PAGE

NUMBERING

AS ORIGINAL

UNIVERSITY OF STRATHCLYDE

THE CONTINUOUS MEDIUM ANALYSIS OF PLANE AND SPATIAL STRUCTURES

BOON CHANTAKSINOPAS

A Thesis presented for the degree of
Doctor of Philosophy
of the University of Strathclyde
in the Department of Civil Engineering

1975

SUMMARY

The continuous medium analyses of two- and three-dimensional multi-storey shear wall structures are presented in this thesis.

The system of planar coupled walls with continuously variable stiffness has been analysed and two methods of solution, the Galerkin and the finite difference methods, proposed. The results of tests on perspex models with tapered width agreed reasonably well with the analytical results.

A new technique which enables important design quantities for uniform coupled wall systems on flexible bases to be evaluated rapidly has been developed. The design curves for several standard load cases, vertical and lateral loads, have been produced. These design curves are applicable to two coupled wall systems or any symmetrical system with three coupled walls.

The lateral-load analysis of symmetrical shear wall and shear wall-frame structures has been presented. The bending and torsional actions of the applied loads are analysed separately. Each separate analysis is reducible to the analysis of an equivalent analogous plane system. The method is particularly suitable for analysing a symmetrical structure which consists of a few distinct groups of coupled wall assemblies. Asymmetrical shear wall and shear wall-frame structures have also been treated.

Finally the structure composed of thin-walled

assemblies has been analysed by using Vlasov's theory for thin-walled beams of open section. The theoretical results were compared with the results of tests on a fourteen-storey perspex model. Reasonable agreement was obtained between theory and experiment.

CONTENTS

CONTENTS (Contd)

CONTENTS (Contd)

CONTENTS (Contd)

CONTENTS (Contd)

CONTENTS (Contd)

CHAPTER 1

INTRODUCTION

1.1 Multi-storey Structures

The relatively high cost and scarcity of land in and around large cities have given rise to a rapid increase in the number of multi-storey buildings for both residential and commercial purposes. With the increasing use of light partitioning and high strength concrete and steel reinforcement in tall buildings, the effects of wind or seismic loads have become more significant, and the provision of adequate lateral stiffness against lateral forces constitutes a major consideration in the design of tall structures.

The structural systems for tall buildings currently in use consist of one or more of the three basic units, namely, frame, wall and tube[32]. Generally, as the height of a building increases, a point is reached beyond which the consideration of lateral stiffness and not strength will govern the design of the structure. Therefore, the choice of the structural system adopted depends, to a large extent, on the number of storeys and the magnitudes of the expected lateral forces. Concrete frame buildings can, generally, be economically built up to the height of between fifteen and twenty storeys. Buildings which derived all of their lateral strength from shear walls are feasible up to between thirty and forty storeys. Hotels and apartment buildings incorporating

shear walls and frames are feasible up to seventy storeys. Above these heights tube-in-tube or multiple frame-tube systems appear to be more economical.

A large proportion of tall concrete buildings is of shear wall construction, i.e. consisting of shear walls only, or shear wall-frame construction which consists of shear walls acting in conjunction with parallel plane frames. The prevalence of these types of structural systems is due to the advantages in the speed of construction, low reinforcing steel requirement and adequate lateral stability to a considerable height. The study made in this research mainly concerns these types of structural systems.

In present building terminology, the term "shear wall" signifies a structural unit in the form of single wall or core capable of withstanding lateral forces. Shear walls may be planar or non-planar and may be connected by either connecting beams or floor slabs or a combination of both. The terms "coupled (shear) walls" and "(shear) walls with openings" are commonly used to describe shear walls in which the connecting members must be considered as moment-resistant elements. If shear walls are connected solely through floor slabs which may be considered as capable of transmitting only in-plane forces, they are commonly described as cantilevered (shear) walls or cantilevered cores.

1.2 Previous Research

In recent years there has been considerable interest

in the analysis and design of multi-storey structures, as witnessed by the large number of published works devoted to the subjects. An extensive review of literature on shear wall structures published prior to 1965 was presented by Coull and Stafford Smith[14]. Present techniques for the analysis of two- and three-dimensional systems were reviewed by a committee of the American Concrete Institute[32] and by Stamato[30]. A selective review of the methods available for the elastic analysis of tall concrete structures, and the classification of the particular techniques most appropriate to the different structural systems was presented by Coull and Stafford Smith[15]. All sources give comprehensive lists of the published literature. In view of the ready availability of the noted papers and the published literature listed in the papers, only a brief review of relevant previous works will be presented here.

The majority of the earlier studies of shear wall structures and many of the more recent works have concentrated on two-dimensional systems. In the analysis of planar coupled shear walls, one of the following three methods, namely, the frame analogy, the finite element method and the continuous medium method, is generally employed. In the frame analogy, the coupled wall system is analysed as a frame, the finite width of the wall being incorporated by a stiff arm connecting the end of the beam to the centroidal axis of the wall[20]. The finite element method replaces the coupled walls by interconnected plane stress elements, and the solution is

obtained using matrix techniques. In the third method, the continuous medium approach, the discrete system of connecting beams is replaced by continuous laminae of equivalent flexural rigidity. By assuming points of contraflexure at the mid-span of the substitute system, conditions of compatibility and equilibrium yield a second-order governing differential equation. A closed form solution for the problem can easily be achieved if the walls are uniform.

Of the three methods of analysis, the frame analogy and the finite element technique which are basically discrete analyses give more accurate results, and are readily adaptable to the variations in geometry of the coupled walls. The amount of computation involved in these two methods, however, is large and increases with height. The use of either of these methods in the design office is rarely justified because of the time and expense involved. The continuous medium method, on the other hand, yields a slightly less accurate result but the computation involved is much less and its accuracy increases with height without additional computation. Although restricted to systems with simple geometry, the analysis can be carried out by hand or small desk calculator. The simplicity of the method has enabled the production of simple design curves[9] which enable a rapid and accurate analysis of the structure for standard load cases.

The technique of replacing the discrete beam system by a continuous medium was first proposed by Chitty[3]

in the analysis of a cantilever composed of a number of parallel beams interconnected by cross bars. Further developments were due to Beck[1], Rosman[25], and Magnus[21], who have extended the original analysis to take account of the axial deformations of the walls, shear deformations of the connecting beams, flexural deformation of walls and beams, and the effects of different foundation conditions. Cases of walls with stepwise variation in cross-sections and walls with linearly tapered thickness were analysed by Coull and Puri[12,13] and Michael[22], respectively.

Several papers on the analysis of shear wall-frame systems were published, notably those by Rosenblueth and Holtz[24], Cardan[2], Rosman[26], Khan and Sbarounis[19], and recently by Heidebrecht and Stafford Smith[18]. The analyses presented were essentially plane analyses since only the displacement in the direction of the applied load was assumed.

Three-dimensional analysis of complete structures were presented by Clough, King and Wilson[4], Gluck[16], Rosman[27], Coull and Irwin[11]. Heidebrecht and Swift[17], and many other authors[32]. Most of the analyses employ the concept of a continuous medium. However, the formulation of the analyses are such that to achieve solutions considerable matrix manipulation is required.

1.3 Scope of the Thesis

This thesis is concerned with the investigation of multi-storey structures by using the continuous medium approach. This approach is adopted because the computation

involved is not excessive and simple design curves may be produced. Furthermore, it is possible to formulate the analysis such that in the case of shear wall structures with a few coupled wall assemblies (or a few groups of identical coupled wall assemblies), the analysis of the complete structures may be carried out manually or with the aid of a small desk calculator.

Two- and three-dimensional shear wall systems have been studied. The first part of the analysis deals with two-dimensional coupled wall structures. Planar coupled walls with continuously variable stiffness subjected to lateral forces have been considered, and theoretical solutions are verified by testing perspex models of coupled walls with tapered width. The analysis is able to deal with coupled walls on elastic foundation. Coupled wall systems of uniform cross-sections (two wall and symmetrical three wall systems) supported on flexible bases and subjected to vertical and lateral loads have been investigated, and design curves presented for several standard load cases applicable to various base conditions.

A study of symmetrical three-dimensional structures subjected to lateral loads has been made. The bending and torsion of symmetrical shear wall structures are analysed as two separate equivalent plane problems. The method is valid for structures composed of planar or non-planar coupled wall assemblies. The analysis is extended to deal with symmetrical shear wall-frame structures. In addition, asymmetrical three-dimensional structures are also treated.

Finally, a general thin-walled shear wall structure is analysed using Vlasov's theory for thin-walled beams of open section, and an experimental investigation was carried out to substantiate the analysis.

In this thesis Figures and Tables are referred to by chapter number and are included at the end of the relevant Chapter.

CHAPTER 2

COUPLED SHEAR WALLS WITH CONTINUOUSLY VARIABLE STIFFNESS

2.1 Notation

The following symbols are used in this Chapter:-

A_1, A_2 = cross-sectional areasof walls 1 and 2

l = distance between the centroids of walls 1 and 2

b = length of connecting beams

I_c = second moment of area of connecting beams

I_r = reduced second moment of area of connecting beams

I_1, I_2 = second moments of area of walls 1 and 2

I = $I_1 + I_2$

h = storey height

E = modulus of elasticity

H = total height of the coupled wall system

M = static applied moment

M_1, M_2 = bending moments in walls 1 and 2

S_1, S_2 = horizontal shear forces in walls 1 and 2

G, ν = shear modulus and Poisson's ratio, respectively

z = co-ordinate of the vertical axis for a coupled wall system, the origin of the vertical axis is at the top of the system.

u = lateral displacement

q = vertical shear distribution in the continuous medium

T = integral shear force = $\int_0^z q \, d\lambda$

λ , ξ = auxiliary vertical ordinates, with the origins at the top of the coupled wall system

η = non-dimensional co-ordinate = $\frac{Z}{H}$

Q = the integral of relative direct stress of the walls

$$= \int_z^H \left[\left(\frac{1}{A_1} + \frac{1}{A_2}\right) \int_0^{\xi} q \, d\lambda \right] d\xi$$

B, R, α, β = structural parameters

K_{v1}, K_{v2} = vertical stiffnesses of foundations under walls 1 and 2 respectively

$K_{\theta 1}$, $K_{\theta 2}$ = rotational stiffnesses of foundations under walls 1 and 2 respectively

EK_b = equivalent stiffness distribution of continuous medium

γ = $\propto H$

Other subsidiary symbols are defined locally in the text.

2.2 Introduction

In the study of coupled shear walls, the continuous medium approach is the method of analysis in which the discrete system of connecting beams is replaced by a continuous medium of equivalent stiffness. The substitute medium is assumed to span the openings throughout the height of the walls. By assuming points of contraflexure at the mid-span positions of the substitute medium, a governing differential equation for the structure may be established.

Earlier works have concentrated on the analysis of uniform walls[1,21,25] or walls with stepwise variations in the cross-sectional dimensions[12,13]. The distance between the centroidal axes of the walls is then either a constant or a step function. The governing differential equations for such systems are essentially second-order equations with constant coefficients.

If the distance between the centroidal axes of the walls is a continuously variable function, for instance coupled walls with tapered width, the order of the governing differential equation will generally be greater than two. The coefficients of the governing equation will also be variable functions. In this Chapter an analysis of coupled shear walls with continuously variable stiffness is presented. The integral of relative direct stress of the walls (resulting from the vertical shear distribution) is used as the redundant function. Two methods of approximate solutions, the finite difference and the Galerkin methods, are proposed.

2.3 General Theory

In the analysis of coupled shear walls by the continuous medium approach, a number of assumptions are postulated in order to simplify the analysis.

2.3.1 Assumptions

The following assumptions are made:-

1. The discrete system of connecting beams is replaced by a continuous medium or a system of laminae which are mutually independent in their deformations.

2. The equivalent stiffness distribution (stiffness per unit height) of the continuous medium is a differentiable function of the height ordinate. Its integral between half a storey above and below any connecting beam must be compatible with the stiffness of the beam.

3. Points of contraflexure occur at the mid-span positions of the substitute laminae.

4. The simple beam theory is taken to be valid for individual wall.

5. The connecting beams are axially rigid so that the deflections of the walls are equal. Thus, the moment carried by each wall is proportional to its second moment of area.

2.3.2 Differential Equation

Consider a general system of coupled walls under lateral loading as shown in Fig. 2.1. The discrete system of connecting beams of the real structure is transformed into an equivalent continuous medium as shown in Fig. 2.2. The equivalent stiffness distribution of the continuous medium is expressed as EK_b, where E is the modulus of elasticity and K_b the equivalent distribution of the second moment of area of the continuous medium.

By making a cut along points of contraflexure of the substitute laminae, i.e. at the mid-span positions, only the vertical shear distributions and axial forces act on the laminae at the cut section since the bending moments are zero by virtue of the property of the point of contra-

flexure. From considerations of the cut structure, the relative vertical displacements δ_1, δ_2, δ_3 of the cut ends of a lamina due to bendings of the walls, bendings of the cantilevered lamina, and axial deformations of the walls are, respectively,

$$\delta_1 = 1 \frac{du}{dz}$$

$$\delta_2 = \frac{b^3}{12EK_b} q$$

$$\delta_3 = \frac{1}{E} \int_z^H \left[\left(\frac{1}{A_1} + \frac{1}{A_2} \right) \int_0^\xi q \, d\lambda \right] d\xi$$

in which,

u = lateral displacement of the walls

z = vertical ordinate, with the origin at the top of the walls

A_1, A_2 = cross-sectional areas of walls 1 and 2

λ , ξ = auxiliary vertical ordinates

1 = distance between centroidal axes of the walls

b = length of connecting beams

q = vertical shear distribution in the continuous medium

H = height of the wall

For compatibility, the relative vertical displacement at the cut ends must vanish, hence,

$$\delta_1 + \delta_2 + \delta_3 = 0$$

or

$$1\,\frac{du}{dz} + \frac{b^3}{12EK_b}\,q + \frac{1}{E}\int_z^H \left[\left(\frac{1}{A_1} + \frac{1}{A_2}\right)\int_0^\xi q\,d\lambda\right] d\xi = 0 \qquad (2.1)$$

From the moment-curvature relationships, the moments in walls 1 and 2 may be written as,

$$M_1 = EI_1\frac{d^2u}{dz^2} = M - g_1\int_0^z q\,d\lambda - M_a \qquad (2.2)$$

$$M_2 = EI_2\frac{d^2u}{dz^2} = -g_2\int_0^z q\,d\lambda + M_a$$

where,

M = static applied moment

M_a = bending moment due to axial forces in the continuous medium

M_1, M_2 = bending moments in walls 1 and 2, respectively

I_1, I_2 = second moments of area of walls 1 and 2, respectively

g_1, g_2 = distances between points of contraflexure and the centroids of walls 1 and 2, respectively

From equation (2.2), the overall moment-curvature relationship for the structure becomes,

$$M_1 + M_2 = EI\frac{d^2u}{dz^2} = M - 1\int_0^z q\,d\lambda \qquad (2.3)$$

in which I is the sum of the second moments of area of walls 1 and 2.

Let,

$$\frac{b^3}{12K_b} = R$$

$$\frac{1}{A_1} + \frac{1}{A_2} = \frac{1}{B} \qquad (2.4)$$

$$\int_z^H \left[\left(\frac{1}{A_1} + \frac{1}{A_2}\right) \int_0^\xi q \, d\lambda \right] d\xi = Q$$

and hence,

$$\frac{dQ}{dz} = -\frac{1}{B} \int_0^z q \, d\lambda \qquad (2.5)$$

$$q = -\left(B\frac{d^2Q}{dz^2} + \frac{dB}{dz} \cdot \frac{dQ}{dz}\right)$$

By differentiating equation (2.1) with respect to z, substituting for $\frac{d^2u}{dz^2}$ from equation (2.3), then multiplying by $-\frac{E}{RB}$ and re-arranging terms, a governing differential equation for the structure is established as,

$$\frac{d^3Q}{dz^3} + \left[\frac{1}{RB} \frac{d(RB^2/1)}{dz}\right] \frac{d^2Q}{dz^2} + \left[\frac{1}{RB} \frac{d(\frac{R}{1} \cdot \frac{dB}{dz})}{dz} - \frac{1}{RB} - \frac{1^2}{IR}\right] \cdot$$

$$\frac{dQ}{dz} - \left[\frac{1}{RB} \cdot \frac{d(1/1)}{dz}\right] Q = \frac{M1}{IRB} \qquad (2.6)$$

or

$$\frac{d^3Q}{dz^3} + C_1 \frac{d^2Q}{dz^2} + C_2 \frac{dQ}{dz} + C_3Q + C_4 = 0 \qquad (2.7)$$

where,

$$C_1 = \frac{1}{RB} \frac{d(RB^2/1)}{dz}$$

$$C_2 = \frac{1}{RB} \frac{d(\frac{R}{1} \frac{dB}{dz})}{dz}$$

$$C_3 = -\frac{1}{RB} \frac{d(1/1)}{dz} \qquad (2.8)$$

$$C_4 = -\frac{M1}{IRB}$$

In general the function C_i will be of the form,

$$C_i = \left(\sum_{j=0}^{m_i} D_j z^j\right) / \left(\sum_{k=0}^{n_i} L_k z^k\right)$$

in which D_j, L_k, m_i, n_i are constants which depend on the applied loads as well as the geometry of the coupled wall system. Therefore, the governing differential equation may generally be expressed as,

$$J_1(z) \frac{d^3Q}{dz^3} + J_2(z) \frac{d^2Q}{dz^2} + J_3(z) \frac{dQ}{dz} + J_4(z)Q + J_5(z) = 0 \qquad (2.9)$$

in which the coefficients $J_i(z)$ are some polynomials of z.

The governing differential equation (2.6) is valid for any coupled wall system provided that the parameters R, B, 1, $\frac{dB}{dz}$ are differentiable functions of z over the interval $0 \leq z \leq H$. The bending moment M may be due to concentrated or distributed loads or a combination of both. If the load system includes concentrated loads, a single moment expression valid over the entire height of the walls may be obtained by employing Macaulay's brackets[6].

Usually the storey height (h) and the second moments of area of connecting beams (I_c) are constant throughout the height of the walls. For such a case, the second moment of area per unit height for the continuous medium is a constant and given by $K_b = I_c/h$. If the second moments of area of the connecting beams are not constant but may be approximately represented by a smooth function $f_I(z)$, the value for K_b may then be taken as $K_b = \frac{f_I(z)}{h}$.

The shear deformations of connecting beams may also be incorporated in the analysis by using the reduced second moments of area of connecting beams. For coupled walls with uniform connecting beams, it may be shown that by taking the shear deformation of connecting beams into account, the second moment of area per unit height of the continuous medium becomes,

$$K_b = \frac{I_r}{h}$$

where,

I_r = reduced second moment of area of connecting beams

$$= \frac{I_c}{(1 + \frac{12EI_c}{b^3GA_s})}$$

G = shear modus of connecting beams = $\frac{E}{2(1+\nu)}$

ν = Poisson's ratio

A_s = effective cross-sectional area of connecting beams

= $\frac{5}{6}$ x cross-sectional area, if connecting beams are

rectangular in cross-sections.

2.3.3 Boundary Conditions

The boundary conditions for the governing differential equation (2.6) are obtained as follows:-

At the top, $z = 0$,

from equation (2.5), $$\frac{dQ}{dz} = 0 \qquad (2.10)$$

At the base, $z = H$,

from equation (2.4), $$Q = 0 \qquad (2.11)$$

At a fixed base the rotation is zero, therefore

$$\frac{du}{dz} = 0 \qquad (2.12)$$

By substituting q from equation (2.5) into equation (2.1), then evaluating at $z = H$, and using equations (2.11) and (2.12), an additional boundary condition at the base is obtained as,

$$\text{at } z = H, \quad \frac{d^2Q}{dz^2} = -\left(\frac{1}{B}\frac{dB}{dz} \cdot \frac{dQ}{dz}\right) \qquad (2.13)$$

The three boundary conditions for the governing differential equation are those given by equations (2.10), (2.11) and (2.13).

2.3.4 Internal Forces and Displacement

The vertical forces in walls 1 and 2 are given by,

$$N_1 = \int_0^z q \, d\lambda$$

$$N_2 = -\int_0^z q \, d\lambda \qquad (2.14)$$

in which N_1 and N_2 are the vertical forces in wals 1 and 2 respectively.

The internal bending moments in walls 1 and 2 are proportional to their second moments of area since both walls deflect equally, and are given by, from equations (2.2) and (2.3),

$$M_1 = \frac{I_1}{I} \left(M - 1 \int_0^z q \, d\lambda \right)$$

$$M_2 = \frac{I_2}{I} \left(M - 1 \int_0^z q \, d\lambda \right) \qquad (2.15)$$

From the expression for $\int_0^z q \, d\lambda$ given in equation (2.5), the vertical forces and internal bending moments in the walls may be written in terms of Q as follows,

$$N_1 = - B \frac{dQ}{dz}$$

$$N_2 = B \frac{dQ}{dz} \qquad (2.16)$$

$$M_1 = \frac{I_1}{I} \left(M + 1 B \frac{dQ}{dz}\right)$$

$$M_2 = \frac{I_2}{I} \left(M + 1 B \frac{dQ}{dz}\right)$$

The lateral wall deflection, u, may be obtained by integrating equation (2.1) once, or integrating equation (2.3) twice. By integrating equation (2.3) twice, the

deflection may be written as,

$$u = \frac{1}{E}\left[\int_z^H \int_\xi^H \frac{M}{I}\, d\lambda\, d\xi + \int_z^H \left(\int_\xi^H \frac{1B}{I}\frac{dQ}{dz}\, d\lambda\right) d\xi\right]$$

$$- (H - z)\left(\frac{du}{dz}\right)_H + (u)_H \qquad (2.17)$$

in which $\left(\frac{du}{dz}\right)_H$ and $(u)_H$ are the rotation and the lateral displacement, respectively, at the bases of the walls.

For walls on a rigid foundation,

$$\left(\frac{du}{dz}\right)_H = (u)_H = 0$$

and equation (2.17) reduces to,

$$u = \frac{1}{E}\left[\int_z^H \int_\xi^H \frac{M}{I}\, d\lambda\, d\xi + \int_z^H \left(\int_\xi^H \frac{1B}{I}\frac{dQ}{dz} \cdot d\lambda\right) d\xi\right] \qquad (2.18)$$

From considerations of the equilibrium of wall elements, the horizontal shear forces in the walls and the distribution of the horizontal force in the continuous medium may be shown to be,

$$S_1 = \frac{dM}{dz} - \frac{dM_a}{dz} = \frac{d\left(M_1 + g_1 \int_0^z q\, d\lambda\right)}{dz}$$

$$S_2 = \frac{dM_a}{dz} = \frac{d\left(M_2 + g_2 \int_0^z q\, d\lambda\right)}{dz} \qquad (2.19)$$

$$w_c = - \frac{dS_2}{dz} \qquad (2.19)$$ contd.

where,

S_1, S_2 = horizontal shear forces in walls 1 and 2 respectively

w_c = distributed axial force in the continuous medium

g_1, g_2, M_a = as defined previously.

The vertical force and the horizontal force in any connecting beam at level z_i may be obtained by integrating the vertical shear distribution q and the distributed axial force w_c respectively, over half a storey height above and below the level concerned, i.e.

$$(V_b)_{z_i} = \int_{z_i - h/2}^{z_i + h/2} q \, d\lambda \qquad (2.20)$$

$$(F_b)_{z_i} = \int_{z_i - h/2}^{z_i + h/2} w_c \, d\lambda$$

where

$(V_b)_{z_i}$ = vertical force in the connecting beam at the level z_i

$(F_b)_{z_i}$ = axial force in the connecting beam at the level z_i

2.3.5 Coupled Wall Systems with Second-order Governing Differential Equation

In deriving the governing differential equation (2.6), it has been assumed that the wall cross-sectional areas, the equivalent stiffness distribution of the continuous medium, and the distance between the centroidal axes of the walls are continuously variable functions of height. If any of these functions is a constant, simplification of the governing differential equation may be achieved.

System with Constant Parameter 1

Consider a coupled wall system with constant distance between the centroidal axes of the walls, for instance walls with tapered thickness. As 1 is constant, the derivative $\frac{d(1/1)}{dz}$ vanishes and the governing differential equation (2.6) becomes,

$$\frac{d^3Q}{dz^3} + \left[\frac{1}{RB^2}\ \frac{d(RB^2)}{dz}\right]\frac{d^2Q}{dz^2} + \left[\frac{1}{RB}\cdot\frac{d(R\frac{dB}{dz})}{dz} - \frac{1}{RB} - \frac{1^2}{IR}\right].$$

$$\frac{dQ}{dz} - \frac{M1}{IRB} = 0 \qquad (2.21)$$

The differential equation (2.21) consists of only the derivatives of Q but not Q itself. Hence, by adopting the first derivative $\frac{dQ}{dz}$ as a new redundant function the differential equation (2.21) may be reduced to a second-order equation.

Define, T = integral shear force = $\int_0^z q\, d\lambda$ (2.22)

Then, from equation (2.4)

$$Q = \int_z^H \frac{T}{B} \, d\lambda$$

$$\frac{dQ}{dz} = - \frac{T}{B}$$

$$\frac{d^2Q}{dz^2} = - \frac{1}{B} \cdot \frac{dT}{dz} + \frac{1}{B^2} \cdot \frac{dB}{dz} \cdot T$$

(2.23)

$$\frac{d^3Q}{dz^3} = - \frac{1}{B} \cdot \frac{d^2T}{dz^2} - \frac{2}{B^2} \cdot \frac{dB}{dz} \cdot \frac{dT}{dz} - \frac{1}{B^2} \frac{d^2B}{dz^2} \cdot T$$

$$+ \frac{2}{B^2} \left(\frac{dB}{dz}\right)^2 T$$

Substitution of $\frac{dQ}{dz}$, $\frac{d^2Q}{dz^2}$, $\frac{d^3Q}{dz^3}$, from equation (2.23) into (2.21) yields a second-order differential equation for T as a function of z as,

$$\frac{d^2T}{dz^2} - \frac{1}{R} \cdot \frac{dR}{dz} \cdot \frac{dT}{dz} - \frac{1}{R} \left(\frac{1}{B} + \frac{l^2}{I}\right)T + \left(\frac{l}{IR}\right)M = 0 \qquad (2.24)$$

Equation (2.24) is valid for coupled wall systems with variable R, B, I provided that the derivative $\frac{dR}{dz}$ exists and l remains constant throughout the height of the walls.

Consider a special case of coupled wall system with tapered thickness, shown in Fig. 2.3. The thicknesses of the walls and the connecting beams are equal and given by,

$$t = t_H \left(1 - \frac{H}{C} + \frac{z}{C}\right)$$

in which t_H is the thickness at the base and C the vertical

distance between the base of the wall and the extrapolated point of zero thickness. It may be shown that the coefficients of T and M in equation (2.24) are constants, and equation (2.23) may be written as,

$$\frac{d^2T}{dz^2} - \frac{1}{(z + C - H)} \frac{dT}{dz} - \alpha^2 T + \beta^2 M = 0 \qquad (2.25)$$

where,

$$\beta^2 = \frac{12}{b^3 h} \left(\frac{I_c}{I}\right) 1 = \text{constant}$$

$$\alpha^2 = \beta^2 1 \mu = \text{constant} \qquad (2.26)$$

$$\mu = 1 + \frac{I}{1^2} \left(\frac{1}{A_1} + \frac{1}{A_2}\right) = \text{constant}$$

I_c = second moment of area of connecting beams.

If both walls of the tapered coupled wall system are identical and completely tapered, the resulting differential equation will be identical to that given by Michael[22].

Systems with Constant Parameter 1 and R

For a coupled wall system with constant distance between the centroidal axes of the walls, and constant cross-sectional dimensions of the connecting beams, the parameters 1 and R become constant and the governing differential equation is reduced further to,

$$\frac{d^2T}{dz^2} - \frac{1}{R} \left(\frac{1}{B} + \frac{1^2}{I}\right) T + \frac{M1}{IR} = 0 \qquad (2.27)$$

Uniform Coupled Walls

For a uniform coupled wall system, all the parameters l, R, B, I do not vary with height. Consequently, the governing differential equation becomes a second-order differential equation with constant coefficients, and may be written as,

$$\frac{d^2T}{dz^2} - \alpha^2 T = -\beta^2 M \qquad (2.28)$$

or, in terms of the vertical shear distribution function q,

$$\frac{d^2q}{dz^2} - \alpha^2 q = -\beta^2 \frac{dM}{dz} \qquad (2.29)$$

in which α^2, β^2 are as given in equation (2.26).

If each coupled wall system is free at the top and fixed to a rigid foundation at the base, the boundary conditions in terms of T are given by,

$$\text{at } z = 0, \quad T = 0$$
$$\text{at } z = H, \quad \frac{dT}{dz} = 0 \qquad (2.30)$$

and in terms of q by,

$$\text{at } z = 0, \quad \frac{dq}{dz} = 0$$
$$\text{at } z = H, \quad q = 0 \qquad (2.31)$$

2.4 Methods of Solution

The governing differential equation (2.6) in its most general form will be an ordinary differential equation with variable coefficients. The coefficients become

constant only when the coupled wall system is uniform. One general method of solving an ordinary differential equation with variable coefficients is the method of undetermined coefficients.

Consider the differential equation (2.9), which is,

$$J_1(z)\,\frac{d^3Q}{dz^3} + J_2(z)\,\frac{d^2Q}{dz^2} + J_3(z)\,\frac{dQ}{dz} + J_4(z)\,Q + J_5(z) = 0$$

A solution in the form of an infinite power series may be first assumed,

$$Q = \sum_{n=0}^{\infty} a_n z^n$$

where a_n are undetermined constant coefficients. Substitution of Q, $\frac{dQ}{dz}$, $\frac{d^2Q}{dz^2}$, $\frac{d^3Q}{dz^3}$ obtained from the assumed solution into the differential equation leads to an expression in terms of powers of z. By grouping the like powers of z together and then imposing the condition that the coefficient of each power of z must vanish - independently, recursive formulae for the undetermined coefficients may be obtained. The solution for Q is then expressible in terms of a few unknown constants. These unknown constants are determined from the known boundary conditions and, hence, the complete solution for Q is obtained.

Each recursive formula will usually involve more than two undetermined coefficients and, consequently, leads to a complicated expression for the solution. The labour involved in evaluating the solution may prove to be prohibitively heavy, since frequently the solution will

be a slowly converging function so that a large number of terms are required to be evaluated. Therefore, any approximate method which can significantly reduce the computational effort at the cost of a slightly less accurate result is preferable. Two such methods of solution are proposed, namely, the Galerkin method and the finite difference method.

2.4.1 Formulation in Terms of an Independent Dimensionless Variable

For convenience in applying the proposed methods of solution, the problem will be formulated in terms of an independent dimensionless co-ordinate. Define the dimensionless co-ordinate η as,

$$\eta = \frac{z}{H}, \qquad 0 \leq \eta \leq 1$$

Then, $z = \eta H$ $\qquad \frac{d\eta}{dz} = \frac{1}{H}$

$$\frac{d^i Q}{dz^i} = \frac{1}{H^i} \frac{d^i Q}{d\eta^i}$$

In terms of the dimensionless variable η, the differential equations (2.6), (2.9) and the boundary condition equations (2.10), (2.11), (2.13) become, respectively,

$$\frac{d^3Q}{d\eta^3} + \left[\frac{1}{RB^2} \frac{d\left(\frac{RB^2}{1}\right)}{d\eta} \right] \frac{d^2Q}{d\eta^2} + \left[\frac{1}{RB} \frac{d\left(\frac{R}{1}\frac{dB}{d}\right)}{d\eta} - \frac{H^2}{RB} - \frac{1^2H^2}{IR} \right] \cdot$$

$$\frac{dQ}{d\eta} - \left[\frac{1H^2}{RB} \frac{d(1/1)}{d\eta} \right] Q - \frac{M1H^3}{IRB} = 0 \qquad (2.32)$$

$$F_1(\eta)\frac{d^3Q}{d\eta^3} + F_2(\eta)\frac{d^2Q}{d\eta^2} + F_3(\eta)\frac{dQ}{d\eta} + F_4(\eta)Q$$

$$+ F_5(\eta) = 0 \qquad (2.33)$$

$$\text{at } \eta = 0, \quad \left(\frac{dQ}{d\eta}\right)_0 = 0$$

$$\text{at } \eta = 1, \quad (Q)_H = 0 \qquad (2.34)$$

$$\text{at } \eta = 1, \quad \left(\frac{d^2Q}{d\eta^2}\right)_H = -\left(\frac{1}{B}\cdot\frac{dB}{d\eta}\cdot\frac{dQ}{d\eta}\right)_H$$

where $F_i(\eta)$ are some polynomials of η. In equation (2.34) and the subsequent analysis, unless defined otherwise, brackets with subscript H or 0 signify that the expression enclosed within the brackets is to be evaluated at $\eta = 1$ or 0, respectively.

The expressions for T, q, $M_t = M_1 + M_2$, $\frac{du}{d\eta}$, $\frac{d^2u}{d\eta^2}$ become, respectively,

$$T = -\frac{B}{H}\frac{dQ}{d\eta}$$

$$q = -\frac{1}{H^2}\left(B\frac{d^2Q}{d\eta^2} + \frac{dB}{d\eta}\frac{dQ}{d\eta}\right)$$

$$M_t = M_1 + M_2 = M + \frac{lB}{H}\frac{dQ}{d\eta} \qquad (2.35)$$

$$\frac{du}{d\eta} = \left(\frac{R}{lH}\left(B\frac{d^2Q}{d\eta^2} + \frac{dB}{d\eta}\frac{dQ}{d\eta}\right) - \frac{HQ}{l}\right)\frac{1}{E}$$

$$\frac{d^2u}{d\eta^2} = \frac{H^2}{EI}\left(M + \frac{lB}{H}\frac{dQ}{d\eta}\right)$$

2.4.2 The Galerkin Method

The Galerkin method assumes an approximate solution in the form,

$$Q_n = \sum_{j=0}^{n} a_j f_j(z)$$

where a_j are constants, and $f_j(z)$ are appropriate functions which satisfy the boundary conditions. The integer n may assume any arbitrary value. The accuracy of the approximate solution Q_n increases with an increasing value of n, but this is also accompanied by an increase in compution. The coefficients a_j are determined by using the criterion of minimizing the absolute value of the error function over the interval of definition of Q_n. The final solution gives an analytical expression for Q_n which is defined over the whole interval[29].

Consider the general governing differential equation (2.33) which may be expressed as,

$$\left(\sum_{j=0}^{m_a} a_j \eta^j\right) \frac{d^3Q}{d\eta^3} + \left(\sum_{j=0}^{m_b} b_j \eta^j\right) \frac{d^2Q}{d\eta^2} + \left(\sum_{j=0}^{m_c} c_j \eta^j\right) \frac{dQ}{d\eta}$$

$$+ \left(\sum_{j=0}^{m_d} d_j \eta^j\right) Q + \left(\sum_{j=0}^{m_e} e_j \eta^j\right) = 0 \qquad (2.36)$$

or simply

$$L(Q) = 0 \qquad (2.37)$$

in which a_j, b_j, c_j, d_j, e_j, m_a, m_b, m_c, m_d, m_e are constants depending on the geometry of the coupled wall system as well as the loading function.

As all the coefficients and the non-homogeneous function of the differential equation (2.36) are polynomial of the variable η , it is convenient to assume an approximate solution as a polynomial of η .

Let the assumed approximate solution, Q_n, be

$$Q_n = \sum_{i=0}^{n} \alpha_i \eta^i \qquad (2.38)$$

where α_i are undetermined constants. The integer n is arbitrary.

As the coupled walls are assumed fixed to rigid foundations, the boundary conditions are those given by equation (2.34),

$$\left(\frac{dQ}{d\eta}\right)_0 = 0$$

$$(Q)_H = 0$$

$$\left(\frac{d^2Q}{d\eta^2}\right)_H = \zeta \left(\frac{dQ}{d\eta}\right)_H$$

in which $\zeta = -\left(\frac{1}{B} \cdot \frac{dB}{d\eta}\right)_H \qquad (2.39)$

Imposing the boundary conditions $\left(\frac{dQ}{d\eta}\right)_0 = (Q)_H = 0$,

$\left(\frac{d^2Q}{d\eta^2}\right)_H = \zeta \left(\frac{dQ}{d\eta}\right)_H$ on the approximation Q_n yields,

respectively,

$$\alpha_1 = 0$$

$$\alpha_0 + \alpha_1 + \ldots \quad \alpha_n = 0 \qquad (2.40)$$

$$2\alpha_2 + 6\alpha_3 + \ldots\ i(i-1)\alpha_i \ldots + n(n-1)\alpha_n =$$

$$\zeta(2\alpha_2 + \ldots\ i\alpha_i \ldots + n\alpha_n)$$

From equation (2.40), it may be shown that

$$\alpha_2 = \frac{1}{2(1-\zeta)} \sum_{i=3}^{n} i\,\alpha_i(\zeta + 1 - i) \tag{2.41}$$

$$\alpha_0 = -\sum_{i=3}^{n}\alpha_i \left[1 + (i(1+\zeta) - i^2)/(2-2\zeta)\right]$$

Substituting $\alpha_1 = 0$, and α_2, α_0 from equation (2.41) into equation (2.38) gives,

$$Q_n = \sum_{i=3}^{n} \alpha_i(\eta^i + \rho_i \eta^2 + \mu_i)$$

or simply (2.42)

$$Q_n = \sum_{i=3}^{n} \alpha_i f_i(\eta)$$

where $$\rho_i = \frac{i(1+\zeta) - i^2}{2(1-\zeta)}$$

$$\mu_i = -\frac{(2-2\zeta) + i(1+\zeta) - i^2}{2(1-\zeta)}$$

$$f_i(\eta) = \eta^i + \rho_i \eta^2 + \mu_i$$

Each of the functions $f_i(\eta)$ satisfies the boundary conditions (2.34) identically, since it may be shown that

$$\frac{df_i(\eta)}{d\eta} = 0 \qquad \text{at} \qquad \eta = 0$$

$$f_i(\eta) = 0 \qquad \text{at} \qquad \eta = 1$$

$$\frac{d^2 f_i(\eta)}{d\eta^2} = \zeta \frac{df_i(\eta)}{d\eta} \quad \text{at} \quad \eta = 1$$

The error resulting from using the approximation Q_n is,

$$\text{error function} = L(Q_n) - L(Q)$$

$$= L(Q_n), \text{ since } L(Q) = 0$$

The minimization of the error function $L(Q_n)$ over the interval $0 \leq \eta \leq 1$ is accomplished by imposing on the error function a set of orthogonality condition[29],

$$\int_0^1 L(Q_n)\ f_k(\eta)\ d\eta = 0 \qquad k = 3, 4, \ldots n$$

or

$$\int_0^1 L\left(\sum_{i=3}^{n} \alpha_i\ f_i(\eta)\right) f_k(\eta)\ d\eta = 0 \qquad (2.43)$$

yielding a set of (n-2) linear algebraic equations for the determination of the constants α_i of the approximate solution.

The required system of (n-2) simultaneous linear equations involving (n-2) unknowns α_i may be obtained by the direct integration of equation (2.43). Upon integrating, it may be established that the general form of the linear equation is,

$$\sum_{i=3}^{n} \alpha_i \left[\sum_{j=0}^{m_a} a_j\ i(i-1)(i-2)\left(\frac{1}{k+j+i-2} + \frac{\rho_k}{j+i} + \frac{\mu_k}{j+i-2}\right.\right.$$

$$\left. + \sum_{j=0}^{m_b} b_j \left\{ i(i-1)\left(\frac{1}{k+j+i-1} + \frac{\rho_k}{j+i+1} + \frac{\mu_k}{j+i-1}\right)\right.\right.$$

$$+ 2\rho_i\left(\frac{1}{k+j+1} + \frac{\rho_k}{j+3} + \frac{\mu_k}{j+1}\right) \Big\}$$

$$+ \sum_{j=0}^{m_c} c_j \Big\{ i\left(\frac{1}{k+j+i} + \frac{\rho_k}{j+i+2} + \frac{\mu_k}{j+i}\right)$$

$$+ 2\rho_i\left(\frac{1}{k+j+2} + \frac{\rho_k}{j+4} + \frac{\mu_k}{j+2}\right) \Big\}$$

$$+ \sum_{j=0}^{m_d} d_j \Big\{ \frac{1}{k+j+i+1} + \frac{\rho_k}{j+i+3} + \frac{\mu_k}{j+i+1}$$

$$+ \rho_i\left(\frac{1}{k+j+3} + \frac{\rho_k}{j+5} + \frac{\mu_k}{j+3}\right) + \mu_i\left(\frac{1}{k+j+1} + \frac{\rho_k}{j+3} + \frac{\mu_k}{j+1}\right) \Big\} \Big]$$

$$+ \sum_{j=0}^{m_e} e_j\left(\frac{1}{k+j+1} + \frac{\rho_k}{j+3} + \frac{\mu_k}{j+1}\right) = 0 \qquad (2.44)$$

where $k = 3, 4, \ldots n$.

The constants α_i, and hence the complete solution for Q_n, are obtained by solving the system of simultaneous linear equation generating by equation (2.44). The integral shear force, vertical shear distribution and bending moment become, from equation (2.35),

$$T = -\frac{B}{H} \sum_{i=3}^{n} \alpha_i \left(i\,\eta^{i-1} + 2\rho_i\eta\right)$$

$$q = -\frac{1}{H^2}\left[B\sum_{i=3}^{n}\alpha_i\left(i(i-1)\,\eta^{i-2} + 2\rho_i\right) + \frac{dB}{d\eta}\sum_{i=3}^{n}\alpha_i \left(i\,\eta^{i-1} + 2\rho_i\eta\right)\right] \qquad (2.45)$$

$$M_t = M + \frac{lB}{H} \sum_{i=3}^{n} \alpha_i \left(i\, \eta^{i-1} + 2\, \beta_i \eta \right) \qquad (2.45)$$
contd.

The lateral deflection u may be obtained by integrating equation (2.1), using the boundary condition of zero deflection at the base,

$$u = \int_{\eta}^{1} \frac{Q_n H^2}{l} \cdot d\bar{n} - \int_{\eta}^{1} \frac{RB}{l} \cdot \frac{d^2 Q_n}{d\eta^2} \cdot d\bar{n}$$

$$- \int_{\eta}^{1} \frac{R}{l} \cdot \frac{dB}{d\eta} \cdot \frac{dQ_n}{d\eta}\, d\bar{n} \qquad (2.46)$$

where the non-dimensional auxiliary ordinate $\bar{n} = \frac{\lambda}{H}$.

2.4.3 The Finite Difference Method

In this method the differential equation is replaced by an approximating difference equation and the continuous interval by a set of discrete points. The interval of η, $0 \leq \eta \leq 1$, is divided into arbitrary n equal sub-intervals of length $rH = \frac{H}{n}$. The discrete points are numbered as shown in Fig. 2.4, where the points 0 and (n+2) are extrapolated points at $\eta = -\frac{1}{n}$ and $\eta = 1 + \frac{1}{n}$ respectively. The central and forward difference operators[28], each with an error of the order $(Hr)^2$, are shown in Appendix I. As the differential equation is of the third-order and only one boundary condition, $\frac{dQ}{d\eta} = 0$, exists at the top; the forward operator for $\frac{d^3Q}{d\eta^3}$ will have to be used in establishing the difference equation for the point at the top of the walls.

From the differential equation (2.33), using the

central difference operators, the difference equations for the points 2 to n may be shown to be

$$F_1(\eta_i)\frac{1}{2r^3}(-Q_{i-2}+2Q_{i-1}-2Q_{i+1}+Q_{i+2})$$

$$+F_2(\eta_i)\frac{1}{r^2}(Q_{i-1}-2Q_i+Q_{i+1})$$

$$+F_3(\eta_i)\frac{1}{2r}(-Q_{i-1}+Q_{i+1})+F_4(\eta_i)Q_i+F_5(\eta_i)=0 \qquad (2.47)$$

where $i = 2, 3, \ldots n$

$\eta_i = (i-1)/n$

Q_i = value of Q at $\eta = \eta_i$

At the point 1, using the forward difference operator for $\frac{d^3Q}{d\eta^3}$ and central difference operators for $\frac{d^2Q}{d\eta^2}$ and $\frac{dQ}{d\eta}$, the difference equation becomes,

$$F_1(0)\frac{1}{2r^3}(-5Q_1+18Q_2-24Q_3+14Q_4-3Q_5)$$

$$+F_2(0)\frac{1}{2r^2}(Q_0-2Q_1+Q_2)+F_3(0)\frac{1}{2r}(-Q_0+Q_2)$$

$$+F_4(0)Q_1+F_5(0)=0 \qquad (2.48)$$

Three additional equations are obtained from the boundary conditions, equation (2.34). Using the central difference operators, the boundary conditions become,

$$\left(\frac{dQ}{d\eta}\right)_0 = 0, \qquad Q_0 - Q_2 = 0$$

$$(Q)_H = 0, \qquad Q_{n+1} = 0 \tag{2.49}$$

$$\left(\frac{d^2Q}{d\eta^2} - \zeta \frac{dQ}{d\eta}\right)_H = 0,$$

$$Q_{n+2} + Q_n + \frac{r}{2} \zeta (Q_n - Q_{n+2}) = 0$$

where ζ is as previously defined in equation (2.39).

Equations (2.47)-(2.49) constitute a system of (n+3) simultaneous linear equations in (n+3) unknowns Q_i, where i = 0, 1, ... (n+2). Hence, the system possesses a unique solution. Theoretically, the accuracy of the solution may be improved indefinitely by increasing the number of the intervals.

Using the central operators, the internal forces become, from equation (2.35),

$$T_i = -\left(\frac{B}{2rH}\right)_i (-Q_{i-1} + Q_{i+1})$$

$$q_i = -\frac{1}{H^2}\left[\left(\frac{B}{r^2}\right)_i (Q_{i-1} - 2Q_i + Q_{i+1}) + \left(\frac{dB}{d\eta}\right)_i \frac{1}{2r} (-Q_{i-1} + Q_{i+1})\right] \tag{2.50}$$

$$(M_t)_i = M_i + \left(\frac{1B}{2Hr}\right)_i (-Q_{i-1} + Q_{i+1})$$

where the subscript i denotes the functional value at $\eta = \eta_i$.

From equation (2.35),

$$\frac{d^2u}{d\eta^2} = \frac{H^2}{EI}\left(M + \frac{1B}{H}\frac{dQ}{d\eta}\right)$$

Therefore, the deflection u_i at the point i becomes, on using the central difference operators,

$$\frac{1}{r^2}(u_{i-1} - 2u_i + u_{i+1}) = \frac{H^2}{E}\cdot\frac{1}{I_i}\cdot \left[M_i + \left(\frac{1B}{H}\right)_i \frac{1}{2r}(-Q_{i-1} + Q_{i+1})\right]$$

(2.51)

For walls on rigid foundations, the displacement and the rotation at the bases must be zero. Therefore, using the central difference operator, the boundary conditions become,

$$(u)_H = 0, \qquad u_{n+1} = 0$$

$$\left(\frac{du}{d\eta}\right)_H = 0, \qquad u_n - u_{n+2} = 0$$

By setting i equal to (n+1) in equation (2.51) and making use of the boundary conditions shown above, the deflection u_n may be determined. The deflections u_i at the other points may then be successively determined.

The finite difference method gives solutions at a set of discrete points, and anywhere else the solutions must be determined by interpolation.

2.4.4 Exact Solutions for Uniform Coupled Wall Systems

The Galerkin and the finite difference methods

presented in the two previous sections are the general methods of solutions, applicable to both uniform and non-uniform coupled wall systems. However, if the coupled wall system is uniform and the loading function relatively simple, an exact closed form solution may be easily achieved using the standard method of solving the differential equation with constant coefficients. A brief treatment of the exact solution will be given here since it acts as a reference solution with which to compare solutions obtained by the two proposed methods of solution.

The governing differential equation for a uniform coupled wall system, equation (2.29), may be written in terms of the non-dimensional variable as,

$$\frac{d^2q}{d\eta^2} - \alpha^2 H\, q = -\beta^2 H \frac{dM}{d\eta} \qquad (2.52)$$

The complete solution for q takes the form,

$$q = K_1 \cosh \gamma\eta + K_2 \sinh \gamma\eta + q_p \qquad (2.53)$$

in which q_p is the particular integral solution which depends on the loading function, and $\gamma = \alpha H$. The constants K_1, K_2 are constants of integration which may be determined from the known boundary conditions at the top and the base. For walls on rigid foundations and free at the top, the boundary conditions are given by,

$$(q)_H = 0$$

$$(\frac{dq}{d\eta})_0 = 0 \qquad (2.54)$$

and the complete solution for q may be shown to be

$$q = \frac{\cosh\gamma\eta}{\gamma\cosh\gamma}\left[\sinh\gamma\left(\frac{dq_p}{d\eta}\right)_{\eta=0} - (q_p)_{\eta=1}\right]$$

$$- \frac{\sinh\gamma\eta}{\gamma}\left(\frac{dq_p}{d\eta}\right)_{\eta=0} + q_p \qquad (2.55)$$

Consider a uniform coupled wall system subjected to three separate standard lateral load cases as shown in Fig. 2.5. The three load cases are,

1. a concentrated load P at the top of the system
2. a uniformly distributed load w per unit height
3. a triangularly distributed load $\upsilon(1 - \eta)$ per unit height.

The particular integral solutions for the standard load cases 1, 2 and 3 are, respectively,

$$(q_p)_P = \frac{P}{1\mu}$$

$$(q_p)_w = \frac{wH}{1\mu}\eta \qquad (2.56)$$

$$(q_p)_\upsilon = \frac{\upsilon H}{1\mu}\left(\eta - \tfrac{1}{2}\eta^2 - \frac{1}{\gamma^2}\right)$$

Hence, the complete solutions for the three standard load cases 1, 2 and 3 become, respectively,

$$q_p = \frac{P}{1\mu}\left(1 - \frac{\cosh\gamma\eta}{\cosh\gamma}\right)$$

$$q_w = \frac{wH}{1\mu}\left[\frac{(\sinh\gamma - \gamma)\cosh\gamma\eta}{\gamma\cosh\gamma} - \frac{\sinh\gamma\eta}{\gamma} + \eta\right] \qquad (2.57)$$

$$q_\upsilon = \frac{\upsilon H}{1\mu}\left[\frac{(\sinh\gamma - \gamma/2 + 1/\gamma)}{\gamma\cosh\gamma}\cosh\gamma\eta\right.$$

$$- \frac{\sinh\gamma\eta}{\gamma} + \eta - \tfrac{1}{2}\eta^2 - \frac{1}{\gamma^2} \Big] \qquad (2.57)\ \text{contd.}$$

The corresponding lateral displacements are,

$$u_P = \frac{PH^3}{EI}\Big[(\tfrac{1}{3} + \tfrac{1}{6}\eta^2 - \tfrac{1}{2}\eta)(1 - \tfrac{1}{\mu})$$

$$- \frac{1}{\mu\gamma^2}\Big\{\eta - 1 - \frac{(\sinh\gamma\eta - \sinh\gamma)}{\gamma\cosh\gamma}\Big\}\Big]$$

$$u_w = \frac{wH^4}{EI}\Big[(\tfrac{1}{8} - \tfrac{1}{6}\eta + \frac{1}{24}\eta^4)(1 - \tfrac{1}{\mu})$$

$$- \frac{1}{\mu\gamma^2}\Big\{\tfrac{1}{2}(\eta^2-1) + \frac{\gamma(\sinh\gamma - \sinh\gamma\eta) - \cosh\gamma(1-\eta)+1}{\gamma^2\cosh}\Big\}\Big]$$

$$u_v = \frac{vH^4}{EI}\Big[(\frac{11}{120} - \tfrac{1}{8}\eta + \frac{1}{24}\eta^4 - \frac{1}{120}\eta^5)(1 - \tfrac{1}{\mu})$$

$$- \frac{1}{\mu\gamma^2}(\tfrac{1}{6} - \tfrac{1}{2}\eta + \tfrac{1}{2}\eta^2 - \tfrac{1}{6}\eta^3)$$

$$- \Big\{\frac{(1/\gamma - \gamma/2)(\sinh\gamma\eta - \sinh\gamma - \gamma\eta\cosh\gamma + \gamma\cosh\gamma) + 1 - \cosh\gamma(1-\eta)}{\mu\gamma^4\cosh\gamma}\Big\}\Big] \qquad (2.58)$$

2.5 Coupled Walls on Flexible Bases

In the preceding analysis the coupled wall system is assumed fixed to a rigid foundation so that the displacements at the bases are all zero. Complete fixity at the bases does not always occur in practice since the foundation is usually flexible. If the foundation is deformable the effects of base movements must be taken into account in the analysis. In the following analysis

it is assumed that each wall is supported on separate elastic foundation which yields vertically and rotationally under the actions of the imposed vertical force and bending moment, respectively.

Let

K_{v1}, K_{v2} = vertical stiffnesses of the foundations under walls 1 and 2 respectively

$K_{\theta 1}$, $K_{\theta 2}$ = rotational stiffnesses of the foundations under walls 1 and 2 respectively.

The relative vertical displacement, δ_H, due to the vertical movements of the bases may be written as,

$$\delta_H = \left(\frac{1}{K_{v1}} + \frac{1}{K_{v2}}\right) \int_0^H q \, d\lambda \qquad (2.59)$$

In consequence, the compatibility condition for the 'cut' continuous medium becomes, cf. equation (2.1),

$$1 \frac{du}{dz} + \left(\frac{b^3}{12EK_b}\right) q + \frac{1}{E} \int_z^H \left[\left(\frac{1}{A_1} + \frac{1}{A_2}\right) \int_0^\xi q \, d\lambda \right] d\xi$$

$$+ \delta_H = 0 \qquad (2.60)$$

Following the same procedure as before, it may be shown that all the governing differential equations derived previously are valid. The boundary conditions $\left(\frac{dQ}{dz}\right)_{z=0} = (Q)_{z=H} = 0$ are still valid, but the boundary condition based on zero rotation at the base needs to be changed.

From the assumption of equal wall displacements the rotation at the bases must be equal, consequently,

$$(M_1)_H = K_{\theta 1}(\frac{du}{dz})_H \qquad (2.61)$$

$$(M_2)_H = K_{\theta 2}(\frac{du}{dz})_H$$

in which $(M_1)_H$, $(M_2)_H$ and $(\frac{du}{dz})_H$ are the bending moments at the bases of walls 1 and 2 and the rotation at the bases respectively. The base rotation may be written as, using equations (2.3) and (2.61),

$$(\frac{du}{dz})_H = \frac{1}{K_\theta}\left((M)_H - 1 \int_0^H q\, d\lambda\right) \qquad (2.62)$$

where,

(M_H)= moment at z = H, due to the applied loads

$K_\theta = K_{\theta 1} + K_{\theta 2}$

From equations (2.59), (2.60), (2.56), and (2.5), a base boundary condition may be established as,

at z = H,

$$(\frac{d^2Q}{dz^2})_H + (\frac{dQ}{dz})_H (\frac{1}{B}\frac{dB}{dz} + \frac{1}{RK_{v1}} + \frac{1}{RK_{v2}} - \frac{1^2}{RK_\theta})_H = (\frac{1M}{RBK_\theta})_H \qquad (2.63)$$

In terms of the non-dimensional variable η, equation (2.63) becomes,

$$(\frac{d^2Q}{d\eta^2})_H + \bar{\varsigma}(\frac{dQ}{d\eta})_H = K \qquad (2.64)$$

where,

$$\bar{\varsigma} = H\,(\frac{1}{HB}\frac{dB}{d\eta} + \frac{1}{R}(\frac{1}{K_{v1}} + \frac{1}{K_{v2}} - \frac{1^2}{K_\theta}))_H \qquad (2.65)$$

$$K = \left(\frac{1}{RBK_\theta}\frac{M}{H}\right) \qquad (2.65)\ \text{contd.}$$

The rest of the analysis, with the exception of the solution by the Galerkin method, may be carried out as before provided that the base boundary condition (2.65) is employed instead of that given by equation (2.13). For the Galerkin method, a slight modification is required. This is necessary since the boundary condition given by equation (2.65) is not homogeneous; ie. the right hand side of the equation does not vanish. Homogeneous boundary conditions may be obtained by choosing a new function, $F_n(\eta)$, defined by

$$F_n(\eta) = \Omega_n(\eta) - \chi(\eta) \qquad (2.66)$$

as the redundant function for the problem.

By assuming that the function $\chi(\eta)$ has the form,

$$\chi(\eta) = \frac{K}{2(1-\bar{\zeta})}(1-\eta^2) \qquad (2.67)$$

the homogeneous boundary conditions in terms of $F_n(\eta)$ may be shown to be,

$$\left(\frac{dF_n}{d\eta}\right)_{\eta=0} = 0$$

$$(F_n)_{\eta=1} = 0 \qquad (2.68)$$

$$\left(\frac{d^2F_n}{d\eta^2}\right)_{\eta=1} + \bar{\zeta}\left(\frac{dF_n}{d\eta}\right)_{\eta=1} = 0$$

Following the same procedure as before, it may be shown that the approximate solution $F_n(\eta)$ is given by,

$$F_n(\eta) = \sum_{i=3}^{n} \alpha_i (\eta^i + \rho_i \eta^2 + \mu_i) \qquad (2.69)$$

where,

$$\rho_i = \frac{i(1 + \bar{\zeta}) - i^2}{2(1 - \bar{\zeta})} \qquad (2.70)$$

$$\mu_i = \frac{i^2 - i(1 + \bar{\zeta}) - 2(1 - \bar{\zeta})}{2(1 - \bar{\zeta})}$$

The system of simultaneous linear equations for the determination of the unknowns α_i is that given by equation (2.44), but with the following terms added to the left hand side of the equation,

$$\sum_{i=3}^{n} \alpha_i \left[\sum_{j=0}^{m_b} b_j \frac{(i)(i-1)\ K}{2(\bar{\zeta} - 1)} \left(\frac{1}{k+1} + \frac{\rho_k}{3} + \mu_k \right) \right.$$

$$+ \sum_{j=0}^{m_c} c_j \frac{(i)\ K}{2(\bar{\zeta} - 1)} \left(\frac{1}{k+2} + \frac{\rho_k}{4} + \frac{\mu_k}{2} \right)$$

$$\left. + \sum_{j=0}^{m_d} d_j \frac{K}{2(\bar{\zeta} - 1)} \left(- \frac{1}{k+1} - \frac{\rho_k}{3} - \mu_k + \frac{1}{k+3} + \frac{\rho_k}{5} + \frac{\mu_k}{3} \right) \right]$$

After the function $F_n(\eta)$ has been determined, the solution for $Q_n(\eta)$ is obtained from equation (2.66).

Although only the case of coupled walls supported on separate elastic foundations have been considered. The analysis may be readily extended to deal with other types of flexible bases, for instance, coupled walls on

a portal frame hinged to a rigid foundation (cf. section 3.4.2).

2.6 Experimental Investigation

Experimental investigation of plane coupled wall structures of tapered width, relatively simple systems of coupled walls of variable stiffness whose behaviour are described by third-order differential equations with variable coefficients, was undertaken. The purposes were to substantiate the theory,to compare the two proposed methods of solution, and to investigate the effects of the taper of the walls.

2.6.1 Model Coupled Walls

Acrylic perspex was chosen as model material due to ease in machining and availability. Perspex has the advantages of having reasonably linear stress-strain relationship and low value of modulus of elasticity which allows for reasonable large deflection under loads. Its undesirable properties are sensitivity to changes in humidity and temperature, and tendency to creep under loads.

Three perspex models of plane coupled walls were constructed and tested. Each model consisted of two identical plane walls connected by a series of evenly spaced connecting beams of uniform cross-section. Apart from the differences in the slopes of the outer edges of the walls, all the three models were geometrically identical. Model 1 with uniform wall cross-sections,

zero wall slope, was used as the datum. The wall slopes of models 2 and 3 were $^{1}/20$ and $^{2}/15$ respectively. All models were made from the same sheet of perspex, 12.6 mm thick, in order to avoid as far as possible any variation in the properties of model material. The connecting beams and the wall openings were made by cutting away the perspex to form rectangular openings. The connecting beams were 6 mm deep and 36 mm long with 24 mm spacing between the beam axes. The geometry of a typical model was shown in Fig. 2.6. The average width of each wall of each model was equal to 72 mm. Each model was cemented into a slot in a 25.4 mm thick perspex base, using Tensol No. 7 cement.

2.6.2 Test Equipment

The test frame was constructed from 6 in x 6 in steel channel sections welded together to form a three-foot high frame on to which a pair of 6 in x 6 in x 2 ft long I-beams rigidly connected by two strips of steel plate were bolted to form the support for the models. In the experiments, the models were mounted horizontally with the plane of the walls lying in a vertical plane. Fifteen light alloy hangers, from which the dead weights were suspended to simulate lateral load on the model, were connected to the model by means of Terylene cord, Fig. 2.7. Five dial gauges with sensitivity of 0.0001 in per division, supported by a Dexion perforated steel angle attached to the frame, were used for measuring the deflections of the models. In addition, three more dial gauges were used to

detect possible rotation and vertical displacements of the perspex base during loading so that any necessary corrections for the measured wall deflections could be made.

Electrical resistance strain gauges, Japanese type PL 10, were used for measuring the strains in the walls. Twenty electrical strain gauges were attached to each model using Eastman 710 adhesive. Four strain gauges were placed along the mid-third storey level, and eight gauges on each side of the model along the mid-second floor level. All the strain gauges were placed normal to the base to measure the longitudinal strains in the walls. The Baldwin-Lima-Hamilton strain indicator equipment which records the strains directly in microstrains was used. Compensating gauges were incorporated in order to eliminate as far as possible errors resulting from variations in the temperature, humidity etc., during the experiments.

Positions of strain gauges, dial gauges and applied loads were shown in Fig. 2.6.

2.6.3 Test Procedure

The base of the model was fixed to the steel plate of the support by means of 2 in x 1 in hollow steel sections strap bolted across the base in an attempt to eliminate base rotation. The verticality of the plane of the walls was ascertained before the model was loaded in order to prevent any twisting of the model under loads. After the model was securely bolted to the frame and the

dial gauges positioned, the reading of all the gauges were recorded in the no-load position.

The loads were applied in equal increments by means of 200 gm dead weights placed on each hanger. Ten load increments were applied to make the final load per load point reached 2 kgf. The deflections and strains readings were recorded for every load increment. Each model was tested at least twice to check the consistency of the results. A standard time of 5 minutes was allowed to elapse after each load increment before gauge readings were taken, to permit the gauges to settle to reasonably stable values. The sequences of the readings of the gauges for every load increment were kept the same.

2.6.4 Experimental Results

Experimental results were evaluated. The deflections of the models and the strains in the walls per load increment were given in Tables 2.1 and 2.2 respectively.

For the purposes of comparison between experimental and theoretical results, the modulus of elasticity and Poisson's ratio of perspex were determined using perspex specimen cut out from the same sheet of perspex from which the models were made. Using the standard beam test, the modulus of elasticity and Poisson's ratio for the model material were found to be 312.3 kgf/mm^2 and 0.38 respectively.

2.6.5 Theoretical Solutions

For the system of tapered coupled walls with

identical connecting beams, the governing differential equation (2.32) reduces to,

$$BIl\frac{d^3Q}{d\eta^3} + I(2l\frac{dB}{d\eta} - B\frac{dl}{d\eta})\frac{d^2Q}{d\eta^2} - H^2(\frac{I}{H^2}\frac{dB}{d\eta}\frac{dl}{d\eta} + \frac{Il}{R} - \frac{l^3B}{R})\cdot$$

$$\frac{dQ}{d\eta} + (\frac{H^2I}{R}\frac{dl}{d\eta})Q - \frac{H^3l^2}{R}M = 0 \qquad (2.71)$$

where

$$B = \frac{A_1A_2}{A_1+A_2}\ , \qquad I = I_1 + I_2$$

$$R = \frac{b^3h}{12I_r}$$

I_r = reduced second moment of area of connecting beams

From a typical model geometry shown in Fig. 2.19,

$$B = 2t(\eta H + g)\ , \qquad \frac{dB}{d\eta} = 2tH$$

$$I = \frac{t}{6}(\eta H + g) \qquad (2.72)$$

$$l = b + \tan\phi\,(\eta H + g)\ , \ \frac{dl}{d\eta} = H\tan\phi$$

where t is the thickness of the wall, ϕ the slope of the wall width, and g the distance between the top of the wall and the point of extrapolated zero wall width.

Substitution of equation (2.72) into (2.71) leads to an expression of the form,

$$(\sum_{j=0}^{5} a_j\,\eta^j)\frac{d^3Q}{d\eta^3} + (\sum_{j=0}^{4} b_j\,\eta^j)\frac{d^2Q}{d\eta^2} + (\sum_{j=0}^{4} c_j\,\eta^j)\frac{dQ}{d\eta}$$

$$+ \left(\sum_{j=0}^{3} d_j \eta^j\right) Q - \frac{H^3}{R} \left(b + \tan \phi \left(\eta H + g\right)\right)^2 M = 0 \qquad (2.73)$$

Where a_j, b_j, c_j, d_j are geometrical parameters which may be readily evaluated using equations (2.71) and (2.72). The expression for M will depend on the applied load. For the three standard load cases, namely a concentrated load P at the top of the wall, a uniformly distributed load w and a triangularly distributed load $\upsilon(1 - n)$, the expressions for M become, respectively,

$$\begin{aligned} M_p &= P \eta H \\ M_w &= \tfrac{1}{2} w(\eta H)^2 \qquad (2.74) \\ M_\upsilon &= \upsilon(\tfrac{1}{2} \eta^2 H^2 - \tfrac{1}{6} \eta^3 H^2) \end{aligned}$$

The theoretical solutions for the experimental models were obtained using both the Galerkin and the finite difference methods of solutions. Computer programmes for both methods were written in FORTRAN. The programmes were used to determine q, N, M_1, u, extreme fibre strains and the relative vertical displacement of the walls, i.e. $\frac{Q}{E}$.

The Galerkin programme allows up to the fifth-order approximation, or five undetermined constants. In the finite difference programme the number of the intervals may be varied from four to thirty. These variations provide a mean to check the convergence of both methods of solutions (c.f. Figs. 2.8 - 2.10).

The exact solution for uniform wall model was also determined in order to compare with the proposed solutions. It was found that the Galerkin solution with five undetermined constants, and the finite different solution with 30 sub-intervals, were indistinguishable from the exact solution.

2.6.6 Comparison and Discussion of Results

Comparison between the Galerkin and the Finite Difference Methods

The agreement between the solutions by the two methods are excellent. The results obtained from the Galerkin method using five undetermined constants and those from the finite difference method with 30 sub-interval are almost identical. These are the values used for comparing with the experimental results.

In order to investigate the convergence of the proposed solutions, the number of the discrete points and the number of the undetermined constants used in the computer programmes were varied. The solutions for Q/E calculated by both methods, with different numbers of discrete points and undetermined constants, are shown in Figs. 2.8 - 2.10. The solutions by both methods converge rapidly, and little more accuracy could be gained by using more than 8 sub-interval for the finite difference method or more than 3 undetermined constants for the Galerkin method. For uniform wall model, which exact closed form solution exists, the Galerkin method with 5 undetermined constants and the finite difference method

with 30 sub-intervals give virtually identical solutions to the exact solution.

The Galerkin method possesses the advantages of giving the solution in analytical form and, for practical purposes, a third-order approximation will be sufficient. The finite difference method, on the other hand, gives only discrete point solutions and for a comparable accuracy about 8-10 subintervals are needed.

Comparison between Experimental and Theoretical Results

Experimental and theoretical strains in wall 1 of each model, at the levels 57 mm and 33 mm above the base, are shown graphically in Figs. 2.11 and 2.12. The agreements between the experimental and theoretical strains are good, the discrepancies are between 5 and 10 per cent. The differences between the deflections as shown in Fig. 2.13 are, on the other hand, considerable. In all cases the experimental deflections are greater than those predicted by the theory. The differences between the theoretical and experimental deflections at the top of the models are between 20 and 35 per cent.

As the strains predicted by the theory were in good agreement with the experimental results, the disparity of the deflections of the models was rather unreasonably large. It was found that under the applied loads support movements occurred as well as base rotations. For the test frame used, which was relatively flexible, it was very difficult to detect all the movements which had some effects on the measured deflections of the model. A

small and undetected base rotation, as small as $\tan^{-1}$ 1/10000, could result in the measured maximum deflection being twice that predicted by the theory. Creep of perspex, elastic deformation of the perspex base plate, and possible relative rotation of the model unit with respect to the perspex base could also contribute to errors in the measured deflections. Most of these sources of errors have the tendency to produce increasingly larger measured deflections for the points further away from the base. These were exactly the results obtained, as shown in Fig. 2.13.

Comparison between Uniform and Tapered Coupled Walls

The effects on forces and displacement in the coupled walls due to tapering wall widths may be deduced from the theoretical curves shown in Figs. 2.14-2.18. The applied load is taken to be a uniformly distributed load.

From Figs. 2.14 and 2.15 it may be seen that considerable reductions of the vertical shear distribution and the axial forces in the walls are obtained when the walls are tapered. The reduction in the vertical shear distribution is fairly constant throughout the height of the wall except near the base. The location of the maximum vertical shear distribution shifts upwards as the wall slope increases.

Fig. 2.16 shows that as the relative flexural rigidity between the top and the base decreases, i.e. the wall slope increases, a greater bending moment is carried

by the lower part of the wall. The differences between the bending moments carried by the tapered and the uniform coupled walls are not very significant. However, remarkable reductions in the maximum wall stresses at the base are obtained with increasing wall slopes as seen in Fig. 2.17. The maximum wall stresses for the models 2 and 3 are, respectively, only 80 and 60 per cent of that of the uniform coupled walls.

Considerable reductions in the maximum wall deflections are also obtained as a result of increasing wall slopes, Fig. 2.18. The maximum deflections of the models 2 and 3 are only 0.88 and 0.63 of that of the uniform coupled walls.

From the analysis based on the three models, it is evident that considerable reduction in the materials used can be achieved if the walls are tapered instead of uniform.

2.7 Conclusions

A continuous medium analysis of coupled shear walls of variable dimensions has been presented. In the analysis the integral of the relative direct stress, $Q = \int_z^H \left[\left(\frac{1}{A_1} + \frac{1}{A_2} \right) \int_0^{\xi} q \, d\lambda \right] d\xi$, has been used as the redundant function. The behaviour of the coupled wall system is found to be governed by an ordinary third-order differential equation. The differential equation is valid for coupled wall systems of arbitrary geometry provided that the parameters R, B, l, $\frac{dB}{dz}$, defined earlier,

are all differentiable functions of z over the interval $0 \leq z \leq H$.

When the distance between the centroidal axes of the walls is constant throughout the height of the system, the third-order differential equation can be reduced to a second-order equation. The differential equation for a coupled wall system with tapered thickness derived by Michael[22] may be directly obtained from the third-order differential equation derived in this Chapter. The second-order differential equation for uniform coupled wall system, which possesses a closed-form solution, is also one of the simplified forms of the general differential equation.

The coefficients of the differential equation are, in general, variables. The differential equation with variable coefficients does not usually render itself to a straightforward integration solution. Therefore, in most cases, only approximate solutions may be achieved. Two methods of approximation have been proposed, the Galerkin method and the finite difference method. The solutions by both methods converge rapidly and are in good agreement with each other.

The validity of the theory has been confirmed by experiments using perspex models. The theory has been used to investigate the behaviour of coupled walls with tapered widths. From the analysis of the tapered coupled wall systems with the same average wall widths, it may be concluded that the deflection, wall stresses and the axial force in the wall become smaller as the wall slope increases.

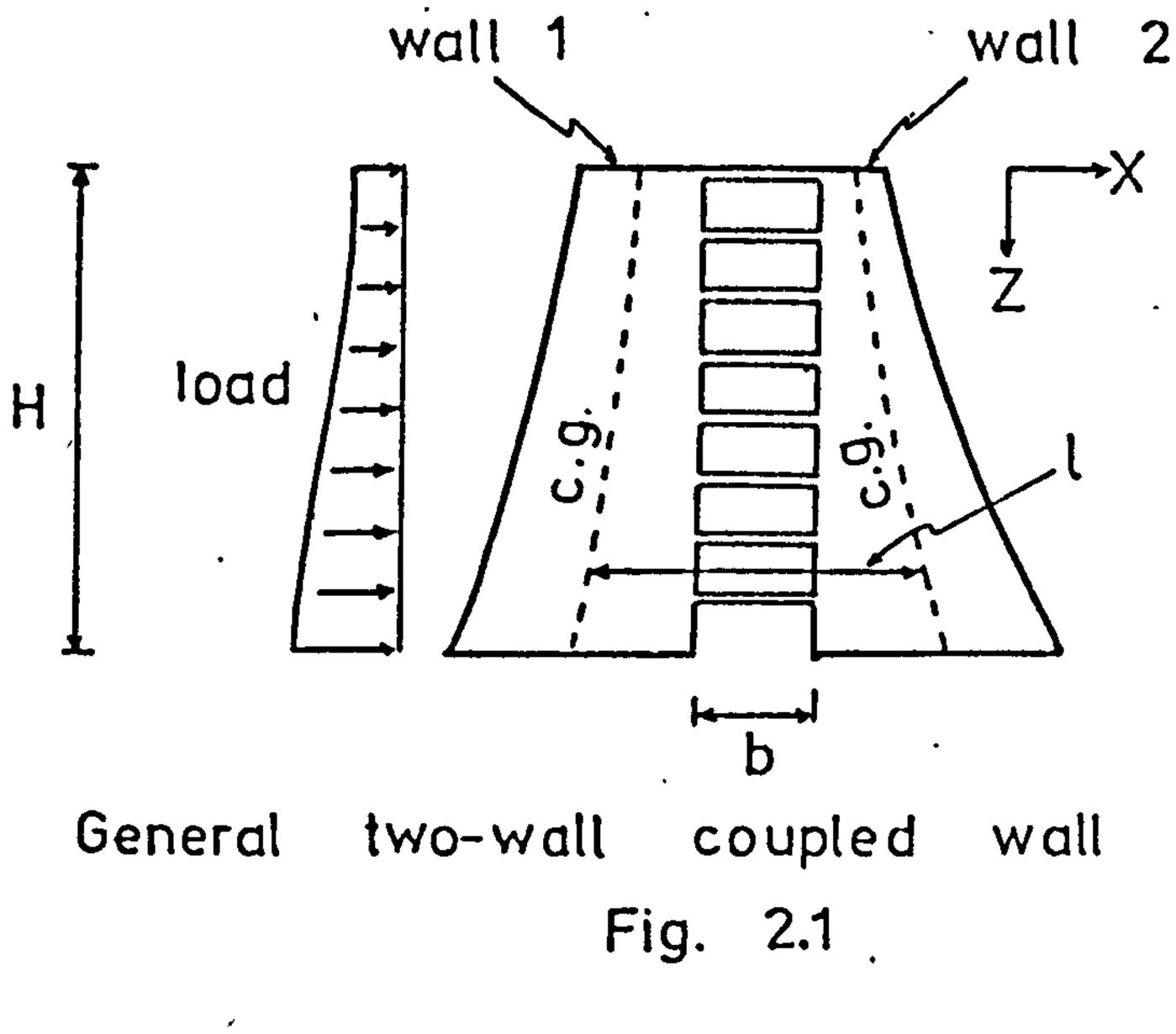

General two-wall coupled wall assembly

Fig. 2.1

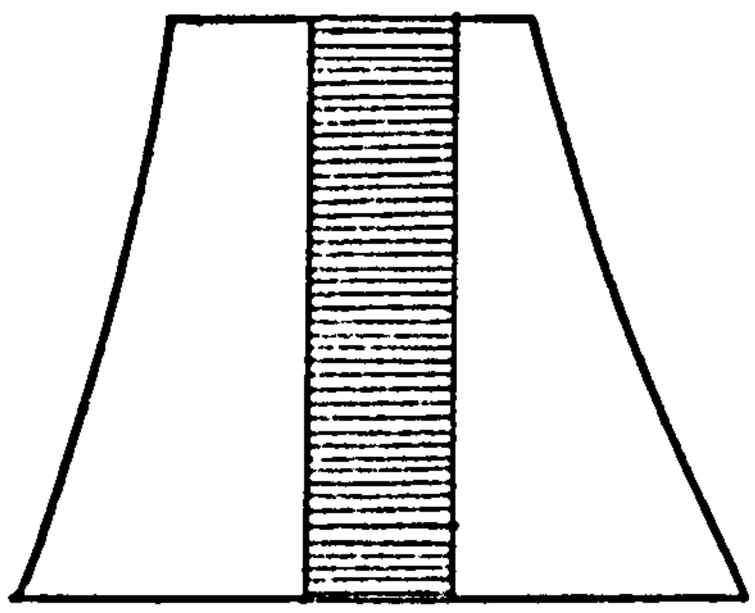

(a) substitute system

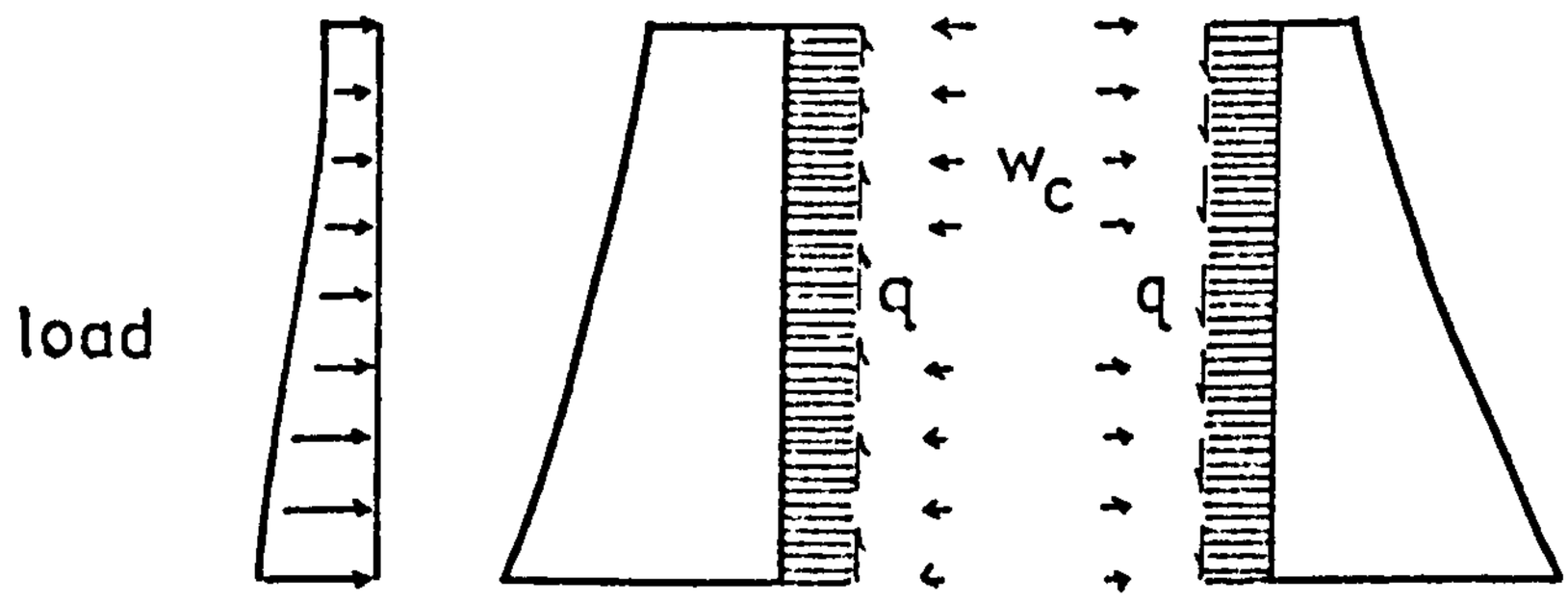

(b) cut-assembly

Equivalent substitute system

Fig. 2.2

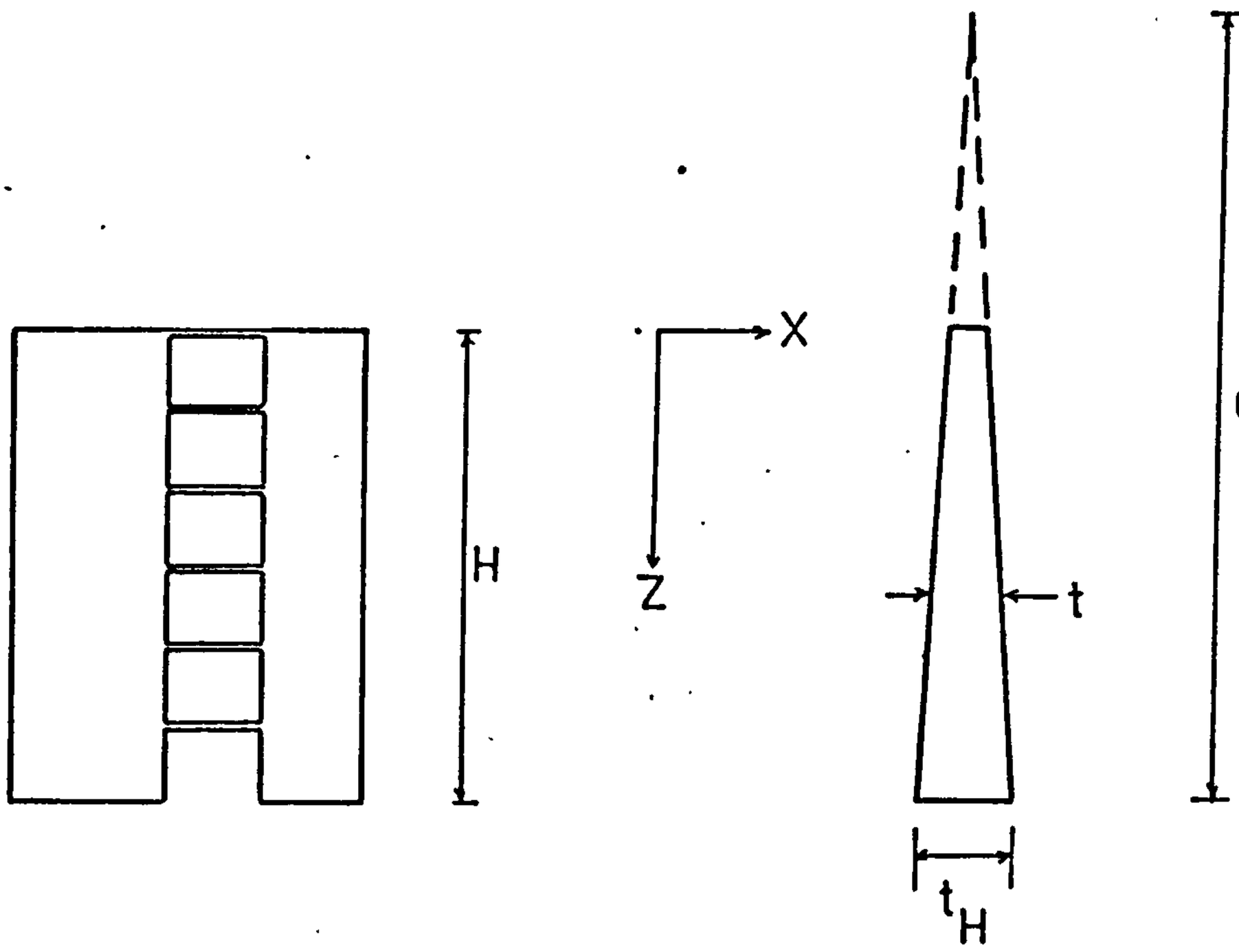

elevation side elevation

Wall with tapered thickness

Fig. 2.3

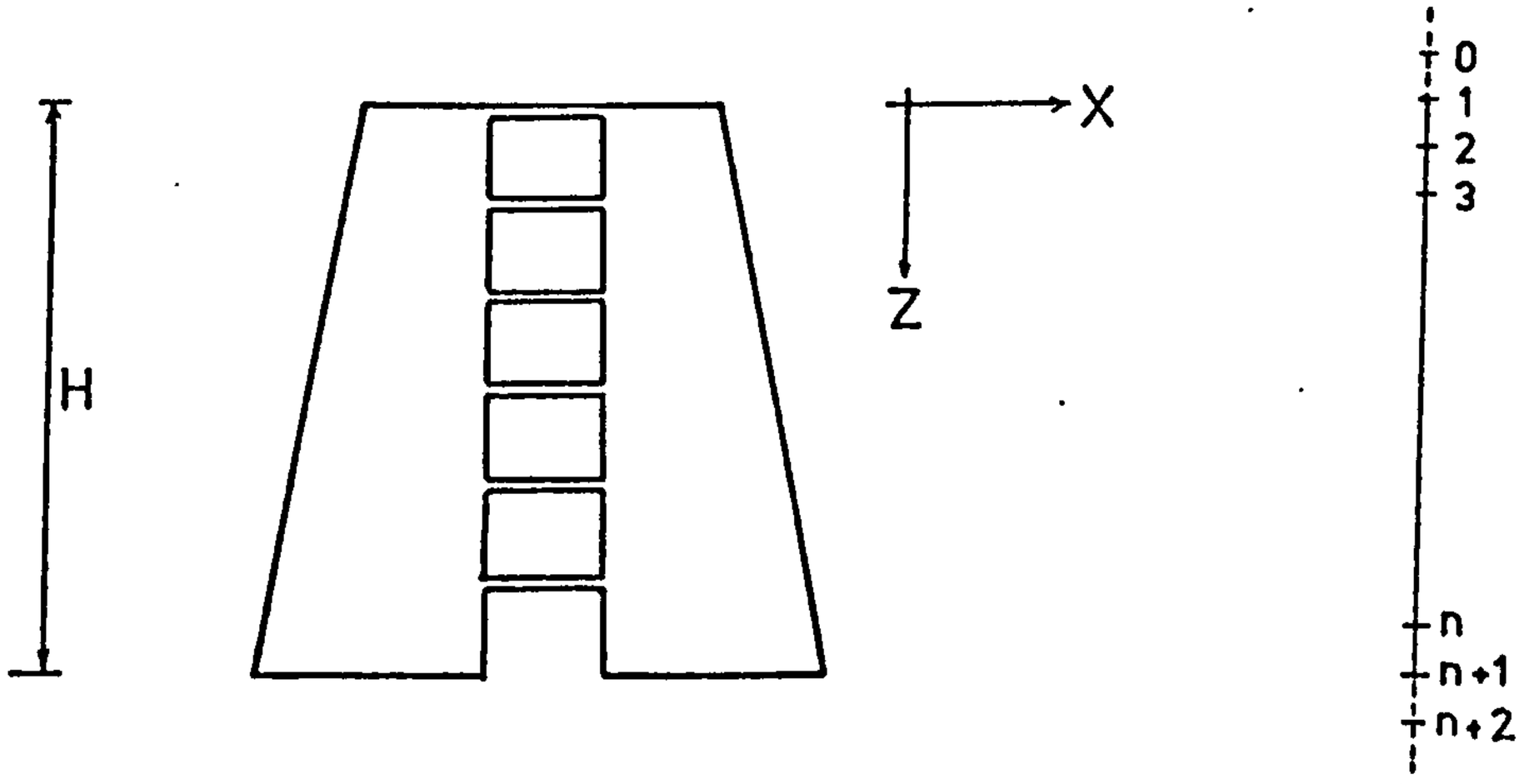

System of reference discrete points

Fig. 2.4

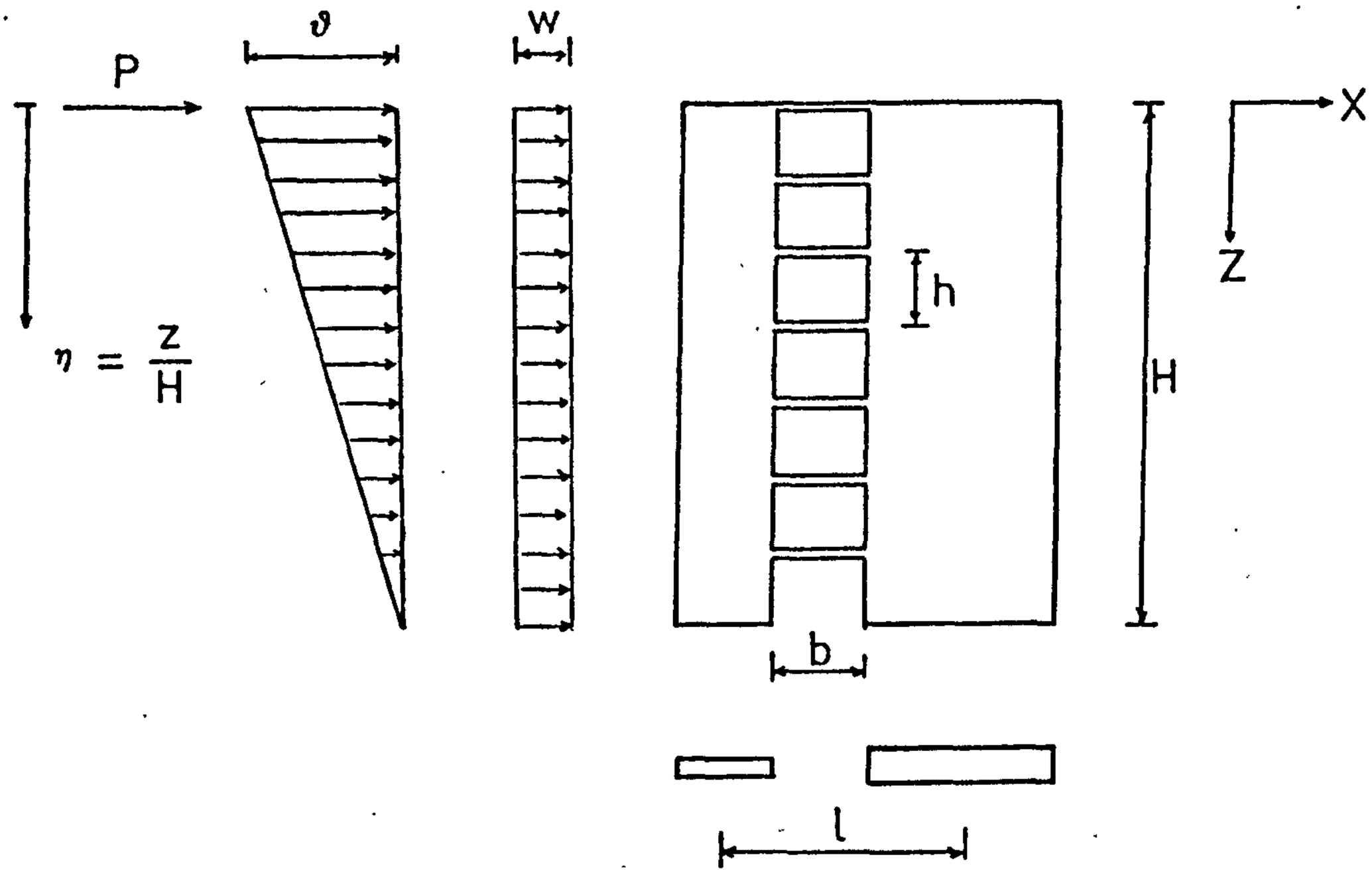

Uniform coupled walls and three standard lateral load cases

Fig. 2.5

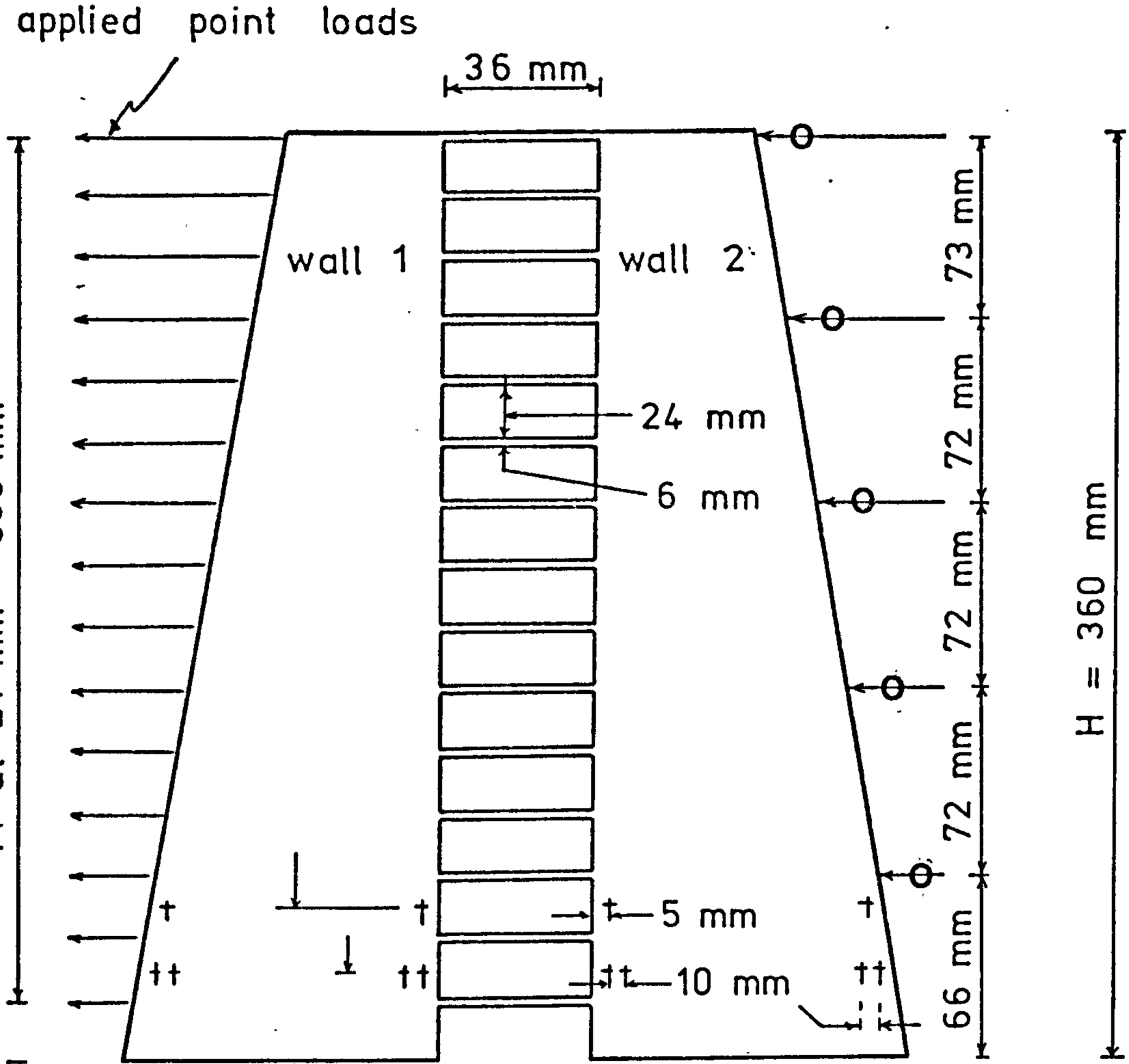

Typical model geometry and positions of gauges and applied loads

Fig. 2.6

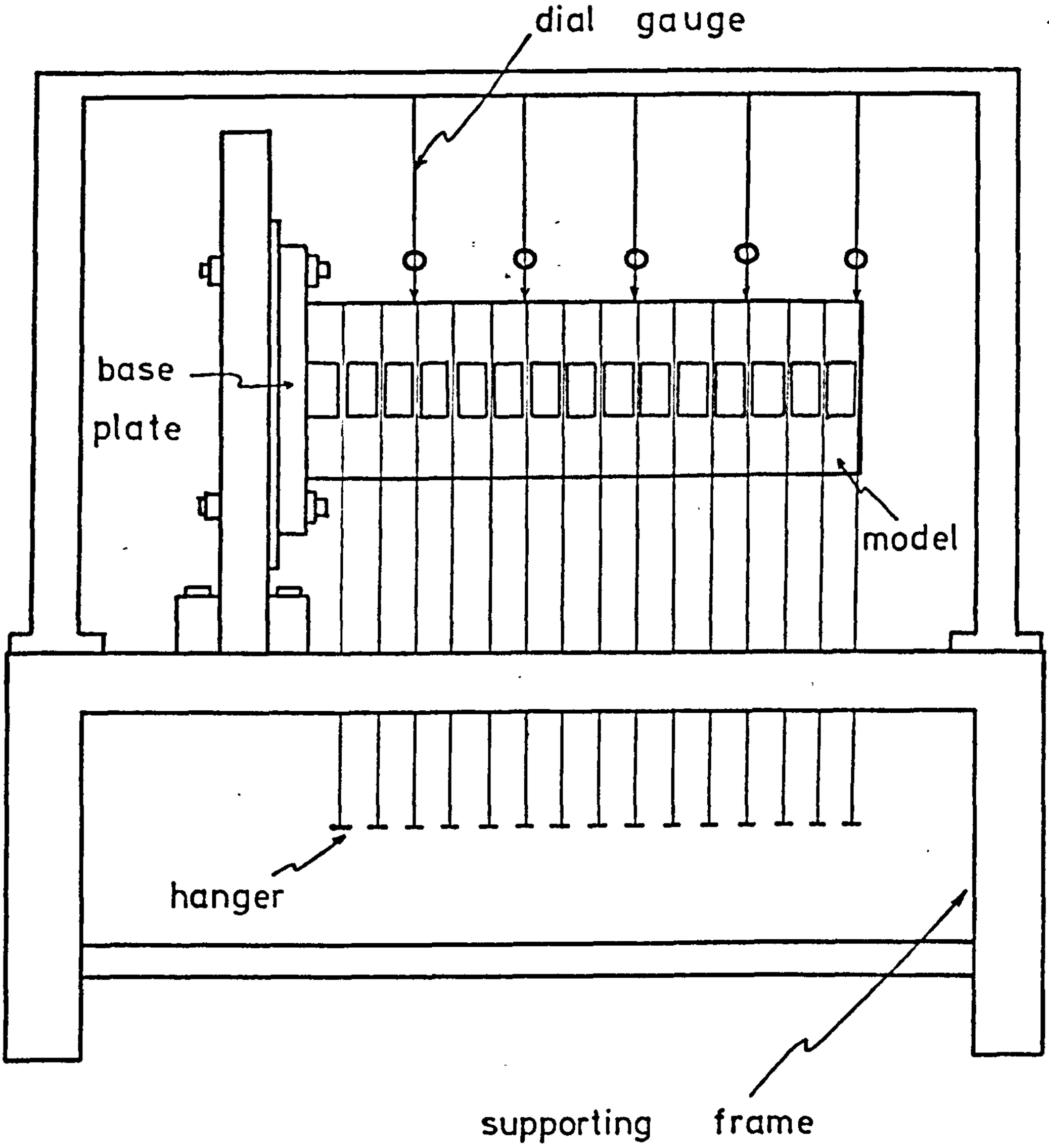

Diagramatic sketch of expeimental set – up

Fig. 2.7

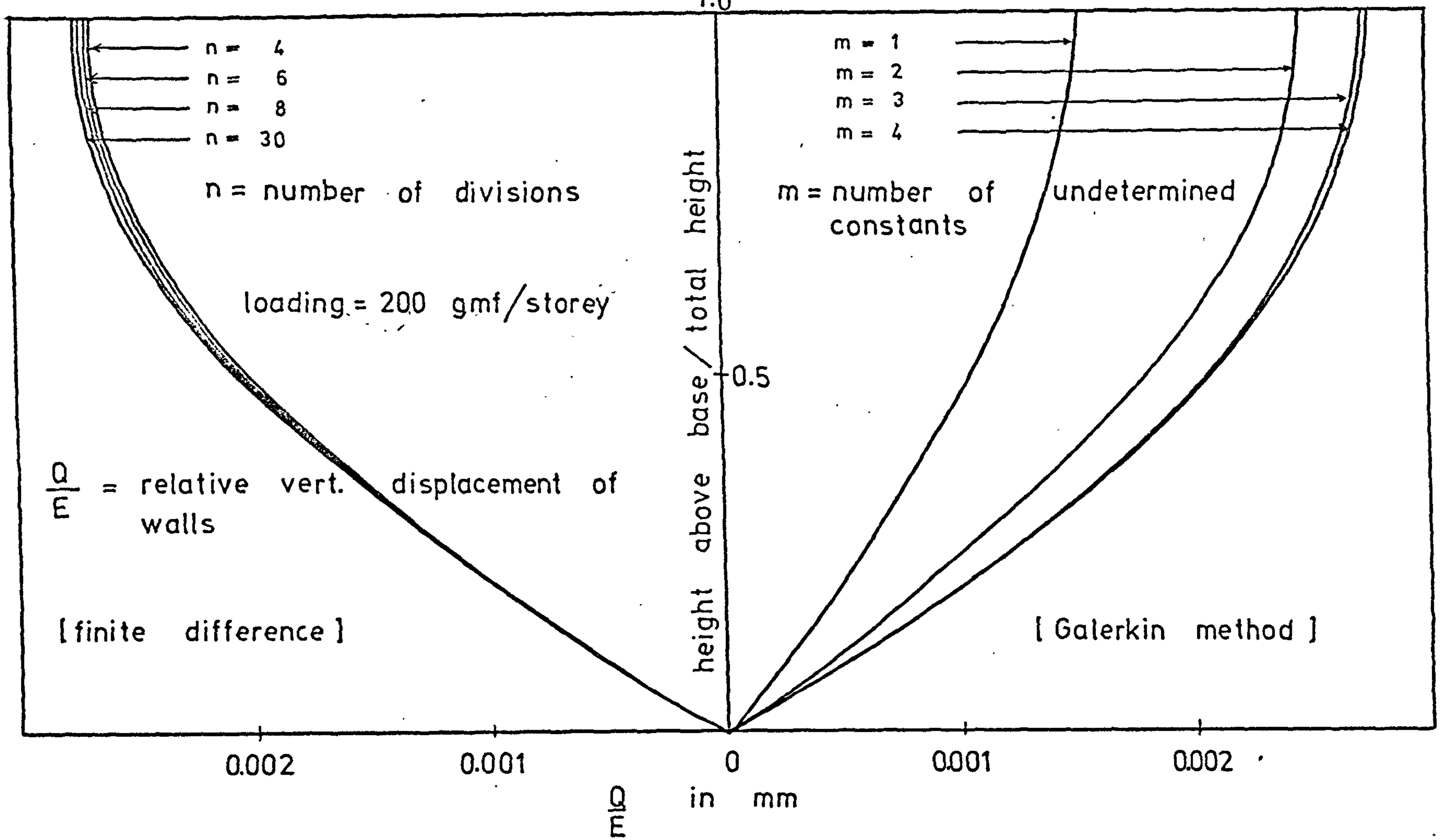

Fig. 2.8 : (Convergence of solutions for model 1)

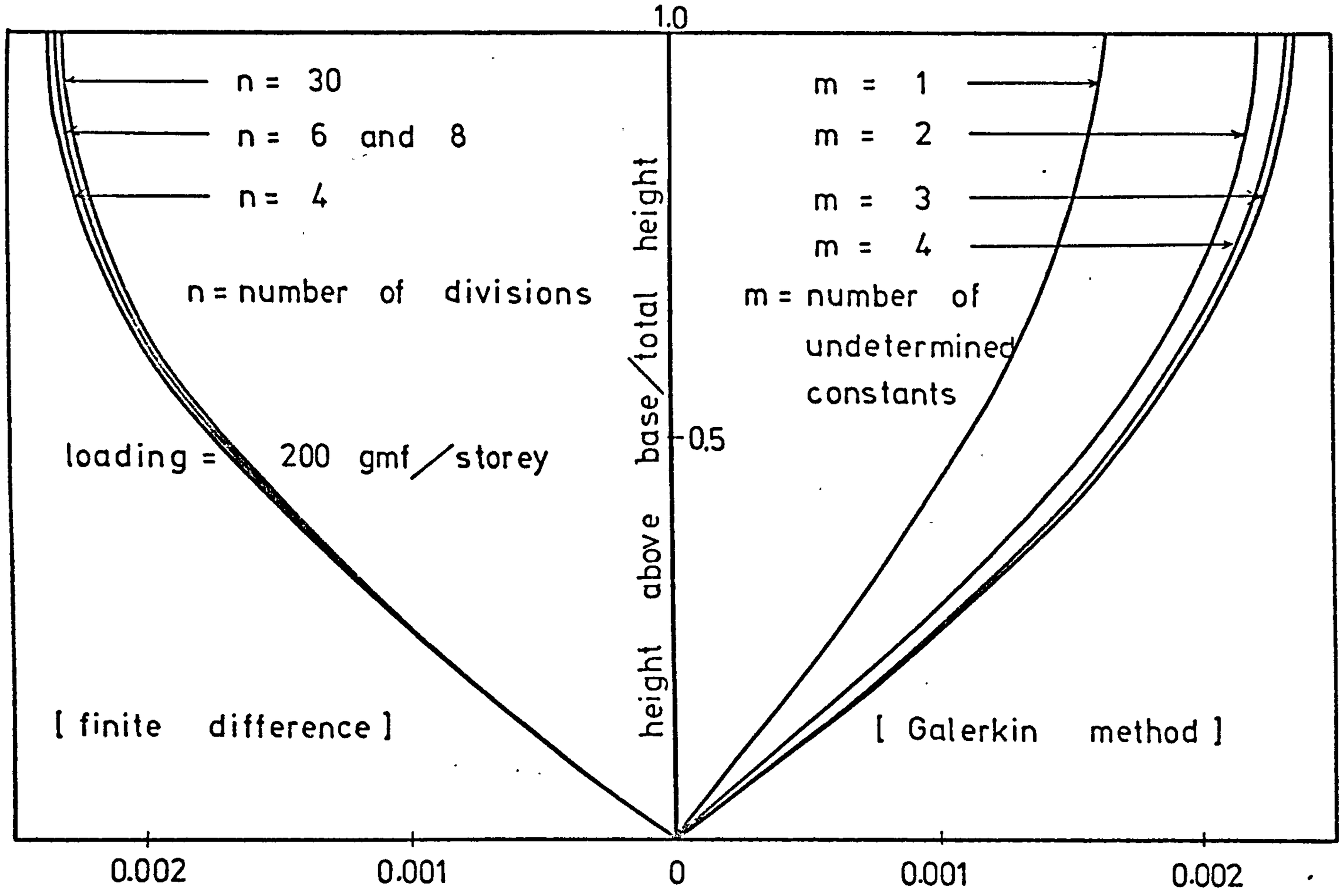

Fig. 2.9 : (Convergence of solutions for model 2)

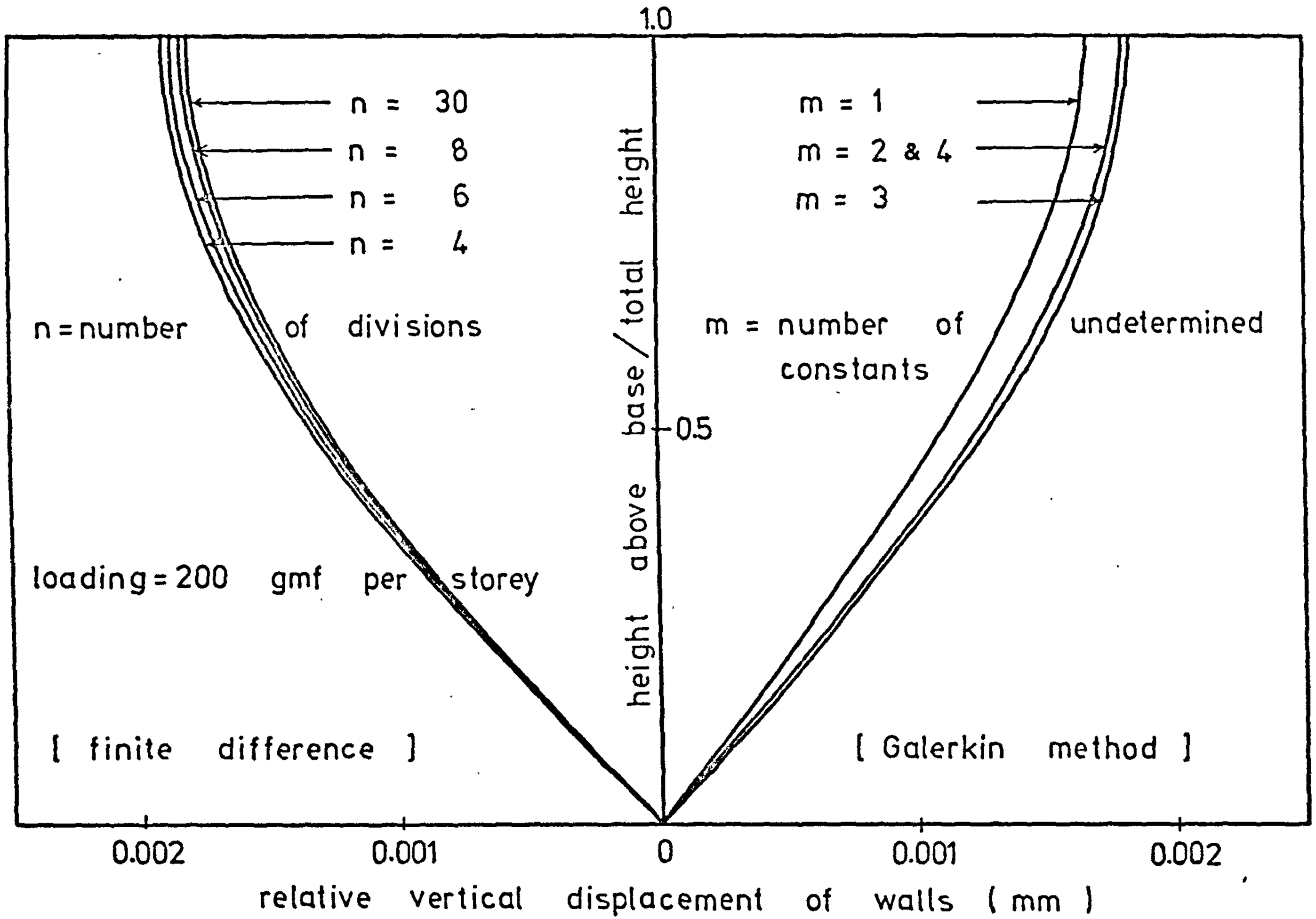

Fig. 2.10 : (Convergence of solutions for model 3)

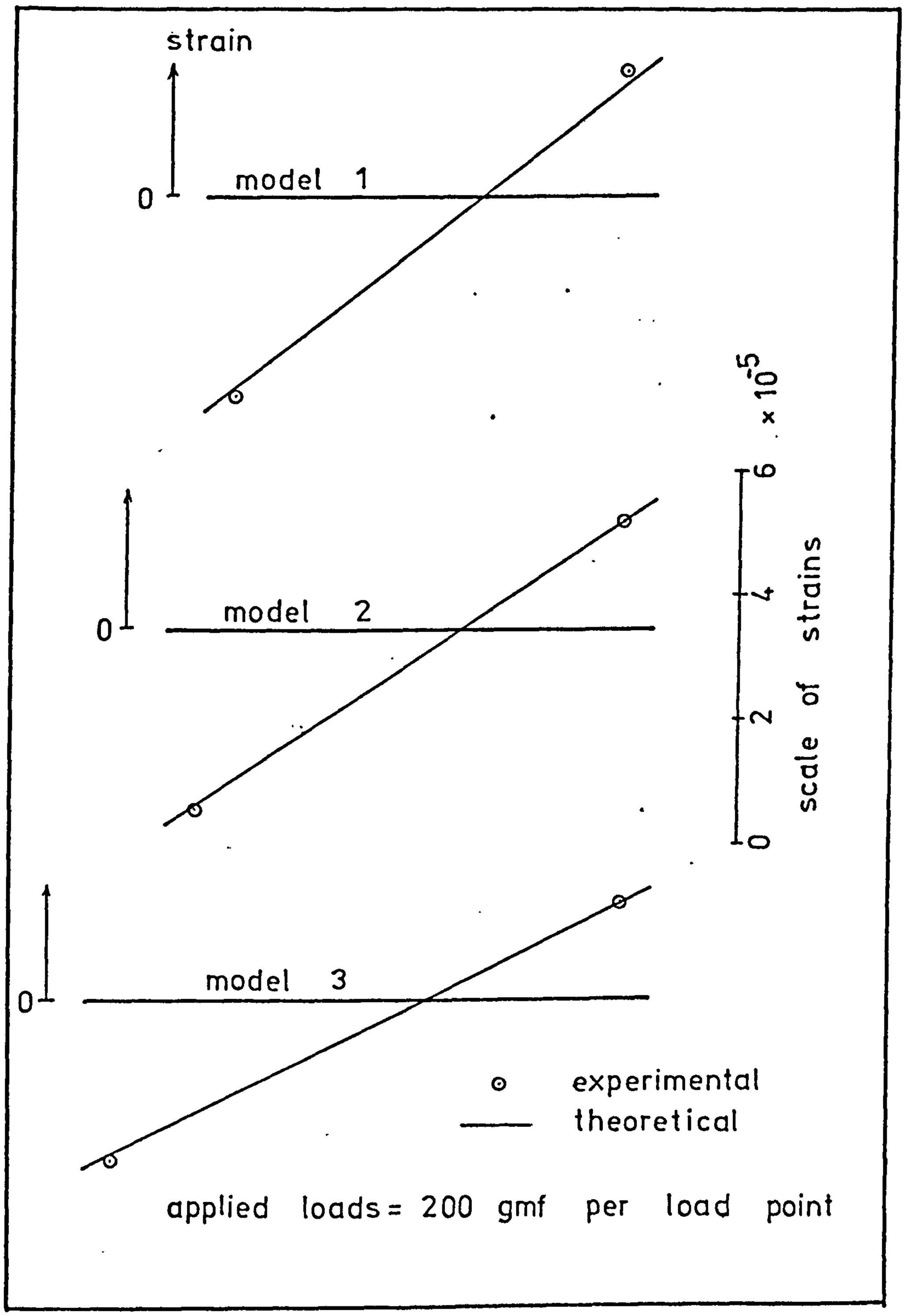

Strain distribution at 57 mm above base (wall 1)

Fig. 2.11

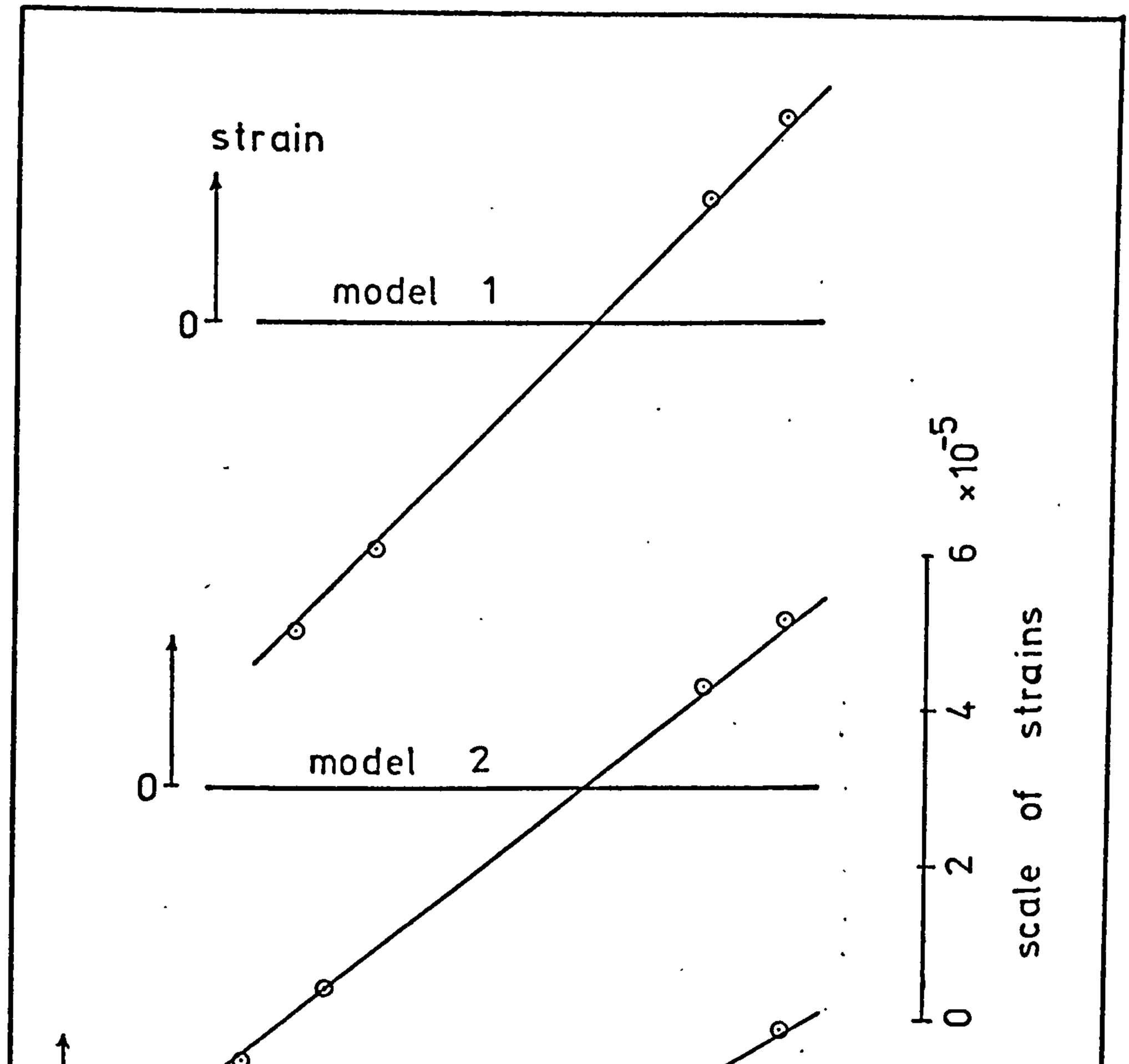

Strain distribution at 33 mm above base (wall 1)

Fig. 2.12

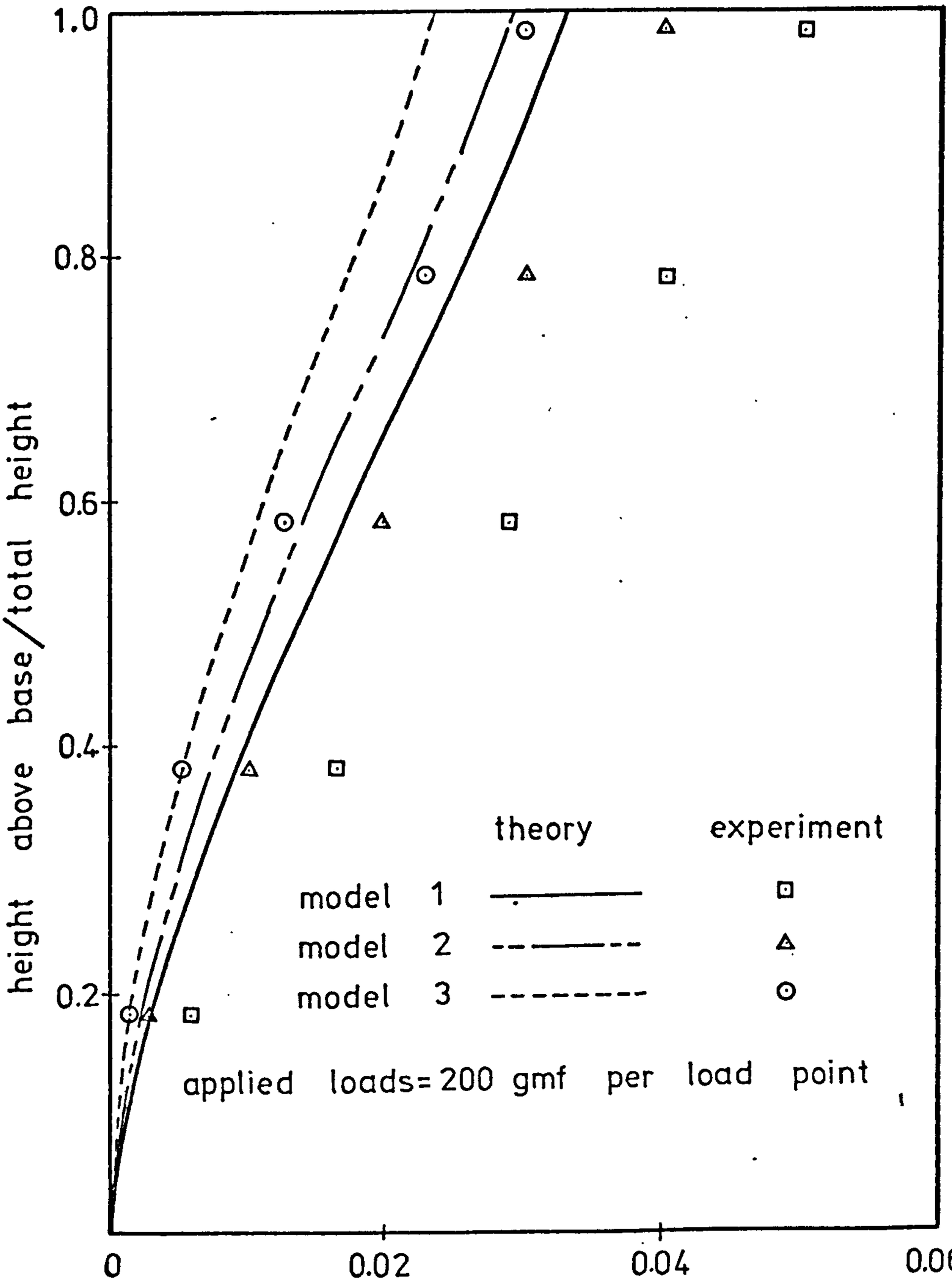

Deflection of model

Fig. 2.13

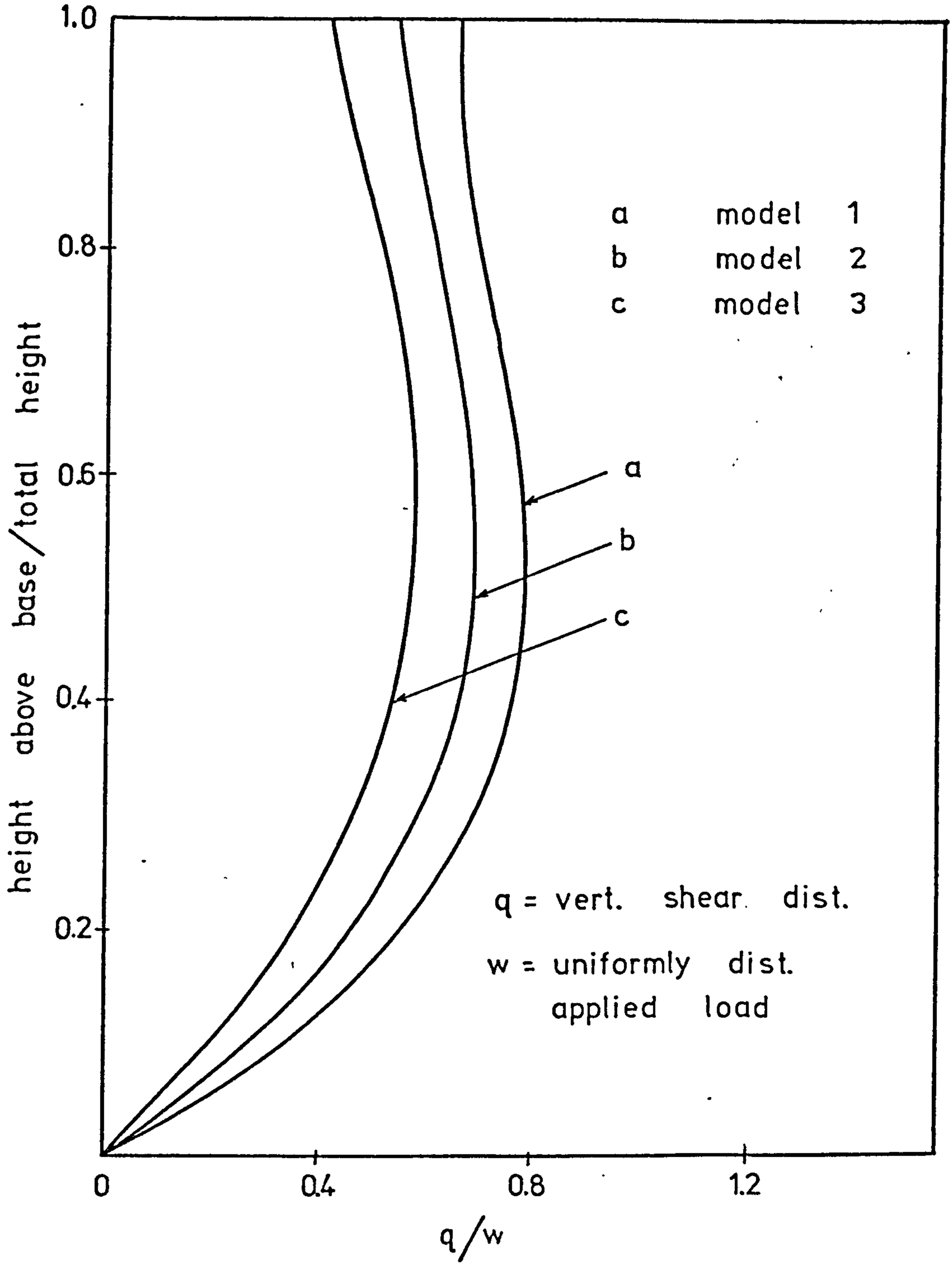

Vert. shear dist./uniformly dist. applied load

Fig. 2.14

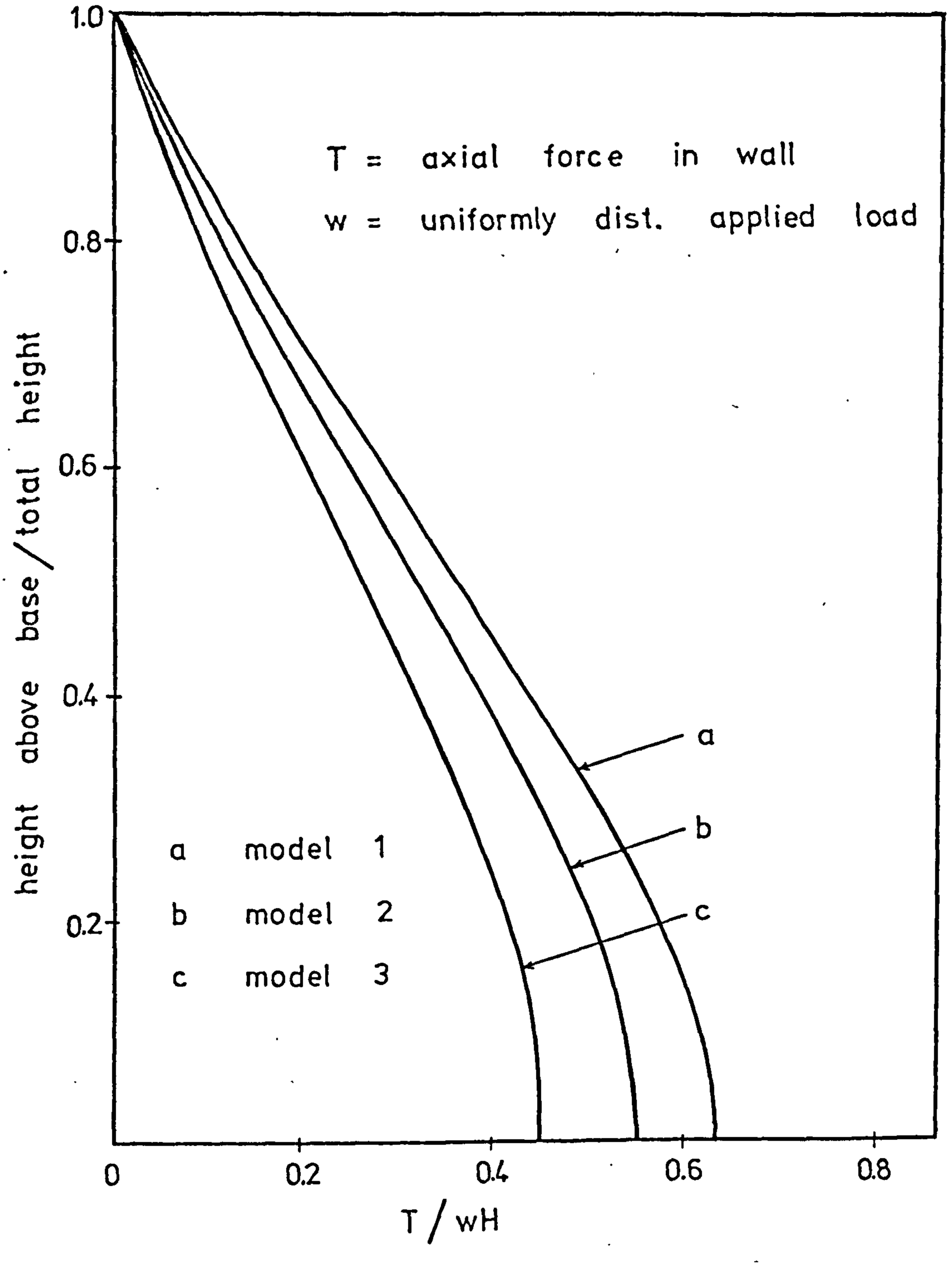
T = axial force in wall
w = uniformly dist. applied load
a model 1
b model 2
c model 3
a
b
c
1.0
0.8
0.6
0.4
0.2
0
0.2
0.4
0.6
0.8
height above base / total height
T / wH
Wall axial force / total lateral load

Fig. 2.15

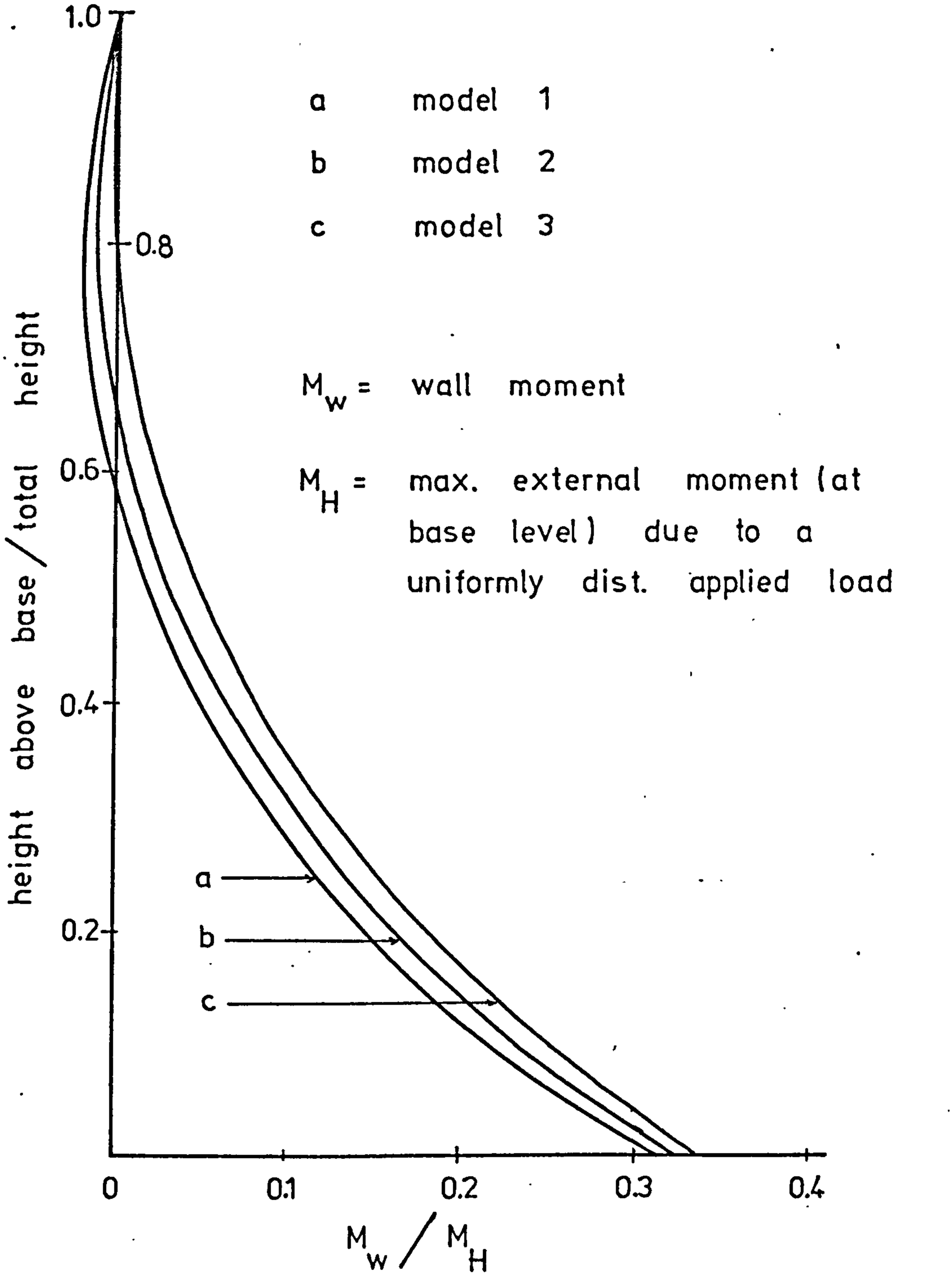
1.0
0.8
0.6
0.4
0.2
0
0.1
0.2
0.3
0.4
height above base / total height
a
b
c
a model 1
b model 2
c model 3
M_w = wall moment
M_H = max. external moment (at base level) due to a uniformly dist. applied load
M_w / M_H
Wall moment / maximum external moment

Fig. 2.16

a model 1

b model 2

c model 3

ϵ_o = strain at outer edge

ϵ_i = strain at inner edge

loading = 1 gmf/mm

(tensile axial force in wall 2)

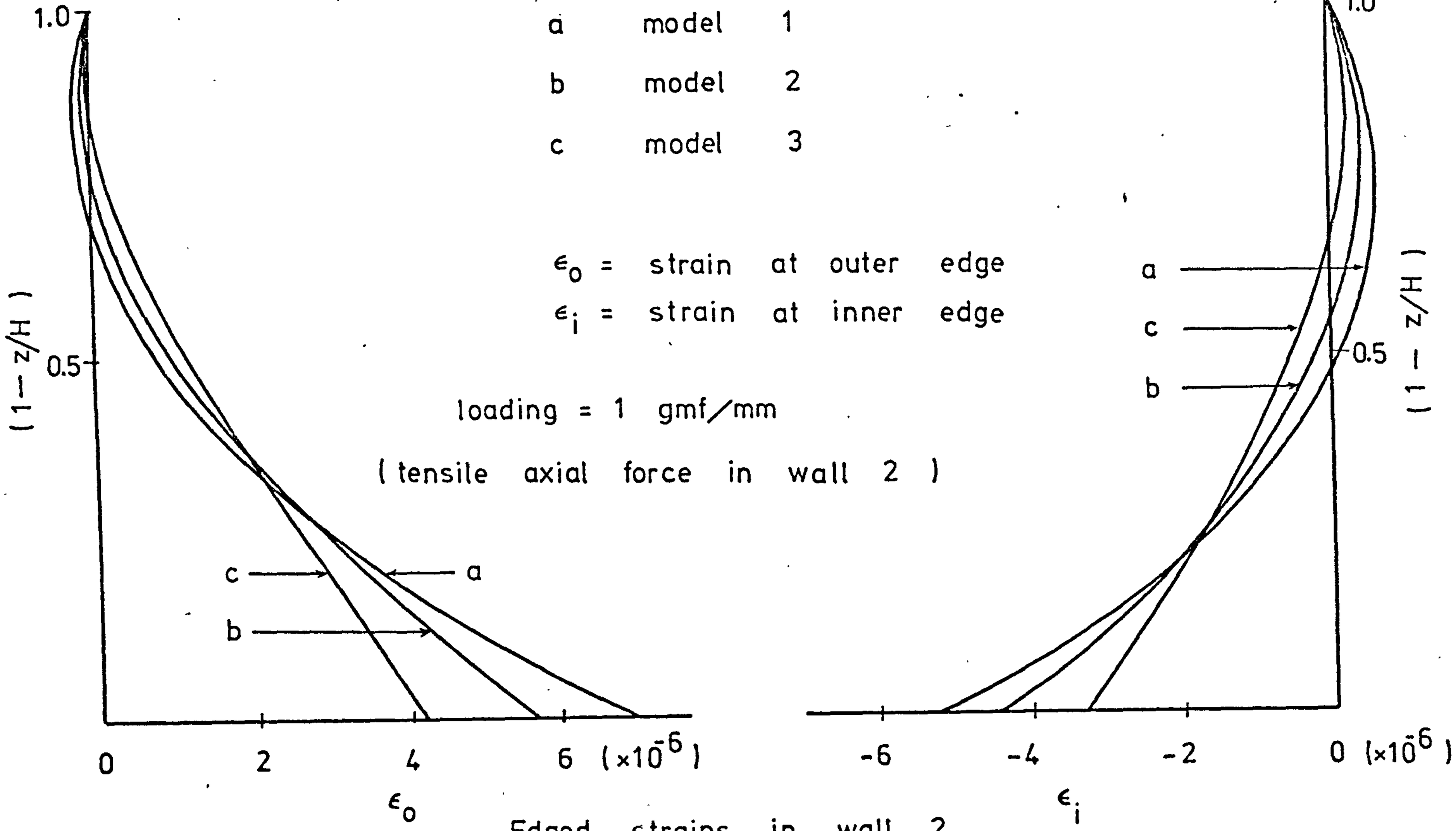

Edged strains in wall 2

Fig. 2.17

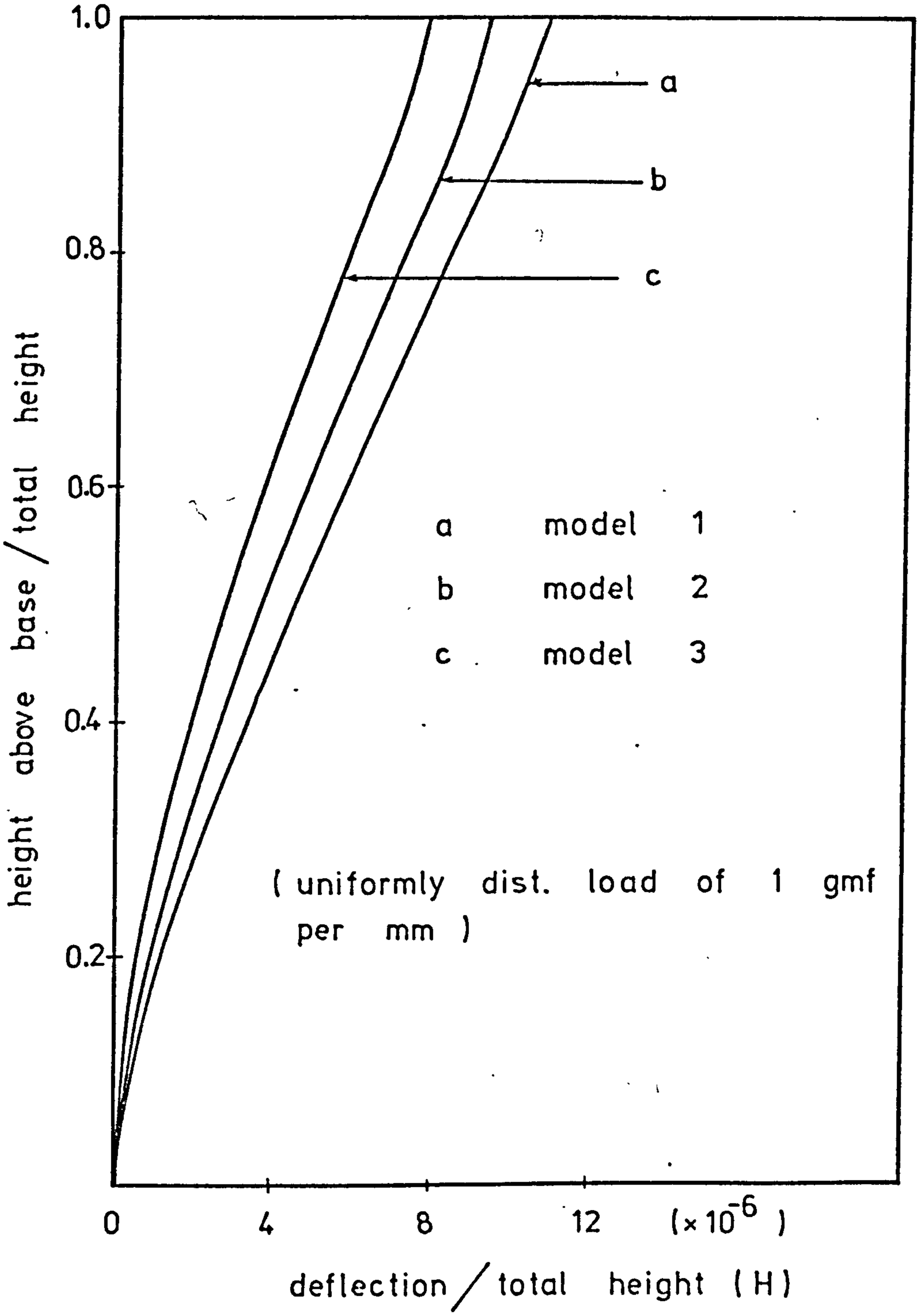
1.0
0.8
0.6
0.4
0.2
height above base / total height
a
b
c
a model 1
b model 2
c model 3
(uniformly dist. load of 1 gmf per mm)
0
4
8
12
(×10⁻⁶)
deflection / total height (H)
Wall deflection / wall height

Fig. 2.18

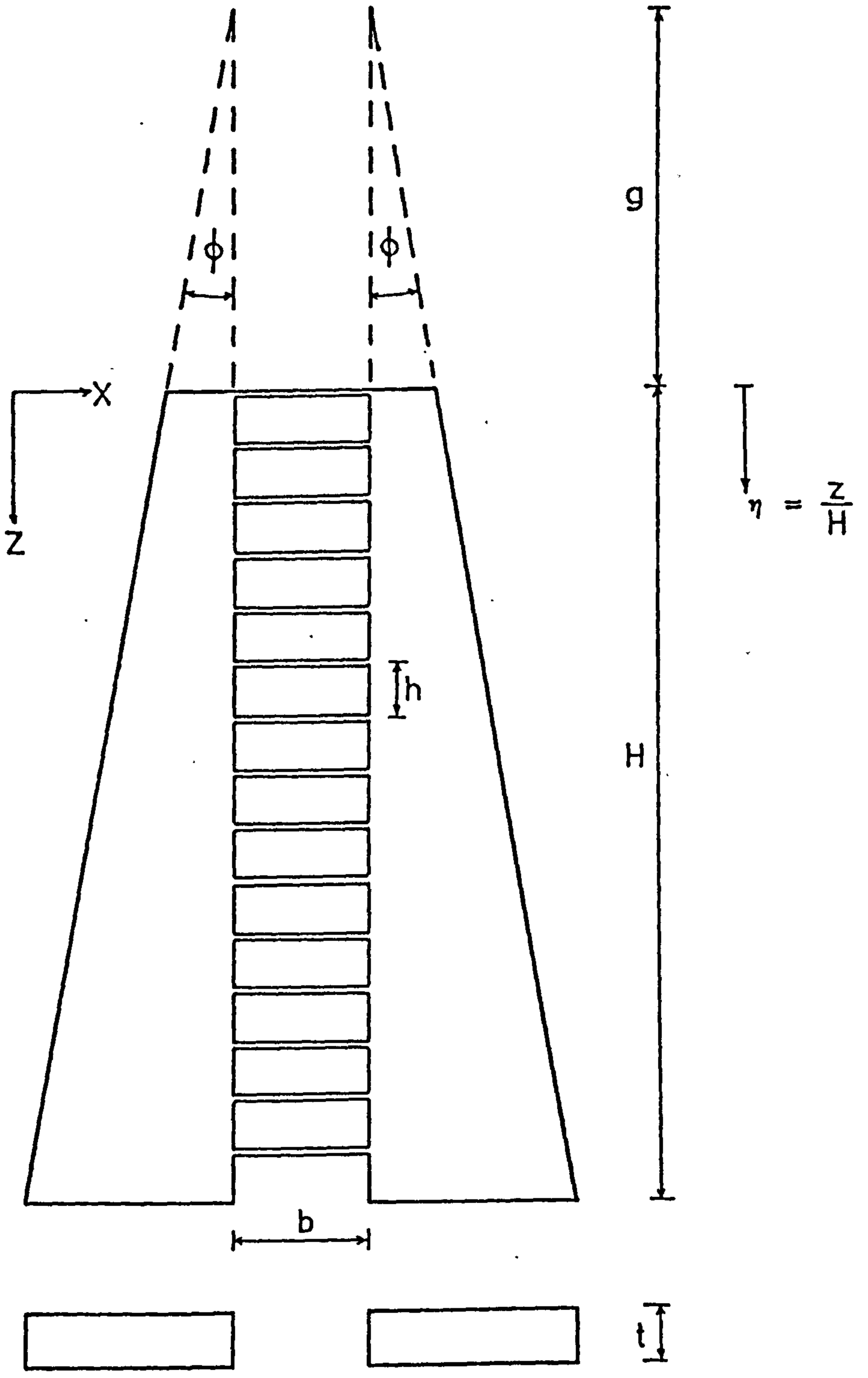

Typical model geometry

Fig. 2.19

Height above base mm	Deflection in mm		
	Model 1	Model 2	Model 3
66	0.0127	0.0089	0.0064
138	0.0279	0.0216	0.0165
210	0.0457	0.0356	0.0292
282	0.0610	0.0546	0.0432
355	0.0762	0.0660	0.0559

Deflections of Coupled Wall Models Due to Loading of 200 gmf per storey

Table 2.1

Height above base mm	Wall	Distance from edge (inner or outer) mm	Strain μ in/in		
			Model 1	Model 2	Model 3
33	1	5 (inner)	26	22.5	18.5
		10 (inner)	16	14	13.5
		5 (outer)	-40	-35	-28.5
		10 (outer)	-30	-26	-22
	2	5 (inner)	-26	-23	-20
		10 (inner)	-15.5	-14	-14
		5 (outer)	40	34	29.5
		10 (outer)	30.5	27.5	23
57	1	5 (inner)	20	17.5	15.5
		5 (outer)	-32.5	-28.5	-26
	2	5 (inner)	-19.5	-18	-17
		5 (outer)	31.5	28	25.5

Strains in Coupled Wall Models Due to Loading of 200 gmf per Storey.

Table 2.2

CHAPTER 3

DESIGN CURVES FOR COUPLED SHEAR WALLS ON FLEXIBLE BASES SUBJECTED TO VERTICAL AND LATERAL LOADS

3.1 Notation

The following symbols are used in this Chapter.

A_1, A_2 = cross-sectional areas of walls 1 and 2

l = distance between the centroids of walls 1 and 2

b = length of connecting beams

I_c = second moment of area of connecting beams

I_0 = second moment of area of the beam of portal frame

I_1, I_2 = second moments of area of walls 1 and 2

h = storey height

h_0 = height of supporting portal frame

H = total wall height

E = modulus of elasticity

K_{v1}, K_{v2} = vertical stiffnesses of elastic foundations under walls 1 and 2

$K_{\theta 1}$, $K_{\theta 2}$ = rotational stiffnesses of elastic foundations under walls 1 and 2

L = distance between bases of columns of portal frame

q = vertical shear distribution in the continuous medium

z = height above base of wall

u = horizontal deflection

η = non-dimensional height co-ordinate, z/H

u_H = deflection at the top

T = integral shear force = $\int_z^H q \, d\lambda$

λ , ξ = auxiliary height co-ordinates

σ = stress in wall

Other subsidiary symbols are defined locally in the text.

3.2 Introduction

In the analysis of uniform coupled walls by the continuous medium approach, the behaviour of the structure has been shown to be governed by a second-order differential equation with constant coefficients. As a closed form solution may be obtained, simple design curves for the determination of forces and displacements may be produced.

Based on this technique, a simple design method was presented[9,10]. The method enables the analysis of a pair of coupled walls or symmetrical three wall system with two bands of connecting beams to be carried out very rapidly. Its simplicity has found favour in design offices and has also been utilised in a design booklet[23]. Curves were produced for three standard lateral load cases, namely, a uniformly distributed load, a triangularly distributed load, and a point load at the top. The latter two cases may be used for seismic design calculations, whilst the superposition of the first two yields a general trapezoidal load distribution. Formulae which allow

similar design curves to be plotted for any load forms which can be described by a polynomial in the height co-ordinate were also presented[7]. All the theories and curves, however, referred to the particular case of walls rigidly built in at foundation level.

Many other base conditions occur in practice. For example, shear walls are often discontinued at the first floor level to provide an open concourse, lobby or other non-uniform structure on the ground floor. In this case the continuous medium analysis may again be used, provided the base is taken at first floor level and the lower boundary conditions are altered to include the load-deformation characteristics of the supporting structure. In other cases, the walls may be supported on independent foundations which yield vertically and rotationally under the actions of wall axial forces and bending moments, respectively.

Although the earlier technique could be used to provide design curves for such situations, a very large number of curves would be needed to describe the behaviour of the structure in view of the large number of parameters required to describe the range of base conditions which might occur in practice. For instance, in the case of flexible foundations a complete set of design curves would be required for each combination of vertical and rotational stiffnesses of each footing. The large number of curves required makes the technique impractical for other than rigid foundation conditions.

A new simple technique which overcomes the disadvan-

tages of the earlier method, and enables a single set of curves to be used for any base condition has been developed. A set of curves is generally required for each standard load case.

A general treatment of uniform coupled walls on flexible bases, and subjected to lateral and vertical loads is presented in this chapter. Four standard lateral load cases, three standard vertical load cases and a special case of concentrated moments at the top are considered. These are, respectively, a concentrated lateral load at the top, a uniformly distributed lateral load per unit height, a triangularly distributed lateral load per unit height, a polynomially distributed lateral load per unit height, concentrated vertical loads at the top passing through the centroids of the walls, uniformly distributed vertical loads per unit height, triangularly distributed vertical load per unit height, and finally, concentrated moments at the top proportional to the second moments of area of the walls. Four sets of design curves, covering all but one of the standard load cases, are produced. A general polynomially distributed lateral load is the standard load case left out, but formulae are given to allow similar design curves to be plotted for a particular power series. Design examples are also given to illustrate the application of the method. A part of the new technique developed, dealing only with lateral load cases, has recently been published as a paper[8].

3.3 General Theory

As the basic continuous medium theory of coupled shear walls has been fully treated in the previous Chapter, only the fundamental assumptions and equations are restated here.

Consider a system of two uniform coupled shear walls subjected to lateral and vertical loadings as shown in Fig. 3.1. The fundamental assumptions of the technique are

1. axial deformations of the connecting beams are considered negligible so that both walls deflect equally; the connecting beams then deform with points of contraflexure at their mid-span positions.
2. the discrete connecting beams, each with second moment of area I_c, may be replaced by a uniform continuous medium of equivalent stiffness EI_c/h per unit height (E and h are modulus of elasticity and storey height respectively); the set of discrete shear forces in the connecting beams may then be replaced by a corresponding continuous vertical shear distribution of intensity q per unit height.

If the substitute medium is 'cut' along the line of points of contraflexure (at mid-span positions), then, under the action of the applied loads and the internal shear and axial forces, no relative movement occurs at the cut. The compatibility equation at any height z may be shown to be

$$1\ \frac{du}{dz} - \left(\frac{b^3 h}{12EI_c}\right)q - \left[\frac{1}{E}\left(\frac{1}{A_1} + \frac{1}{A_2}\right)\int_0^z \int_\xi^H q\ d\lambda\ d\xi\right.$$

$$- \frac{1}{EA_1} \int_0^z \int_\xi^H V_1 \, d\lambda \, d\xi + \frac{1}{EA_2} \int_0^z \left(\int_\xi^H V_2 \, d\lambda \, d\xi \right] \right]$$

$$+ \left[\frac{1}{EA_1} \int_0^z p_1 H \, d\lambda - \frac{1}{EA_2} \int_0^z p_2 H \, d\lambda \right] + \delta = 0 \qquad (3.1)$$

Where the five terms represent the relative vertical displacements at the cut ends due to, respectively, the slope of the walls, the cantilever bending action of the cut lamina, the axial deformations of the walls resulting from the distributed vertical load and the concentrated vertical load at the top, and the movements of the bases.

H = total wall height

l = distance between the centroidal axes of walls 1 and 2

A_1, A_2 = cross-sectional areas of walls 1 and 2

u = lateral deflection

z = height above base of walls

λ , ξ = auxiliary height co-ordinates

V_1, V_2 = intensity (per unit height) of the distributed vertical loads acting on walls 1 and 2

p_1H, p_2H = concentrated vertical loads passing through the centroidal axes of walls 1 and 2 respectively

b = length of connecting beams

From the moment-curvature relationships, the total internal bending moment for the coupled wall system may be written as,

$$M_t = EI \frac{d^2u}{dz^2} = M - 1T \qquad (3.2)$$

where,

M_t = sum of moments in walls 1 and 2

$= M_1 + M_2$

I = sum of second moments of area of walls 1 and 2

$= I_1 + I_2$

M = moment due to applied loads

$= M_v + M_l$

M_l = moment resulting from lateral loads

$$= \int_z^H p'(\lambda)(\lambda - z)\, d\lambda + p_0 H\,(H - z)$$

$p'(\lambda)$ = intensity of distributed lateral load

$p_0 H$ = concentrated lateral load at the top

M_v = moment due to distributed vertical loads

$$= \int_z^H V_1\, e_1\, d\lambda - \int_z^H V_2\, e_2\, d\lambda$$

e_1, e_2= eccentricities of distributed vertical loads V_1 and V_2 with respect to the centroidal axes of walls 1 and 2, respectively; positive if it lies between the centroidal axes of the walls

T = integral shear force $= \int_Z^H q\, d\lambda$

As both walls deflect equally the curvatures are equal, and the moment carried by each wall is proportional to its second moment of area. Therefore, the bending moments in walls 1 and 2 are, respectively,

$$M_1 = \frac{I_1}{I} M_t$$

$$M_2 = \frac{I_2}{I} M_t \qquad (3.3)$$

On differentiating equation (3.1) with respect to z, substituting for $\frac{d^2u}{dz^2}$ from equation (3.2), and them differentiating again, the governing differential equation may be written as,

$$\frac{d^2q}{dz^2} - \alpha^2 q = \beta^2 \left(\frac{dM}{dz} - \frac{I}{I} \frac{d\psi}{dz}\right) \qquad (3.4)$$

where,

$$\beta^2 = \frac{12 I_c l}{b^3 h I}$$

$$\alpha^2 = \beta^2 \, l \mu \qquad (3.5)$$

$$\mu = 1 + \frac{I}{l^2} \left(\frac{1}{A_1} + \frac{1}{A_2}\right)$$

$$\psi = \frac{1}{A_2} \left(p_2 H + \int_z^H V_2 d\lambda\right) - \frac{1}{A_1} \left(p_1 H + \int_z^H V_1 \, d\lambda\right) \qquad (3.6)$$

The general solution of equation (3.4) is

$$q = B_1 \cosh \alpha z + B_2 \sinh \alpha z + q_p \qquad (3.7)$$

where B_1 and B_2 are constants of integration which must be evaluated from the known boundary conditions at the top and the base, and q_p is the particular integral part of the solution which depends only on the form of the

applied loading.

If the walls are free at the top as is usually the case, there is no bending moment in the substitute system at the top and the curvature, $\frac{d^2u}{dz^2}$, there must be zero. By differentiating equation (3.1) with respect to z, then evaluating at $z = H$, the top boundary condition in terms of the vertical shear distribution q becomes,

$$\text{at } z = H, \quad \left(\frac{dq}{dz}\right)_H = \beta^2 \frac{I}{I} \left(\psi\right)_H \tag{3.8}$$

$$\text{where} \quad \left(\psi\right)_H = H\left(\frac{p_1}{A_1} - \frac{p_2}{A_2}\right) \tag{3.9}$$

From equations (3.7) and (3.8), the coefficient B_2 may be eliminated and the general solution for q becomes, for the coupled wall system which is free at the top,

$$q = B_1 \frac{\cosh\gamma(1-\eta)}{\cosh\gamma} - \frac{H \sinh\gamma\eta}{\gamma\cosh\gamma}\left(\left(\frac{dq_p}{dz}\right)_H - \beta^2 \frac{I}{I}\left(\psi\right)_H\right) + q_p \tag{3.10}$$

where,

$$\eta = \frac{z}{H}$$

$$\gamma = \alpha H \tag{3.11}$$

$\left(\frac{dq_p}{dz}\right)_H$ = value of $\frac{dq_p}{dz}$ evaluated at $z = H$

The integral shear force T and the internal wall moment M_t become, respectively,

$$T = B_1 \frac{H \sinh\gamma(1-\eta)}{\gamma\cosh\gamma} + \phi \tag{3.12}$$

$$M_t = M - B_1 H l \frac{\sinh \gamma (1 - \eta)}{\gamma \cosh \gamma} - 1 \phi \qquad (3.13)$$

where,

$$\phi = \int_z^H q_p \, d\lambda + \frac{H^2}{\gamma^2} \left[\left(\frac{dq_p}{dz}\right)_H - \beta^2 \frac{I}{l} (\psi)_H \right].$$

$$\left[\frac{\cosh \gamma \eta}{\cosh \gamma} - 1 \right] \qquad (3.14)$$

On integrating equation (3.2) and putting in the boundary conditions at the base, the maximum deflection u_H at the top of the structure becomes,

$$u_H = B_1 \frac{H^3 l}{EI} \left(\frac{\tanh \gamma}{\gamma^3} - \frac{1}{\gamma^2}\right) + \frac{\rho}{EI} + H\left(\frac{du}{dz}\right)_0 + (u)_0 \qquad (3.15)$$

where,

$$\rho = - \frac{H^4 l}{\gamma^4} \left(\left(\frac{dq_p}{dz}\right)_H - \beta^2 \frac{I}{l} (\psi)_H \right) \left(1 - \frac{1}{\cosh \gamma} - \tfrac{1}{2} \gamma^2\right)$$

$$- 1 \int_0^H \int_0^z \int_\xi^H q_p \, d\lambda \, d\xi \, dz + \int_0^H \int_0^\xi M \, d\lambda \, d\xi \qquad (3.16)$$

and $\left(\frac{du}{dz}\right)_0$ and $(u)_0$ are the rotational and lateral displacements, respectively, at the base level of the coupled wall system resulting from flexibility of the foundations or supporting structure.

In the subsequent analysis, unless defined otherwise, brackets with subscript H or 0 signify that the expression enclosed within the brackets is to be evaluated at $z = H$ or 0, respectively.

The axial forces N_1 and N_2 in walls 1 and 2

respectively are given by,

$$N_1 = B_1 H \frac{\sinh \gamma (1 - \eta)}{\gamma \cosh \gamma} + \phi - p_1 H - \int_z^H V_1 \, d\lambda \qquad (3.17)$$

$$N_2 = -B_1 H \frac{\sinh \gamma (1 - \eta)}{\gamma \cosh \gamma} - \phi - p_2 H - \int_z^H V_2 \, d\lambda \qquad (3.18)$$

tensile force being considered positive.

3.4 Base Conditions

The lower boundary condition, and hence the constant B_1 in the previously derived equations, depends on the properties of the supporting structure (or foundation) as well as the form of connection between the walls and supporting structure. In this study two main types of base configurations are considered, namely walls on footings supported on elastic foundations, and walls supported on trapezoidal or rectangular portal frames hinged to a rigid foundation. For walls on a portal frame, it is assumed that the axial deformations of the columns may be neglected in comparison with the relative vertical displacement of the tops of the columns due to sway of the frame.

3.4.1 Walls on Separate Elastic Foundations

For this type of base configuration it is assumed that each wall is supported on an elastic foundation such that the rotation and vertical displacement of each footing is proportional to the imposed bending moment and axial force at the base. The special case of a rigid foundation may be obtained by putting the foundation rotational

and vertical stiffnesses equal to infinity.

As both walls deflect equally because of the high in-plane stiffness of the connecting beams and associated floor slabs, the slope at the base will be the same for each. The base rotation condition becomes,

$$\left(\frac{du}{dz}\right)_0 = \frac{(M_t)_0}{K_{\theta 1} + K_{\theta 2}} = \frac{\left(\frac{d^2u}{dz^2}\right)_0}{K_{\theta 1} + K_{\theta 2}} \qquad (3.19)$$

in which $K_{\theta 1}$ and $K_{\theta 2}$ are the rotational stiffnesses of the foundations under walls 1 and 2 respectively.

The relative vertical displacement at the base is

$$\delta = \frac{(N_1)_0}{K_{v1}} - \frac{(N_2)_0}{K_{v2}}$$

$$= (T)_0\left(\frac{1}{K_{v1}} + \frac{1}{K_{v2}}\right) + \frac{1}{K_{v2}}\left(p_2 H + \int_0^H V_2 \, d\lambda\right) \qquad (3.20)$$

$$- \frac{1}{K_{v1}}\left(p_1 H + \int_0^H V_1 \, d\lambda\right)$$

where K_{v1} and K_{v2} are the vertical stiffnesses of the foundations under walls 1 and 2 respectively.

On evaluating equation (3.1) at $z = 0$, then substituting for $(q)_0$, $\left(\frac{du}{dz}\right)_0$, by using the expressions derived earlier, the constant B_1 may be obtained as,

$$B_1 = \frac{K_a\left(\frac{(M)_0}{1} - K_b(\phi)_0 + K_c(\zeta)_0\right) - (q_p)_0}{\left(1 + HK_a K_b \frac{\tanh\gamma}{\gamma}\right)} \qquad (3.21)$$

where,

$$K_a = \left(\frac{12I_c}{b^3h}\right) \frac{l^2E}{(K_{\theta 1} + K_{\theta 2})}$$

$$K_b = 1 + \frac{1}{l^2}(K_{\theta 1} + K_{\theta 2})\left(\frac{1}{K_{v1}} + \frac{1}{K_{v2}}\right)$$

$$K_c = \frac{(K_{\theta 1} + K_{\theta 2})}{l^2 K_{v1}} \qquad (3.22)$$

$$(\phi)_0 = \frac{H^2}{\gamma^2}\left(\left(\frac{dq_p}{dz}\right)_H - \beta^2 \frac{I}{l}(\psi)_H\right)\left(\frac{1}{\cosh\gamma} - 1\right) +$$

$$\int_0^H q_p \, d\lambda$$

$$(\varsigma)_0 = \left(p_1 H + \int_0^H V_1 \, d\lambda\right) - \left(\frac{K_{v1}}{K_{v2}}\right)\left(p_2 H + \int_0^H V_2 \, d\lambda\right)$$

$(M)_0$ = moment (due to applied loads) at $z = 0$

$(q_p)_0$ = the particular integral solution evaluated at $z = 0$

If the walls are fixed to footings which rest on elastic foundations of subgrade modulus K, the stiffnesses K_{v1}, K_{v2}, $K_{\theta 1}$, $K_{\theta 2}$ are given by,

$$K_{v1} = KA_{f1}$$

$$K_{v2} = KA_{f2} \qquad (3.23)$$

$$K_{\theta 1} = KI_{f1}$$
$$K_{\theta 2} = KI_{f2} \qquad (3.23)\ \text{contd.}$$

where

A_{f1}, A_{f2} = cross-sectional areas of the footings under walls 1 and 2 respectively

I_{f1}, I_{f2} = second moments of area of the footings under walls 1 and 2 respectively

For walls hinged to separate footings it may be shown that

$$B_1 = \frac{(M)_0/1 - (\phi)_0}{(H \frac{\tanh \gamma}{\gamma})} \qquad (3.24)$$

The lateral deflection at the base of the walls is usually zero, therefore,

$$(u)_0 = 0$$

and from equations (3.1) and (3.20), the rotation at the base is given by

$$(\frac{du}{dz})_0 = \frac{1}{1}(\frac{b^3h}{12EI_c})(q)_0 + \frac{(T)_0}{1}(\frac{1}{K_{v1}} + \frac{1}{K_{v2}})$$
$$- \frac{1}{1K_{v1}}(p_1H + \int_0^H V_1\, d\lambda\ )$$
$$+ \frac{1}{1K_{v2}}(p_2H + \int_0^H V_2\, d\lambda\ ) \qquad (3.25)$$

3.4.2 Walls on Trapezoidal Frame

For a coupled wall system supported on a trapezoidal

portal frame hinged to a rigid foundation as shown in Fig. 3.2(a), it is assumed that the portal beam also deforms with a point of contraflexure at its mid-clear span, the length of the beam under each wall being assumed rigid. The force system acting on the portal frame is then as shown in Fig. 3.2(b). The expression for the shear force Q_0 in the portal beam may be obtained from statics and, subsequently, using the compatibility equation for the 'cut' portal beam in conjunction with the compatibility equation (3.1) for the cut lamina at $z = 0$, the expression for B_1 becomes

$$B_1 = \frac{(\frac{1}{hL})(\frac{I_c}{I}) \left[(M)_0 - (\phi)_0 L - h_0 \left((\frac{dM_1}{dz})_0 + C \right)\right] - (q_p)_0}{(1 + (\frac{HI_c}{hI_0}) \frac{\tanh \gamma}{\gamma})} \qquad (3.26)$$

where

I_0 = second moment of area of the portal beam

h_0 = height of the portal frame

L = distance between the bases of columns 1 and 2

$$C = \tan \theta_1 \left(p_1 H + \int_z^H V_1 \, d\lambda \right) - \tan \theta_2 \left(p_2 H + \int_z^H V_2 \, d\lambda \right) \qquad (3.27)$$

θ_1, θ_2 = the angles between the vertical axis and columns 1 and 2, respectively; the angle is positive if the base of the column slopes outwards (cf. Fig. 3.2(a)).

In the limiting case of walls resting on columns,

i.e. $I_0 = 0$, the constant B_1 reduces to

$$B_1 = \frac{(M_0) - h_0 \left(\frac{dM_1}{dz}\right)_0 - h_0 C - (\phi)_0 L}{(1 \; H \; \frac{\tanh \gamma}{\gamma})} \qquad (3.28)$$

If the walls are hinged to separate rigid columns which are fixed to a rigid foundation, it may be shown that the expression for B_1 is that given by equation (3.24).

From the deformed configuration of the portal frame, tacitly assumed that the columns are rigid, the lateral displacement and the relative vertical displacement of the tops of the columns may be shown to be, respectively,

$$(u)_0 = h_0 \left(\frac{du}{dz}\right)_0$$

$$\delta = - (L - 1) \left(\frac{du}{dz}\right)_0$$

On substituting the expression for δ into equation (3.1), then evaluating at $z = 0$, the rotation at the base of the walls becomes,

$$\left(\frac{du}{dz}\right)_0 = \left(\frac{1}{L}\right) \left(\frac{b^3 h}{12EI_c}\right) (q)_0 \qquad (3.29)$$

and hence, from the expression for the lateral displacement at the tops of the columns,

$$(u)_o = \left(\frac{h_0}{L}\right) \left(\frac{b^3 h}{12EI_c}\right) (q)_0 \qquad (3.30)$$

3.5 Solutions for Standard Load Cases

All the equations derived are applicable to lateral and vertical loading systems. They are valid for complex combination of loading situations which may consist of concentrated lateral load at the top, concentrated vertical loads at the tops passing through the centroidal axes of the walls, and distributed lateral and vertical loads of whatever forms.

In general, the codified design loading systems may be obtained by superimposing a few standard load cases, each of which possesses a simple solution and may be readily evaluated. Initially seven standard load cases consisting of four lateral load cases and three vertical load cases are considered.

The seven standard load cases are as follows:-

(a) Concentrated lateral load at the top, $p_0 H$.

(b) A uniformly distributed lateral load per unit height, w_0.

(c) A triangularly distributed lateral load per unit height, $v_0 \eta$.

(d) A distributed polynomial lateral load per unit height, $P_n \eta^n$.

(e) Concentrated vertical loads $p_1 H$, $p_2 H$, passing through the centroidal axes of walls 1 and 2 respectively.

(f) Uniformly distributed vertical loads per unit height w_1, w_2, with eccentricities e_1, e_2, acting on walls 1 and 2 respectively.

(g) Triangularly distributed vertical loads per unit

height, $\vartheta_1(1-\eta)$, $\vartheta_2(1-\eta)$ with eccentricities e_1, e_2, acting on walls 1 and 2 respectively.

The particular integral solution q_p, and the complete solution for q, for each of the seven standard load cases are as follows:-

(a) $$q_p = \frac{p_o H}{1\mu} \qquad (3.31)$$

$$q = B_1 \frac{\cosh \gamma(1-\eta)}{\cosh\gamma} + q_p$$

(b) $$q_p = \frac{w_o H}{1\mu}(1-\eta) \qquad (3.32)$$

$$q = B_1 \frac{\cosh \gamma(1-\eta)}{\cosh\gamma} + \frac{\sinh\gamma\eta}{\gamma\cosh\gamma}\left(\frac{w_o H}{1\mu}\right) + q_p$$

(c) $$q_p = \frac{\vartheta_o H}{1\mu}\left(\tfrac{1}{2} - \tfrac{1}{2}\eta^2 - \frac{1}{\gamma^2}\right) \qquad (3.33)$$

$$q = B_1 \frac{\cosh \gamma(1-\eta)}{\cosh\gamma} + \frac{\sinh\gamma\eta}{\gamma\cosh\gamma}\left(\frac{\vartheta_o H}{1\mu}\right) + q_p$$

(d) $$q_p = \frac{P_n H}{1\mu}\left(\frac{1}{(n+1)} - \sum_{r=-1}^{n}\left(\frac{n!}{(n-r)!}\frac{\sin^2\left(\frac{r\pi}{2}\right)}{\gamma^{r+1}}\eta^{n-r}\right)\right)$$

$$q = B_1 \frac{\cosh\gamma(1-\eta)}{\cosh\gamma} + \left(\frac{\sinh\gamma\eta}{\gamma\cosh\gamma}\frac{P_n H}{1\mu}\right)\cdot$$

$$\left(\sum_{r=-1}^{n}\frac{n!}{(n-r-1)!}\frac{\sin^2\left(\frac{r\pi}{2}\right)}{\gamma^{r+1}}\right) + q_p \qquad (3.34)$$

(e) $q_p = 0$

$$q = B_1 \frac{\cosh \gamma(1 - \eta)}{\cosh\gamma} + \left(\frac{\sinh\gamma\eta}{\gamma\cosh\gamma}\right). \qquad (3.35)$$

$$\left(\frac{\gamma^2}{1\mu}\right)\left(\frac{I}{1}\right)\left(\frac{P_1}{A_1} - \frac{P_2}{A_2}\right)$$

(f) $$q_p = \frac{w_1}{1\mu}\left(e_1 + \frac{I}{1A_1}\right) - \frac{w_2}{1\mu}\left(e_2 + \frac{I}{1A_2}\right) \qquad (3.36)$$

$$q = B_1 \frac{\cosh \gamma(1 - \eta)}{\cosh\gamma} + q_p$$

(g) $$q_p = \left(\upsilon_1\left(e_1 + \frac{I}{1A_1}\right) - \upsilon_2\left(e_2 + \frac{I}{1A_2}\right)\right).$$

$$\left(\frac{1 - \eta}{1\mu}\right) \qquad (3.37)$$

$$q = B_1 \frac{\cosh \gamma(1 - \eta)}{\cosh\gamma} + \left(\frac{\sinh\gamma\eta}{1\mu\gamma\cosh\gamma}\right).$$

$$\left(\upsilon_1\left(e_1 + \frac{I}{1A_1}\right) - \upsilon_2\left(e_2 + \frac{I}{1A_2}\right)\right)$$

$$+ q_p$$

The solutions given in equations (3.31) to (3.37) are obtained on the assumption that the eccentricities e_1 and e_2 are constant throughout the height of the walls.

3.6 Symmetrical Three Coupled Wall System

Many pierced shear walls, particularly those at the

end faces of the building, contain two symmetrical bands of openings. For a symmetrical three coupled wall system (Fig. 3.3) supported on a base structure which is symmetrical with respect to both geometry and force-deformation characteristics, and subjected to lateral loads or anti-symmetrical vertical loads or a combination of both load systems, the mode of deformation will be anti-symmetric with respect to the axis of symmetry. If the walls are acted upon by a symmetrical vertical load system the mode of deformation will be symmetric. In either case, it can be shown that the behaviour of the structure may be completely described by a single second-order governing differential equation.

When the actual vertical load system is neither symmetric nor anti-symmetric but equivalent to a combination of both types of loadings, the analysis for each type of vertical loading may be carried out independently. The forces and displacements are then superimposed to give the actual values.

Symmetrical Three Coupled Walls under Lateral Load or Anti-symmetrical vertical Load Systems or a Combination of the Two Load Systems

For this particular type of loading the vertical shear distributions in the substitute laminae are equal and opposite and, hence, the axial force in the middle wall is zero. Following the same procedure as before, it may be shown that the equations (3.4), (3.10), (3.12) (3.14), (3.15), (3.17), (3.21), (3.24) to (3.26) and

(3.31) to (3.37) are still applicable provided that the following parameters are redefined as,

$$V_2 = p_2 = w_2 = \vartheta_2 = 0$$

$$M_v = 2 \int_z^H V_1 e_1 \, d\lambda$$

$$I = 2I_1 + I_2$$

$$\mu = 2 + \frac{I}{A_1 l^2}$$

$$K_a = \frac{12 I_c}{b^3 h} \quad \frac{l^2 E}{(2K_{\theta 1} + K_{\theta 2})}$$

$$K_b = 2 + \frac{(2K_{\theta 1} + K_{\theta 2})}{K_{v1} l^2}$$

$$K_c = \frac{2}{K_{v1} l^2} \quad (K_{\theta 1} + K_{\theta 2})$$

$$K_{v2} = \infty$$

$$\rho = 2 \left[\frac{H^4 l}{\gamma^4} \quad \left(\frac{dq_p}{dz}\right)_H - \left(\beta^2 \frac{I}{l} \left(\psi \right)_H \right) \cdot \right.$$

$$\left(\tfrac{1}{2} \gamma^2 + \frac{1}{\cosh \gamma} - 1 \right) - 1 \int_0^H \int_0^z \int_\xi^H q_p d\lambda \, d\xi \, dz$$

$$\left. + \tfrac{1}{2} \int_0^H \int_0^\xi M \, d\lambda \, d\xi \right]$$

The wall moment, axial force in the middle wall, rotational and lateral displacements at the base, z = 0,

become, respectively,

$$(M_t)_0 = M - 2(B_1 H1 \frac{\sinh \gamma (1 - \eta)}{\gamma \cosh \gamma} + 1 \phi)$$

$$(N_2)_0 = 0$$

$$(\frac{du}{dz})_0 = \frac{2}{L} (\frac{b^3 h}{12EI_c})(q)_0 \text{ , for walls on frame} \qquad (3.38)$$

$$(u)_0 = \frac{2h_0}{L} (\frac{b^3 h}{12EI_c}) (q)_0 \text{ , for walls on frame}$$

Symmetrical Three Coupled Walls Under Symmetrical Vertical Loading

From the symmetry of the structure and loading system it follows that the lateral deflection of the middle wall must be zero and the vertical shear distributions in the substitute laminae are equal. As the connecting beams are axially stiff, the end walls also have zero deflection. Therefore, the bending moments in all the walls vanish identically.

Following the same procedure of analysis as before, it may be shown that equations (3.4), (3.10), (3.12), (3.14), (3.17), (3.21), (3.26) and (3.35) are valid provided that the following parameters are redefined as,

$$I = 2I_1 + I_2$$

$$\mu = \frac{I}{l^2} (\frac{1}{A_1} + \frac{2}{A_2})$$

$$K_a = (\frac{12 I_c}{b^3 h}) \, l^2 E$$

$$K_b = \frac{1}{l^2}\left(\frac{1}{K_{v1}} + \frac{2}{K_{v2}}\right)$$

$$K_c = \frac{1}{l^2 K_{v1}}$$

$$C = -\frac{L}{2h_0}\left(p_2 H + \int_0^H V_2 \, d\lambda\right)$$

Equations (3.36) and (3.37) may also be used provided e_1 and e_2 are deleted from the equations.

For walls hinged to separate footings supported on elastic foundations, the constant B_1 must be evaluated from equation (3.21). The rotational and lateral displacements of the system at all levels are zero.

The axial force in the middle wall is to be evaluated from,

$$N_2 = -2\left(B_1 H \frac{\sinh\gamma(1-\eta)}{\gamma\cosh\gamma} + \phi\right) - p_2 H - \int_z^H V_2 \, d$$

(3.39)

3.7 Design Method

3.7.1 Basis of Design Method

The non-homogeneous part of the general governing differential equation (3.4) is a function of the form of the applied loads, the positions of the vertical loads and the wall structural parameters. Therefore, the

particular integral solution q_p and its integral or derivative and, hence, the functions ϕ and p will also be functions of the same set of parameters. From consideration of equations (3.10), (3.12), (3.13), (3.15), (3.17), (3.18), (3.25), (3.29) and (3.30) it is evident that all the expressions for generalised forces and displacements consist of two distinct parts. One part depends on the applied loads and wall parameter alone whereas the other part depends on, in addition, the lower boundary condition. Any desired quantity may then be expressed as,

$$\text{quantity} = B_1 k_1 F_1(\gamma, \eta) + F_3 + (\text{load} \times k_2) \times F_2(\gamma, \eta, \text{load form}) \qquad (4.40)$$

where k_1, k_2 are simple structural constants and F_1, F_2 are functions of γ and η. Function F_2 is dependent on load form but F_1 is completely independent of load form. The term F_3 exists only in the case of displacement u but it is dependent on load form and base conditions (cf. equations (3.15), (3.25), (3.29), (3.30)). Therefore, for a specified standard load case, it is possible to prepare design curves which are applicable to any base configuration. Any desired design quantity may be obtained by superposition of the two distinct parts. The influence of a particular base configuration is reflected in the parameters B_1 and the term F_3.

In order to facilitate the production of design curves, the forces and displacement of interest will be

expressed in non-dimensional terms. These quantities are expressed mathematically in the form,

$$f^Q = BF_1^Q + F_2^Q + F_3^Q \qquad (3.41)$$

The superscript Q denotes a generalised force or displacement quantities (i.e. Q refers to q, T, M_t or u_H), and

f^Q = non-dimension generalised force or displacement quantity

B = a function of B_1 and other wall parameters

F_1^Q = a function of γ , η (does not depend on load form)

F_2^Q = a function of γ , η (depends on load form)

F_3^Q = a constant which depends on load form, base conditions and other structural parameters (exists only for f^{u_H}).

Following equation (3.41), the non-dimensional force and displacement parameters f^q, f^T, f^{u_H} are given by,

$$f^q = B\,F_1^q + F_2^q \qquad (3.42)$$

$$f^T = B\,F_1^T + F_2^T \qquad (3.43)$$

$$f^{u_H} = B\,F_1^{u_H} + F_2^{u_H} + F_3^{u_H} \qquad (3.44)$$

The parameters B, $F_3^{u_H}$ and functions F_1^Q, F_2^Q of equations (3.42)to (3.44) for different load cases will be given subsequently in the Chapter.

To systemmatise the design method, classification of structures and standard load cases considered are

given as follows.

Wall-load Categories

The wall-load interactions are grouping into three main categories, namely,

A:- Two coupled walls subjected to vertical or lateral loads.

B:- Symmetrical three coupled wall system subjected to lateral or anti-symmetrical vertical loads.

C:- Symmetrical three coupled wall system subjected to symmetrical vertical loads.

Load Cases

a: Concentrated lateral load at the top, $p_0 H$

b: A uniformly distributed lateral load per unit height, w_0

c: A triangularly distributed lateral load per unit height, $\vartheta_0 \eta$

d: A polynomially distributed lateral load per unit height, $P_n \eta^n$

e: Concentrated vertical loads $p_1 H$, $p_2 H$ passing through the centroidal areas of walls 1 and 2 respectively

f: Uniformly distributed vertical load per unit height, w_1, w_2 with eccentricities e_1, e_2 acting on walls 1 and 2 respectively

g: Triangularly distributed vertical loads per unit height, $\vartheta_1(1-\eta)$ and $\vartheta_2(1-\eta)$ with eccentricities e_1, e_2 acting on walls 1 and 2 respectively

e': Concentrated vertical loads, $p_1 H$, $-p_1 H$ passing through the centroidal axes of walls 1 and 3

respectively.

e": Concentrated vertical loads, p_1H, p_2H, p_1H passing through the centroidal axes of walls 1, 2 and 3 respectively.

f': Uniformly distributed vertical loads per unit height, w_1, - w_1 with eccentricities e_1, e_1 acting on walls 1 and 3 respectively.

f": Uniformly distributed vertical loads per unit height, w_1, w_2, w_1 with eccentricities e_1, 0, e_2 acting on walls 1, 2 and 3 respectively.

g': Triangularly distributed vertical loads per unit height, $\vartheta_1(1-\eta)$, - $\vartheta_1(1-\eta)$ with eccentricities e_1, e_1 acting on walls 1 and 3 respectively.

g": Triangularly distributed vertical loads per unit height, $\vartheta_1(1-\eta)$, $\vartheta_2(1-\eta)$, $_1(1-\eta)$ with eccentricities e_1, 0, e_1 acting on walls 1, 2 and 3 respectively.

The load cases g, g', g" are included to permit cases with linearly varying vertically distributed load (a linear function of height) to be treated. If the actual vertical load acting on a symmetrical three coupled wall system is equivalent to a combination of symmetrical and anti-symmetrical standard load cases, the solutions for the actual loading may be obtained by combining the solutions for the standard load cases.

Walls with Moments at the Tops

Under certain circumstances the tops of the walls may be subjected to concentrated moments, for instance,

when the walls are subjected to concentrated vertical loads which do not pass through the centroidal axes of the walls. In such a case, the method of analysis carried out previously is valid provided that the ratio of the moments at the tops and the ratio of the second moment of areas of the walls are equal. This is necessary because of the assumption of equal wall deflection.

Two additional load cases are then considered:-

m: concentrated moments m_1H, m_2H acting at the tops of walls 1 and 2 respectively, with the ratio $\frac{m_1}{m_2} = \frac{I_1}{I_2}$, (two coupled wall system)

m': concentrated moments m_1H, m_2H, m_1H acting at the tops of walls 1, 2 and 3 respectively, with the ratio $\frac{m_1}{m_2} = \frac{I_1}{I_2}$

With the applied moments at the tops, the top boundary condition becomes,

$$\text{at } z = H \qquad \left(\frac{dq}{dz}\right)_H = \beta^2 (M)_H \tag{3.45}$$

where

$(M)_H$ = total moment at the top

$$= H(m_1 + m_2) \quad \text{for load case m} \tag{3.46}$$

$= H(2m_1 + m_2)$ for load case m'

and the solution for q becomes

$$q = B_1 \frac{\cosh \gamma(1 - \eta)}{\cosh \gamma} + H \frac{\sinh \gamma\eta}{\gamma \cosh \gamma} \beta^2 (M)_H \tag{3.47}$$

Following the earlier procedure, the displacement and forces in the walls may be similarly obtained.

Classification of Structural-load System

The structural-load system will be classified as Y_y, where the capital letter Y and the lower case letter y refer to wall-load group and applied load case respectively. The whole range of structural-load systems considered are then,

A_a, A_b, A_c, A_d, A_e, A_f, A_g, A_m

B_a, B_b, B_c, B_d, $B_{e'}$, $B_{f'}$, $B_{g'}$, $B_{m'}$

$C_{e''}$, $C_{f''}$, $C_{g''}$

Parameters in the Expressions for Forces and Displacement Functions

Define:-

R = 1, 2, 2 for wall-load categories A, B, C respectively

R_1 = 1, 2, 0 for wall-load categories A, B, C respectively

$G_1 = p_1, w_1, \vartheta_1$ for load cases e or e' or e'', f or f' or f'', g or g' or g'', respectively; otherwise $G_1 = 0$

$G_2 = p_2, w_2, \vartheta_2$ for load cases e or e' or e'', f or f' or f'', g or g' or g'' respectively; otherwise $G_2 = 0$

$G_0 = p_0, w_0, \vartheta_0, P_n$ for load cases a, b, c, d respectively; otherwise $G_0 = 0$

$\varkappa$ = 0 for load cases a, b, c, d; otherwise $\varkappa = 1$

$$I = RI_1 + I_2$$

$$W = \varkappa\left(G_1\left(R_1 e_1 + \frac{I}{lA_1}\right) - G_2\left(R_2 e_2 + \frac{I}{lA_2}\right)\right) + (1 - \varkappa)G_0 H + \frac{(M)_H}{H} \qquad (3.48)$$

The structural-load parameters β^2, α^2, μ, γ which are valid for all structural-load systems may then be expressed as,

$$\beta^2 = \frac{12 I_c}{b^3 h I}$$

$$\alpha^2 = \beta^2 l \mu$$

$$\mu = R_1 + \frac{I}{l^2}\left(\frac{1}{A_1} + \frac{(2-R_1)}{A_2}\right) \qquad (3.49)$$

$$\gamma = \alpha H$$

From equations (3.10), (3.13), (3.15), the non-dimensional quantities f^q, f^T, f^{u_H} are obtained as, in the form of equations (3.42) to (3.44),

$$f^q = \left(\frac{l \mu}{W}\right) q = B F_1^q + F_2^q$$

$$f^T = \left(\frac{l \mu}{WH}\right) T = B F_1^T + F_2^T \qquad (3.50)$$

$$f^{u_H} = \frac{1}{R}\left(\frac{EI \mu}{WH^3}\right) u_H = B F_1^{u_H} + F_2^{u_H} + F_3^{u_H}$$

where

$$B = \left(\frac{l \mu}{W}\right) B_1$$

$$F_1^q = \frac{\cosh \gamma (1-\eta)}{\cosh \gamma} \qquad \text{all structural-load systems and all load cases} \qquad (3.51)$$

$$F_1^T = \frac{\sinh \gamma (1-\eta)}{\gamma \cosh \gamma}$$

$$F_1^{u_H} = \frac{\tanh \gamma}{\gamma^3} - \frac{1}{\gamma^2}$$

Expressions for F_2^q, F_2^T, $F_2^{u_H}$ for different load cases are given in tables 3.1 to 3.4. The parameters

B and $F_3^{u_H}$ depend on load form, wall-load category and base conditions and, in general, must be determined for each different combination of these variables.

Using equations for B_1, $(\frac{du}{dz})_0$, $(u)_0$, derived earlier and equation (3.15), the parameters B and $F_3^{u_H}$ for different combinations of load forms, wall-load categories and support systems may be determined. As a large number of different combinations is involved, it will be cumbersome to give expressions for B and $F_3^{u_H}$ for all different combinations considered. However, by introducing a number of new parameters, it is possible to reduce the formulae to a small number. The following parameters are introduced.

Structural-load Parameters

$$J_1 = \varkappa(\frac{R_1}{D})(G_1e_1 - G_2e_2)(\frac{1}{W}) + (1 - \varkappa)$$

$$J_2 = \frac{R_1}{D}\ \frac{H}{W}\ (G_1 \tan\ \theta_1 - G_2 \tan\ \theta_2)$$

$$J_3 = \frac{1}{D}\ \frac{H}{W}\ (G_1 - \frac{K_{v1}}{K_{v2}}\ G_2) \qquad (3.52)$$

$$J_4 = \frac{1}{D}\ (\frac{H}{2W})\ G_2$$

where

D = 2 for load cases g or g' or g", otherwise D = 1

θ_1, θ_2 = as defined previously in section 3.4.2.

Wall-base Parameters

Let

D_1 = 0, for walls hinged to footings, otherwise D_1=1 (3.53)

B and $F_3^{u_H}$ depend on load form, wall-load category and base conditions and, in general, must be determined for each different combination of these variables.

Using equations for B_1, $(\frac{du}{dz})_0$, $(u)_0$, derived earlier and equation (3.15), the parameters B and $F_3^{u_H}$ for different combinations of load forms, wall-load categories and support systems may be determined. As a large number of different combinations is involved, it will be cumbersome to give expressions for B and $F_3^{u_H}$ for all different combinations considered. However, by introducing a number of new parameters, it is possible to reduce the formulae to a small number. The following parameters are introduced.

Structural-load Parameters

$$J_1 = \varkappa(\frac{R_1}{D})(G_1e_1 - G_2e_2)(\frac{1}{W}) + (1 - \varkappa)$$

$$J_2 = \frac{R_1}{D}\ \frac{H}{W}\ (G_1 \tan\ \theta_1 - G_2 \tan\ \theta_2)$$

$$J_3 = \frac{1}{D}\ \frac{H}{W}\ (G_1 - \frac{K_{v1}}{K_{v2}}\ G_2) \qquad (3.52)$$

$$J_4 = \frac{1}{D}\ (\frac{H}{2W})\ G_2$$

where

D = 2 for load cases g or g' or g'', otherwise D = 1

θ_1, θ_2 = as defined previously in section 3.4.2.

Wall-base Parameters

Let

D_1 = 0, for walls hinged to footings, otherwise D_1=1 (3.53)

$D_2 = 1$, for walls on a portal frame or on columns,

otherwise $D_2 = 0$

$D_3 = 0$, for walls on columns, otherwise $D_3 = 1$

$K_{v1}, K_{v2} = \infty$, for walls on a portal frame or

$$\beta_f = R\left(\frac{12I_c}{b^3h}\right)\frac{l^2_{HE}}{(R_1K_{\theta 1} + K_{\theta 2})} \quad \begin{matrix}\text{columns}\\ \text{for walls on footings}\end{matrix} \qquad (3.53)\ \text{contd.}$$

$$= \frac{HI_c}{hI_0}\ ,\ 0\ ,$$ for walls on a portal frame and on columns, respectively

$$\mu_f = \frac{R_1}{R} + D_1\left(1 - \frac{R_1}{R}\right) + \left[\left(\frac{1}{Rl^2}\right)\cdot\right.$$

$$(D_3 + (D_1 - 1)\frac{R_1}{R})(R_1K_{\theta 1} + K_{\theta 2})\cdot$$

$$\left.\left(\frac{1}{K_{v1}} + \frac{(2 - D_1R_1)}{K_{v2}}\right)\right]$$

The wall-base parameters, r_1 to r_7, are defined as,

$$r_1 = \left(\frac{\mu l}{L}\right)\left[1 + D_1(D_3 + (D_1 - 1)\frac{R_1}{R})(\beta_f - 1)\right]$$

$$r_2 = \mu_f\left[1 + (D_3 + (D_1 - 1)\frac{R_1}{R})(\beta_f - 1)\right]$$

$$r_3 = D_3 + (D_1 - 1)\frac{R_1}{R} \qquad (3.54)$$

$$r_4 = \frac{EI}{Hl^2}\left(\frac{1}{K_{v1}} + \frac{(2 - R_1)}{K_{v2}}\right)$$

$$r_5 = 1 + D_2(R_1\frac{1}{L} - 1)$$

$$r_6 = \frac{\gamma^2 EI}{lH^2K_{v1}}$$

$$r_7 = D_2\left(\left(1 - \frac{R_1}{R}\right)\frac{l\mu}{H}\quad \beta_f\right)$$

Using the parameters introduced, it may be shown that only a few formulae for B and $F_3^{u_H}$ need to be given, since many of them have the same expressions. For instance, the formulae for structural-load systems A_a, A_f, B_a, $B_{f'}$, $C_{f''}$ are given by,

$$B = (1-\varkappa)\ \frac{r_1(1+\frac{h_0}{H}) - r_2(F_2^T)_0 - r_3(F_2^q)_0}{r_3 + r_2(F_1^T)_0}$$

$$+\ \varkappa\ \frac{r_1(J_1 + \frac{h_0}{H}J_2) + r_6J_3 - r_2(F_2^T)_0 - r_3(F_2^q)_0 + r_7J_4}{r_3 + r_2(F_1^T)_0}$$

$$F_3^{u_H} = \frac{1}{R}\ \Big[r_5\Big(r_4(f^T)_0 + \frac{\mu}{\gamma^2}\big(\ (f^q)_0 - r_6J_3\big)$$

$$+\ \frac{\mu}{3}\big(\ (1-R)(1-\varkappa) + \varkappa(J_1 - 1)\big)\ \Big] \qquad (3.55)$$

where, $(F_2^q)_0$, $(F_2^T)_0$, $(F_1^T)_0$, $(f^q)_0$, $(f^T)_0$ are values of the appropriate functions at $z = 0$. All other parameters are as defined previously.

For simplicity, and in order that important parameters and expressions may be obtained rapidly, the following tables are presented.

Table 3.1 Expressions for f^Q, F_i^Q and B for structural-load systems A_a, A_f, B_a, $B_{f'}$, $C_{f''}$

Table 3.2 Expressions for f^Q, f_i^Q and B for structural-load systems A_b, A_g, B_b, $B_{g'}$, $C_{g''}$

Table 3.3 Expressions for f^Q, f_i^Q and B for structural-load systems A_c, B_c

Table 3.4 Expressions for f^Q, F_i^Q and B for structural-load systems A_e, A_m, B_e', B_m', C_e''

Table 3.5 Expressions for structural-load parameters, (i.e. R, R_1, $\varkappa$, W, J_1, J_2, J_3, J_4, I, μ , γ), for structural-load systems A_a, A_b, A_c, A_d, A_e, A_f, A_g and A_m

Table 3.6 Structural-load parameters for structural-load systems B_a, B_b, B_c, B_d, B_e', B_f', B_g', B_m'

Table 3.7 Structural-load parameters for structural-load systems C_e'', C_f'', C_g''

Table 3.8 Wall-base parameters, (i.e. r_1 to r_7), for all support systems considered.

In addition, expressions for f^Q, F_i^Q and B for structural-load systems A_d and B_d are also given in Appendix II.

3.7.2 Maximum Shear Distribution in the Continuous Medium.

The height η at which the maximum vertical shear distribution in the continuous medium occurs may be determined by solving the equation obtained by differentiating equation (3.42) and equating to zero. That is,

$$B \frac{dF_1^q}{d\eta} + \frac{dF_2^q}{d\eta} = 0 \qquad (3.56)$$

The maximum vertical shear distribution is then evaluated from equation (3.42).

Using the expressions given in Tables 3.1-3.4, equation (3.56) becomes,

For standard load cases a, f, f', f''

$$\sinh \gamma (1 - \eta) = 0 \qquad (3.57)$$

For standard load cases b, g, g', g''

$$B \gamma \sinh \gamma(1 - \eta) = \cosh\gamma\eta - \cosh\gamma \qquad (3.58)$$

For standard load case c,

$$B \gamma \sinh \gamma(1 - \eta) = \cosh\gamma\eta - \eta\cosh\gamma - \frac{\sinh \gamma(1 - \eta)}{\gamma} \qquad (3.59)$$

For standard load case e, e', e'', m, m'

$$B \sinh \gamma(1 - \eta) = \gamma\cosh\gamma\eta \qquad (3.60)$$

For standard load case d,

$$B \gamma \sinh \gamma(1 - \eta) = \cosh\gamma \sum_{r=-1}^{n-1} \left[\frac{n!}{(n-r-1)!} \left(\frac{\sin^2 \left(\frac{r\pi}{2} \right)}{\gamma^{r+1}} \right) \cdot \eta^{(n-r-1)} \right] - \cosh\gamma\eta \sum_{r=-1}^{n} \frac{n!}{(n-r-1)!} \frac{\sin^2 \left(\frac{r\pi}{2} \right)}{\gamma^{r+1}} \qquad (3.61)$$

From equation (3.52) it may be seen that the maximum vertical shear distribution for each of the standard load cases a, f, f', f'' invariably occurs at the tops of the walls, i.e. at $\eta = 1$, for negative value of B.

3.7.3 Stresses in the Walls

Since all walls deflect equally, the bending moment carried by each wall is proportional to its flexural rigidity. The bending stresses are then obtained using ordinary beam theory, and, by superimposing the axial stresses due to the axial force, N, the total stress distribution may be evaluated.

For a general two-wall system such as that shown in Fig. 3.4, the extreme fibre stresses may be readily shown to be

$$\sigma_A = \sigma \left(f^T\left(\frac{I}{A_1 l^2} - \frac{\lambda_1}{l}\right) + F\left(\frac{\lambda_1}{l} J_1 - \frac{I}{A_1 l^2} K_1\right)\right)$$

$$\sigma_B = \sigma \left(f^T\left(\frac{I}{A_1 l^2} + \frac{\lambda_2}{l}\right) - F\left(\frac{\lambda_2}{l} J_1 + \frac{I}{A_1 l^2} K_1\right)\right)$$

(3.62)

$$\sigma_C = \sigma \left(-f^T\left(\frac{I}{A_2 l^2} + \frac{\lambda_3}{l}\right) + F\left(\frac{\lambda_3}{l} J_1 - \frac{I}{A_2 l^2} K_2\right)\right)$$

$$\sigma_D = \sigma \left(-f^T\left(\frac{I}{A_2 l^2} - \frac{\lambda_4}{l}\right) - F\left(\frac{\lambda_4}{l} J_1 + \frac{I}{A_2 l^2} K_2\right)\right)$$

For a general symmetrical three coupled walls system such as that shown in Fig. 3.5, the extreme fibre stresses are given by

$$\sigma_E = \sigma \left(f^T\left(\frac{I}{A_1 l^2} - 2\left(\frac{R_1}{R}\right)\frac{\lambda_5}{l}\right) + F\left(\left(\frac{R_1}{R}\right)\frac{\lambda_5}{l} J_1 - \frac{I}{A_1 l^2} K_1\right)\right)$$

$$\sigma_F = \sigma \left(f^T\left(\frac{I}{A_1 l^2} + 2\left(\frac{R_1}{R}\right)\frac{\lambda_6}{l}\right) - F\left(\left(\frac{R_1}{R}\right)\frac{\lambda_6}{l} J_1 + \frac{I}{A_1 l^2} K_1\right)\right)$$

(3.63)

$$\sigma_G = \sigma \left(-f^T\left(1 - \frac{R_1}{R}\right) \frac{I}{A_2 l^2} + 2\left(\frac{R_1}{R}\right) \frac{\lambda_7}{l}\right)$$

$$+ F \left(\left(\frac{R_1}{R}\right) \frac{\lambda_7}{l} J_1 - \frac{I}{A_2 l^2} K_2\right)\right)$$

$$\sigma_H = \sigma \left(-f^T\left(1 - \frac{R_1}{R}\right) \frac{I}{A_2 l^2} - 2\left(\frac{R_1}{R}\right) \frac{\lambda_7}{l}\right)$$

$$- F\left(\left(\frac{R_1}{R}\right) \frac{\lambda_7}{l} J_1 - \frac{I}{A_2 l^2} K_2\right)\right)$$

$$\sigma_I = \sigma \left(-f^T \left(\frac{I}{A_1 l^2} + 2\left(\frac{R_1}{R}\right) \frac{\lambda_6}{l}\right)\right.$$

$$+ F \left(\left(\frac{R_1}{R}\right) \frac{\lambda_6}{l} J_1 - \frac{I}{A_1 l^2} K_1\right)\right)$$

$$\sigma_J = \sigma \left(-f^T \left(\frac{I}{A_1 l^2} - 2\left(\frac{R_1}{R}\right) \frac{\lambda_5}{l}\right)\right.$$

$$- F \left(\left(\frac{R_1}{R}\right) \frac{\lambda_5}{l} J_1 + \frac{I}{A_1 l^2} K_1\right)\right) \qquad (3.63)$$

(3.63) contd.

where

$$\sigma = \frac{WHl}{\mu I}$$

$$K_1 = \frac{G_1 l}{W}, \quad K_2 = \frac{G_2 l}{W} \qquad (3.64)$$

$F = \mu (1 - \eta)$ for standard load cases a, f, f' and f"

$$= \frac{\mu}{2}(1-\eta)^2 \quad \text{for standard load cases b, g, g' and g''}$$

$$= \mu\left(\frac{1}{3} - \frac{\eta}{2} + \frac{\eta^3}{6}\right) \quad \text{for standard load case c}$$

$$= \mu\left[\frac{1}{(n+2)} - \frac{\eta}{(n+1)} + \left(\frac{1}{(n+1)} - \frac{1}{(n+2)}\right)\eta^{n+2}\right]$$

for standard load case d

$$= \mu \quad \text{for standard load case e, e', e'', m, m'}$$

(3.64) contd.

λ_i = distance between the point at which the stress is evaluated and the centroid of the corresponding wall.

Equations (3.62) and (3.63) are valid for all structural-load systems.

3.7.4 Design Curves

The design curves for the relevant non-dimensional functions for each standard load case may be conveniently produced from the expressions given in Tables 3.1-3.4. It has been stated earlier in the Chapter that usually a set of design curves is required for each standard load case. This follows from the fact that the particular integral solutions of different standard load cases will, in general, be different. However, whenever the

particular integral solutions of any two load cases are proportional to each other, there will be correspondences of the expressions of forces and displacement functions due to these load cases. The design curves for both load cases will then be identical. From consideration of Tables 3.1-3.4, it is evident that there are correspondences between the following standard load cases:-

1. Triangularly distributed vertical loads and a uniformly distributed lateral load.
2. Uniformly distributed vertical loads and a concentrated lateral load at the top.
3. Concentrated vertical loads at the tops passing through the centroidal axes of the walls and concentrated moments at the tops of the walls.

Both of the standard load cases which are paired together have identical design curves. The correspondences between the lateral and vertical load cases are shown diagrammatically in Fig. 3.13.

Four sets of design curves, Figs. 3.6-3.9, corresponding to structural-load systems (A_a, A_f, B_a, B_f', C_f''), (A_b, A_g, B_g, B_g', C_g''), (A_c, B_c), (A_e, A_m', B_e', B_m', C_e''), respectively, are presented for a semi-graphical determination of q, T, u_H, the wall extreme fibre stresses and the position of the maximum vertical shear distribution. The curves cover the range of combinations of wall configurations and loading systems likely to be encountered in practice. In addition,

similar design curves for any lateral polynomial load form applicable to structural-load systems A_d and B_d may be produced, using equation (3.61) and Appendix II.

3.7.5 Use of Design Curves

For a given structural-load system, for instance the structural-load system A_a, the structural-load parameters and the wall-base parameters are first determined from Tables 3.5 and 3.8 respectively. The parameter B is then evaluated from the expression given in Table 3.1, making use of the design curves in Fig. 3.6.

The vertical shear distribution and the integral shear force at any level are obtained using equations (3.42), (3.43) and the design curves for F_i^q and F_i^T. The wall extreme fibre stresses are obtained from equations (3.62). The position of the maximum value of the vertical shear distribution may be rapidly determined from the design curves B against γ . The maximum deflection at the top is obtained using equation (3.44) and the design curves for $F_i^{u_H}$. The design quantities for other structural-load systems may be obtained in a similar manner provided that the appropriate Tables and curves are used.

3.8 Example Problems

In order to illustrate the use of the design curves and to show the changes in design quantities resulting from changes in base conditions, a few design examples are presented.

Example 1: Two coupled walls under lateral load.

The system of coupled walls shown in Fig. 3.10 is considered. The walls, of total height 54 m and storey height 2.7 m, are supported on a portal frame of 3 m in height. The second moment of area of the portal beam is 0.02 m^4. The walls and connecting beams are 0.30 m thick, and the depth of each connecting beam is 0.40 m. The elastic modulus of the concrete is taken to be 2.394×10^7 KN/m^2. Assume that the wall system is subjected to a uniformly distributed load of intensity 15.47 KN/m.

With the given data

H	= 54.0 m	I_0	= 0.02 m^4
h	= 2.7 m	I_c	= 0.0016 m^4
A_1	= 2.1 m^2	I_1	= 8.575 m^4
A_2	= 3.0 m^2	I_2	= 25.0 m^4
l	= 10.5 m	h_0	= 3.0 m

The structural-load system is of the type A_b (cf. section 3.7.1). Therefore, the structural-load parameters are, from Table 3.5,

R	= 1	J_1	= 1.0
R_1	= 1	J_2	= 0
$\varkappa$	= 0	J_3	= 0
W	= 835.38 KN	J_4	= 0
μ	= 1.2465	I	= 33.575
γ	= 3.2567		

The wall-base parameters become, from Table 3.8,

$r_1 = 1.9944$ $r_2 = 1.6$ $r_3 = 1$

$r_4 = 0$ $r_5 = 1$ $r_6 = r_7 = 0$

As the structural-load system is A_b, the appropriate set of design curves to be used is that given in Fig. 3.7. From the design curves,

$(F_1^q)_0 = 1.0$ $(F_1^T)_0 = 0.315$

$(F_2^q)_0 = 1.0$ $(F_2^T)_0 = 0.595$

On substituting relevant parameters into the expression for B given in Table 3.2, the value for B is found to be

$$B = -0.5612$$

From the design curves, Table 3.2, equations (3.42) to (3.44) and the value of B which has been determined, the non-dimensional quantities f^q, f^T, f^{u_H} and, hence, other design quantities may be rapidly evaluated.

From Table 3.2 and equation (3.44) it is found that

$$f^{u_H} = 0.08086$$

therefore, the deflection at the top relative to the base of the wall becomes,

$$u_H = \frac{R\ W\ H^3}{I\ E\ \mu}\ f^{u_H}$$

$$= 0.0086 \text{ m}$$

Consider the typical case of the base of the structure, $\eta = 0$. On evaluating $(f^T)_0$ using equation (3.43) and the design curves, then substituting $(f^T)_0$

and other relevant parameters into equation (3.62), the extreme fibre stresses at points A, B, C, D (Fig. 3.10) are found to be,

$$\sigma_A = 1460 \quad KN/m^2$$

$$\sigma_B = -87 \quad KN/m^2$$

$$\sigma_C = 625 \quad KN/m^2$$

$$\sigma_D = -1585 \quad KN/m^2$$

From Fig. 3.7(d) it is found that the maximum shear intensity, q_{max}, occurs at a height $\eta = 0.21$, hence,

$$q_{max} = \frac{W}{l\mu} \quad (f^q)_{\eta=0.21}$$

and on substituting the appropriate values of parameters,

$$q_{max} = 34.15 \quad KN/m$$

If it is assumed, conservatively, that q_{max} may be used to calculate the maximum bending moment, M_{max}, in any connecting beam, then

$$M_{max} = \tfrac{1}{2}(34.15 \times 2.7 \times 2) = 91 \text{ KN-m}$$

To show the effects of different base conditions on design quantities, it is assumed that the coupled walls are supported on elastic foundation of subgrade modulus K. Three different values of subgrade modulus are assumed, and the resulting calculation tabulated in Table 3.9. In each set of calculations it is assumed that the footings and the walls have the same cross-sectional dimensions. The differential settlement, δ , between the bases of the

walls is calculated from equation (3.20).

From Table 3.9 it may be seen that the maximum deflection, the differential settlement and the maximum intensity of vertical shear distribution increase with decreasing foundation stiffness (subgrade modulus).

Example 2: Two coupled walls under vertical loads.

The coupled wall system of the previous example is again considered. The floor slab is taken to be 0.20 m thick and the weight of the concrete 2307 Kgf/m^3. A live load of 1.5 KN/m^2 is assumed acting on each floor, and the contributary loading area of each floor is as shown in Fig. 3.11. It is assumed that the vertical load acting on each wall can be considered as distributed uniformly throughout the height of the wall.

From the given loading data, the uniformly distributed vertical loads and the corresponding eccentricities are found to be,

w_1 = 168.95 KN/m

w_2 = 234.66 KN/m

e_1 = 0.36981 KN/m

e_2 = 0.36609 KN/m

The structural-load system is of the type A_f, and the corresponding set of design curves to be used is Fig. 3.6.

Following the same design method illustrated in the previous example, similar design quantities may be rapidly

evaluated. Three different values of sub-grade modulus are considered, and the resulting calculation shown in Table 3.10.

The differential settlement is evaluated from equation (3.20), i.e.

$$\delta = (T)_0 \left(\frac{1}{K_{v1}} + \frac{1}{K_{v2}}\right) - \frac{w_1 H}{K_{v1}} + \frac{w_2 H}{K_{v2}}$$

The minus values of the shear intensity and the maximum deflection indicate that the shear distribution acts downwards on wall 1 and the walls deflect to the left.

From the results it may be seen that the maximum shear intensity and the extreme fibre stresses of the walls are not greatly affected by the changes in the stiffness of the foundation, although the maximum deflection and the differential settlement are considerably affected.

Comparisons between the lateral and vertical loadings, Tables 3.9 and 3.10, show that the wall extreme fibre stresses and the differential settlement due to a practical vertical loading are more significant than those due to lateral loading, and the opposite occurs regarding the maximum deflection and the vertical shear distribution. However, the maximum deflection and the vertical shear distribution due to the vertical loading may become significant if the load parameter W is not small. This situation may arise if the floor load is far from uniform so that the eccentricities are of opposite signs. For

example, assuming that in the previous example the vertically distributed load w_1 has the eccentricity of -0.36981 m instead of + 0.36981 m. The load parameter W is then found to be -141.253 KN. Following the same calculation as before, similar design quantities are obtained and these are tabulated in Table 3.11. From Tables 3.10 and 3.11 it may be seen that the maximum deflection and the maximum intensity of vertical shear distribution increase considerably.

Example 3: Symmetrical three coupled walls under lateral load.

Consider a typical symmetrical three coupled wall system shown in Fig. 3.12. The width of the walls 1 and 2 are 4.5 m and 6 m respectively. Other geometrical dimensions and the elastic modulus of the concrete are identical to those used in the earlier examples. The cross-sectional dimensions of the footings are taken to be the same as those of the walls above them. A lateral loading, w_0, of intensity 15.47 KN/m is again assumed.

From the given data, the structural parameters are found to be,

$l = 7.25$ m $\qquad I_c = 0.0016 \ m^4$

$A_1 = 1.35 \ m^2 \qquad I_1 = 2.2781 \ m^4$

$A_2 = 1.8 \ m^2 \qquad I_2 = 5.4 \ m^4$

The structural-load system belongs to the type B_b. The structural-load parameters then become,

R	= 2	J_1	= 1	μ	= 2.14031
R_1	= 2	J_2	= 0	γ	= 5.4115
$\varkappa$	= 0	J_3	= 0	I	= 9.95625
W	= 835.38 KN	J_4	= 0		

The set of design curves to be used is Fig. 3.7. The rest of the calculations are carried out in a similar manner to those of the two coupled wall system, except that the extreme fibre stresses are determined from equation (3.63). The resulting calculation is shown in Table 3.12. The relative vertical displacement, δ , is the differential settlement between the outer and middle walls.

3.9 Conclusion

Based on the continuous medium method of analysis, a new technique which enables the design of coupled shear walls on flexible bases to be carried out rapidly has been developed. The technique is applicable to any load form which can be described by analytical function. The load system may be either lateral or vertical loads or a combination of both.

Curves have been presented for the evaluation of forces, wall extreme fibre stresses, the maximum deflection, position of the maximum vertical shear distribution, in a system of two coupled walls or a symmetrical three coupled wall system. Four sets of design curves have been produced, covering load cases and base conditions likely to be encountered in practice.

In addition, formulae for a general polynomial load form have been given in Appendix II.

For each standard load case, the complete solution for a coupled wall system on any base condition may be obtained using only one set of design curves. The variation of important design quantities under different base conditions can be rapidly investigated.

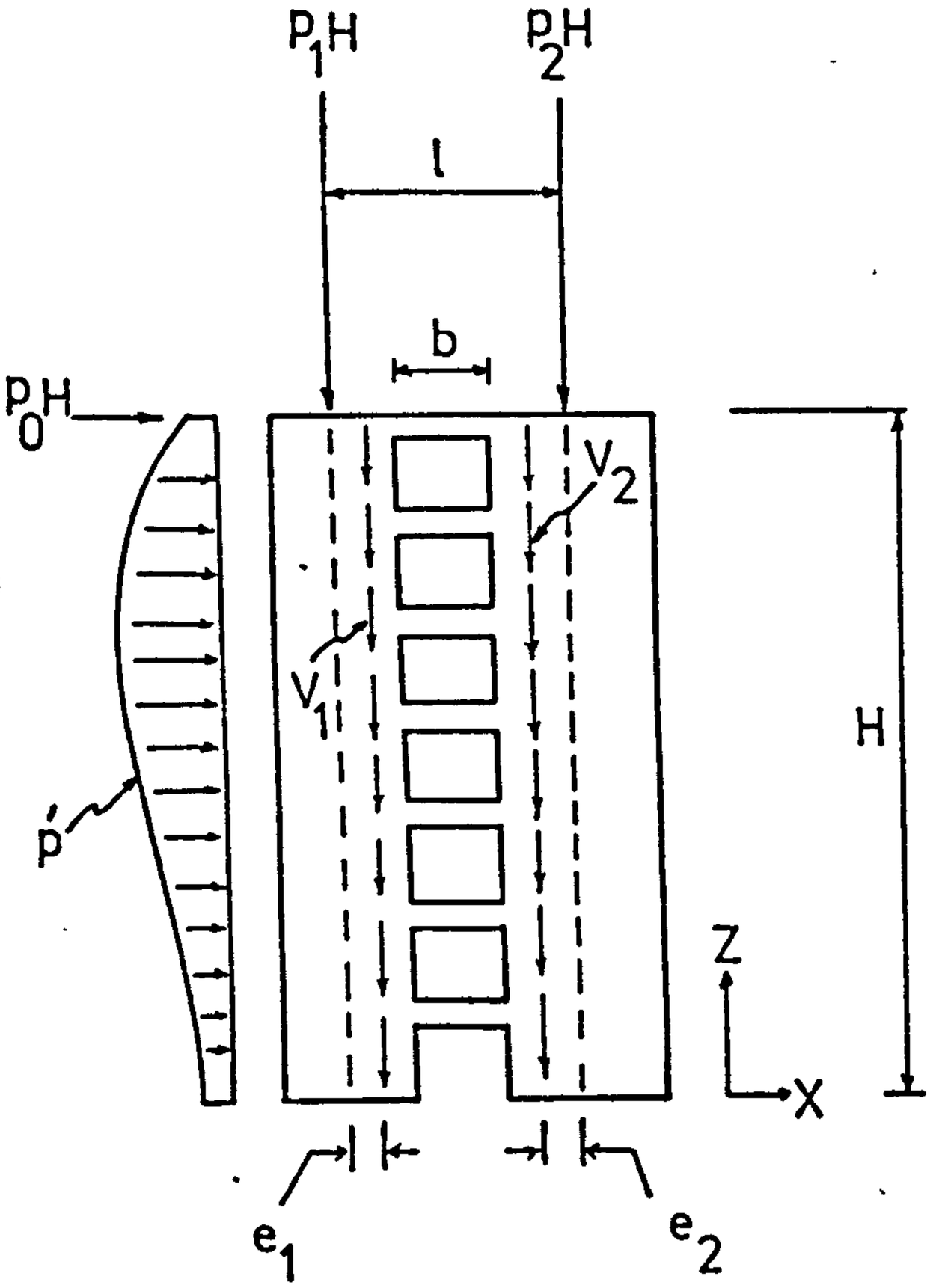

General loading of coupled walls

Fig. 3.1

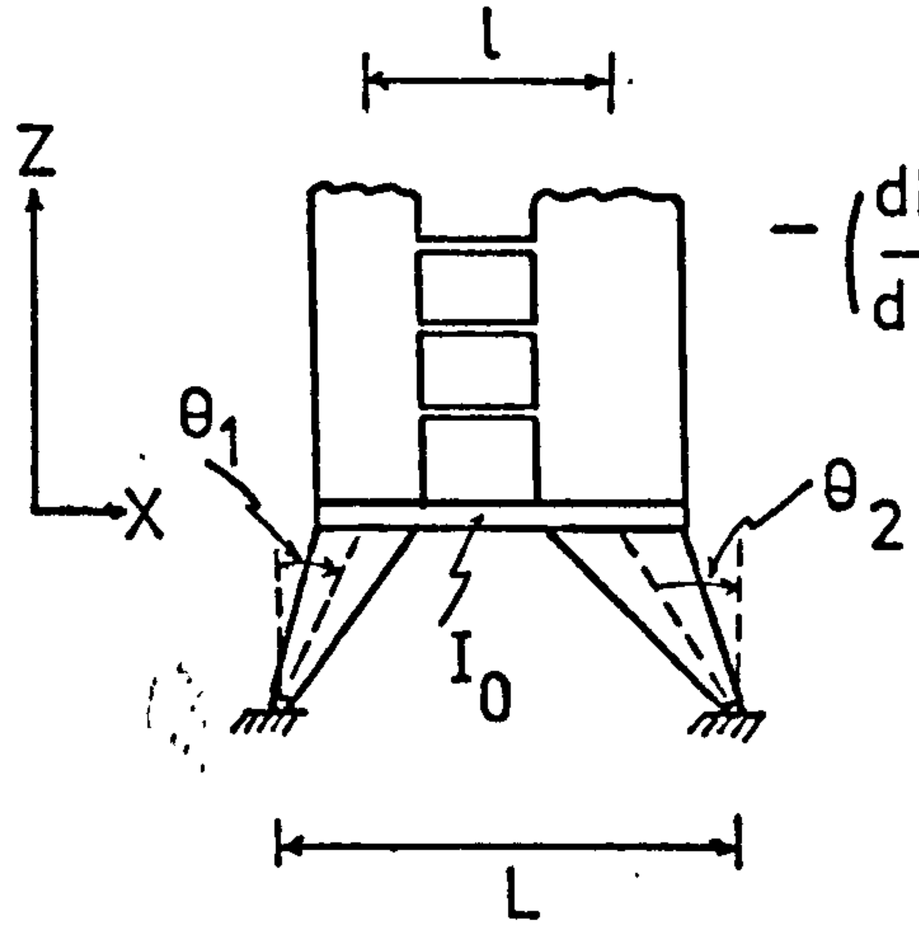

(3.2a) elevation

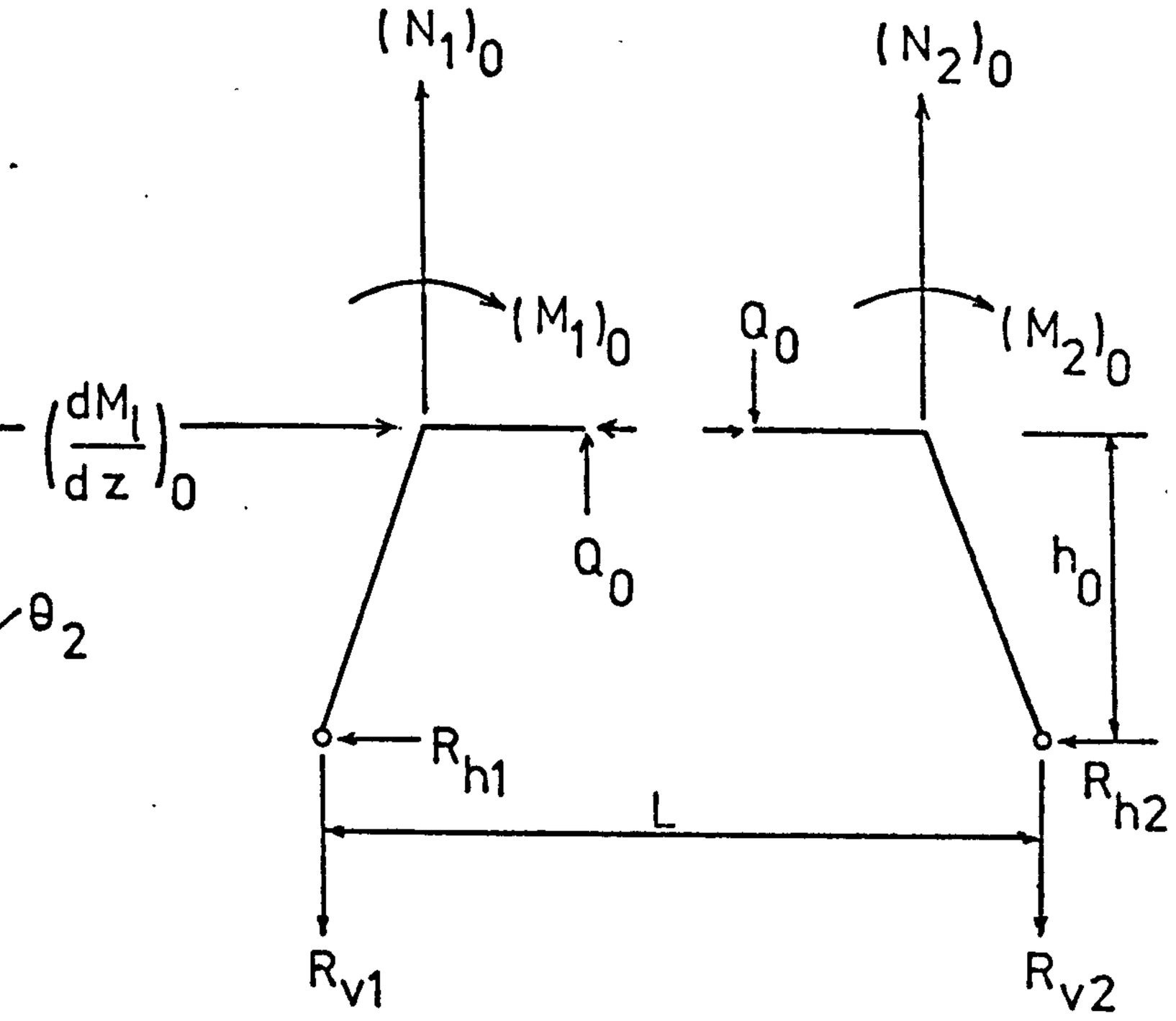

(3.2b) forces on portal frame

Coupled walls on portal frame

Fig. 3.2

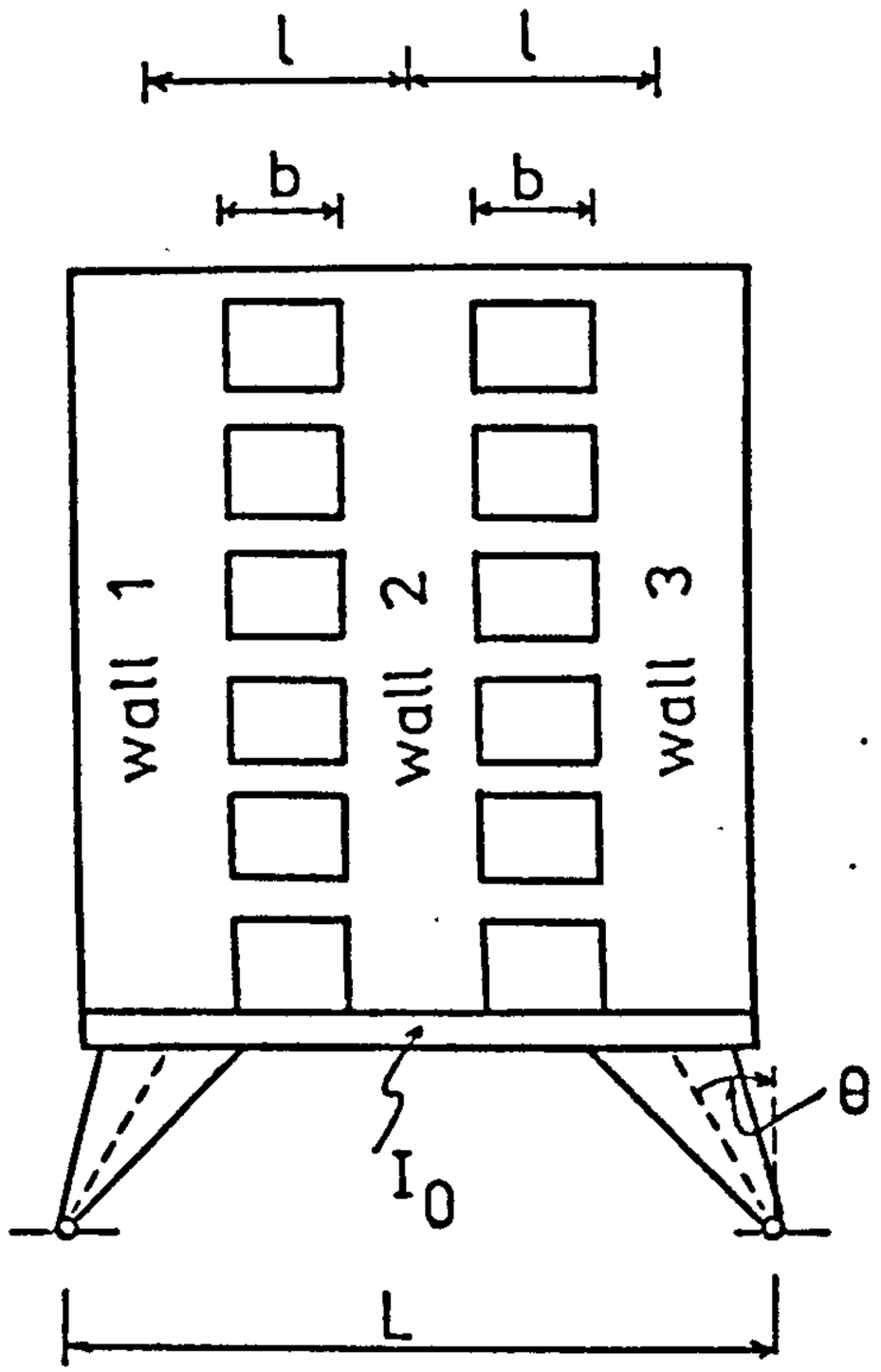

Symmetrical three coupled wall system

Fig. 3.3

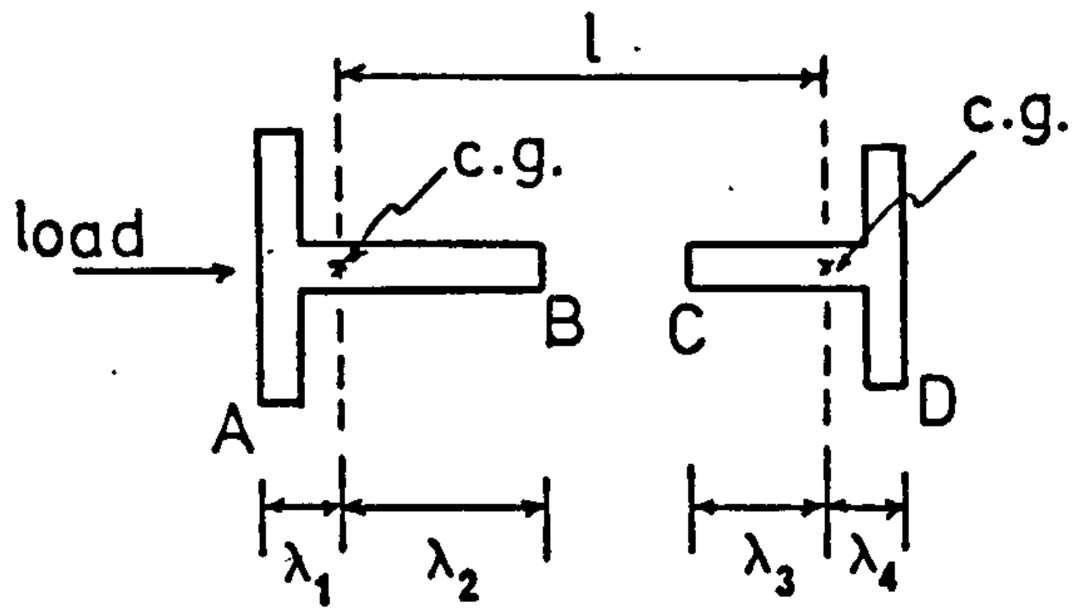

Plan of two coupled wall system

Fig. 3.4

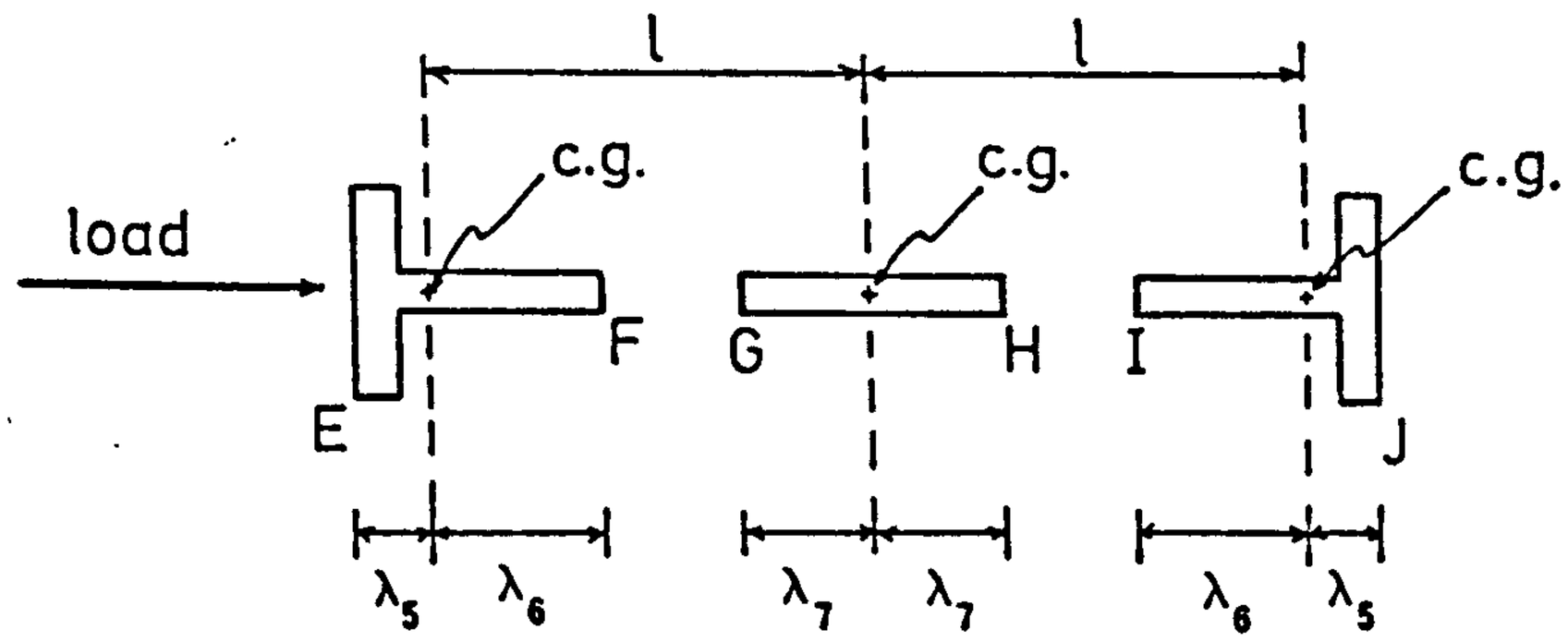

Plan of symmetrical three coupled wall system

Fig. 3.5

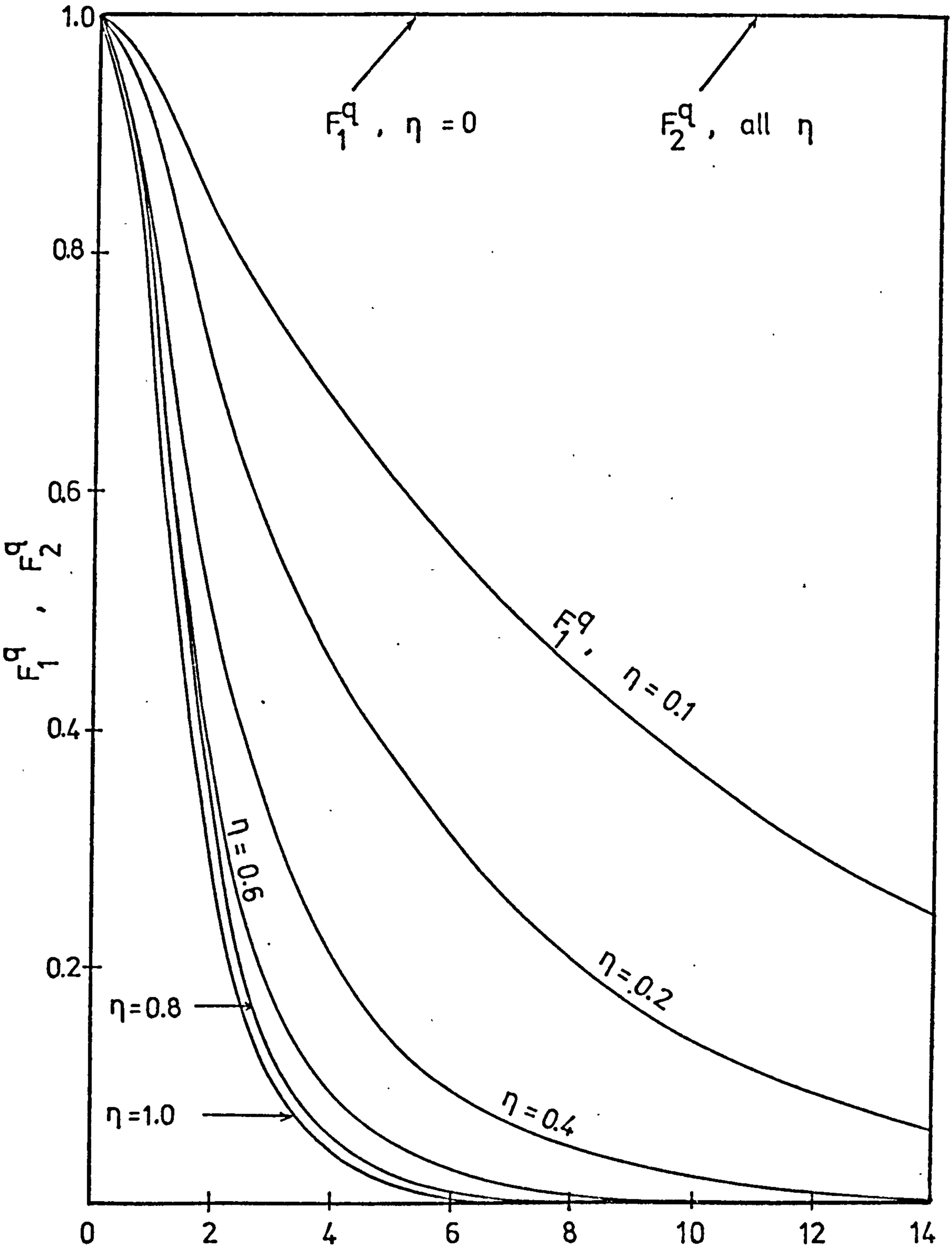

Variation of design functions F_1^q and F_2^q for standard load cases a, f, f′, f″

Fig. 3.6(a)

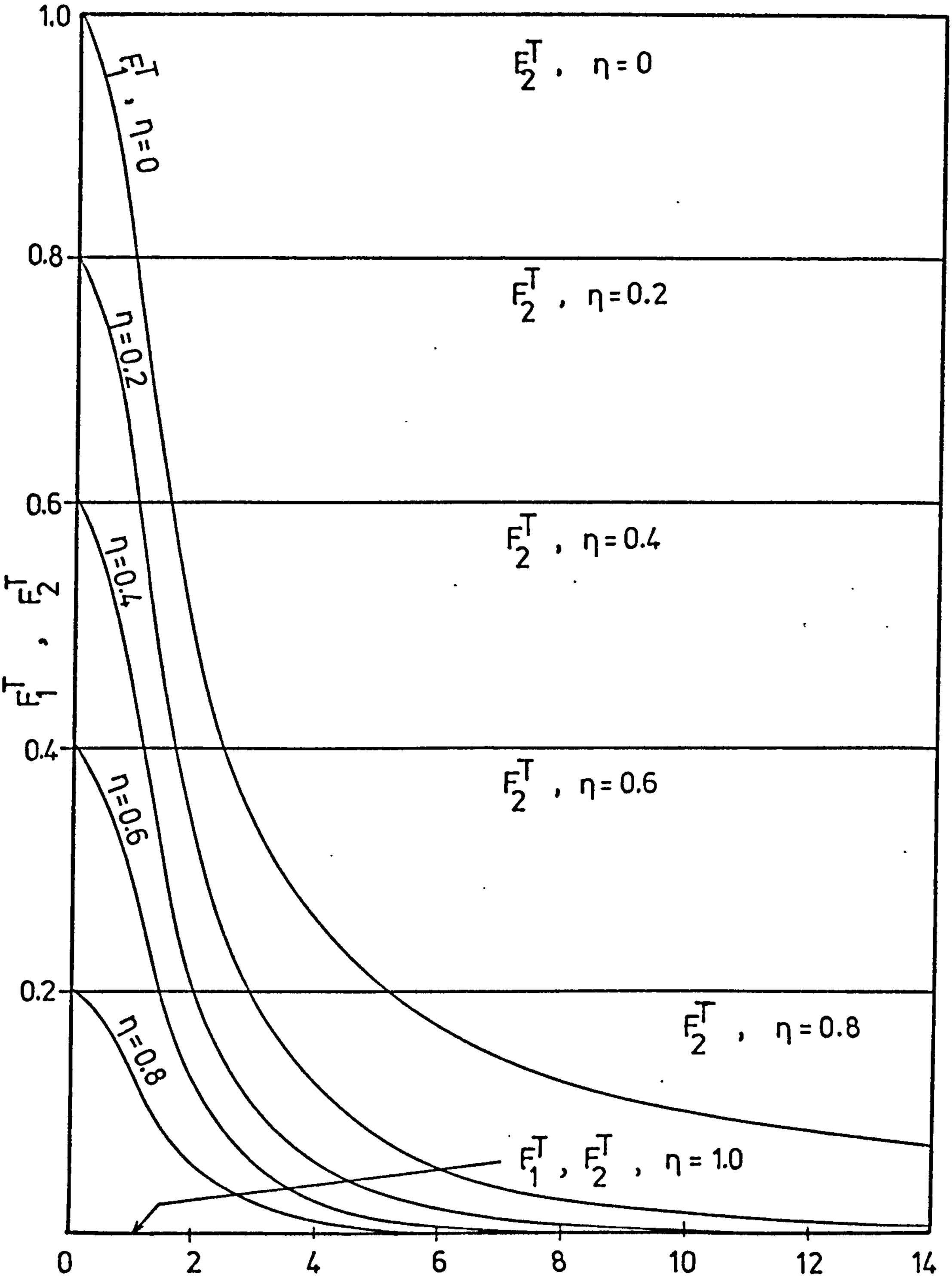

Variation of design functions F_1^T and F_2^T for standard load cases a , f , f' , f''

Fig. 3.6(b)

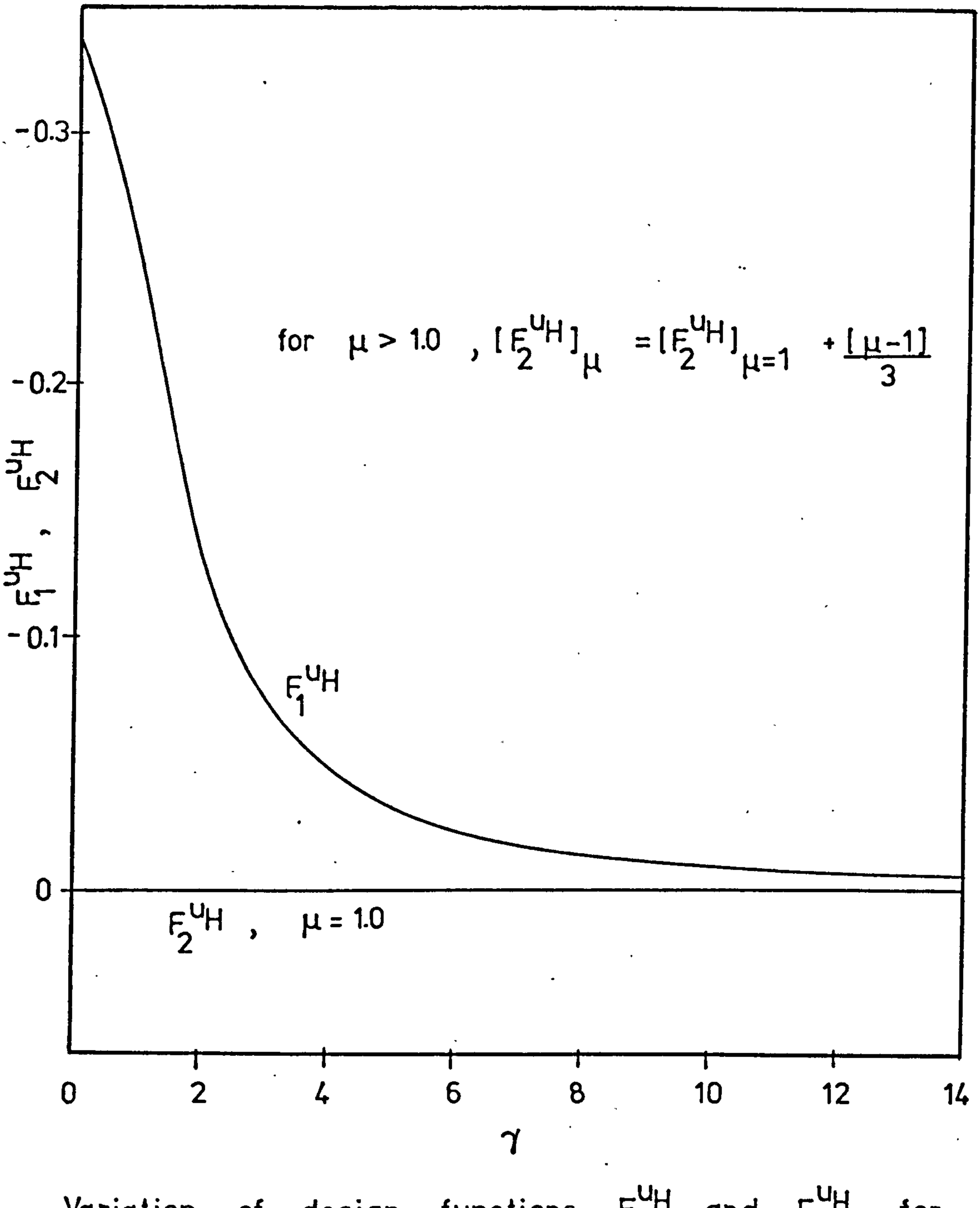

Variation of design functions F_1^{uH} and F_2^{uH} for standard load cases a, f, f′, f″

Fig. 3.6(c)

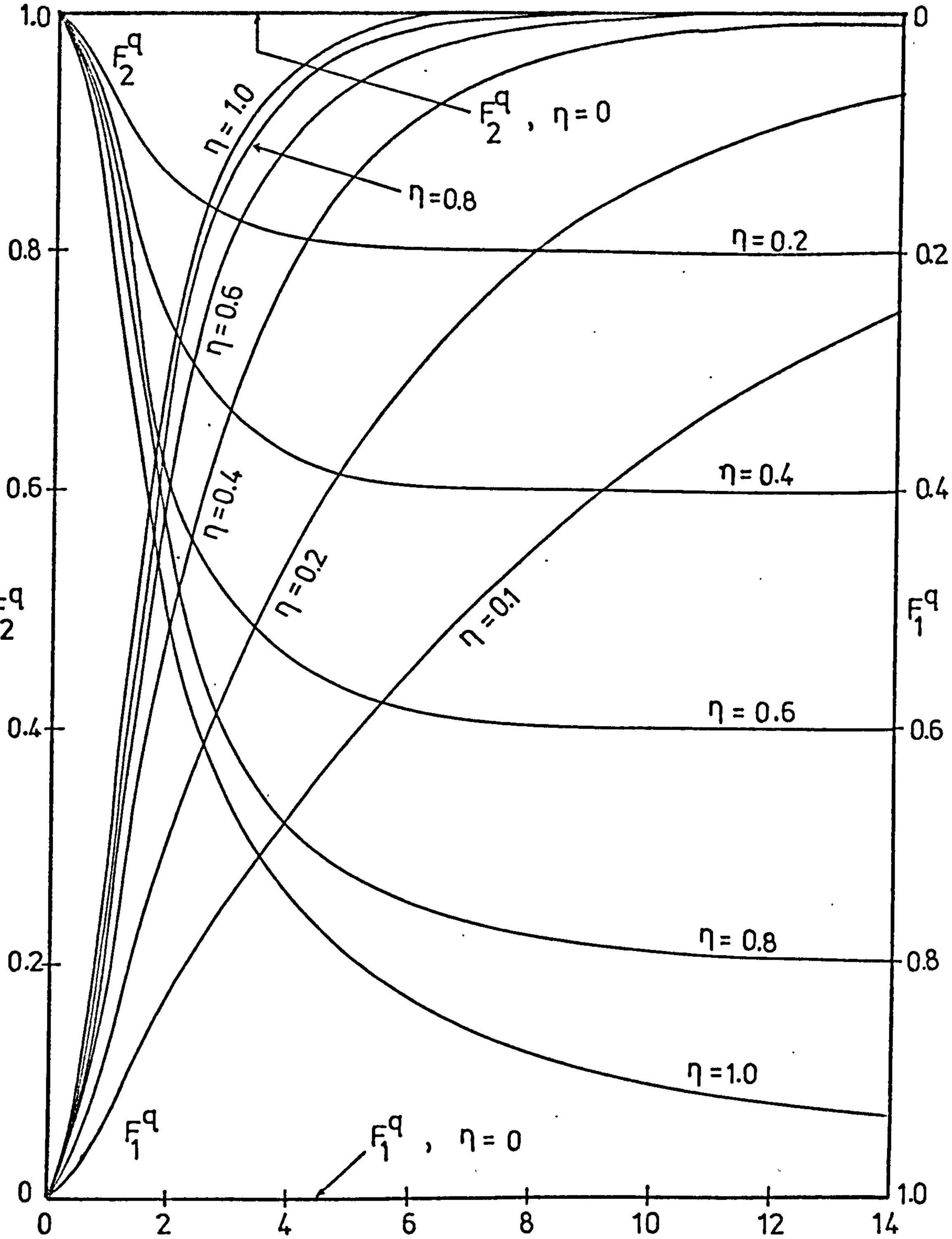

Variation of design functions F_1^q and F_2^q for standard load cases b, g, g′, g″

Fig. 3.7(a)

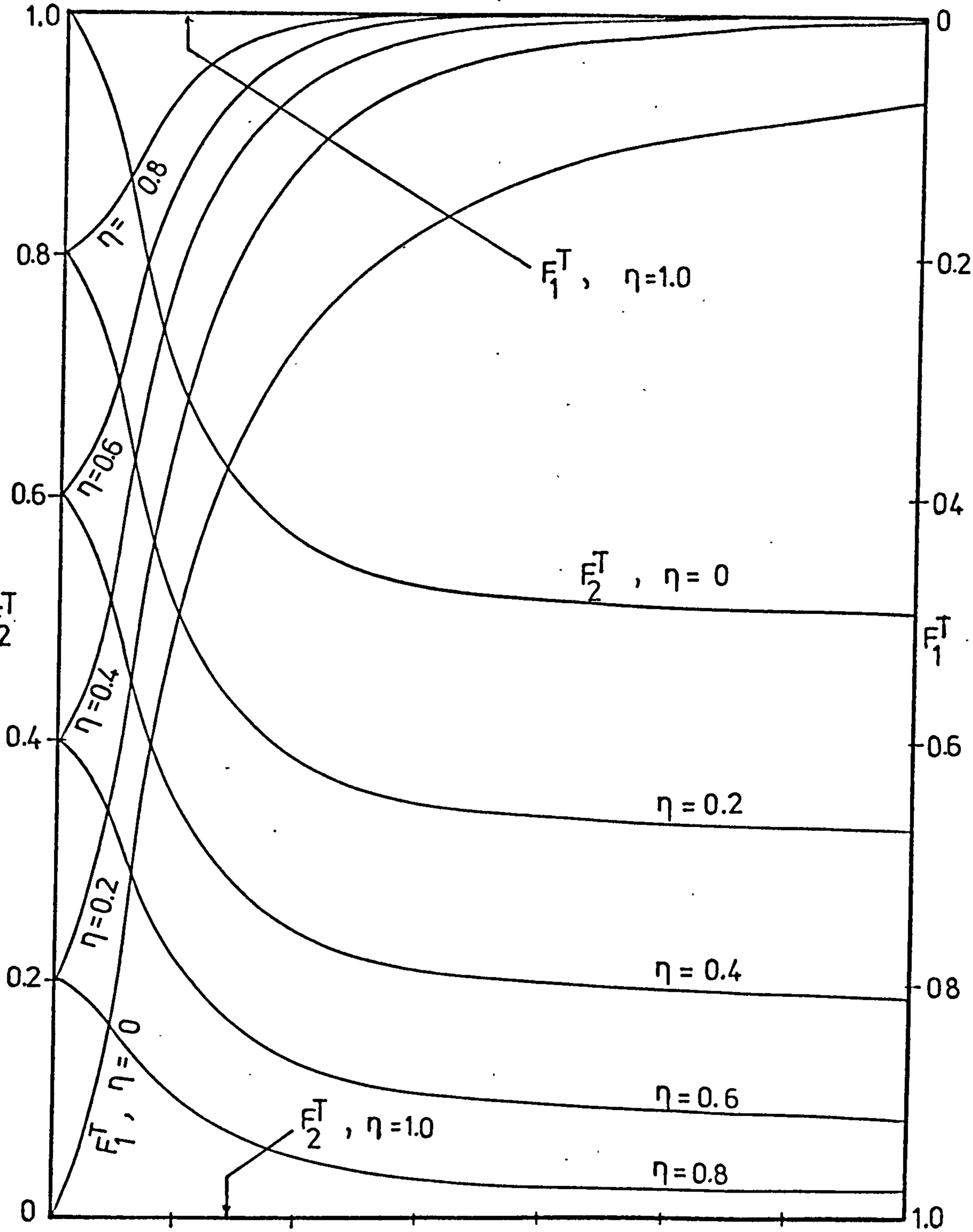

Variation of design functions F_1^T and F_2^T for standard load cases b, g, g′, g″

Fig. 3.7(b)

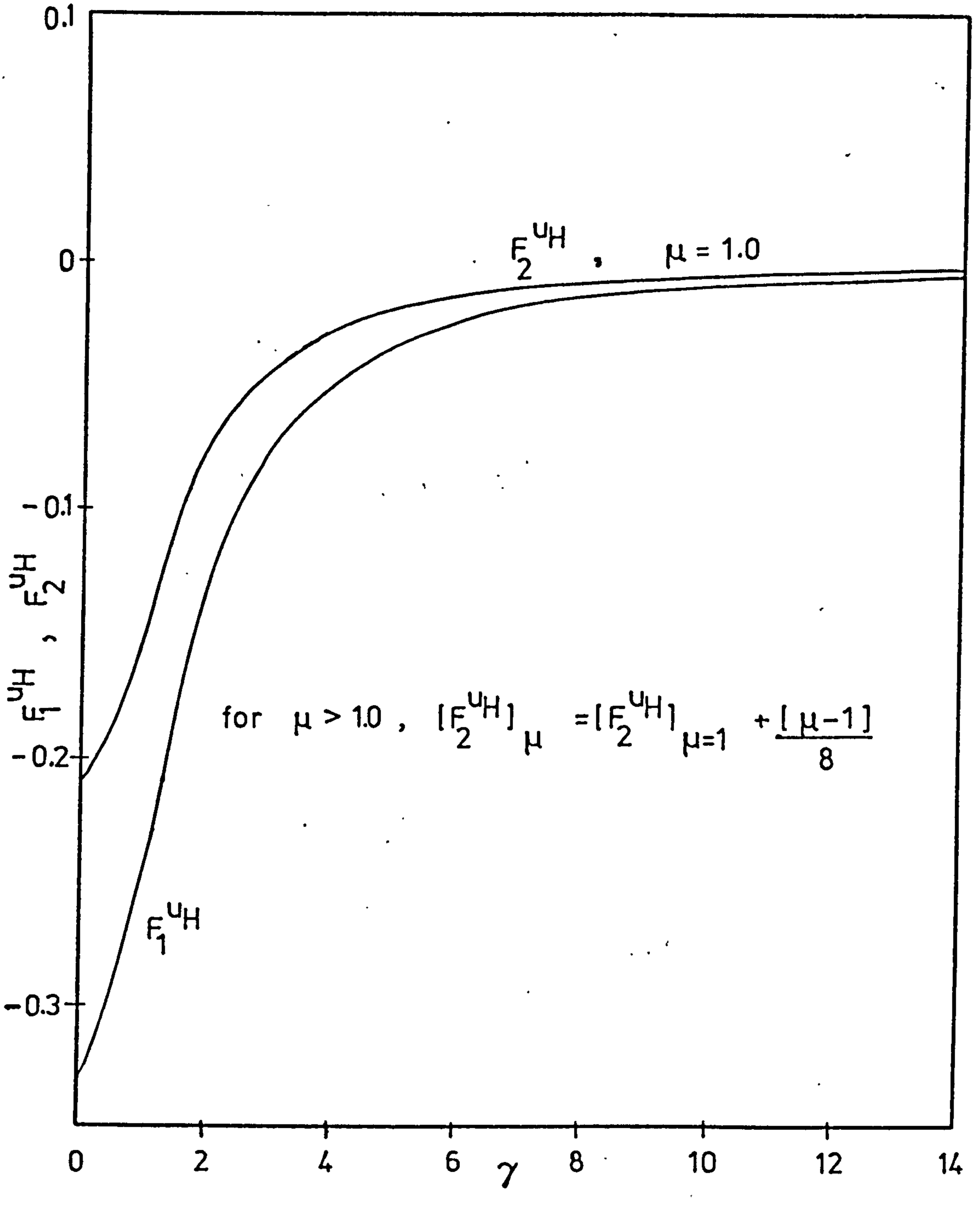

Variation of design functions F_1^{uH} and F_2^{uH} for standard load cases b, g , g′, g″

Fig. 3.7(c)

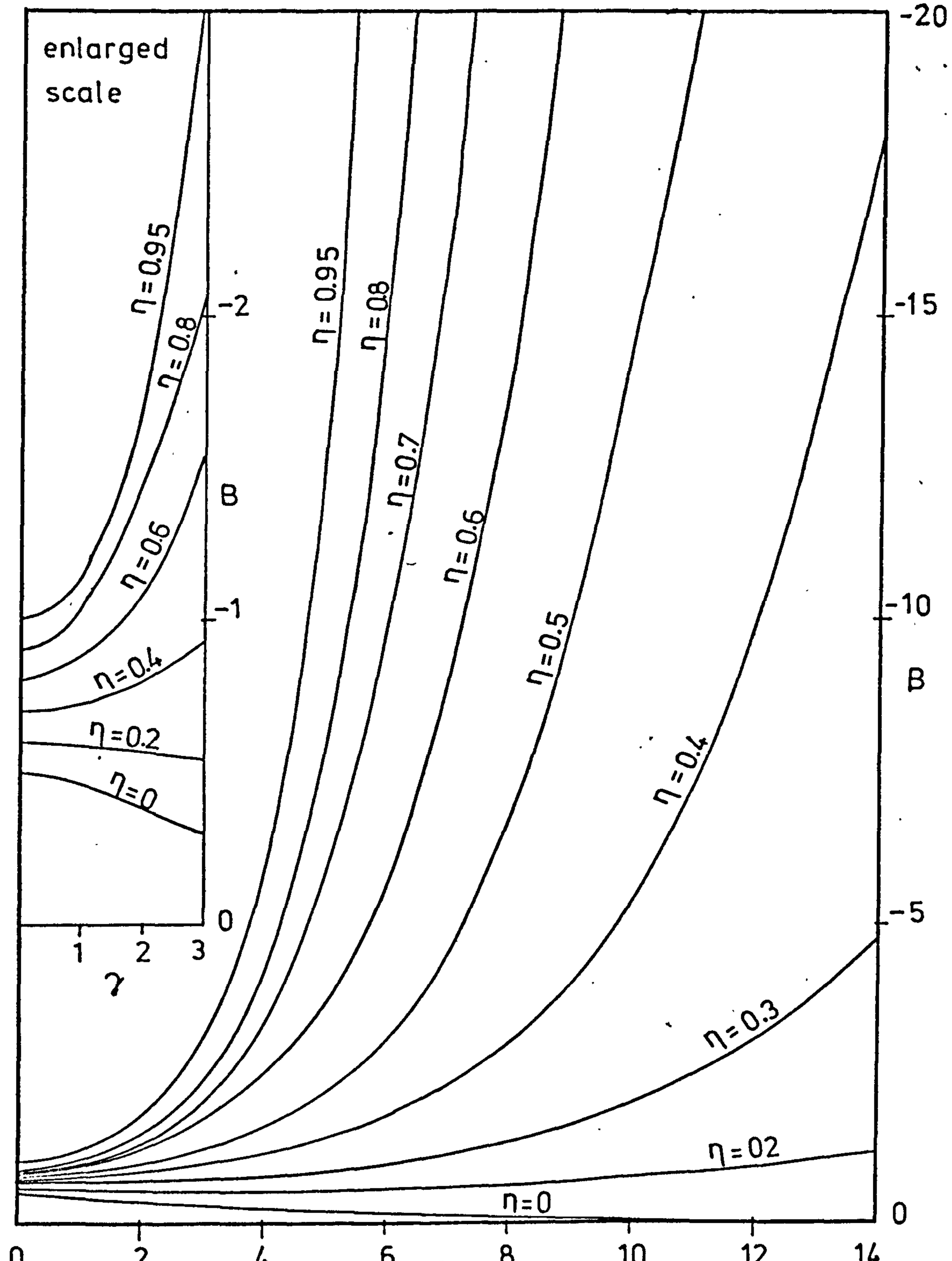

Position of maximum vertical shear distribution for standard load cases b, g, g′, g″

Fig. 3.7(d)

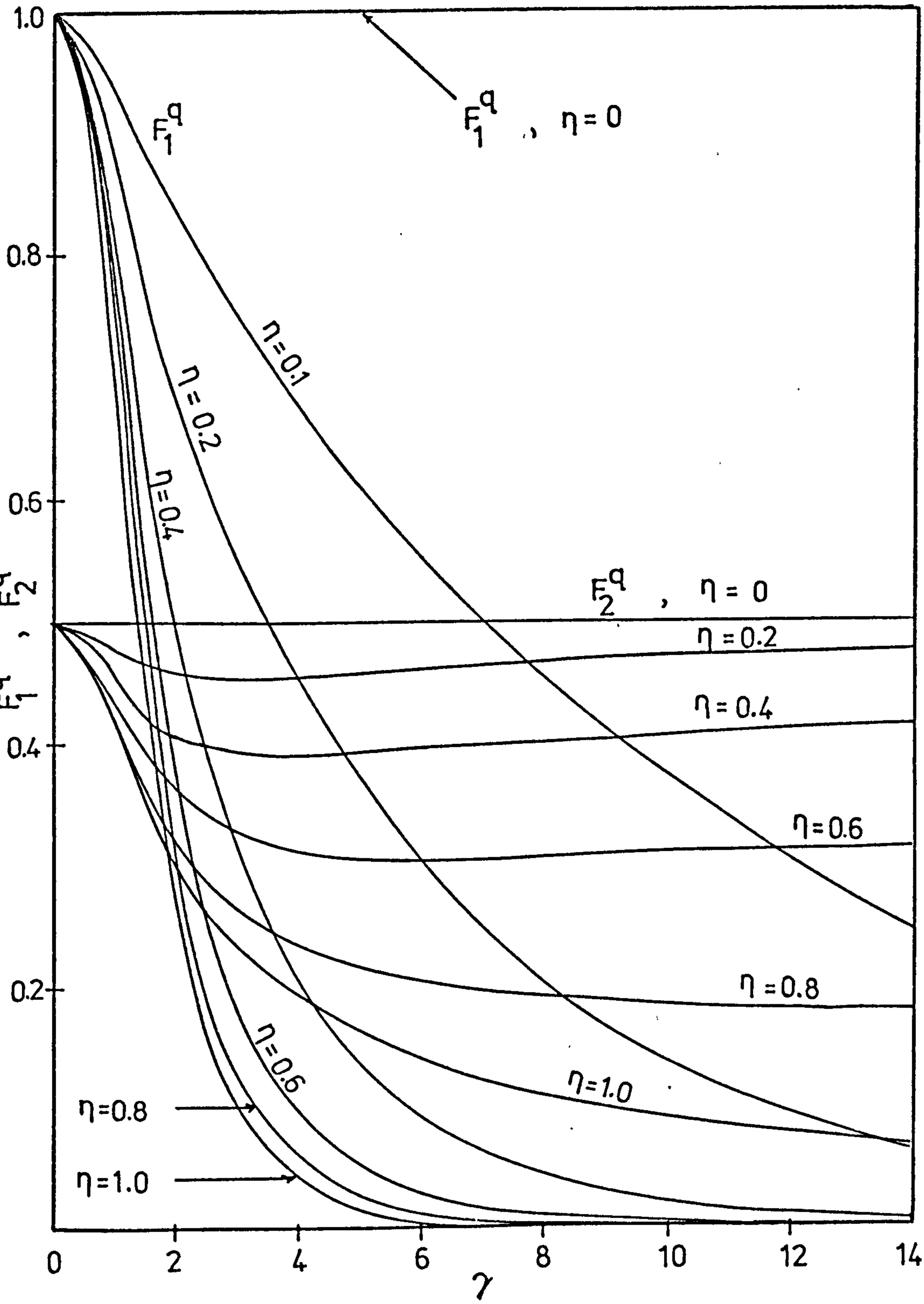

Variation of design functions F_1^q and F_2^q for standard load case c

Fig. 3.8(a)

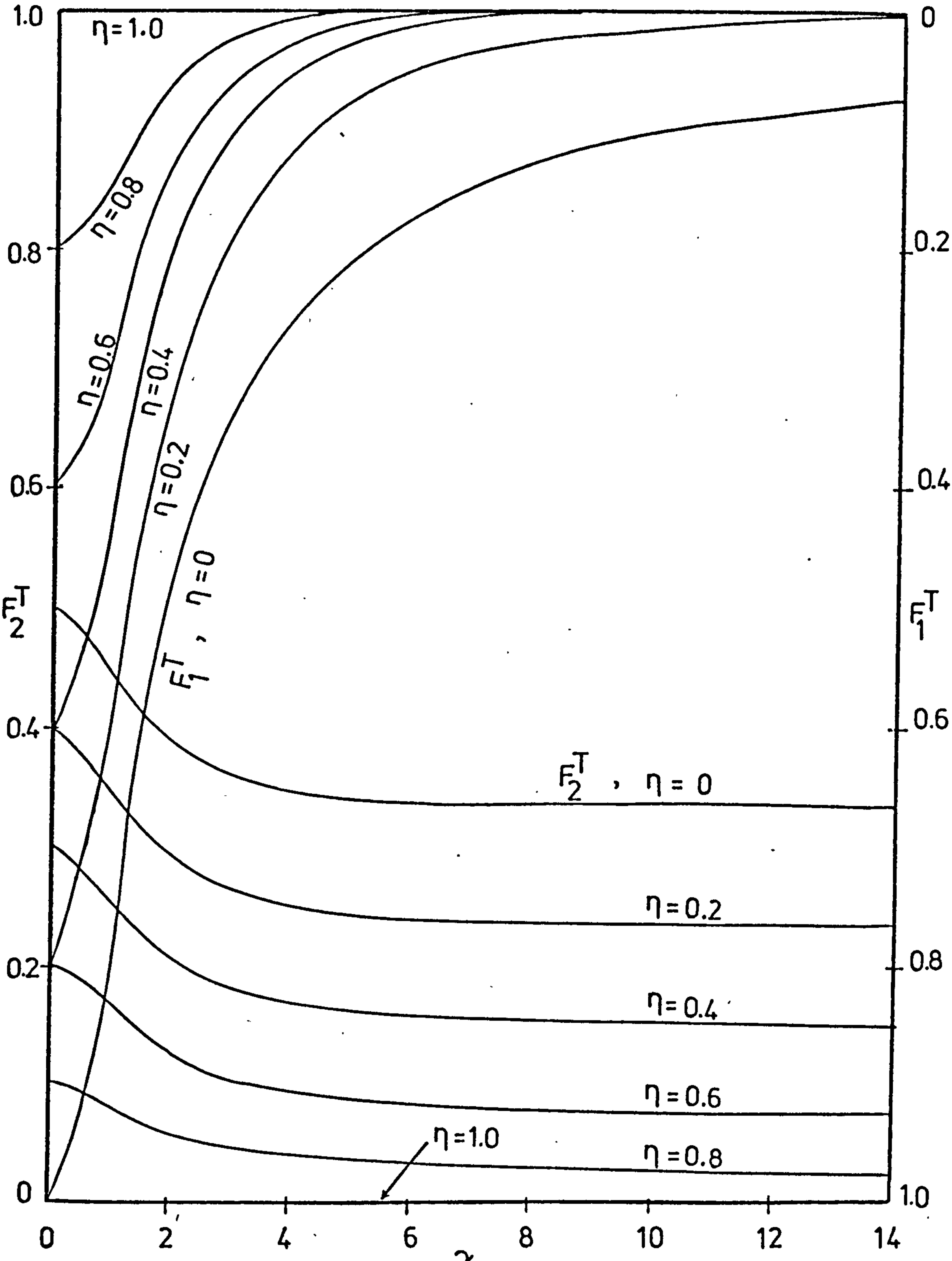

Variation of design functions F_1^T and F_2^T for standard load case c

Fig. 3.8(b)

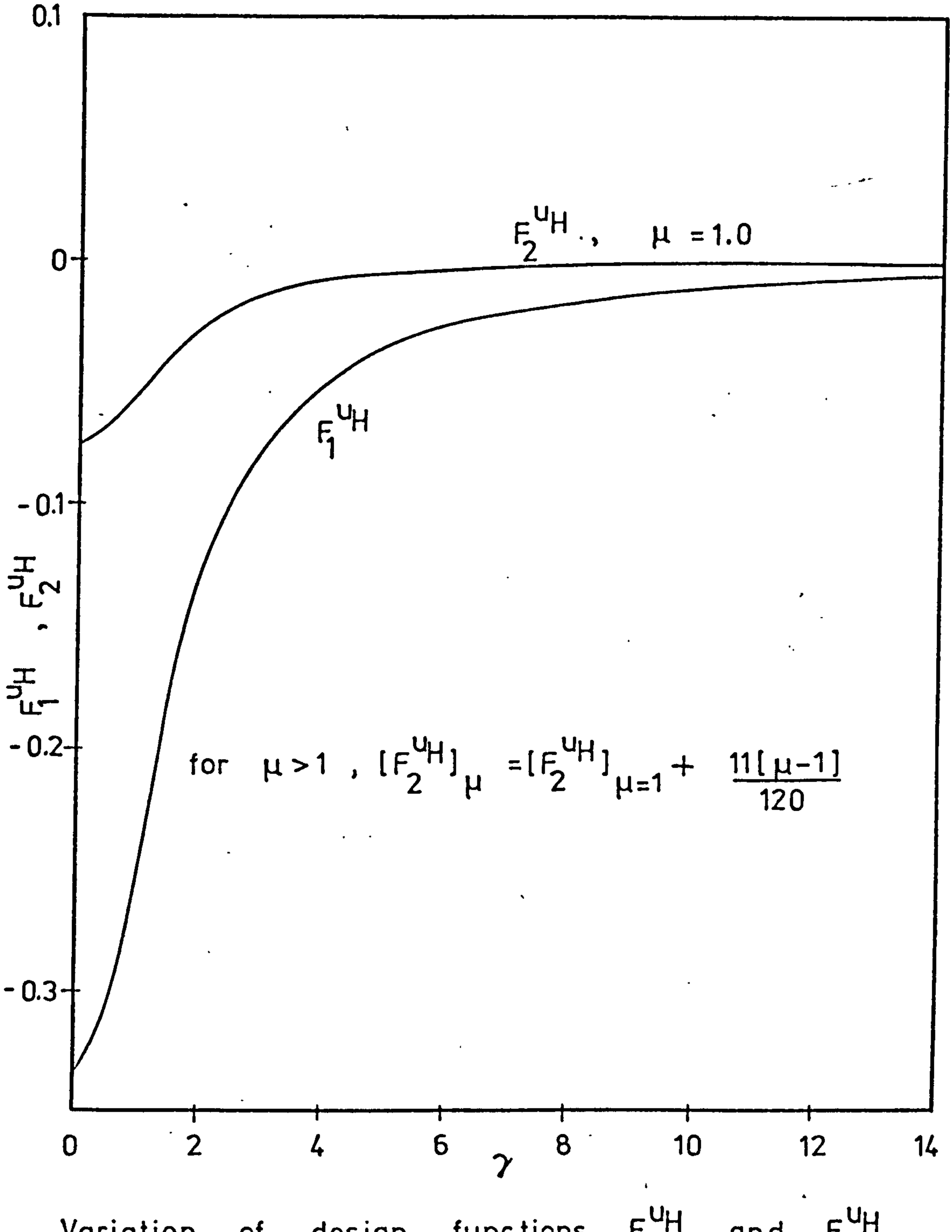

Variation of design functions F_1^{UH} and F_2^{UH} for standard load case c

Fig. 3.8(c)

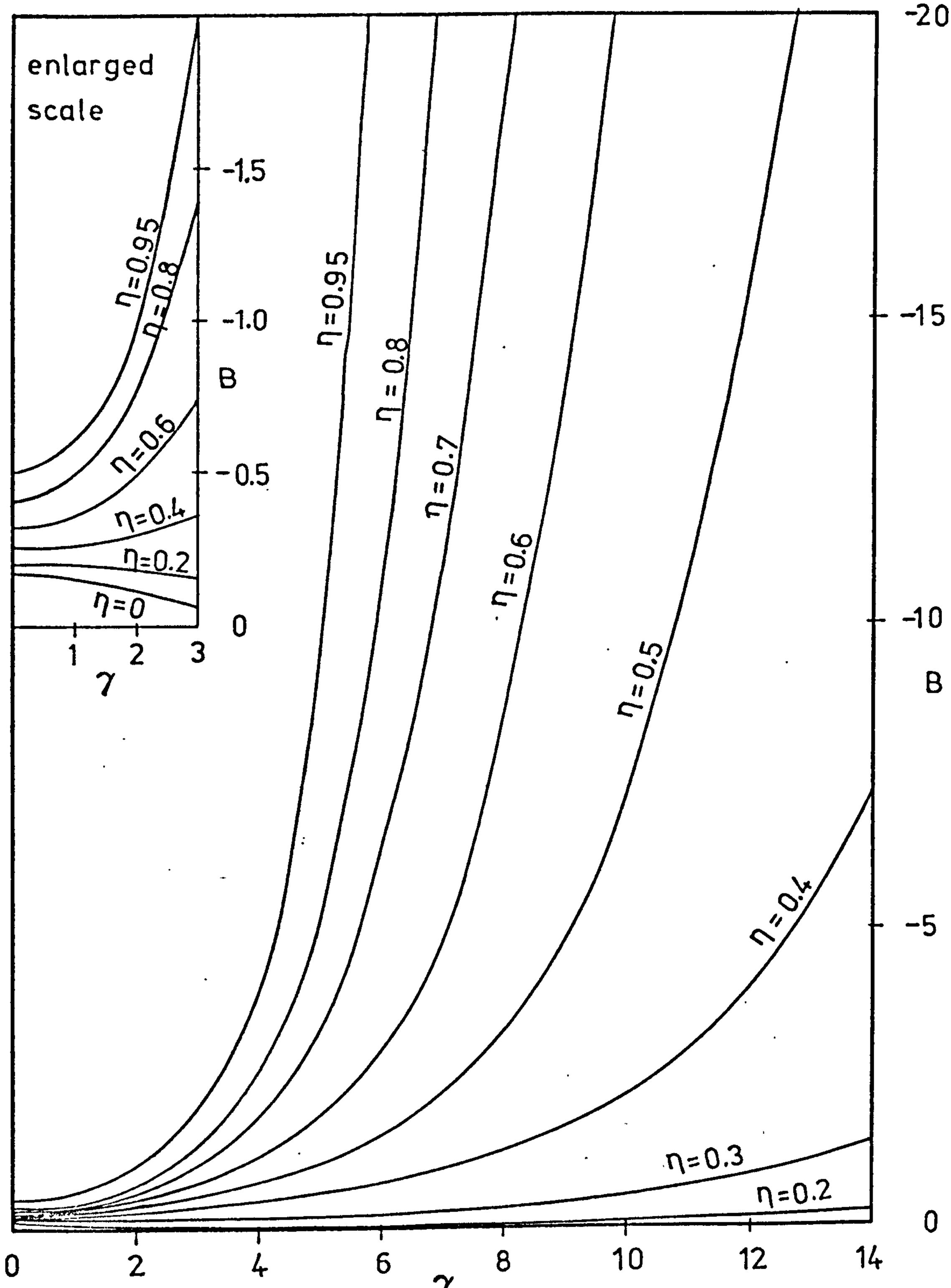

Position of maximum vertical shear distribution for standard load case c

Fig. 3.8(d)

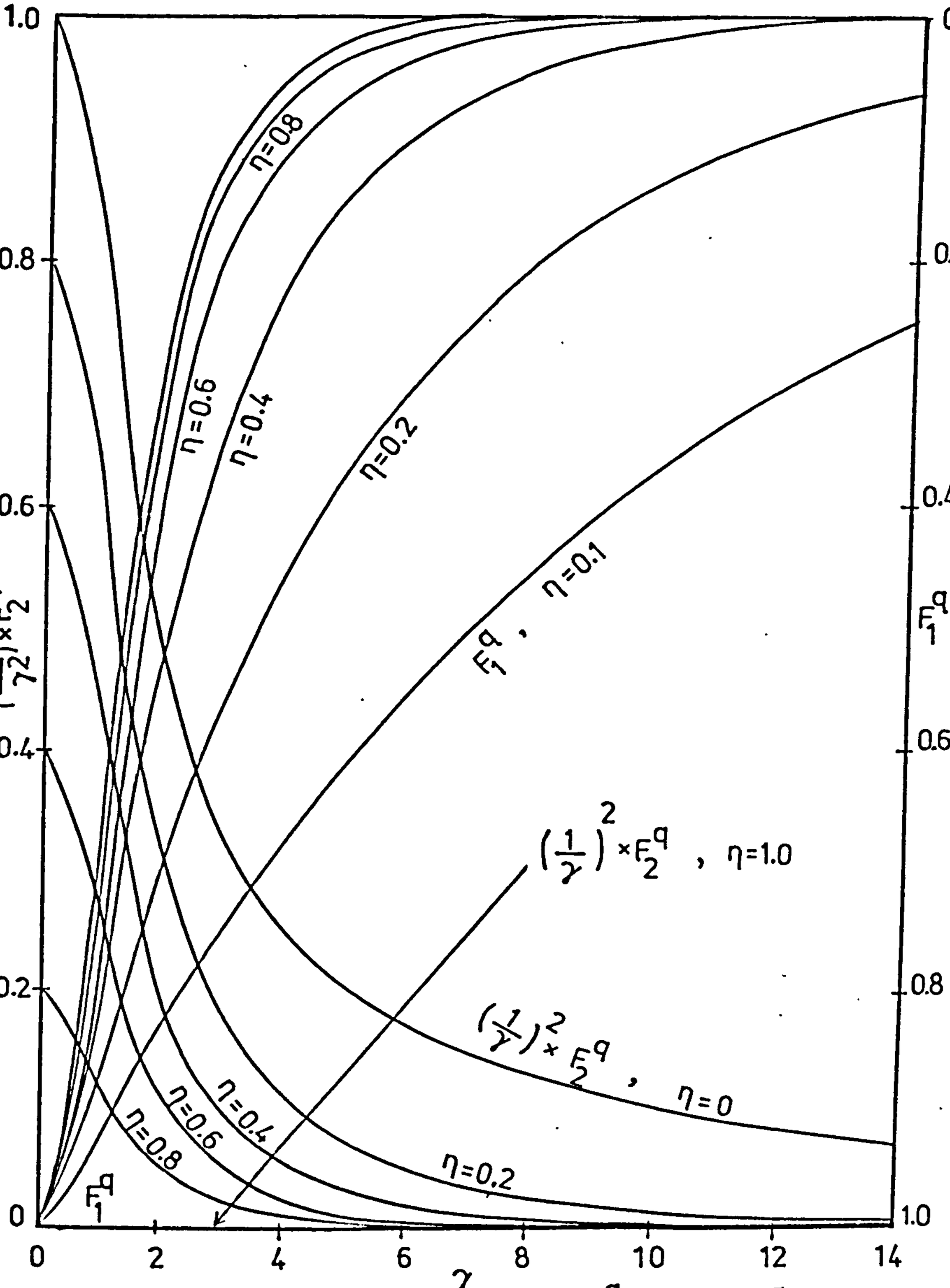

Variation of design functions F_1^q and F_2^q for standard load cases e, e′, e″, m, m′

Fig. 3.9(a)

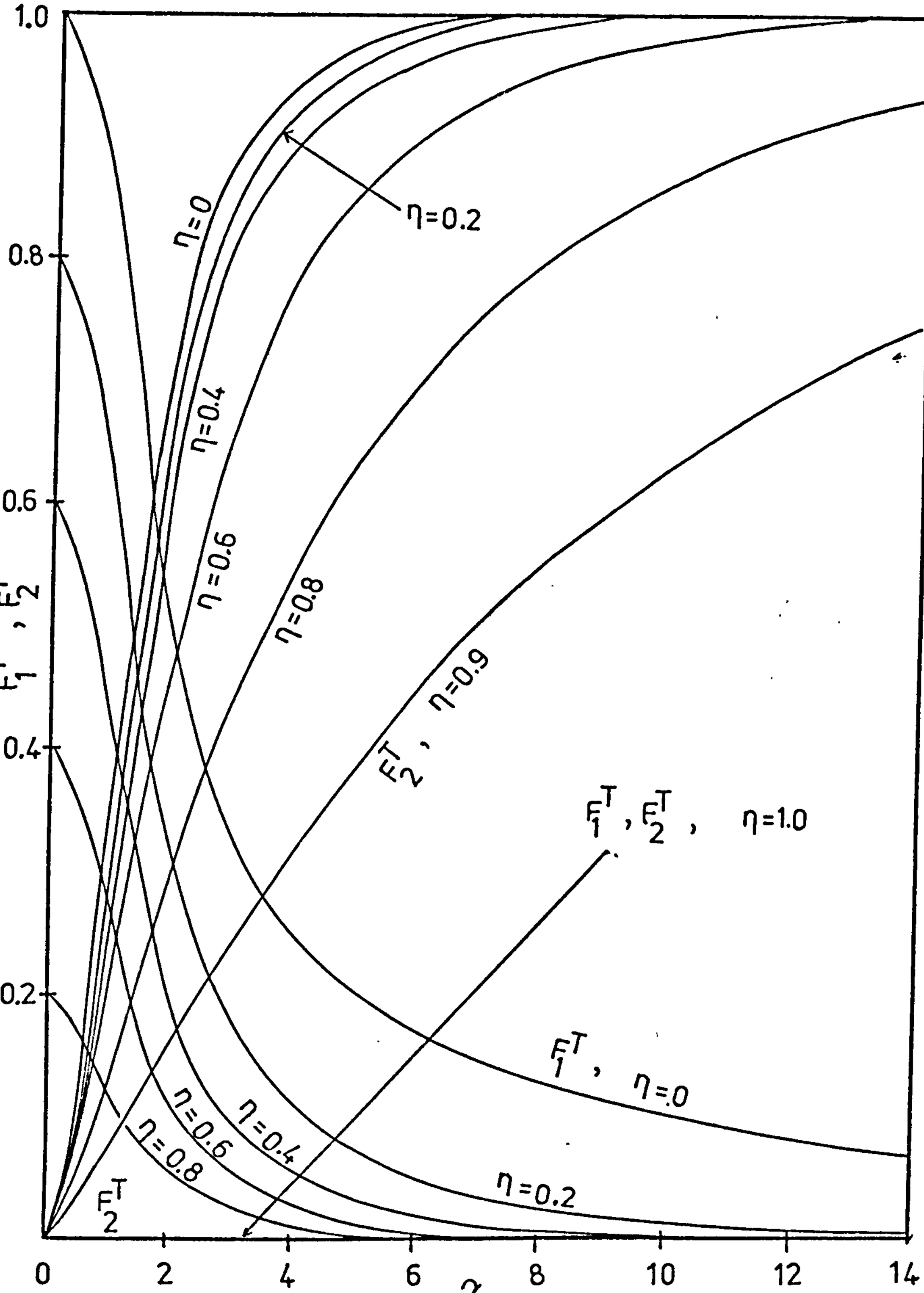

Variation of design functions F_1^T and F_2^T for standard load cases e, e′, e″, m, m′

Fig. 3.9(b)

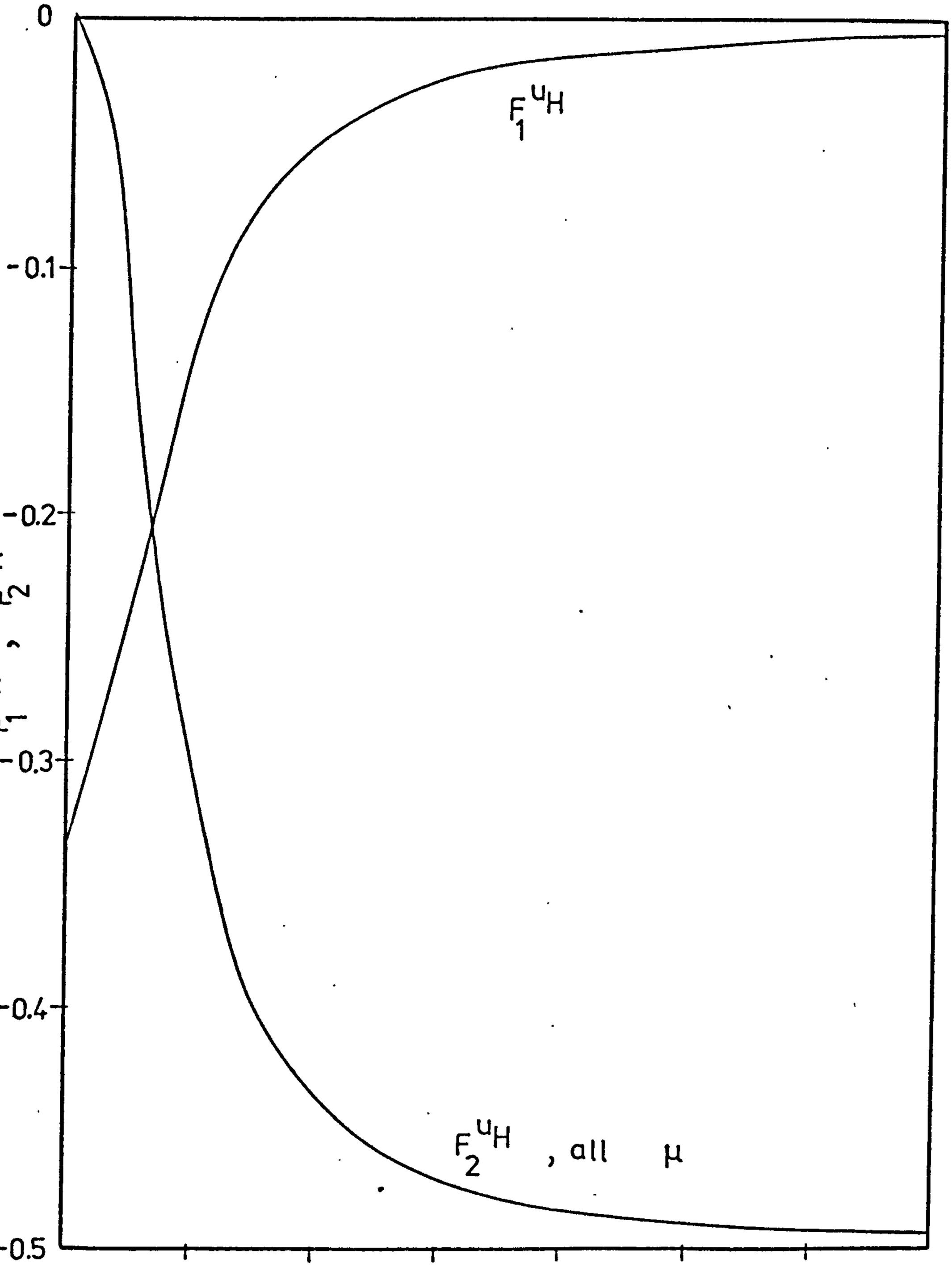

Variation of design functions F_1^{uH} and F_2^{uH} for standard load cases e, e', e'', m, m'

Fig. 3.9(c)

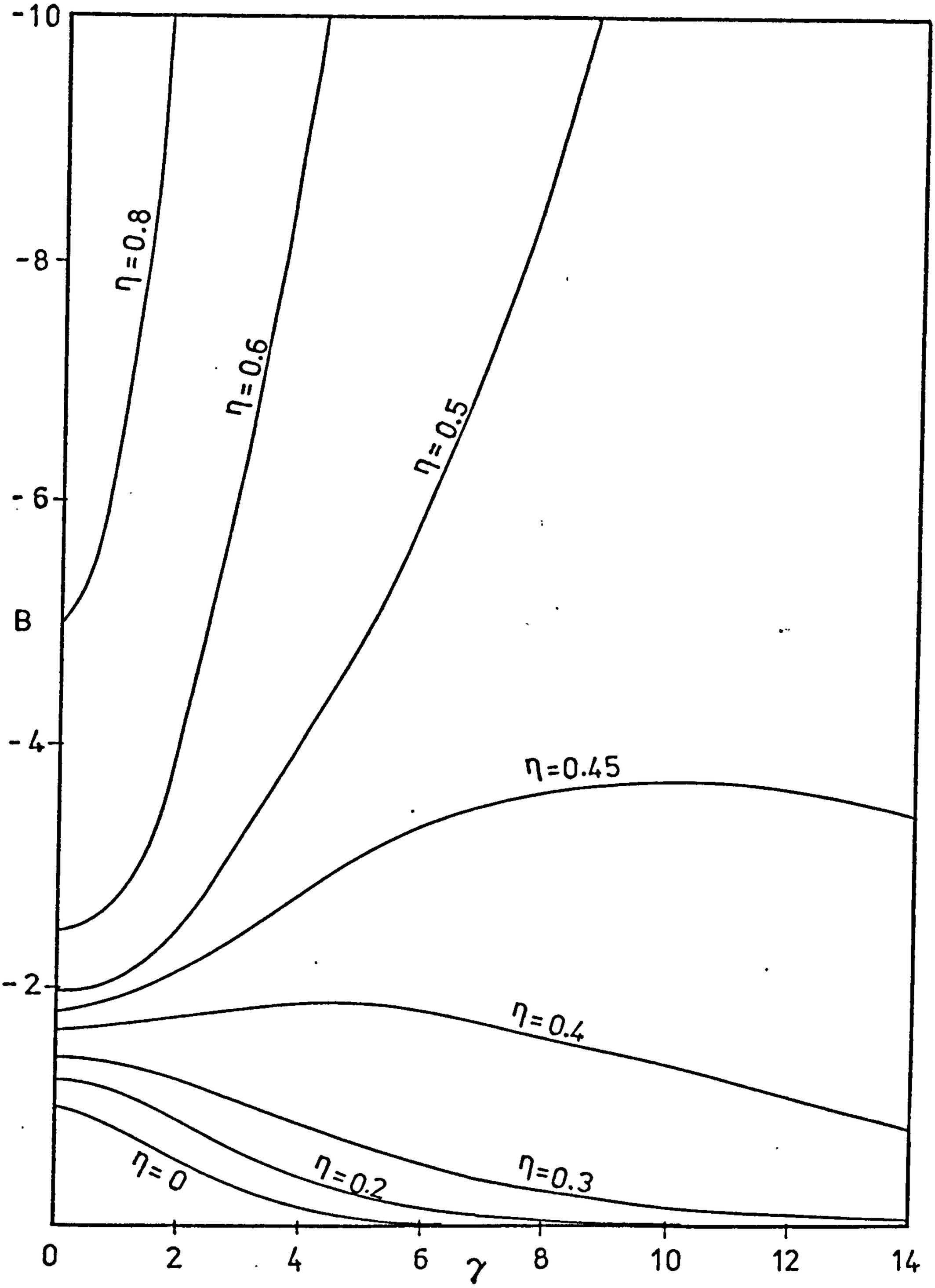

Position of maximum vertical shear distribution for standard load cases e, e′, e″, m, m′

Fig. 3.9(d)

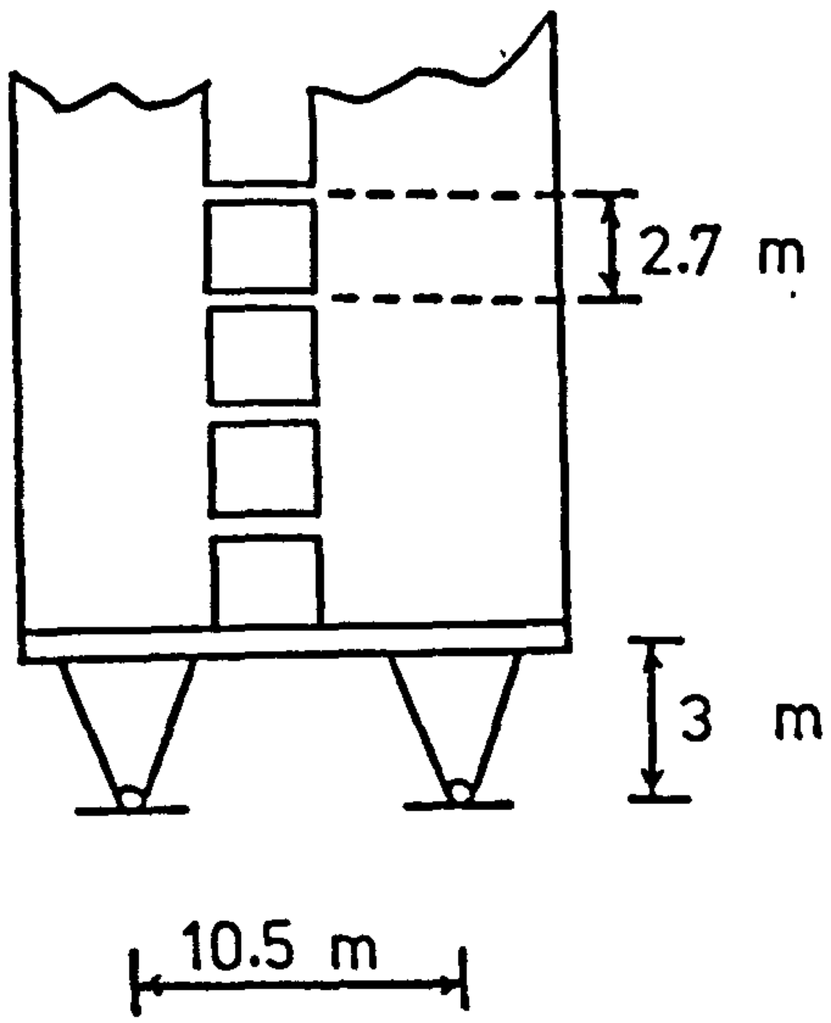

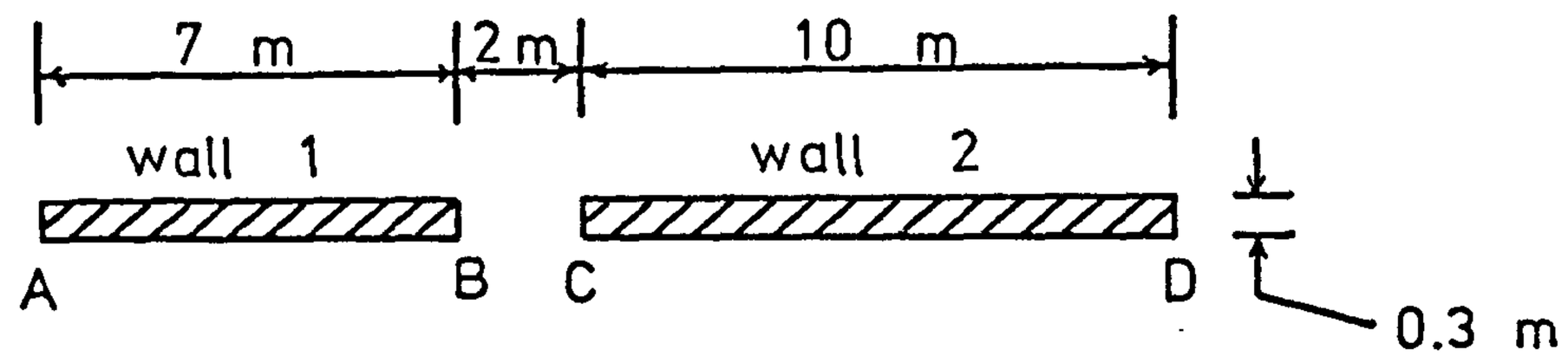

Example problem 1

Fig. 3.10

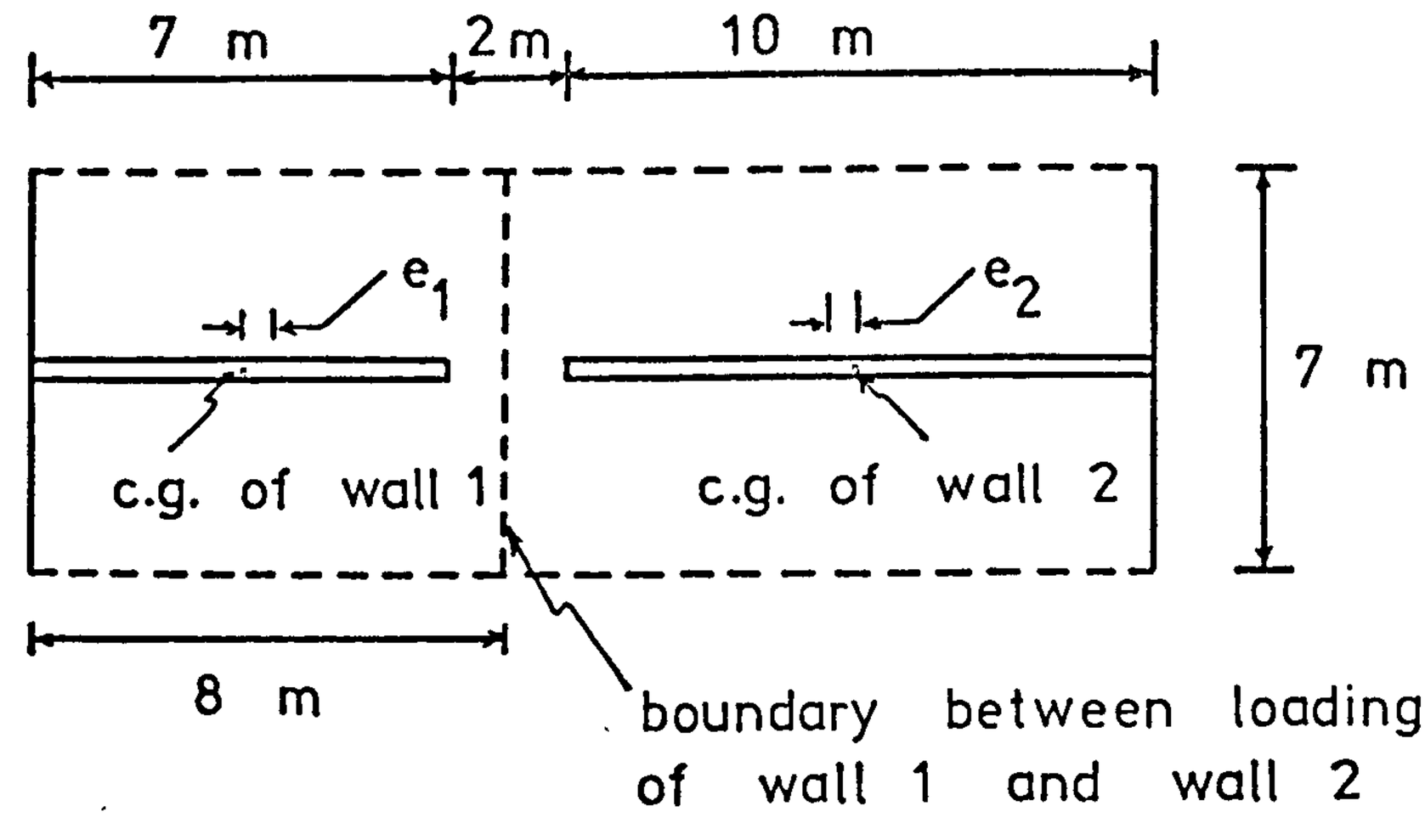

Example problem 2

Fig. 3.11

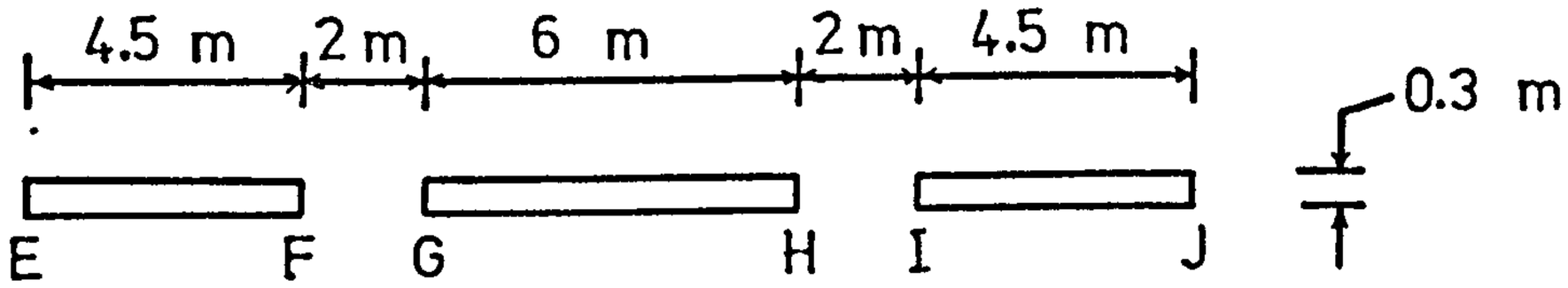

Example problem 3

Fig. 3.12

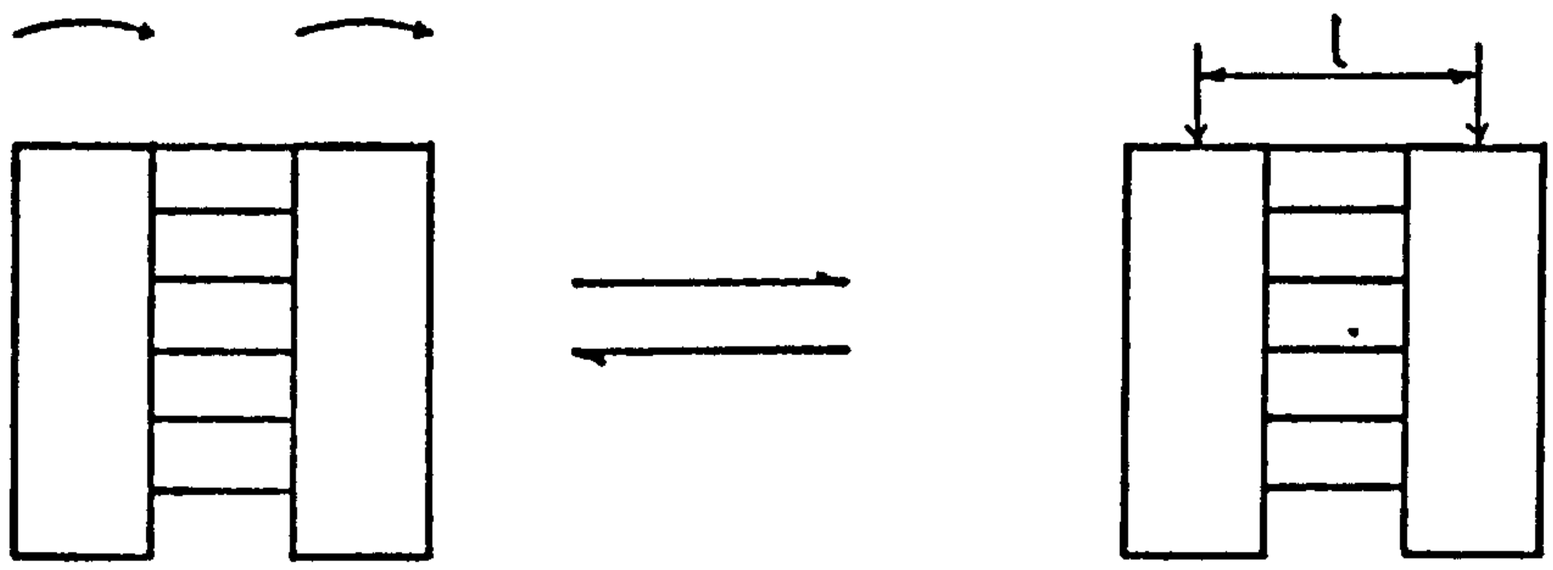

(1) concentrated moments at the tops

concentrated vert. loads at the tops passing through the centroidal axes of the walls

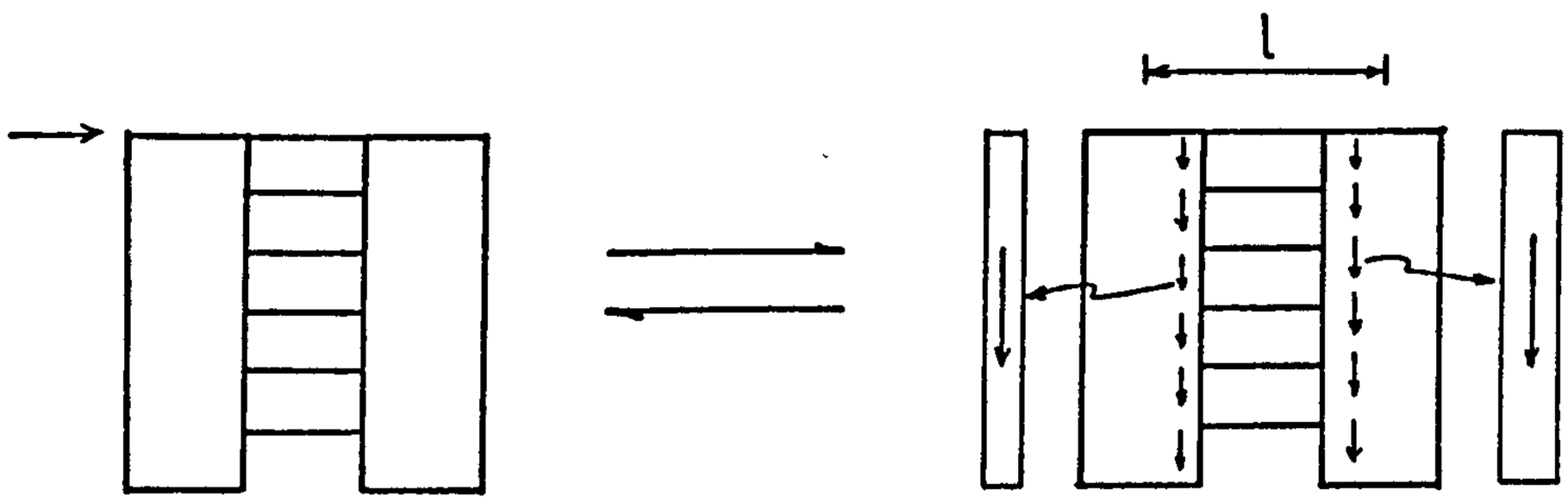

(2) concentrated lateral load at the top

uniformly dist. vert. loads per unit height

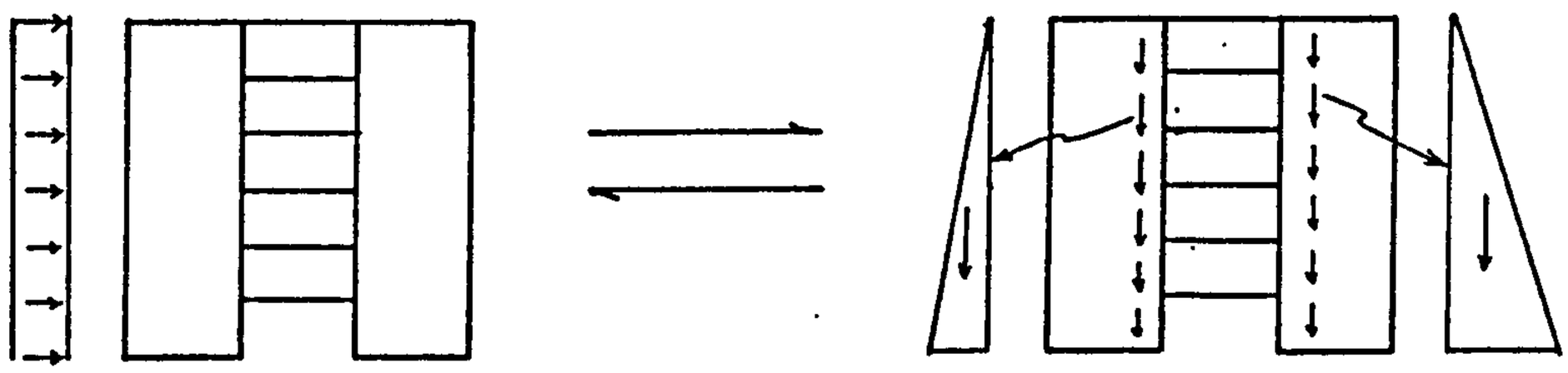

(3) uniformly dist. lateral load

triangularly dist. vert. loads per unit height

Correspondences between standard load cases

Fig. 3.13

Function	Expression
f^q	$\frac{ql\,\mu}{W}$
f^T	$\frac{Tl\,\mu}{WH}$
* f^{u_H}	$\frac{EI\,\mu}{RWH^3}\ u_H$
F_1^q	$\frac{\cosh\gamma(1-\eta)}{\cosh\gamma}$
F_1^T	$\frac{\sinh\gamma(1-\eta)}{\gamma\cosh\gamma}$
* $F_1^{u_H}$	$\frac{\tanh\gamma}{\gamma^3} - \frac{1}{\gamma^2}$
F_2^q	1
F_2^T	$(1-\eta)$
* $F_2^{u_H}$	$\frac{1}{3}(\mu - 1)$
* $F_3^{u_H}$	$\frac{r_5}{R}\left[r_4(f^T)_0 + \frac{\mu}{\gamma^2}\left((f^q)_0 - r_6 J_3\right)\right]$ $+\frac{\mu}{3R}\left[(1-R)(1-\varkappa) + \varkappa(J_1 - 1)\right]$
B	$(1-\varkappa)\left[\frac{r_1(1+\frac{h_0}{H}) - r_2(F_2^T)_0 - r_3(F_2^q)_0}{r_3 + r_2(F_1^T)_0}\right]$ $+\varkappa\left[\frac{r_1(1+\frac{h_0 J_2}{H}) + r_6 J_3 - r_2(F_2^T)_0 - r_3(F_2^q)_0 + r_7 J_4}{r_3 + r_2(F_1^T)_0}\right]$

Note:- * Not applicable to wall-load category C

Design Expressions for Load Cases a, f, f', f''
Applicable to Structural-load Systems
A_a, A_f, B_a, B_f', C_f''
(Design Curves Fig. 3.6)

Table 3.1

Function	Expression
f^{q}	$ql\,\mu/W$
f^{T}	$Tl\,\mu/WH$
* f^{u_H}	$EI\,\mu\,u_H/WH^3R$
F_1^q	$\cosh\gamma(1-\eta)/\cosh\gamma$
F_1^T	$\sinh\gamma(1-\eta)/(\gamma\cosh\gamma)$
* $F_1^{u_H}$	$(\tanh\gamma/\gamma^3) - (1/\gamma^2)$
F_2^q	$(1-\eta) + \sinh\gamma\eta\ /(\gamma\cosh\gamma)$
F_2^T	$\frac{1}{2}(1-\eta)^2 + (1/\gamma^2) - \cosh\gamma\eta\ /(\gamma^2\cosh\gamma)$
* $F_2^{u_H}$	$\frac{1}{8}(\mu-1) - (1/2\gamma^2) - (1/\gamma^4\cosh\gamma) + 1/\gamma^4$
* $F_3^{u_H}$	$(\frac{r_5}{R})\ \left[r_4(f^T)_0 + \frac{\mu}{\gamma^2}((f^q)_0 - r_6J_3)\right]$ $+\frac{\mu}{8R}\ \left[(1-\varkappa)(1-R) + \varkappa(2J_1 - 1)\right]$
B	$(1-\varkappa)\left[\frac{r_1(\frac{1}{2}+\frac{h_0}{H}) - r_2(F_2^T)_0 - r_3(F_2^q)_0}{r_3 + r_2(F_1^T)_0}\right]$ $+\varkappa\left[\frac{r_1(J_1+\frac{h_0J_2}{H})+r_6J_3-r_2(F_2^T)_0-r_3(F_2^q)_0+r_7J_4}{r_3 + r_2(F_1^T)_0}\right]$

Note * Not applicable to wall-load category C

Design Expressions for Load Cases b, g, g', g"
Applicable to Structural-Load Systems A_b, A_g,
B_b, B_g', $C_g"$
(Design Curves Fig. 3.7)

Table 3.2

Function	Expression
f^q	$\frac{1}{W}\ (ql\,\mu\ )$
f^T	$\frac{1}{WH}\ (Tl\,\mu\ )$
f^{u_H}	$\frac{1}{RWH^3}(EI\,\mu\ )u_H$
F_1^q	$\frac{\cosh\ \gamma(1-\eta\ )}{\cosh\gamma}$
F_1^T	$\frac{\sinh\ \gamma(1-\eta\ )}{\gamma\cosh\gamma}$
$F_1^{u_H}$	$\frac{\tanh\gamma}{\gamma^3} - \frac{1}{\gamma^2}$
F_2^q	$\frac{1}{2}(1-\eta^2) + \frac{\sinh\gamma\eta}{\gamma\cosh\gamma} + \frac{\cosh\ \gamma(1-\eta\ )}{\gamma^2\cosh\gamma} - \frac{1}{\gamma^2}$
F_2^T	$\frac{1}{3}-\frac{1}{2}\eta\ + \frac{1}{6}\eta^3 + \frac{\eta}{\gamma^2} + \frac{\sinh\ \gamma(1-\eta\ )}{\gamma^3\cosh\gamma} - \frac{\cosh\gamma\eta}{\gamma^2\cosh\gamma}$
$F_2^{u_H}$	$\frac{11}{120}(\mu-1) + \frac{\tanh\gamma}{\gamma^5} - \frac{1}{\gamma^4\cosh\gamma} - \frac{1}{6\ \gamma^2}$
$F_3^{u_H}$	$\frac{r_5}{R}(\ r_4(f^T)_0 + \frac{\mu}{\gamma^2}\ (f^q)_0\ )\ + \frac{11\ \mu}{120R}\ (1-R)$
B	$\frac{r_1(\frac{1}{3} + \frac{1}{2}\ \frac{h_0}{H}) - r_2\ (F_2^T)_0 - r_3(F_2^q)_0}{r_3 + r_2\ (F_1^T)_0}$

Design Expressions for Load Case c
Applicable to Structural-load Systems
A_c, B_c

(Design Curves Fig. 3.8)

Table 3.3

Function	Expression
f^q	$\frac{1}{W}\ (ql\,\mu\ )$
f^T	$\frac{1}{WH}\ (Tl\,\mu\ )$
$*\ f^{u_H}$	$\frac{1}{RWH^3}\ (EI\,\mu\ )u_H$
F_1^q	$\frac{\cosh\ \gamma(1-\eta\ )}{\cosh\gamma}$
F_1^T	$\frac{\sinh\ \gamma(1-\eta\ )}{\gamma\cosh\gamma}$
$*\ F_1^{u_H}$	$\frac{\tanh\ \gamma}{\gamma^3} - \frac{1}{\gamma^2}$
F_2^q	$\frac{\gamma\sinh\gamma\eta}{\cosh\gamma}$
F_2^T	$1 - \frac{\cosh\gamma\eta}{\cosh\gamma}$
$*\ F_2^{u_H}$	$\frac{1}{\gamma^2} - \frac{1}{\gamma^2\ \cosh\gamma} - \frac{1}{2}$
$*\ F_3^{u_H}$	$\frac{r_5}{R}\ \left[r_4(f^T)_0 + \frac{\mu}{\gamma^2}\ ((f^q)_0 - r_6J_3)\right]\ + \frac{\mu\ J_1}{2R}$
B	$\frac{r_1(J_1+\ \frac{h_0J_2}{H}) + r_6J_3 - r_2(F_2^T)_0 - r_3(F_2^q)_0 + r_7J_4}{r_3 + r_2\ (F_1^T)_0}$

Note * Not applicable to wall-load category C

Design Expressions for Load Cases e, e', e", m, m' Applicable to Structural-load Systems A_e, A_m, B_e', B_m', C_e"

(Design Curves Fig. 3.9)

Table 3.4

Parameter	Structural-load System							
	A_a	A_b	A_c	A_d	A_e	A_f	A_g	A_m
R	1	1	1	1	1	1	1	1
R_1	1	1	1	1	1	1	1	1
χ	0	0	0	0	1	1	1	0
W	p_0H	w_0H	ϑ_0H	p_nH	$p_1 \frac{I}{lA_1} - p_2 \frac{I}{lA_2}$	$w_1(e_1 + \frac{I}{lA_1})$ $-w_2(e_2 + \frac{I}{lA_2})$	$\vartheta_1(e_1 + \frac{I}{lA_1})$ $-\vartheta_2(e_2 + \frac{I}{lA_2})$	$m_1 + m_2$
J_1	1	1	1	1	$\frac{1}{W}(p_1e_1 - p_2e_2)$	$\frac{1}{W}(w_1e_1 - w_2e_2)$	$\frac{1}{2W}(\vartheta_1e_1 - \vartheta_2e_2)$	1
J_2	0	0	0	0	$\frac{Hp_1}{W}\tan\theta_1$ $-\frac{Hp_2}{W}\tan\theta_2$	$\frac{Hw_1}{W}\tan\theta_1$ $-\frac{Hw_2}{W}\tan\theta_2$	$\frac{H\vartheta_1}{2W}\tan\theta_1$ $-\frac{H\vartheta_2}{2W}\tan\theta_2$	0
J_3	0	0	0	0	$\frac{H}{W}(p_1 - \frac{K_{v1}}{K_{v2}}p_2)$	$\frac{H}{W}(w_1 - \frac{K_{v1}}{K_{v2}}w_2)$	$2\frac{H}{W}(\vartheta_1 - \frac{K_{v1}}{K_{v2}}\vartheta_2)$	0
J_4	0	0	0	0	$\frac{Hp_2}{2W}$	$\frac{Hw_2}{2W}$	$\frac{H\vartheta_2}{4W}$	0
I	$I_1 + I_2$							
μ	$1 + \frac{I}{l^2}(\frac{1}{A_1} + \frac{1}{A_2})$							
γ^2	$\frac{12\, I_c\, l^2\, H^2\, \mu}{b^3hI}$							

Structural-load Parameters for Structural-load Systems A_a, A_b, A_c, A_d, A_e, A_f, A_g, A_m

Table 3.5

Parameter	Structural-load System							
	B_a	B_b	B_c	B_d	$B_{e'}$	$B_{f'}$	$B_{g'}$	$B_{m'}$
R	2	2	2	2	2	2	2	2
R_1	2	2	2	2	2	2	2	2
$\varkappa$	0	0	0	0	1	1	1	0
W	p_0H	w_0H	ϑ_0H	P_nH	$2p_1e_1+\frac{p_1I}{lA_1}$	$2w_1e_1+\frac{w_1I}{lA_1}$	$2\vartheta_1e_1+\frac{1^I}{lA_1}$	$m_1 + m_2$
J_1	1	1	1	1	$\frac{2p_1e_1}{W}$	$\frac{2w_1e_1}{W}$	$\frac{\vartheta_1e_1}{W}$	1
J_2	0	0	0	0	$\frac{2Hp_1\tan\theta_1}{W}$	$\frac{2Hw_1\tan\theta_1}{W}$	$\frac{H\vartheta_1\tan\theta_1}{W}$	0
J_3	0	0	0	0	$\frac{H}{W}p_1$	$\frac{H}{W}w_1$	$\frac{1}{2}\frac{H}{W}\vartheta_1$	0
J_4	0	0	0	0	$\frac{1}{2}\frac{H}{W}p_2$	$\frac{1}{2}\frac{H}{W}w_2$	$\frac{1}{4}\frac{H}{W}\vartheta_2$	0
I	$2I_1 + I_2$							
μ	$2 + \frac{I}{l^2A_1}$							
γ^2	$\frac{12I_cl^2H^2\mu}{b^3hI}$							

Structural-load Parameters for Structural-load Systems B_a, B_b, B_c, B_d, $B_{e'}$, $B_{f'}$, $B_{g'}$, $B_{m'}$

Table 3.6

Para-meter	Structural-load System		
	$C_{e''}$	$C_{f''}$	$C_{g''}$
R	2	2	2
R_1	0	0	0
$\varkappa$	1	1	1
W	$\frac{p_1 I}{lA_1} - \frac{p_2 I}{lA_2}$	$\frac{w_1 I}{lA_1} - \frac{w_2 I}{lA_2}$	$\frac{\vartheta_1 I}{lA_1} - \frac{\vartheta_2 I}{lA_2}$
J_1	0	0	0
J_2	0	0	0
J_3	$\frac{H}{W}(p_1 - \frac{K_{v1}}{K_{v2}} p_2)$	$\frac{H}{W}(w_1 - \frac{K_{v1}}{K_{v2}} w_2)$	$\frac{H}{2W}(\vartheta_1 - \frac{K_{v1}}{K_{v2}} \vartheta_2)$
J_4	$\frac{Hp_2}{2W}$	$\frac{Hw_2}{2W}$	$\frac{H \vartheta_2}{4W}$
I	$2I_1 + I_2$		
μ	$\frac{I}{l^2} (\frac{1}{A_1} + \frac{2}{A_2})$		
γ^2	$\frac{12 I_c l^2 H^2}{b^3 h I} \mu$		

Structural-load Parameters for Structural-load Systems $C_{e''}$, $C_{f''}$, $C_{g''}$

Table 3.7

Parameters	Support System			
	Portal[a] frame	Columns[b] (two coupled walls)	Elastic Foundations (Fixed connection)	Elastic Foundations (Hinged Connection)
r_1	$\frac{1HI_c}{LhI_0}\mu$	$\frac{1}{L}\mu$	$\frac{\gamma^2 EI}{H(R_1 K_{\theta 1} + K_{\theta 2})}$	$\frac{\mu}{R}$
r_2	$\frac{HI_c}{hI_0}$	1	$\frac{\gamma^2 EI}{\mu H}\ \frac{R_1}{(R_1 K_{\theta 1} + K_{\theta 2})}$ $+ \frac{1}{1^2}\left(\frac{1}{K_{v1}} + \frac{(2-R_1)}{K_{v2}}\right)$	$(1 - \frac{R_1}{R})\frac{\gamma^2 EI}{\mu H1^2}\left(\frac{1}{K_{v1}}\right.$ $\left. + \frac{2}{K_{v2}}\right) + \frac{R_1}{R}$
r_3	1	0	1	$(1 - \frac{R_1}{R})$
r_4	0	0	$\frac{EI}{H1^2}\left(\frac{1}{K_{v1}} + \frac{(2 - R_1)}{K_{v2}}\right)$	
r_5	$R_1 \frac{1}{L}$[c]	$R_1 \frac{1}{L}$[d]	1	
r_6	0	0	$\frac{\gamma^2 EI}{H^2 1 K_{v1}}$	
r_7	$\mu \frac{1I_c}{hI_0}(1-\frac{R_1}{R})$	0	0	

Note

(a), (b): The bases of both columns are hinged to a rigid foundation.

(c), (d): for deflection relative to the tops of columns; for the maximum deflection relative to the base of the frame the parameter r_5 should be replaced by $r_5(1 + h_0/H)$.

Wall-base Parameters

Table 3.8

Subgrade Modulus (KN/m3)	Wall Stresses at Base Level (KN/m^2)				Relative Settlement (m)	Max. Deflection (m)	Max. Vertical Shear Distribution (KN/m)
	σ_A	σ_B	σ_C	σ_D			
∞	1754	-835	1528	-2172	0	0.0079	22.98
2.7143×10^5	1358	171	312	-1383	0.0048	0.0362	38.61
2.7143×10^4	1294	334	115	-1256	0.051	0.2744	43.87

Example 1. Two Coupled Walls under Lateral Load.

Table 3.9

Subgrade Modulus (KN/m^3)	Wall Stresses at Base Level (KN/m^2)				Relative Settlement (m)	Max. Deflection (m)	Max. Vertical Shear Distribution (KN/m)
	σ_A	σ_B	σ_C	σ_D			
∞	-4447	-4286	-4502	-3993	0	-0.0008	-1.4533
$2.7143x1-^5$	-4436	-4312	-4533	-3978	0.0108	-0.0053	-1.2289
$2.7143x10^4$	-4435	-4318	-4539	-3976	0.1123	-0.0340	-1.2430

Note:- Axial force in wall 1 is compressive force.

Example 2:- Two Coupled Walls under Vertical Loads
(Positive eccentricities e_1 and e_2)

Table 3.10

Subgrade Modulus (KN/m^3)	Wall Stresses at Base Level (KN/m^2)				Relative Settlement (m)	Max. Deflection (m)	Max. Vertical Shear Distribution (KN/m)
	σ_A	σ_B	σ_C	σ_D			
∞	-4931	-4150	-6191	-2665	0	- 0.0037	- 9.9287
2.7143×10^5	-4840	-4380	-6469	-2533	0.0127	- 0.0155	-10.6528
2.7143×10^4	-4825	-4419	-6517	-2511	0.1256	- 0.1166	-10.7758

Note:- Axial force in wall 1 is compressive force.

Example 2:- Two Coupled Walls under Vertical Loads
(eccentricity e_1 is negative, and e_2 positive)

Table 3.11

Subgrade Modulus (KN/m^3)	Wall Stresses at Base Level (KN/m^2)			Relative Settlement (m)	Max. Deflection (m)	Max. Vertical Shear Distribution (KN/m)
	$6_B=-6_J$	$6_F=-6_I$	$6_G=-6_H$			
∞	1883	-787	1780	0	0.0032	30.32
2.7143×10^5	1124	415	472	0.0046	0.0219	43.05
2.7143×10^4	1050	533	344	0.0455	0.1574	51.50

Note:- Relative settlement is the differential settlement between outer and middle walls.

Example 3:- Symmetrical Three Coupled Walls under Lateral Loads.

Table 3.12

CHAPTER 4

SYMMETRICAL THREE DIMENSIONAL SHEAR WALL STRUCTURES

4.1 Notation

The following symbols are used in this Chapter:-

A	=	cross-sectional area of a wall
l	=	distance between the centroids of walls a and b of a coupled wall assembly
b	=	length of connecting beam
I_c	=	second moment of area of connecting beams
I	=	second moment of area in general
I_m, I_n	=	second moments of area about the major and minor principal axes, respectively, of a wall
h	=	storey height
E	=	modulus of elasticity
K	=	stiffness, or number of groups of coupled wall assemblies
X, Y, Z	=	structural co-ordinate axes
z	=	height co-ordinate (along the vertical Z axis)
λ , ξ	=	auxiliary height co-ordinates
u	=	horizontal displacement
θ	=	horizontal rotation
M	=	moment in general
S	=	shear force in general
C	=	cosine of an angle
R	=	horizontal projection of a vector on a horizontal axis
q	=	vertical shear distribution in the substitute

lamina of a coupled wall assembly

Q = analogous vertical shear distribution

Other subsidiary symbols are defined locally in the text.

4.2 Introduction

The development of multi-storey residential and hotel buildings has led to the extensive use of coupled shear walls and service cores as the main load-bearing elements. Although it is theoretically possible to analyse completely a three-dimensional shear wall structure using modern computer-orientated techniques, the large increase in the number of degrees of freedom inherent in the three dimensional analysis often causes the techniques to be either extremely lengthy or beyond the capacity of available computers. Simpler techniques, usually involving simplifying assumptions, which enable solutions to be achieved with less computation are, therefore, desirable. One technique which promises a great reduction in the computational effort is the continuous medium approach, since the amount of computation involved in this approach does not depend on the number of storeys of the structures.

The functional and practical requirements of multi-storey residential and hotel buildings tend to evolve structures with regular assemblies of coupled shear walls interspersed with service cores. Many of these buildings also possess overall plan forms which are symmetrical.

An analysis of regular symmetrical cross-wall

structures by the continuous medium approach has been recently presented[5]. In this Chapter, a continuous medium method of analysis for general symmetrical three-dimensional structures consisting of uniform coupled wall assemblies and cantilevered walls is presented. It is shown that the analysis of symmetrical structures can be reduced to the analyses of simple analogous plane systems. The method is particularly useful if the coupled wall assemblies are identical and in-plane symmetrical (i.e. the plane of the connecting beams is a plane of symmetry of the coupled wall assembly). For such a case, the analysis of the complete structure can be rapidly performed since closed form solutions may be obtained.

4.3 Analysis of Plane Systems with Rigid Pin-ended Connecting Links

Consider initially a plane system consisting of three coupled wall assemblies and one cantilevered core constrained to act together by a system of rigid pin-ended connecting links, as shown in Fig. 4.1. The structure is subjected to a lateral in-plane load W. It is assumed that the connecting beams deform with points of contraflexure at their mid-length, but are axially rigid so that all the walls have equal horizontal deflections. Ordinary beam theory is taken to be valid for individual wall or core.

4.3.1 Governing Differential Equations

Using the usual assumptions of the continuous medium

technique, the compatibility equations for the 'cut' laminae of the coupled wall assemblies 1, 2 and 3 are, respectively,

$$l_i \frac{du}{dz} - \frac{1}{E}\left(\frac{b_i^3 h}{12 I_{ci}}\right) q_i - \frac{1}{E}\left(\frac{1}{A_{ai}} + \frac{1}{A_{bi}}\right) \int_0^z \int_\xi^H q_i \, d\lambda \, d\xi$$

$$i = 1,2,3$$

$$- \delta_i = 0 \qquad (4.1)$$

where the four terms represent the relative vertical displacements at the cut edges resulting from, respectively, the slopes of the walls, the deflections of the connecting beams, the axial deformations of the walls and the settlements of the walls.

u = horizontal deflection

l_i = distance between the centroids of walls a and b of assembly i

ai, bi = symbols referred to walls a and b respectively of coupled wall assembly i

q_i = vertical shear distribution in the continuous medium of coupled wall assembly i

H, h, E = total height of walls, storey height, and modulus of elasticity, respectively

δ_i = relative vertical displacement between the bases of walls ai and bi

I_{ci}, b_i = second moment of area and clear span of the connecting beams respectively, of coupled wall assembly i

A_{ai}, A_{bi} = cross-sectional areas of walls ai and bi

z = height ordinate

λ , ξ = auxiliary height ordinates.

Using the differential equation for the deflected curve, the moment-curvature relationship for any individual wall r (coupled wall or cantilevered core) may be written as,

$$EI_r \frac{d^2u}{dz^2} = M_r = M_{rv} + M_{rh} \qquad (4.2)$$

I_r = second moment of area of wall r

M_r = internal moment of wall r

M_{rv}, M_{rh} = moments due to the vertical and horizontal forces respectively, acting externally to wall r.

Addition of the moment-curvature relationships of all the walls in the structure leads to an overall moment-curvature relationship of the form,

$$EI \frac{d^2u}{dz^2} = M - \sum_{i=1}^{3} l_i \int_z^H q_i \, d\lambda \qquad (4.3)$$

M = moment due to externally applied load W

I = sum of second moments of area of all the walls

$$= \sum_{i=1}^{3} (I_{ai} + I_{bi}) + I_{cr}$$

I_{ai}, I_{bi}, I_{cr} = second moments of area of walls ai, bi and the cantilevered core respectively

On differentiating equation (4.1) with respect to

z, combining with (4.3), and then differentiating again, the following governing differential equations for the plane system are obtained,

$$\frac{d^2 q_i}{dz^2} - \alpha_i^2 q_i - \beta_i^2 \left(\sum_{k=1}^{3} l_k q_k - l_i q_i\right) = \beta_i^2 \frac{dM}{dz} \qquad (4.4)$$

$$i = 1, 2, 3$$

where

$$\beta_i^2 = \frac{12 l_i I_{ci}}{b_i^3 h I}$$

$$\alpha_i^2 = \beta_i^2 l_i \mu_i \qquad (4.5)$$

$$\mu_i = 1 + \frac{I}{l_i^2}\left(\frac{1}{A_{ai}} + \frac{1}{A_{bi}}\right)$$

4.3.2 Boundary Conditions

The boundary conditions for the system of differential equations (4.4) are determined from the known conditions at the tops and the bases of the walls.

At the upper free end, the bending moments in all the walls are zero, so that the curvature $\frac{d^2 u}{dz^2}$ is zero. Hence, on differentiating equation (4.1), the upper boundary conditions in terms of the vertical shear distributions become,

$$\text{at } z = H, \quad \frac{dq_i}{dz} = 0, \qquad i = 1, 2, 3 \qquad (4.6)$$

If the walls are rigidly built in at the lower end, the slope $\frac{du}{dz}$ is zero and, from equation (4.1), the lower boundary conditions become,

$$\text{at } z = 0, \qquad q_i = 0 , \qquad i = 1, 2, 3 \qquad (4.7)$$

4.3.3 Forces and Displacement

From the known boundary conditions, equations (4.6) and (4.7), the complete solutions for the vertical shear distribution functions q_i may be obtained by solving the set of differential equations (4.4). The deflection and forces may then be obtained as follows:-

Horizontal Deflection

The deflection, u, may be determined by integrating equation (4.1) once, or integrating equation (4.3) twice. By integrating equation (4.3) twice, the horizontal deflection becomes,

$$u = \frac{1}{EI} \left(\int_0^z \int_0^{\xi} M \, d\lambda \, d\xi - \int_0^z \int_0^{\xi} \sum_{i=1}^{3} l_i q_i \, d\lambda \, d\xi \right)$$

$$- \left(\frac{du}{dz}\right)_0 z - u_0 \qquad (4.8)$$

in which $\left(\frac{du}{dz}\right)_0$ and u_0 are the rotation and horizontal deflection at the base, i.e. $z = 0$, respectively. For an infinitely rigid foundation, the rotation and horizontal deflection at the base are both equal to zero.

Axial Forces in the Walls

The axial vertical force in the cantilevered core

will be zero because the rigid pin-ended links transmit only axial forces. The axial forces in the coupled walls are given by,

$$N_{ai} = \int_z^H q_i \, d\lambda = - N_{bi} \qquad (4.9)$$

in which N_{ai} and N_{bi} are the axial forces in coupled walls ai and bi respectively. The forces may be tensile or compressive depending on the direction of q_i.

Moments in the Walls

As the curvatures of all the walls are equal, the moment in each wall will be proportional to its flexural rigidity. From equation (4.2) and (4.3) the internal wall moment, M_r, may be written as,

$$M_r = EI_r \frac{d^2u}{dz^2}$$

$$= \frac{I_r}{I} \left(M - \sum_{i=1}^{3} l_i \int_z^H q_i \, d\lambda \right) \qquad (4.10)$$

Shear Forces and Lateral Forces

From considerations of the equilibrium of the cut-sections of coupled walls and the equilibrium of an elemental wall element, Fig. 4.2, the horizontal shear force and the distributed lateral force on any coupled wall may be shown to be,

$$S_r = - \frac{dM_{rh}}{dz} = - \frac{dM_r}{dz} + \frac{dM_{rv}}{dz} \qquad (4.11)$$

$$W_r = -\frac{dS_r}{dz} = \frac{d^2M_r}{dz^2} - \frac{d^2M_{rv}}{dz^2} \qquad (4.12)$$

where

S_r = horizontal shear force in an individual wall r

W_r = distributed horizontal force (arising from the distributed forces transmitted by the rigid pin-ended connecting links and the externally applied distributed load acting directly on the wall) acting externally on an individual wall r

M_r = internal wall moment = $M_{rv} + M_{rh}$

M_{rh} = component of moment due to horizontal forces acting externally on wall r

M_{rv} = component of moment due to vertical shear distribution acting on wall r

The expressions for M_{rv} for the coupled walls ai and bi are given by,

$$\text{for wall ai,} \qquad M_{rv} = -g_{ai} \int_z^H q_i \, d\lambda \qquad (4.13)$$

$$\text{for wall bi,} \qquad M_{rv} = -g_{bi} \int_z^H q_i \, d\lambda$$

in which g_{ai} and g_{bi} are the distances between points of contraflexure and the centroids of walls ai and bi respectively.

Equations (4.11) and (4.12) are also valid for the cantilevered core. As the connecting links are assumed to be incapable of transmitting vertical forces, the component of moment due to the vertical forces will be

zero for the cantilevered core.

Generally the shear force at the top of each wall, obtained by evaluating equation (4.11) at z = H, does not vanish. To produce this shear force, a resultant concentrated lateral force must be acting at the top of the wall. Hence it can be deduced that concentrated axial forces exist in the top connecting links and the top substitute laminae. Using equation (4.11), the resultant concentrated lateral force at the top of any wall r may be written as,

$$P_r = \left(\frac{dM_r}{dz}\right)_{z=H} - \left(\frac{dM_{rv}}{dz}\right)_{z=H} \qquad (4.14)$$

in which P_r is the resultant concentrated lateral force at the top of wall r.

For any coupled wall assembly i, (i = 1, 2 or 3), the lateral forces acting externally on the assembly become, from equations (4.10) to (4.14),

$$W_i = W_{ai} + W_{bi} = \frac{E(I_{ai} + I_{bi})}{I} \frac{d^4u}{dz^4} - l_i \frac{dq_i}{dz} \qquad (4.15)$$

$$P_i = P_{ai} + P_{bi} = \left[- \frac{E(I_{ai} + I_{bi})}{I} \frac{d^3u}{dz^3} + l_i q_i \right]_{z=H}$$

W_i, P_i = distributed lateral force and resultant concentrated lateral force at the top respectively, acting externally on coupled wall assembly i

Axial Forces in the Connecting Links and the Substitute Lamina

From the equations derived earlier in the Chapter it may be seen that the vertical shear distributions, internal wall moments, horizontal shear forces, lateral forces on each wall, and the deflection of the structure are independent of the actual wall-wise distribution of the applied loads. These functions are dependent only on the resultant applied load W. However, as will be seen subsequently, the axial forces in the connecting links and the substitute lamina are dependent on the wall-wise distribution of the applied loads. Therefore, to determine these axial forces the actual applied load on each wall must be known.

Assume that the resultant applied load W is of the form,

$$W = \sum_{i=1}^{3} (\bar{W}_{ai} + \bar{W}_{bi}) + \bar{W}_{cr}$$

where,

$\bar{W}_{ai}$, $\bar{W}_{bi}$ = distributed lateral applied loads on coupled walls ai and bi respectively

$\bar{W}_{cr}$ = distributed lateral applied load on the cantilevered core.

By making a fictitious vertical cut along any series of rigid pin-ended connecting links and then considering the equilibrium of a horizontal element of either part of the partitioned structure, the axial forces in the rigid pin-ended links may be determined. The

axial forces in any substitute lamina may also be determined in a similar manner. For instance, the axial forces in the connecting links between the coupled wall assemblies 1 and 2, and the axial forces in the substitute lamina of the assembly 2 may be shown to be,

$$w_{1,2} = -\frac{E(I_{a1} + I_{b1})}{I}\frac{d^4u}{dz^4} + l_1\frac{dq_1}{dz} + \bar{w}_{a1} + \bar{w}_{b1}$$

$$C_{1,2} = \frac{E(I_{a1} + I_{b1})}{I}\left(\frac{d^3u}{dz^3}\right)_{z=H} - l_1(q_1)_{z=H} \qquad (4.16)$$

$$\bar{w}_2 = -\frac{E(I_{a1} + I_{b1} + I_{a2})}{I}\frac{d^4u}{dz^4} + l_1\frac{dq_1}{dz} + g_{a2}\frac{dq_2}{dz} + \bar{w}_{a1} + \bar{w}_{b1} + \bar{w}_{a2}$$

$$\bar{C}_2 = \frac{E(I_{a1} + I_{b1} + I_{a2})}{I}\left(\frac{d^3u}{dz^3}\right)_{z=H} - g_{a2}(q_2)_{z=H} - l_1(q_1)_{z=H}$$

where,

$w_{1,2}$ = distributed axial force in the connecting links between the assemblies 1 and 2

$C_{1,2}$ = concentrated axial force in the top connecting link between the assemblies 1 and 2

$\bar{w}_2$ = distributed axial force in the substitute lamina of the assembly 2

$\bar{C}_2$ = concentrated axial force in the top substitute

lamina of the assembly 2.

From consideration of equation (4.16) it is evident that the axial forces in the connecting links and the substitute lamina depend on the actual wall-wise distribution of the applied loads.

4.3.4 Plane Systems with Groups of Identical Coupled Wall Assemblies

Consider a general plane system consisting of m cantilevers (walls and cores) and K distinct groups of coupled walls. The numbers of the coupled wall assemblies in groups 1, 2, 3 ... K, are n_1, n_2, n_3 ...n_K; respectively, and the coupled wall assemblies within the same group are identical.

Following the same procedure as before, it may then be shown that there will be K independent second-order governing differential equations of the form,

$$\frac{d^2Q_i}{dz^2} - \alpha_i^2 Q_i - \beta_i^2 \left(\sum_{j=1}^{K} 1_j Q_j - 1_i Q_i\right) = \beta_i^2 \frac{dM}{dz} \qquad (4.17)$$

$$i = 1, 2, 3 \ldots K$$

where,

$$\beta_i^2 = \frac{12\ \bar{I}_{ci} 1_i}{b_i^3\ h\ \bar{I}}$$

$$\bar{I}_{ci} = n_i\ I_{ci} \qquad (4.18)$$

$$\bar{I} = \sum_{i=1}^{K} (\bar{I}_{ai} + \bar{I}_{bi}) + \bar{I}_{cr}$$

$\bar{I}_{ai} = n_i I_{ai}$

$\bar{I}_{bi} = n_i I_{bi}$

$\bar{I}_{cr}$ = sum of second moments of area of all the cantilevers

$$\alpha_i^2 = \beta_i^2 l_i \mu_i$$

$$\mu_i = 1 + \frac{\bar{I}}{l_i^2} \left(\frac{1}{\bar{A}_{ai}} + \frac{1}{\bar{A}_{bi}}\right) \qquad (4.18)$$ contd.

$\bar{A}_{ai} = n_i A_{ai}$

$\bar{A}_{bi} = n_i A_{bi}$

$Q_i = n_i q_i$

q_i = vertical shear distribution in each assembly of coupled wall group i

The parameters l_i, b_i, I_{ci}, I_{ai}, I_{bi}, A_{ai}, A_{bi} are those of a typical assembly of coupled wall group i.

Comparison of equations (4.4), (4.5) and (4.17), (4.18) shows that the general plane system can be transformed into an analogous plane system consisting of one simple cantilever and K coupled wall assemblies. The stiffness components, $\bar{I}_{ci}$, $\bar{A}_{ai}$, $\bar{A}_{bi}$, $\bar{I}_{ai}$, $\bar{I}_{bi}$ of the analogous coupled wall assembly i are the combined values of the corresponding properties of the real assemblies of

coupled wall group i. The stiffness $\bar{I}_{cr}$ of the analogous cantilever is the combined second moments of area of all the cantilevers.

All the equations derived previously are valid for the analogous plane system, recognising that the transformed analogous properties are to be used. The forces in any real assembly of coupled wall group i, except the axial forces in the substitute lamina, are equal to $1/n_i$ of the corresponding forces in the analogous coupled wall assembly i. The forces in any real cantilever are proportional to those of the analogous cantilever, where the proportional ratii are the ratii of the second moments of area of the real and analogous cantilevers. The deflections of the real and analogous structures will be equal.

The axial forces in the rigid pin-ended connecting links and the substitute laminae must be determined from the actual structural configuration and actual loading of the system.

4.4 Assumptions and Basis of the Reduction of Symmetrical Three-dimensional Structures to Equivalent Plane Systems

In the analysis of three-dimensional structures, the following assumptions are made:

1. The floor slabs are infinitely rigid in their own planes so that the overall cross-sections of the structures suffer only rigid body displacements in their own planes.

2. Resistance to out of plane deformations of the floor slabs are negligible so that the floor slabs may be considered as transmitting only in-plane axial forces.
3. Ordinary beam theory is taken to be valid for individual walls.
4. St. Venant's torsion may be neglected due to the relatively small thickness of each wall.
5. The usual assumptions of the continuous medium approach are valid.

Consider a symmetrical three-dimensional shear wall structure, the plan of which is shown in Fig. 4.3, consisting of a number of coupled wall assemblies and cantilevered elements such as open-section cores and plane walls. The vertical axis of symmetry OZ is the line of intersection of the planes of symmetry OZX and OZY. The loading function W is assumed acting obliquely to the planes of symmetry.

The applied load W can be replaced by a statically equivalent load system consisting of the loads W_x and W_y, acting in the planes of symmetry OZX and OZY respectively, and the accompanying torsional moment M_T. For a linear structure, the actions of these three load vectors may be analysed independently and then superimposed to give the solution to the actual loading system.

Under the action of the load W_y which passes through the axis of symmetry OZ, the symmetrical structure will be deflected in the Y direction only. The displacements

of all the walls must be equal because they are constrained to act together by the assumed infinitely rigid floor slabs. The analysis then becomes that of a plane system since only one deflection function, deflection in the Y direction, will be sufficient to describe the behaviour of the structure. From the assumption that only the horizontal in-plane forces are transmitted through the floor slab, the reduced plane system can be considered as having rigid pin-ended connecting links and, hence, the method of analysis described earlier in the Chapter is applicable. The behaviour of the structure subjected to the load W_x may be analysed in a similar manner.

Under the action of the torsional moment M_T, the symmetrical structure will rotate about the axis of symmetry OZ. The resultant horizontal displacement of each wall will be proportional to its distance from the axis of rotation OZ by virtue of the assumption 1. The proportional constant is the horizontal rotation about the vertical axis.

According to the assumption 4, the torsional resistance of the structure is due entirely to the differential shearing action of each wall. Using ordinary beam theory, the torsional equilibrium equation may be established in terms of the unknown vertical shear distributions in the laminae and the third derivative of the horizontal rotation. From the continuity equations for the 'cut' laminae and the overall torsional equili-

brium equation, a system of simultaneous second-order governing differential equations for the structure may be obtained. The system of differential equations thus obtained may be shown to be identical to those derived from an analogous plane system with rigid pin-ended connecting links subjected to a lateral loading function. The structural properties and the loading function of the analogous plane system are the transformed values of those of the real structure. The transformation characteristics depend on the relative orientation of the principal axes as well as the types (planar or non-planar) of the walls in the real structure.

The analyses of different classes of symmetrical three-dimensional shear wall structures are presented in detail in the subsequent sections.

4.5 Structures Composed of Cantilevered Wall and In-plane Symmetrical Coupled Wall Assemblies

A coupled wall assembly is termed in-plane symmetrical if the connecting beams axes lie in a vertical plane of symmetry of the assembly. The plan of a typical symmetrical structure composed of cantilevers and in-plane symmetrical coupled wall assemblies is shown in Fig. 4.3. The structure consists of three distinct groups of coupled wall assemblies, designated as groups 1, 2 and 3, and a number of cantilevers. Any lateral load W may be replaced by the statically equivalent loads W_x, W_y acting in the planes of symmetry OZX and OZY respectively, and the accompanying torsional moment M_T.

The numbers of the cantilevers and the coupled wall assemblies in groups 1, 2, 3 are denoted as n_{cr}, n_1, n_2, n_3 respectively. For the structure shown in Fig. 4.3, the values of n_{cr}, n_1, n_2, n_3 are 4, 8, 4, 4 respectively. Throughout the analysis the shear centre axis of each wall is taken as the vertical wall axis.

Several variable integer notations and letter-integer notations are used in the analysis, these are defined as follows:-

i-j	: refers to assembly j of coupled wall group i
cr-k	: refers to cantilever cr-k
ai, bi	: refer to walls a and b, respectively, of a typical assembly of coupled wall group i
ai-j, bi-j	: refer to walls a and b, respectively, of coupled wall assembly i-j

4.5.1 Analysis of Pure Bending Action

For simplicity, it will be assumed that the major principal axes of the walls a and b of each in-plane symmetrical coupled wall assembly are perpendicular to the axes of the connecting beams. Under the action of the applied load W_x, passing through the axis of symmetry OZ, all the walls deflect equally in the X direction and with zero component of deflection in the Y direction. The continuity equations for the 'cut' substitute laminae of the coupled wall groups 1, 2 and 3 may be written as, respectively,

$$l_1 \, C_{1-i} \, \frac{du}{dz} - \frac{1}{E}\left(\frac{b_1^3 h}{12 I_{c1}}\right) q_{1-i} - \frac{1}{E}\left(\frac{1}{A_{a1}} + \frac{1}{A_{b1}}\right) \cdot$$

$$\int_0^z \int_\xi^H q_{1-i} \, d\lambda \, d\xi - \delta_{1-i} = 0$$

$$i = 1, 2, \ldots n_1$$

(4.19)

$$l_2 \, C_{2-j} \, \frac{du}{dz} - \frac{1}{E}\left(\frac{b_2^3 h}{12 I_{c2}}\right) q_{2-j} - \frac{1}{E}\left(\frac{1}{A_{a2}} + \frac{1}{A_{b2}}\right) \cdot$$

$$\int_0^z \int_\xi^H q_{2-j} \, d\lambda \, d\xi - \delta_{2-j} = 0$$

$$j = 1, 2, \ldots n_2$$

$$l_3 \, C_{3-k} \, \frac{du}{dz} - \frac{1}{E}\left(\frac{b_3^3 h}{12 I_{c3}}\right) q_{3-k} - \frac{1}{E}\left(\frac{1}{A_{a3}} + \frac{1}{A_{b3}}\right) \cdot$$

$$\int_0^z \int_\xi^H q_{3-k} \, d\lambda \, d\xi - \delta_{3-k} = 0$$

$$k = 1, 2 \ldots n_3$$

where,

q_{i-j} = vertical shear distribution in the substitute lamina of assembly i-j

δ_{i-j} = relative vertical displacement between the bases of walls ai-j and bi-j

A_{ai}, A_{bi} = cross-sectional areas of walls a and b respectively, of a typical assembly of coupled wall group i

l_i, b_i, I_{ci} = distances between the centroids of walls a and b, clear distance between walls a and b, and second moment of area of connecting beams, respectively, of a typical assembly of coupled wall group i

C_{i-j} = cosine of the angle the vertical plane of connecting beams of assembly i-j makes with the X axis

u = horizontal displacement of the structure in the X direction

However, as will be shown subsequently in section 4.7.1, under the pure bending action the vertical shear distributions in the in-plane symmetrical coupled wall assemblies which are identical are proportional to one another. The proportional ratios are the ratios of the displacements of the assemblies along the planes of their connecting beams. Therefore, for the case considered, the relationships between the vertical shear distributions of the assemblies of the same group may be written as,

$$q_{i-j} = \frac{C_{i-j}}{C_{i-k}} q_{i-k} \qquad (4.20)$$

In consequence, only one independent continuity equation exists for each group of the coupled walls. Adopting the coupled wall assemblies 1-1, 2-1, and 3-1, as the reference assemblies for groups 1, 2 and 3 respectively, a set of three independent continuity equations for the structure may be written as,

$$C_{i-1}{}^{1}{}_{i}\,\frac{du}{dz} - \frac{1}{E}\left(\frac{b_i^3 h}{12 I_{ci}}\right) q_{i-1} - \frac{1}{E}\left(\frac{1}{A_{ai}} + \frac{1}{A_{bi}}\right)\cdot$$

$$\int_0^z \int_\xi^H q_{i-1}\, d\lambda\, d\xi \;-\; \delta_{i-1} = 0 \qquad (4.21)$$

$$i = 1,\ 2,\ 3$$

Using the differential equation of the deflected curve of a beam, (cf. equation (4.2)), and the linear property of the system, the moment equilibrium of the structure may be established as,

$$C_{1-1}^2\, E\, \bar{I}\, \frac{d^2u}{dz^2} = M - \sum_{i=1}^{3} \sum_{j=1}^{n_i} \left(\frac{{}_1C_{i-j}^2}{C_{i-1}}\right) \int_z^H q_{i-1}\, d\lambda \qquad (4.22)$$

in which,

$$I = I_1 + I_2 + I_3 + I_{cr}$$

$$\bar{I}_i = \frac{(I_{m,ai} + I_{m,bi})}{C_{1-1}^2} \sum_{j=1}^{n_i} C_{i-j}^2\,, \quad i = 1,\ 2,\ 3$$

$$\bar{I}_{cr} = \frac{1}{C_{1-1}^2}\left[\sum_{k=1}^{n_{cr}} \left(C_{cr-k}^2\, I_{m,cr-k} + (1 - C_{cr-k}^2) I_{n,cr-k} \right) + \sum_{i=1}^{3} \sum_{j=1}^{n_i} (I_{n,ai} + I_{n,bi})(1 - C_{i-j}^2)\right] \qquad (4.23)$$

C_{cr-k} = cosine of the angle the minor principal axis of cantilever cr-k makes with the X axis.

$I_{m,cr-k}$, $I_{n,cr-k}$ = the major and minor principal second

moments of area, respectively, of cantilever cr-k

$I_{m,ai}$, $I_{m,bi}$ = the major principal second moments of area of walls ai and bi respectively

$I_{n,ai}$, $I_{n,bi}$ = the minor principal second moments of area of walls ai and bi

M = moment about the Y axis, due to the applied load W_x

From equations (4.21) and (4.22), the set of governing differential equations for the structure under the action of the load W_x may be shown to be,

$$\frac{d^2Q_i}{dz^2} - \alpha_i^2 Q_i - \beta_i^2 \left(\sum_{j=1}^{3} 1_j Q_j - 1_i Q_i \right) = \beta_i^2 \frac{d(M/C_{1-1})}{dz} \qquad (4.24)$$

$$i = 1, 2, 3$$

where,

$$Q_i = B_i V_{i-j} q_{i-j}$$

$$V_{i-j} = \frac{C_{1-1}}{C_{i-j}}$$

$$B_i = \sum_{j=1}^{n_i} (C_{i-j}^2/C_{1-1}^2) \qquad (4.25)$$

$$\beta_i^2 = \frac{12\ 1_i\ I_{ci}\ B_i}{b_i^3\ h\ \bar{I}}$$

$$\alpha_i^2 = \beta_i^2\ 1_i\ \mu_i$$

$$\mu_i = 1 + \frac{\bar{I}}{B_i l_i^2}\left(\frac{1}{A_{ai}} + \frac{1}{A_{bi}}\right) \qquad (4.25)\ \text{contd.}$$

For the structure free at the top and rigidly fixed to an undeformable foundation, the boundary conditions for the set of differential equations (4.24) may be shown to be,

$$\text{at } z = H, \quad \frac{dQ_i}{dz} = 0 \ , \quad i = 1, 2, 3$$
$$\text{at } z = 0, \quad Q_i = 0 \ , \quad i = 1, 2, 3 \qquad (4.26)$$

Inspections of equations (4.17), (4.18), (4.24) and (4.25) show that the analysis of pure bending action can be reduced to the analysis of an analogous plane system. It may be shown that the set of differential equations given by equation (4.24) is identical to that obtained from an analogous plane system consisting of three analogous coupled wall assemblies and one cantilever, and subjected to a horizontal loading system which produces a total moment at any level equal to $\frac{M}{C_{1-1}}$.

There are direct correspondences between the parameters of the analogous coupled wall assemblies and those of the real coupled wall assemblies. The parameters of an analogous coupled wall assembly i are the transformed parameters of the real assemblies of coupled wall group i. The transformation relationships may be shown to be as follows:-

$$\hat{I}_{m,ai} = B_i I_{m,ai}$$
$$\hat{I}_{m,bi} = B_i I_{m,bi} \qquad (4.27)$$

$$\hat{I}_{ci} = B_i I_{ci}$$

$$\hat{A}_{ai} = B_i A_{ai}$$

$$\hat{A}_{bi} = B_i A_{bi}$$

$$\hat{b}_i = b_i \qquad \text{(4.27) contd.}$$

$$\hat{l}_i = l_i$$

$$\hat{h} = h$$

Where the parameters with the upper hat, $\hat{}$, are the analogous parameters.

For the analogous cantilever, its second moment of area is given by,

$$\hat{I}_{cr} = \bar{I}_{cr} \qquad (4.28)$$

where $\bar{I}_{cr}$ is the same as that given in equation (4.23).

The analogous loading system is a linear transformation of the actual load W_x, cf. equations (4.4) and (4.24), and given by,

$$\hat{W} = \frac{W_x}{C_{1-1}} \qquad (4.29)$$

where $\hat{W}$ is the analogous applied load.

The analogous plane system considered is based on the plane of connecting beams of the datum assembly 1-1 since all the transformations are related to that plane, i.e. involving C_{1-1}. In general, any assembly may be chosen as the datum assembly but the parameters of the analogous system must be changed accordingly.

The behaviour of the structure under the action of

the load W_y may be similarly analysed, and an equivalent analogous plane system obtained. If the assembly 1-1 is chosen again as the datum assembly, the equations derived earlier are applicable provided that,

(i) W_x is replaced by W_y

(ii) u is redefined as the deflection in the direction of the applied load W_y

(iii) C_{i-j} and C_{cr-k} are redefined as sines, instead of cosines, of the corresponding angles.

4.5.2 Analysis of Pure Torsional Action

Under the action of the torsional moment M_T, the symmetrical structure will rotate about the axis of symmetry OZ. The resultant horizontal displacement of any wall will be proportional to its distance from the axis of rotation due to the assumed infinite in-plane rigidity of the floor slabs. Therefore, for any wall,

$$d = \theta \times L \qquad (4.30)$$

where d is the resultant horizontal displacement, L the magnitude of horizontal vector of the shear centre of the wall, and θ the horizontal angle of rotation. The component of horizontal displacement in any direction may be obtained by resolving d vectorially.

Using the continuous medium technique, the continuity equation for each coupled wall assembly may be obtained. However, as will be shown subsequently in section 4.7.2, the vertical shear distributions in identical in-plane symmetrical coupled wall assemblies

under the pure torsional action are proportional to one another. The proportional ratios are the ratios of the distances of the planes of connecting beams of the assemblies from the axis of rotation. In consequence, only one independent continuity equation may be obtained from each distinct group of coupled walls. Adopting the assemblies 1-1, 2-1, 3-1 as the reference assemblies for coupled wall groups 1, 2, 3 respectively, a set of independent continuity equations for the structure may be shown to be,

$$l_i \; R_{i-1} \; \frac{d\theta}{dz} - \frac{1}{E} \left(\frac{b_i^3 h}{12 I_{ci}}\right) q_{i-1} - \frac{1}{E} \left(\frac{1}{A_{ai}} + \frac{1}{A_{bi}}\right) \cdot$$

$$\int_0^z \int_\xi^H q_{i-1} \, d\lambda \, d\xi - \delta_{i-1} = 0 \qquad (4.31)$$

$$i = 1, 2, 3$$

where R_{i-j} is defined as the distance of the plane of connecting beams of coupled wall assembly i-j from the axis of rotation.

Using ordinary beam theory, the moments in each individual wall about its principal axes may be written as,

$$M_m = M_{mh} + M_{mv} = EI_m \; R_m \; \frac{d^2\theta}{dz^2}$$

$$(4.32)$$

$$M_n = M_{nh} + M_{nv} = EI_n \; R_n \; \frac{d^2\theta}{dz^2}$$

where,

M_m, M_n = internal wall moments about the major and minor

principal axes respectively

M_{mh}, M_{nh} = moments about the major and minor principal axes respectively, due to horizontal loads

M_{mv}, M_{nv} = moments about the major and minor principal axes respectively, due to vertical loads

R_m, R_n = projections on the major and minor principal axes,respectively, of the horizontal vector of the shear centre of the wall (a horizontal vector of any point is the component vector which is perpendicular to the axis OZ)

On differentiating equation (4.32), the orthogonal horizontal shear forces in each wall become,

$$S_m = - \frac{dM_{nh}}{dz} = - EI_n R_n \frac{d^3\theta}{dz^3} + \frac{dM_{nv}}{dz} \qquad (4.33)$$

$$S_n = - \frac{dM_{mh}}{dz} = - EI_m R_m \frac{d^3\theta}{dz^3} + \frac{dM_{mv}}{dz}$$

in which S_m and S_n are the horizontal cross-sectional shear forces in the directions parallel to the major and minor principal axes respectively. The expressions of M_{nv} and M_{mv} for any coupled wall may be obtained from equation (4.13).

For practical structure, the thickness of each wall is usually small in comparison with its other dimensions. Consequently, the St. Venant's torsion is comparatively insignificant and can usually be neglected. Therefore, by neglecting the St. Venant's torsion, the torsional resistance of the structure consists entirely of the torsional resistances developed by the cross-sectional

shear forces. Hence, for the torsional equilibrium of the structure,

$$M_T = \sum_{\text{all walls}} (S_m R_n + S_n R_m) \qquad (4.34)$$

where $\sum_{\text{all walls}} (S_m R_n + S_n R_m)$ is the summation of the torsional resistance developed by each wall.

On substituting the expressions for shear forces given in equation (4.33) into equation (4.34), the overall torsional equilibrium equation becomes, for the structure considered,

$$R_{1-1}^2 \; EI_t \frac{d^3\theta}{dz^3} = - M_T + \sum_{i=1}^{3} \sum_{j=1}^{n_i} \left(\frac{l_i R_{i-j}^2}{R_{i-1}}\right) q_{i-1} \qquad (4.35)$$

where,

$$I_t = \frac{1}{R_{1-1}^2} \sum_{i=1}^{3} \sum_{j=1}^{n_i} (R_{i-j}^2)(I_{m,ai} + I_{m,bi}) + I_{t,cr}$$

$$I_{t,cr} = \frac{1}{R_{1-1}^2} \sum_{i=1}^{3} \sum_{j=1}^{n_i} (I_{n,ai} R_{n,ai-j}^2 + I_{n,bi} R_{n,bi-j}^2)$$

$$+ \frac{1}{R_{1-1}^2} \sum_{k=1}^{n_{cr}} (I_{m,cr-k} R_{m,cr-k}^2 + I_{n,cr-k} R_{n,cr-k}^2) \qquad (4.36)$$

$R_{n,ai-j}$ = projection of the horizontal vector of the shear centre of wall ai-j on its minor principal axis.

$R_{n,bi-j}$ = projection of the horizontal vector of the shear centre of wall bi-j on its minor principal axis.

$R_{m,cr-k}$, $R_{n,cr-k}$ = projections of the horizontal vector of

the shear centre of cantilever cr-k on its major and minor principal axes respectively.

On multiplying the continuity equations for the assemblies 1-1, 2-1, 3-1, by $\frac{1}{R_{1-1}^2} \sum_{j=1}^{n_1} R_{1-j}^2$,

$\frac{1}{R_{1-1}R_{2-1}} \sum_{j=1}^{n_2} R_{2-j}^2$, $\frac{1}{R_{1-1}R_{3-1}} \sum_{j=1}^{n_3} R_{3-j}^2$, respectively, then differentiating twice and substituting for $\frac{d^3\theta}{dz^3}$ from equation (4.35), the set of governing differential equations for the structure under pure torsion may be obtained as,

$$\frac{d^2Q_i}{dz^2} - \alpha_i^2 Q_i - \beta_i^2 \left(\sum_{j=1}^{3} 1_j Q_j - 1_i Q_i\right) = - \beta_i^2 \frac{M_T}{R_{1-1}}$$

$$i = 1, 2, 3 \qquad (4.37)$$

where,

$$\begin{aligned} Q_i &= D_i\, t_{i-j}\, q_{i-j} \\ D_i &= \frac{1}{R_{1-1}^2} \sum_{j=1}^{n_i} R_{i-j}^2 \\ t_{i-j} &= \frac{R_{1-1}}{R_{i-j}} \\ \beta_i^2 &= \frac{12\, I_{ci}\, l_i\, D_i}{b_i^3\, h\, I_t} \end{aligned} \qquad (4.38)$$

$$\alpha_i^2 = \beta_i^2\, l_i\, \mu_i$$

$$\mu_i = 1 + \frac{I_t}{D_i l_i^2} \left(\frac{1}{A_{ai}} + \frac{1}{A_{bi}}\right)$$

For the structure free at the top and rigidly fixed to an undeformable foundation, the boundary conditions are the same as those given by equation (4.26).

Comparisons between equations (4.17), (4.18), (4.37) and (4.38) show that the pure torsional analysis can be reduced to the analysis of an analogous plane system. The set of governing differential equations obtained from equation (4.37) is identical to the system of differential equations for an analogous plane system consisting of three analogous coupled wall assemblies and one analogous cantilever, subjected to a horizontal loading system which produces a total horizontal shear at any level equal to $\frac{M_T}{R_{1-1}}$. The analogous parameters are given by,

$$
\begin{aligned}
\check{A}_{ai} &= D_i A_{ai} \\
\check{A}_{bi} &= D_i A_{bi} \\
\check{I}_{m,ai} &= D_i I_{m,ai} \\
\check{I}_{m,bi} &= D_i I_{m,bi} \\
\check{I}_{ci} &= D_i I_{ci} \\
\check{I}_{cr} &= \check{I}_{t,cr}
\end{aligned}
\qquad (4.39)
$$

where the parameters with the upper inverted hat, $\check{}$, are the analogous parameters.

The analogous loading system is an equivalent horizontal loading which produces a total horizontal shear

at any level equal to $\frac{M_T}{R_{1-1}}$, i.e.

$$\frac{d\check{M}}{dz} = - \frac{M_T}{R_{1-1}} \qquad (4.40)$$

in which $\check{M}$ is the moment at any level resulting from the analogous loading system.

The analogous plane system considered is based on the datum assembly 1-1, since all the transformations are related to the assembly 1-1, i.e. involving the constant R_{1-1}. Generally any assembly may be chosen as the datum assembly, but the analogous parameters must be changed accordingly.

4.5.3 Relationship between Real and Analogous Forces and Displacements

The analyses of pure bending and pure torsional actions can be conveniently carried out using the equivalent analogous plane systems. After the analogous forces and displacements have been determined they can be transformed back to give the real forces and displacements in the real structure.

Pure Torsional Action

From considerations of equations (4.3) and (4.35), it may be shown that the displacement of the analogous system is the in-plane displacement of the plane of the connecting beams of the datum assembly. Therefore, for the system considered in which the assembly 1-1 is chosen as the datum assembly, the horizontal rotation of the structure may be expressed as,

$$\theta = \frac{d_a}{R_{1-1}} \qquad (4.41)$$

where d_a and θ are the analogous displacement and the horizontal angle of rotation of the structure respectively. The sense of the rotation θ will be the same as that of the applied torsional moment M_T. From considerations of equations (4.30), (4.32), (4.33) and (4.38) it may be established that the magnitudes of the real and analogous forces are related by,

$$F_r = f_s f_d F_a \qquad (4.42)$$

in which F_r, F_a, f_s, f_d are the real force, the corresponding analogous force, the corresponding real-analogous stiffness factor and the corresponding real-analogous action factor respectively.

The factors f_s and f_d may be expressed as,

$$f_s = \frac{K_r}{K_a}$$

$$f_d = \frac{G_r}{G_a} \qquad (4.43)$$

where,

K_r = real stiffness appropriate to the force considered

K_a = corresponding appropriate analogous stiffness

G_r = distance between the plane (vertical) of action of the force considered and the axis of rotation OZ

G_a = distance between the axis of rotation OZ and the datum plane upon which the analogous system is based

The plane of action of any vertical shear distribution q_{i-j} is the plane of connecting beams of assembly i-j. The planes of actions of moment and shear forces (moments about the principal axes and shear forces in the directions parallel to the principal axes) of any wall are taken to be the planes which pass through the shear centre of the wall, since the shear centre axis of each wall is used as the reference wall axis. The appropriate stiffnesses for the transformations of the vertical shear distributions are the cross-sectional areas of the coupled wall assemblies. For the transformations of bending moments and shear forces the appropriate stiffnesses are the second moments of area. However, it is to be noted that in using equation (4.42) to determine the internal moment and shear force in the plane perpendicular to the connecting beams of each coupled wall the corresponding appropriate analogous forces and stiffnesses are those of the analogous cantilever.

From equations (4.42) and (4.43), the expressions for real forces can be easily obtained. For instance, the vertical shear distribution q_{i-j}, and the moment $M_{m,cr-k}$ are given by, respectively,

$$q_{i-j} = \frac{1}{D_i} \frac{R_{i-j}}{R_{1-1}} Q_i$$

$$M_{m,cr-k} = \frac{I_{m,cr-k}}{\check{I}_{cr}} \cdot \frac{R_{m,cr-k}}{R_{1-1}} \check{M}_{cr} \qquad (4.44)$$

in which $\check{M}_{cr}$ is the moment in the analogous cantilever.

The horizontal forces, parallel to the plane of connecting beams, acting externally on any real coupled wall assembly i-j are given by, cf. equation (4.12),

$$W_{i-j} = - \frac{d}{dz} (S_{n,ai-j} + S_{n,bi-j}) \qquad (4.45)$$

$$P_{i-j} = - (S_{n,ai-j} + S_{n,bi-j})_{z=H}$$

where

W_{i-j} = distributed horizontal force, parallel to the plane of connecting beams, acting externally on assembly i-j

P_{i-j} = concentrated horizontal force at the top, parallel to the plane of connecting beams, acting externally on assembly i-j

$S_{n,ai-j}$, $S_{n,bi-j}$ = shear forces in the walls ai-j and bi-j, respectively, acting parallel to the plane of the connecting beams

The force W_{i-j} (or P_{i-j}) is positive if its direction has the same sense as that of the component of displacement along the plane of the connecting beams.

It has been shown in section 4.3.3 that the axial forces in the substitute lamina, and hence in the connecting beams, depend on the actual distributions of the loads on the walls a and b of the assembly. Therefore, to determine the axial forces in the substitute lamina of any real coupled wall assembly a pattern of wall-wise distribution of the loads, trans-

mitted through the floor slabs, must be postulated. As an illustration, suppose that the loads transmitted through the floor slabs and acting on each coupled wall assembly i-j are divided between wall ai and bi in proportion to their second moments of area. The distributed axial force $\bar{w}_{i-j}$ and the top concentrated axial force $\bar{C}_{i-j}$ in the substitute lamina of any coupled wall assembly i-j may then be shown to be, respectively.

$$\bar{w}_{i-j} = \frac{d}{dz}\left(S_{n,ai-j}\right) + \varkappa\, W_{i-j}$$

$$\bar{C}_{i-j} = -\left(S_{n,ai-j}\right)_{z=H} + \varkappa\, P_{i-j} \qquad (4.46)$$

in which $\varkappa$ is equal to $\dfrac{I_{m,ai-j}}{(I_{m,ai-j} + I_{m,bi-j})}$

Pure Bending Action

In the case of pure bending action, the analogous displacement is the component of real displacement along the plane of connecting beams of the datum assembly. The relationships between the real and the analogous forces given by equation (4.42), and the expressions given by equations (4.45), (4.46) are valid provided that the parameters G_a and G_r are redefined as follows:

G_a = cosine of the angle the plane of connecting beams of the datum assembly makes with the direction of the applied load which causes the pure bending action.

G_r = cosine of the angle the plane of connecting beams of

the assembly considered makes with the direction of the applied load.

4.6 Structures on Elastic Foundations

In the preceding analysis it has been assumed that full fixity exists at the base of the structure. However, the theory can be extended to deal with flexible foundation conditions. It will be assumed that each wall is supported on a linearly elastic foundation such that the rotational and vertical displacements of the base are proportional to the imposed bending moment and vertical force, respectively. It is further assumed that the foundations under the walls which are identical possess identical force-deformation characteristics.

4.6.1 Lower Boundary Conditions for Pure Bending Action

Consider the pure bending action, under the load W_x, of the structure shown in Fig. 4.3. From the moment-curvature relationships and equation (4.9), it can be shown that the rotation at the base of each wall and the relative vertical displacement between the bases of walls a and b of any coupled wall assembly i-j may be written as,

$$\left(\frac{du}{dz}\right)_{z=0} = \frac{E\bar{I}}{K_\theta}\left(\frac{d^2u}{dz^2}\right)_{z=0} \tag{4.47}$$

$$\delta_{i-j} = \left(\frac{1}{K_{v,ai}} + \frac{1}{K_{v,bi}}\right) \int_0^H q_{i-j}\, d\lambda$$

where,

$$K_{\theta} = \frac{1}{C_{1-1}^2} \left[\sum_{i=1}^{3} \sum_{j=1}^{n_i} \left\{ C_{i-j}^2 \, (K_{\theta m,ai} + K_{\theta m,bi}) \right. \right.$$

$$\left. + (1 - C_{i-j}^2)(K_{\theta n,ai} + K_{\theta n,bi}) \right\}$$

$$\left. + \sum_{k=1}^{n_{cr}} C_{cr-k}^2 \, K_{\theta m,cr-k} + (1 - C_{cr-k}^2) K_{\theta n,cr-k} \right] \qquad (4.48)$$

K_{θ} = sum of the transformed rotational stiffnesses of the foundation under each wall

$K_{\theta m,ai}$ = rotational stiffness, about the major principal axis of a typical wall ai of coupled wall group i, of the foundation under the wall

$K_{\theta n,ai}$ = similarly defined as $K_{\theta m,ai}$, but referred to the minor principal axis of the wall

$K_{v,ai}$, $K_{v,bi}$ = vertical stiffnesses of the foundations under walls ai and bi, respectively, of a typical assembly of coupled wall group i,

$K_{\theta m,bi}$, $K_{\theta n,bi}$, $K_{\theta m,cr-k}$, $K_{\theta n,cr-k}$ are defined in a similar manner, and C_{i-j}, $\bar{I}$ are as previously defined in section 4.5.1.

From equations (4.21), (4.22), (4.24), (4.47), (4.48) the lower boundary conditions for Q_i may be shown to be,

at $z = 0$,

$$Q_i = \beta_i^2 \, E\bar{I} \left[\frac{M_{z=0}}{K_\theta C_{1-1}} - \frac{1}{l_i \, B_i} \left(\frac{1}{K_{v,ai}} + \frac{1}{K_{v,bi}} \right) \cdot \right.$$

$$\left. \int_0^H Q_i \, d\lambda \; - \frac{1}{K_\theta} \sum_{j=1}^{3} l_j \int_0^H Q_j \, d\lambda \right] \qquad (4.49)$$

$$i = 1, 2, 3$$

where Q_i, β_i, B_i are as previously defined in equation (4.25).

It may be shown that the boundary conditions given by equation (4.49) are identical to the lower boundary conditions for the equivalent analogous plane system. The rotational and vertical stiffnesses of the analogous foundations are related to those of the real foundations by the following relationships,

$$\hat{K}_{v,ai} = B_i \, K_{v,ai}$$

$$\hat{K}_{v,bi} = B_i \, K_{v,bi}$$

$$\hat{K}_{\theta m,ai} = B_i \, K_{\theta m,ai} \qquad (4.50)$$

$$\hat{K}_{\theta m,bi} = B_i \, K_{\theta m,bi}$$

$$\hat{K}_{\theta,cr} = \frac{1}{C_{1-1}^2} \sum_{i=1}^{3} \sum_{j=1}^{n_i} (K_{\theta n,ai} + K_{\theta n,bi}) - \sum_{i=1}^{3} (B_i) \cdot$$

$$(K_{\theta n,ai} + K_{\theta n,bi}) + \frac{1}{C_{1-1}^2} \sum_{k=1}^{n_{cr}} (C_{cr-k}^2) \cdot$$

$$(K_{\theta m,cr-k} - K_{\theta n,cr-k}) + \frac{1}{C_{1-1}^2} \sum_{k=1}^{n_{cr}} K_{\theta n,cr-k}$$

= rotational stiffness of the analogous cantilever

where the parameters with the upper hat, ^ , are the analogous parameters.

4.6.2 Lower Boundary Conditions for Pure Torsional Action

Consider the pure torsional action, under the torsional moment M_T, of the structure shown in Fig. 4.3. In a similar manner as in the case of pure bending action, the horizontal rotation of the structure at the base and the relative vertical displacement between the bases of walls a and b of any coupled wall assembly may be shown to be, respectively,

$$\left(\frac{d\theta}{dz}\right)_{z=0} = \frac{EI_t}{K_{t\theta}} \left(\frac{d^2\theta}{dz^2}\right)_{z=0} \tag{4.51}$$

$$\delta_{i-j} = \left(\frac{1}{K_{v,ai}} + \frac{1}{K_{v,bi}}\right) \int_0^H q_{i-j}\, d\lambda \tag{4.52}$$

where,

$$\begin{aligned} K_{t\theta} = {} & \frac{1}{R_{1-1}^2} \sum_{i=1}^{3} \sum_{j=1}^{n_i} \left(R_{m,ai-j}^2 K_{\theta m,ai} + R_{m,bi-j}^2 K_{\theta m,bi}\right) \\ & + \frac{1}{R_{1-1}^2} \sum_{i=1}^{3} \sum_{j=1}^{n_i} \left(R_{n,ai-j}^2 K_{\theta n,ai} + R_{n,bi-j}^2 K_{\theta n,bi}\right) \\ & + \frac{1}{R_{1-1}^2} \sum_{k=1}^{n_{cr}} \left(R_{m,cr-k}^2 K_{\theta m,cr-k} + R_{n,cr-k}^2 K_{\theta n,cr-k}\right) \end{aligned} \tag{4.53}$$

and other parameters are as defined or given earlier.

On integrating equation (4.35), making use of the

upper boundary conditions of zero moments at the top, the second derivative of the horizontal rotation of the structure at $z = 0$ may be written as,

$$\left(\frac{d^2\theta}{dz^2}\right)_{z=0} = \frac{1}{EI_t}\left(\frac{1}{R_{1-1}^2}\int_0^H M_T\, d\lambda + \frac{1}{R_{1-1}}\sum_{i=1}^{3} l_i \int_0^H Q_i d\lambda\right) \tag{4.54}$$

in which Q_i, $i = 1, 2, 3$, are as previously given in equation (4.38).

From equations (4.31), (4.37), (4.38), (4.51) and (4.52), the lower boundary conditions for Q_i may be shown to be,

at $z = 0$.

$$Q_i = \beta_i^2 EI_t \left[\frac{1}{R_{1-1}K_{t\theta}}\int_0^H M_T\, d\lambda - \left(\frac{1}{D_i l_i}\right)\cdot\right.$$

$$\left.\left(\frac{1}{K_{v,ai}} + \frac{1}{K_{v,bi}}\right)\int_0^H Q_i\, d\lambda - \frac{1}{K_{t\theta}}\sum_{j=1}^{3} l_j \int_0^H Q_j d\lambda\right]$$

$$i = 1, 2, 3 \tag{4.55}$$

in which D_i, $i = 1, 2, 3$, are as given previously in equation (4.38).

As in the case of pure bending action, the lower boundary conditions given by equation (4.55) may be obtained from the equivalent analogous plane system supported on the elastic foundations. The rotational and vertical stiffnesses of the analogous foundations are related to those of the real foundations by the

following relationships,

$$\check{K}_{\theta m,ai} = D_i K_{\theta m,ai}$$

$$\check{K}_{\theta m,bi} = D_i K_{\theta m,bi}$$

$$\check{K}_{v,ai} = D_i K_{v,ai}$$

$$\check{K}_{v,bi} = D_i K_{v,bi}$$

$$\check{K}_{\theta,cr} = \frac{1}{R^2_{1-1}} \sum_{i=1}^{3} \sum_{j=1}^{n_i} (R^2_{n,ai-j} K_{\theta n,ai} + R^2_{n,bi-j} K_{\theta n,bi})$$

$$+ \frac{1}{R^2_{1-1}} \sum_{k=1}^{n_{cr}} (R^2_{m,cr-k} K_{\theta m,cr-k} + R^2_{n,cr-k} K_{\theta n,cr-k}) \quad (4.56)$$

where the parameters with the upper inverted hat, $\check{}$, are the analogous parameters.

4.7 Constrained Displacements of Identical Non-planar Coupled Wall Assemblies

From the analysis presented so far in this Chapter, it is evident that by using the continuous medium approach the analysis of any symmetrical structure composed of cantilevers and in-plane symmetrical coupled wall assemblies may be reduced to the analyses of the analogous plane systems for bending and torsional actions. The behaviour of the analogous plane system for either bending or torsional action is described by a system of second-order governing differential equations with the vertical shear distributions as dependent variables. Although there may be a large number of coupled wall

assemblies in the structure, the number of the independent differential equations for the system will be at most n, where n is the number of the distinct groups of coupled wall assemblies. The reduction of the total number of the differential equations, generally one equation for each coupled wall assembly, to a system of n (or less than n) equations is possible because of the linear relationships between the vertical shear distributions in the identical in-plane symmetrical coupled wall assemblies. It may be noted that the linear relationships between the vertical shear distributions in the identical in-plane symmetrical coupled wall assemblies under both the pure bending and torsional actions have been stated and used in sections 4.5.1 and 4.5.2, without proofs being given. The validity of the statements will be substantiated in this section.

If the coupled wall assemblies are not in-plane symmetrical, the vertical shear distributions in the assemblies will not generally be linearly related although the assemblies are identical. Consequently, the number of the independent differential equations are usually greater than the number of the distinct groups of coupled wall assemblies present in the structure. The exact number of the independent differential equations for either the bending or torsional actions will depend on the relative positions and orientations of the assemblies. The behaviours of non-planar coupled wall assemblies which are identical and subjected to the constrained

translation and the constrained rotation, i.e. corresponding to the pure bending action and the pure torsional action respectively of symmetrical structures, will be investigated in the present section.

4.7.1 Constrained Translation

Consider the two identical non-planar coupled wall assemblies, 1 and 2, shown in plan in Fig. 4.4. Assume initially that both assemblies undergo independent translational displacements, and define,

$\underset{\sim}{U}_i$ = resultant horizontal displacement vector of the assembly i, i = 1 or 2,

$\underset{\sim}{C}_i$ = the centroidal vector, a horizontal vector passing through the centroids of both walls a and b, of assembly i

ϕ_i = the angle the vector $\underset{\sim}{U}_i$ makes with the vector $\underset{\sim}{C}_i$

centroidal plane = the plane which contains the centroidal axes of both walls of each assembly

Using the continuous medium approach, the continuity equations for the assemblies 1 and 2 may be written as, respectively,

$$1 \cos \phi_1 \frac{dU_1}{dz} - \frac{1}{E}\left(\frac{b^3 h}{12 I_c}\right) q_1 - \frac{1}{E}\left(\frac{1}{A_a} + \frac{1}{A_b}\right) \int_0^z \int_\xi^H q_1 d\lambda \, d\xi - \delta_1 = 0$$

$$1 \cos \phi_2 \frac{dU_2}{dz} - \frac{1}{E}\left(\frac{b^3 h}{12 I_c}\right) q_2 - \frac{1}{E}\left(\frac{1}{A_a} + \frac{1}{A_b}\right) \int_0^z \int_\xi^H q_2 d\lambda \, d\xi - \delta_2 = 0 \qquad (4.57)$$

in which 1 is the distance between the centroids of walls a and b. From ordinary beam theory, it may be shown that the bending moments in the centroidal planes of the assemblies 1 and 2 are, respectively,

$$M_1 = EI_1 \cos \phi_1 \frac{d^2U_1}{dz^2} = M_{e1} - 1 \int_z^H q_1 \, d\lambda$$

$$M_2 = EI_2 \cos \phi_2 \frac{d^2U_2}{dz^2} = M_{e2} - 1 \int_z^H q_2 \, d\lambda \qquad (4.58)$$

where,

M_1, M_2 = internal bending moments in the centroidal planes of assemblies 1 and 2 respectively

M_{e1}, M_{e2} = external moments about the axes perpendicular to the centroidal planes of assemblies 1 and 2

$$I_i = \frac{1}{\cos \phi_i} \Big[I_{m,a} \cos(\phi_i + \psi_{na}) \cos \psi_{na} + (I_{n,a}) \cdot \cos(\phi_i + \psi_{ma}) \cos \psi_{ma} + I_{m,b} \cos(\phi_i + \psi_{nb}) \cos \psi_{nb} + I_{n,b} \cos(\phi_i + \psi_{mb}) \cos \psi_{mb} \Big]$$

$$i = 1, 2 \qquad (4.59)$$

ψ_{ma}, ψ_{na} = the angles the centroidal vector of the assembly make with the major and minor principal axes, respectively, of wall a

ψ_{mb}, ψ_{nb} = similarly defined as ψ_{ma} and ψ_{na}, but referred to wall b

$I_{m,a}$, $I_{n,a}$ = second moments of area about the major and minor principal axes respectively, of wall a

$I_{m,b}$, $I_{n,b}$ = similarly defined as $I_{m,a}$ and $I_{n,a}$, but referred to wall b

From equations (4.57) and (4.58) the governing differential equations for the assemblies become,

$$\frac{d^2 q_i}{dz^2} - \alpha_i^2 q_i = \beta_i^2 \frac{dM_{ei}}{dz} , \quad i = 1 \text{ or } 2 \tag{4.60}$$

in which,

$$\beta_i^2 = \frac{12 I_c 1}{b^3 h I_i} \tag{4.61}$$

$$\alpha_i^2 = \beta_i^2 1 \left[1 + \frac{I_i}{I_2} \left(\frac{1}{A_a} + \frac{1}{A_b}\right)\right]$$

If the assemblies are constrained to move together so that U_1 and U_2 are equal(such as that in the case of the pure bending of a structure) and I_1 is equal to I_2, the following differential equation may be derived,

$$\frac{d^2 Q}{dz^2} - \frac{12 I_c}{b^3 h} \left(\frac{1}{A_a} + \frac{1}{A_b}\right) Q = 0 \tag{4.62}$$

in which,

$$Q = \frac{q_1}{\cos \phi_1} - \frac{q_2}{\cos \phi_2} \tag{4.63}$$

The solution for Q, assume that the assemblies are free at the tops, is trivial, i.e. Q = 0. Therefore, from equation (4.63),

$$\frac{q_1}{q_2} = \frac{\cos \phi_1}{\cos \phi_2} \qquad (4.64)$$

or the ratio of the vertical shear distributions is equal to the ratio of the displacements in the directions of the centroidal vectors of the assemblies.

It may be shown, by substituting relevant parameters into equation (4.59), that the equality of I_1 and I_2 is always satisfied for the following simple cases:-

(i) The angles between the resultant horizontal displacement and the centroidal planes of assemblies 1 and 2 are equal.

(ii) The centroidal vector is the common principal axis for both walls a and b of the assembly, in which case $q_1 = q_2 \frac{\cos \phi_1}{\cos \phi_2}$. An in-plane symmetrical coupled wall assembly belongs to this category of non-planar coupled walls since the plane of symmetry is the common principal plane for both walls.

4.7.2 Constrained Rotation

Consider the two identical non-planar coupled wall assemblies, 1 and 2, shown in plan in Fig. 4.5. The assemblies are assumed to be constrained to rotate about the vertical axis OZ.

Define,

$\underset{\sim}{U}_{ai}$, $\underset{\sim}{U}_{bi}$ = resultant horizontal displacement vectors for the shear centre axes of walls a and b of assembly i, i.e. walls ai and bi

$\underset{\sim}{C}_i$ = centroidal vector, a horizontal vector passing through the centroids of both walls a and b, of assembly i

$\underset{\sim}{S}_i$ = shear centre vector, a horizontal vector passing through the shear centres of both walls a and b, of assembly i

ϕ_{ai}, ϕ_{bi} = the angles the vectors $\underset{\sim}{U}_{ai}$ and $\underset{\sim}{U}_{bi}$ make with the vector $\underset{\sim}{S}_i$

θ = horizontal angle of rotation of each assembly, about the axis OZ

ρ = the angle between the vectors $\underset{\sim}{C}_i$ and $\underset{\sim}{S}_i$

R_{ai}, R_{bi} = distances between the axis of rotation OZ and the shear centres of walls ai and bi, respectively

R_i = perpendicular distance between the axis of rotation OZ and the plane of the shear centres (shear centre plane) of assembly i

r_a, r_b = horizontal distances between points of contra-flexure of the substitute lamina and the centroids of walls a and b, respectively.

J_{ai}, J_{bi} = projections of r_a and r_b on the vectors $\underset{\sim}{U}_{ai}$ and $\underset{\sim}{U}_{bi}$, respectively

The continuity equations for the substitute laminae of the assemblies 1 and 2 may be written as,

$$(R_{ai}J_{ai} + R_{bi}J_{bi})\frac{d\theta}{dz} - \frac{1}{E}\left(\frac{b^3h}{12I_c}\right)q_i - \frac{1}{E}\left(\frac{1}{A_a} + \frac{1}{A_b}\right)\cdot$$

$$\int_0^z \int_\xi^H q_i \, d\lambda \, d\xi - \delta_i = 0 \qquad (4.65)$$

$$i = 1,2$$

Using ordinary beam theory, bending moments in the shear centre planes of assemblies 1 and 2 are given by, respectively,

$$M_1 = R_1 I_{t1} \frac{d^2\theta}{dz^2} = M_{e1} - 1 \cos\rho \int_z^H q_1 \, d\lambda \qquad (4.66)$$

$$M_2 = R_2 I_{t2} \frac{d^2\theta}{dz^2} = M_{e2} - 1 \cos\rho \int_z^H q_2 \, d\lambda$$

where,

$$I_{ti} = \frac{R_{ai}}{R_i} \left[I_{m,a} \cos(\phi_{ai} + \psi_{n,ai}) \cos \psi_{n,ai} + I_{n,a} \cos(\phi_{ai} + \psi_{m,ai}) \cos \psi_{m,ai} \right] + \frac{R_{bi}}{R_i} \left[I_{m,b} \cos(\phi_{bi} + \psi_{n,bi}) \cos \psi_{n,bi} + I_{n,bi} \cos(\phi_{bi} + \psi_{m,bi}) \cos \psi_{m,bi} \right]$$

$$i = 1, 2 \qquad (4.67)$$

$\psi_{m,ai}$, $\psi_{n,ai}$ = the angles the vector $\underset{\sim}{S}_i$ make with the major and minor principal axes, respectively, of wall ai

$\psi_{m,bi}$, $\psi_{n,bi}$ = similarly defined as $\psi_{m,ai}$ and $\psi_{n,ai}$, but referred to wall bi

M_1, M_2 = redefined as the components of internal moments in the shear centre planes of assemblies 1 and 2 respectively

M_{e1}, M_{e2} = redefined as the external moments about

the axes perpendicular to the shear centre planes of assemblies 1 and 2

and the other parameters are as defined earlier.

From equations (4.65), (4.66), the governing differential equations for the assemblies may be written as,

$$\frac{d^2 q_i}{dz^2} - \alpha_i^2 q_i = \beta_i^2 \frac{dM_{ei}}{dz} \qquad (4.68)$$

$$i = 1, 2$$

in which,

$$\beta_i^2 = \frac{12 I_c}{b^3 h I_{ti}} \bar{I}_i$$

$$\bar{I}_i = \frac{1}{R_i} (R_{ai} J_{ai} + R_{bi} J_{bi}) \qquad (4.69)$$

$$\alpha_i^2 = \beta_i^2 \, l \cos\rho \left[1 + \frac{\bar{I}_{ti}}{l \bar{I}_i \cos} \left(\frac{1}{A_a} + \frac{1}{A_b} \right) \right]$$

Generally the vertical shear distributions q_1 and q_2 are not linearly related, and the governing differential equations are independent. However, if the parameters I_{t1} and I_{t2} are equal and $\bar{I}_1$ is equal to $\bar{I}_2$, then, from equation (4.66),

$$M_{e1} = \frac{R_1}{R_2} \left(M_{e2} - l \cos\rho \int_z^H q_2 \, d\lambda \right) + l \cos\rho \int_z^H q_1 \, d\lambda \qquad (4.70)$$

From equations (4.65), (4.68) and (4.70) it may be shown that the vertical shear distributions in the

assemblies are proportional to each other. The relationship between q_1 and q_2 is given by,

$$q_1 = \frac{R_1}{R_2} q_2 \qquad (4.71)$$

The validity of equation (4.71) depends on the equalities of I_{t1} and I_{t2}, and $\bar{I}_1$ and $\bar{I}_2$. It can be shown that these equalities are always satisfied for the following simple cases:-

(i) $R_{a1} = R_{a2}$ and $R_{b1} = R_{b2}$, in which case $q_1 = q_2$ irrespective of the geometry of the walls.

(ii) The plane of the connecting beams is the centroidal plane and the shear centre plane, in which case $\frac{q_1}{q_2} = \frac{R_1}{R_2}$. An in-plane symmetrical coupled wall assembly belongs to this type of non-planar coupled walls.

4.8 Structures with General Non-planar Coupled Wall Assemblies

It has been shown in the previous section that the constrained translation and rotation, corresponding to the pure bending and the pure torsional actions of symmetrical structures respectively, of general non-planar coupled wall assemblies, which are identical do not necessarily ensure that the vertical shear distributions in the assemblies are linearly related. However, from the geometry of the assemblies and the positions and orientations of the assemblies in the structures, it can generally be determined which assemblies have vertical

shear distributions which are linearly related.

As an illustration, consider the symmetrical structure shown in plan in Fig. 4.6. Each coupled wall assembly is a non-planar assembly, and there are only two distinct groups of coupled wall assemblies. Under the pure bending action due to the load W_y, the vertical shear distributions in identical assemblies which have the same relative orientation with respect to the Y axis, i.e. the angles between the Y axis and the centroidal planes of the assemblies are the same, will be linearly related. Therefore, all the assemblies may be divided into three bending groups, namely,

bending group 1:- assemblies 1, 8, 9, 16

bending group 2:- assemblies 3, 4, 5, 6, 11, 12, 13, 14

bending group 3:- assemblies 2, 7, 10, 15

The vertical shear distributions in the assemblies of the same groups will be linearly related and, consequently, the behaviour of the structure under the pure bending action may be described by a system of three independent differential equations.

Under the pure torsional action, the vertical shear distributions in identical assemblies which have the same relative positions and orientations with respect to the axis of symmetry OZ, i.e. $R_{ai} = R_{aj}$ and $R_{bi} = R_{bj}$, will be equal. Therefore, all the assemblies may be divided into four torsion groups, namely,

torsion group 1:- assemblies 1, 8, 9, 16

torsion group 2:- assemblies 3, 6, 11, 14

torsion group 3:- assemblies 4, 5, 12, 13

torsion group 4:- assemblies 2, 7, 10, 15

In consequence, the behaviour of the structure under the pure torsional action may be described by a system of four independent differential equations.

It may be noted that the assemblies which behave similarly, i.e. the vertical shear distributions in the assemblies are linearly related, under the pure bending action may behave differently under the pure torsional action, for instance, the assemblies 3 and 4.

Whether the symmetrical structure consists of planar or non-planar coupled wall assemblies or a combination of both types, the procedures for establishing the equivalent analogous plane systems presented earlier are applicable. The final forms of the analogous differential equations are the same as those given earlier. However, the expressions for the analogous parameters will be slightly different since the plane of the connecting beams may not be the centroidal plane and the shear centre plane of the assembly.

4.8.1 Pure Bending Action

As noted earlier, from the geometry of the structure it is possible to determine which coupled wall assemblies behave similarly under the pure bending action or the pure torsional action. Assume that under a pure bending action, the coupled wall assemblies of a symmetrical structure can be separated into K groups such that the vertical shear distributions of the assemblies within the

same group are linearly related. The numbers of the coupled wall assemblies in groups 1, 2, 3 ... K are n_1, n_2, ... n_k respectively. Assume that the structure also consists of, in addition, n_{cr} cantilevers.

Following the same procedure carried out in section 4.5.1, it may be shown that the differential equations and the expressions of the parameters given by equations (4.24) and (4.25) respectively are valid, provided that some of the parameters are redefined as follows:-

C_{i-j} = cosine of the angle the centroidal plane of the assembly i-j makes with the direction of the displacement of the structure

$$\bar{I} = \sum_{i=1}^{K} (\bar{I}_{i,a} + \bar{I}_{i,b}) + \bar{I}_{cr}$$

$$\bar{I}_{i,a} = \frac{1}{C_{1-1}^2} \sum_{j=1}^{n_i} \left(I_{m,a} C_{ma,i-j}^2 + I_{n,a}(1-C_{ma,i-j}^2) \right)$$

$$\bar{I}_{i,b} = \frac{1}{C_{1-1}^2} \sum_{j=1}^{n_i} \left(I_{m,b} C_{mb,i-j}^2 + I_{n,b}(1-C_{mb,i-j}^2) \right)$$

$$\bar{I}_{cr} = \frac{1}{C_{1-1}^2} \sum_{k=1}^{n_{cr}} \left(I_{m,cr-k} C_{cr-k}^2 + I_{n,cr-k}(1-C_{cr-k}^2) \right)$$

(4.72)

$C_{ma,i-j}$, $C_{mb,i-j}$ = cosines of the angles the centroidal plane of assembly i-j make with the major principal axes of walls ai-j and

bi-j respectively.

In a similar manner as in the case of symmetrical structures with in-plane symmetrical coupled wall assemblies, the relationships between the real and analogous stiffnesses may be established. The displacement of the analogous plane system is the component of the real displacement along the centroidal plane of the datum assembly 1-1. After the analogous vertical shear distributions and displacement have been determined, all other real forces may be easily evaluated.

4.8.2 Pure Torsional Action

By following a similar procedure established in section 4.5.2, but taking into account the fact that the coupled wall assemblies may be non-planar assemblies, the differential equations for an analogous plane system for the pure torsional action may be shown to be,

$$\frac{d^2Q_i}{dz^2} - \alpha_i^2 Q_i - \beta_i^2\left(\sum_{j=1}^{K} L_j Q_j - L_i Q_i\right) = - \beta_i^2 \frac{M_T}{R_{1-1}}$$

$$i = 1, 2, \ldots K \qquad (4.73)$$

where,

M_T = the torsional moment applied to the structure

K = number of groups of coupled walls which behave differently (i.e. the vertical shear distributions in the assemblies of different groups are not linearly related)

$Q_i = D_i\, t_{i-j}\, q_{i-j}$

$$t_{i-j} = \frac{R_{1-1}}{R_{i-j}}$$

$$D_i = \sum_{j=1}^{n_i} \left(\frac{R_{i-j}}{R_{1-1}}\right)^2$$

R_{i-j} = distance of the shear centre plane of assembly i-j from the axis of symmetry of the structure

R_{1-1} = distance of the shear centre plane of the datum assembly 1-1 from the axis of symmetry

Q_i = vertical shear distribution in the analogous coupled wall assembly i

n_i = number of coupled wall assemblies in coupled wall group i

n_i

$$L_i = \sum_{j=1} G_{i-j}$$

$$G_{i-j} = \frac{1}{R_{i-j}} \left(R_{m,ai-j} J_{n,ai-j} + R_{n,ai-j} J_{m,ai-j} + R_{m,bi-j} J_{n,bi-j} + R_{n,bi-j} J_{m,bi-j}\right)$$

$J_{m,ai-j}, J_{n,ai-j}$ = projections of a line between a point of contraflexure, of assembly i-j, and the centroid of wall ai-j, on its major and minor principal axes, respectively

$J_{m,bi-j}, J_{n,bi-j}$ = similarly defined as $J_{m,ai-j}$ and $J_{n,ai-j}$, but referred to wall bi-j

$$\beta_i^2 = \frac{12 I_{ci}}{b_i^3 h I_t} \sum_{j=1}^{n_i} \bar{L}_{i-j}$$

$$\bar{L}_{i-j} = \frac{R_{i-j}}{R_{1-1}^2} \left(R_{ai-j} J_{ai-j} + R_{bi-j} J_{bi-j}\right)$$

R_{ai-j}, R_{bi-j} = distances of the shear centres of walls ai-j and bi-j from the axis of rotation, respectively

J_{ai-j} = projection of a line between a point of contraflexure of assembly i-j and the centroid of wall ai-j on an axis parallel to the horizontal displacement of the shear centre of wall ai-j

J_{bi-j} = similarly defined as J_{ai-j}, but referred to wall bi-j

$$I_t = \sum_{i=1}^{K} \sum_{j=1}^{n_i} I_{i-j} + I_{t,cr}$$

$$I_{i-j} = \frac{1}{R_{1-1}^2} \left(I_{m,ai} R_{m,ai-j}^2 + I_{n,ai} R_{n,ai-j}^2 + I_{m,bi} R_{m,bi-j}^2 + I_{n,bi} R_{n,bi-j}^2\right)$$

$$I_{t,cr} = \frac{1}{R_{1-1}^2} \sum_{k=1}^{n_{cr}} \left(I_{m,cr-k} R_{m,cr-k}^2 + I_{n,cr-k} R_{n,cr-k}^2\right)$$

$R_{m,ai-j}$ = projection of the horizontal vector of the shear centre of wall ai-j on its major

principal axis

$R_{m,bi-j}$ = similarly defined as $R_{m,ai-j}$, but referred to wall bi-j

$$\alpha_i^2 = \beta_i^2 L_i \mu_i$$

$$\mu_i = 1 + \frac{I_t}{\psi_i} \left(\frac{1}{A_{ai}} + \frac{1}{A_{bi}}\right)$$

$$\psi_i = \sum_{j=1}^{n_i} G_{i-j} \bar{L}_{i-j}$$

other parameters are as defined previously in this Chapter.

If the coupled wall assemblies are in-plane symmetrical, then,

$$G_{i-j} = l_i$$

$$\bar{L}_{i-j} = l_i \left(\frac{R_{i-j}}{R_{1-1}}\right)^2$$

and all the parameters reduce to those given in equation (4.38).

4.9 Closed Form Solutions for Standard Load Cases

Any structure which is reducible to analogous plane systems with no more than one analogous coupled wall assembly for each system can be analysed rapidly since closed form solutions may be easily obtained. Example of the structures which fall into this category are shown in Fig. 4.7. For such structures, the analogous

governing differential equations for the pure bending action and the pure torsional action are given by, respectively,

$$\frac{d^2 Q_B}{dz^2} - \alpha_B^2 Q_B = \beta_B^2 \frac{d(M/\cos \phi)}{dz} \qquad (4.74)$$

$$\frac{d^2 Q_T}{dz^2} - \alpha_T^2 Q_T = - \beta_T^2 \frac{M_T}{R} \qquad (4.75)$$

in which,

M = moment due to the lateral load system which acts in the plane of symmetry of the structure

M_T = applied torsional moment

ϕ = the angle the direction of the applied load makes with the centroidal plane of the datum assembly

R = the distance between the shear centre plane of the datum assembly and the axis of symmetry of the structure

and the analogous parameters β_B^2, α_B^2 and β_T^2, α_T^2 are the parameters evaluated from equations (4.25) and (4.38) respectively.

For the three standard lateral load cases, namely, a concentrated load P at the top, a uniformly distributed load w per unit height and a triangularly distributed load $\vartheta(\frac{z}{H})$ per unit height, the solutions for the pure bending actions due to these loads are, respectively,

$$(Q_B)_P = \frac{P}{l\mu} \sec \phi \left(1 - \frac{\cosh \gamma(1 - \eta)}{\cosh \gamma} \right)$$

$$(Q_B)_w = \frac{wH}{1\mu}\sec\phi\left[\frac{(\sinh\gamma - \gamma)\cosh\gamma(1-\eta)}{\gamma\cosh\gamma} - \frac{\sinh\gamma(1-\eta)}{\gamma} + (1-\eta)\right]$$

$$(Q_B)_\vartheta = \frac{\vartheta H}{1\mu}\sec\phi\left[\frac{(\sinh\gamma - \gamma/2 + 1/\gamma)\cosh\gamma(1-\eta)}{\gamma\cosh\gamma} - \frac{\sinh\gamma(1-\eta)}{\gamma} + \frac{1}{2} - \frac{1}{2}\eta^2 - \frac{1}{\gamma^2}\right]$$

(4.76)

in which $\eta = \frac{z}{H}$ and $\gamma = \alpha_B H$

The corresponding analogous displacements, u, may be shown to be,

$$(u)_P = \frac{PH}{EI}\sec\phi\left[\left(\frac{1}{3} - \frac{(1-\eta)^3}{6} - \frac{1}{2}(1-\eta)\right)\left(1 - \frac{1}{\mu}\right) - \frac{1}{\mu}\left(\frac{\sinh\gamma(1-\eta) - \sinh\gamma}{\gamma^3\cosh\gamma} - \frac{\eta}{\gamma^2}\right)\right]$$

$$(u)_w = \frac{wH^4}{EI}\sec\phi\left[\left(\frac{1}{8} - \frac{(1-\eta)}{6} + \frac{(1-\eta)^4}{24}\right)\left(1 - \frac{1}{\mu}\right) - \frac{1}{\mu\gamma^2}\left(\frac{\eta^2}{2} - \eta + \frac{\gamma\sinh\gamma - \gamma\sinh\gamma(1-\eta) - \cosh\gamma\eta + 1}{\gamma^2\cosh\gamma}\right)\right]$$

$$(u)_\vartheta = \frac{\vartheta H^4}{EI}\sec\phi\left[\left(\frac{11}{120} - \frac{(1-\eta)}{8} - \frac{(1-\eta)^4}{24} - \frac{(1-\eta)^5}{120}\right)\cdot\left(1 - \frac{1}{\mu}\right) - \frac{1}{\mu\gamma^2}\cdot\left(\frac{1}{6}\eta^3 + \eta^2 - \eta\right) - \left\{\frac{(1/\gamma - \gamma/2)}{\mu\gamma^4\cosh\gamma}\right\}\cdot\left\{\sinh\gamma(1-\eta) - \cosh\gamma(1-\eta) - \sinh\gamma + \eta\gamma\cosh\gamma + 1\right\}\right]$$

(4.77)

The marameters I and μ are the analogous parameters for the pure bending action, and Q_B and u are the analogous solutions.

If the applied loads do not pass through the axis of symmetry of the structure but act with eccentricity e, the structure will also be subjected to torsion. For constant eccentricity e, it may be shown that the analogous solutions for the pure torsional actions due to the three standard load cases are those given by equations (4.76), (4.77), provided that sec ϕ is replaced by $\frac{e}{R}$ and the analogous torsional parameters are used instead of the analogous bending parameters.

4.10 Example Problem

To illustrate the application of the analysis, a symmetrical three dimensional shear wall structure shown in Fig. 4.8 has been chosen as an example problem. A number of structures of this nature have been constructed recently for hotel buildings. The structure considered possesses three planes of symmetry, namely, the vertical planes OZX_a, OZX_b and OZX_c. The coupled wall assemblies, 1 to 18, are identical, and the walls 19 to 21 are plane cantilevered walls. For the purposes of analyses, it is assumed that the bending action is produced by a uniformly distributed load of 1 KN/m acting in the plane of symmetry OZX_a, and the torsional action is produced by a uniformly distributed torsional moment of 1 KN-m/m. The modulus of elasticity for the material is taken to be 24,000,000 KN/m^2.

As all the coupled wall assemblies are in-plane

symmetrical, there is only one analogous coupled wall assembly in each of the equivalent analogous plane systems for the bending and the torsional actions. Therefore, the solutions for the analogous vertical shear distributions and the analogous displacements given by equations (4.76) and (4.77) respectively are applicable. The analogous bending parameters and the analogous torsional parameters are those given by equations (4.25) and (4.38) respectively.

From the geometry of the structure (Figs. 4.8-4.9), equations (4.25), (4.38), and adopting assembly 1 as the datum assembly, the following relevant parameters are obtained,

$H = 75$ m $\qquad I_c = 0.0026042$ m^4

$h = 3$ m $\qquad E = 24{,}000{,}000$ KN/m^2

$b = 1.7$ m $\qquad A_a = A_b = 1.875$ m^2

$l = 9.2$ m

bending		torsion	
ϕ	$= \frac{\pi}{6}$	R	$= 30.5$ m
B	$= 12$	D	$= 9.5102$
μ	$= 1.2669$	μ	$= 1.2257$
I	$= 254.13$ m^4	I	$= 170.33$ m^4
γ	$= 7.7709$	γ	$= 8.3115$
w	$= 1$ KN/m	we	$= 1$ kN-m/m

With these parameters, the following functions have been evaluated.

Bending Action

(i) vertical shear distribution in the assembly 1

(ii) horizontal displacement of the structure

(iii) total shear force (in the direction of the applied load) taken by the three cantilevers

Torsional Action

(i) vertical shear distribution in the assembly 1

(ii) rotation of the structure

(iii) total torsional resistance contributed by the three cantilevers

Variations of these functions with height are shown graphically in Figs. 4.10-4.12. As noted earlier in this Chapter, inspection of Fig. 4.12 shows that concentrated lateral forces exist at the top of the walls.

4.11 Conclusion

It has been shown that the analyses of the pure bending and the pure torsional actions of any symmetrical shear wall structure consisting of in-plane symmetrical coupled wall assemblies are reducible to the analyses of analogous plane systems. The properties of the analogous plane systems are the transformed properties of the real structure. Generally any assembly may be chosen as the datum assembly, however, the transformation relationships based on different datum assemblies are usually different.

The theory has been extended to deal with structures supported on elastic foundations, and structures consisting of planar and non-planar coupled wall assemblies. Closed form solutions for the three standard lateral load cases, namely, a top concentrated load, a uniformly

distributed load and a triangularly distributed load, have been presented. The solutions are valid for any structure which is reducible to equivalent analogous plane systems with only one analogous coupled wall assembly for each system. The solutions presented are also applicable to the three standard torsional loadings, namely, a concentrated torsional moment at the top, a uniformly distributed torsional moment per unit height and a triangularly distributed torsional moment per unit height.

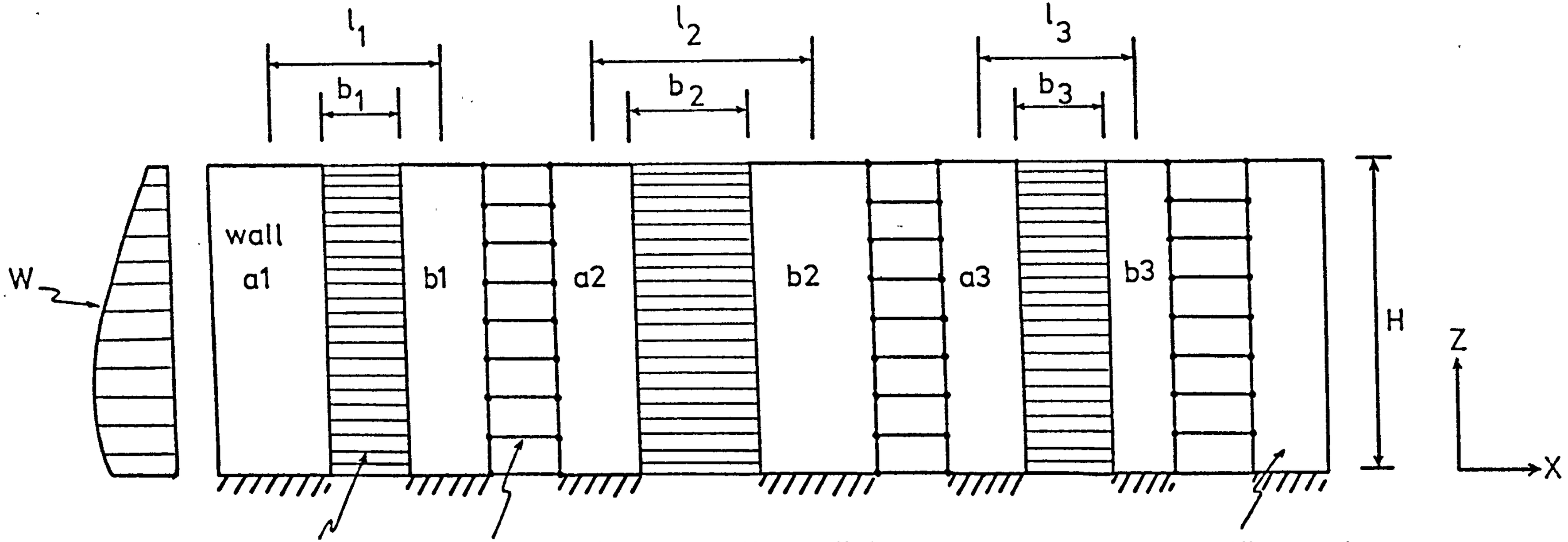

Plane system with rigid pin-ended connecting links

Fig. 4.1

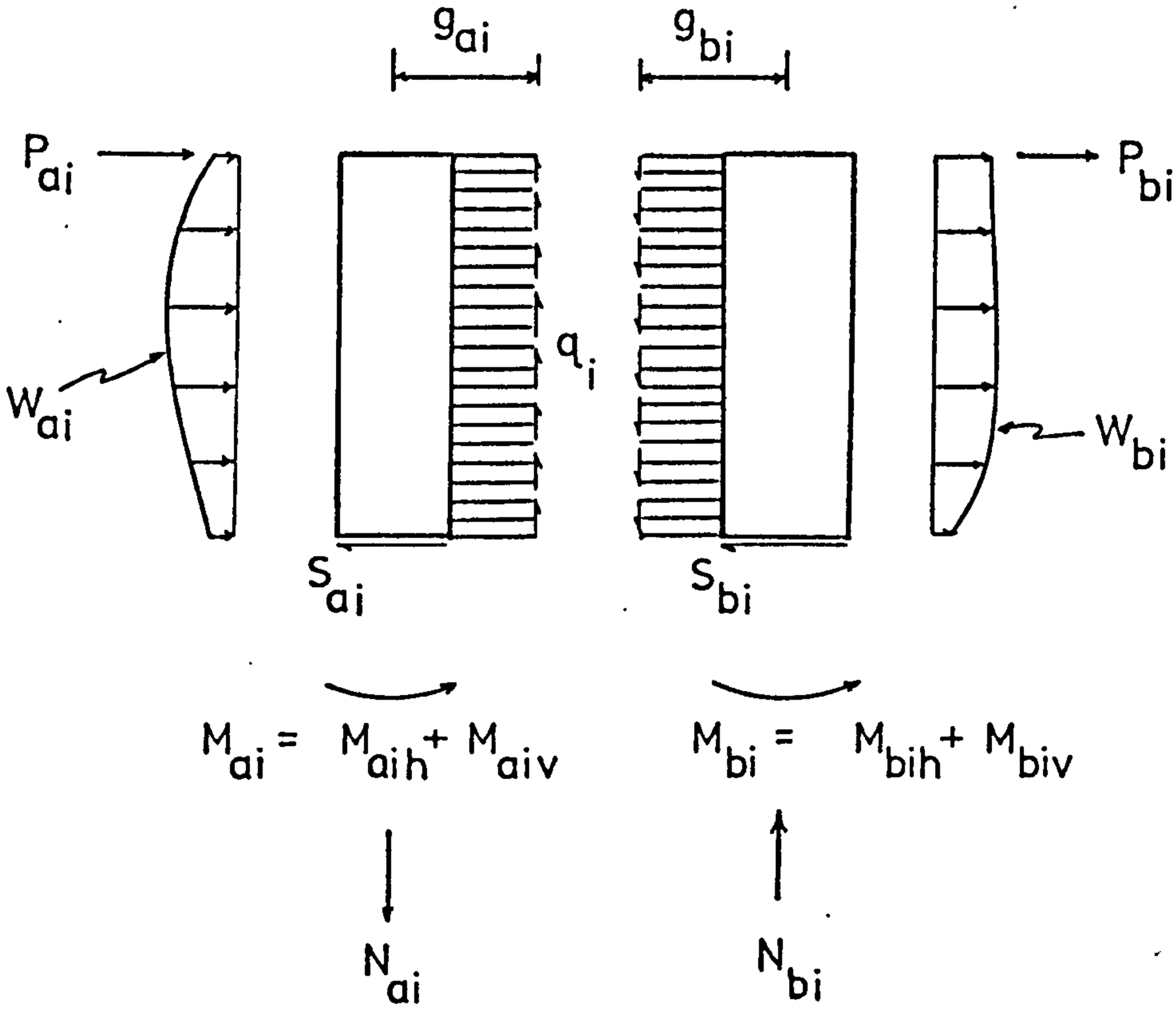

(a) cut-sections of coupled walls

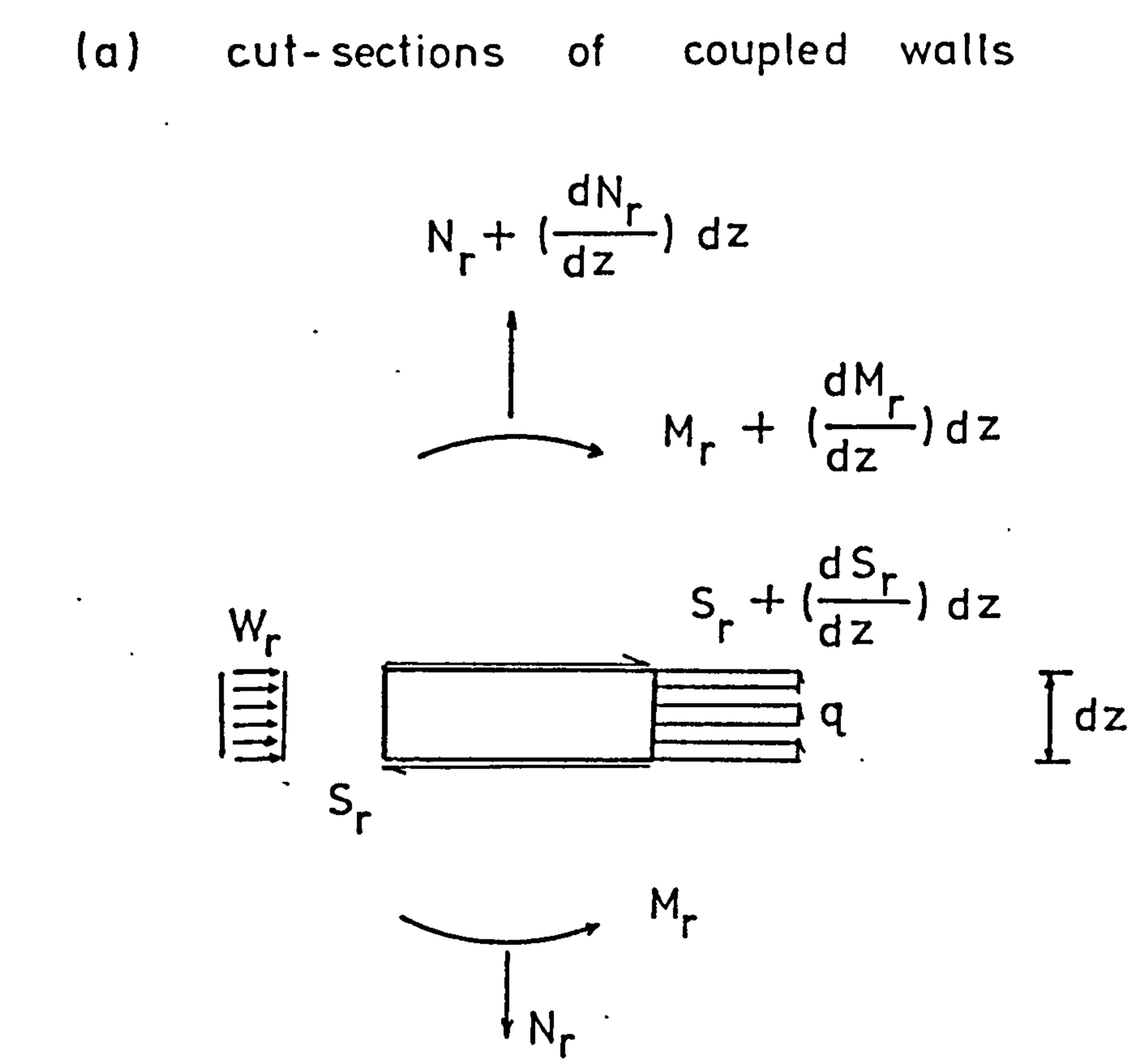

(b) wall element of an individual wall r

Forces on wall cut-sections and wall element

Fig. 4.2

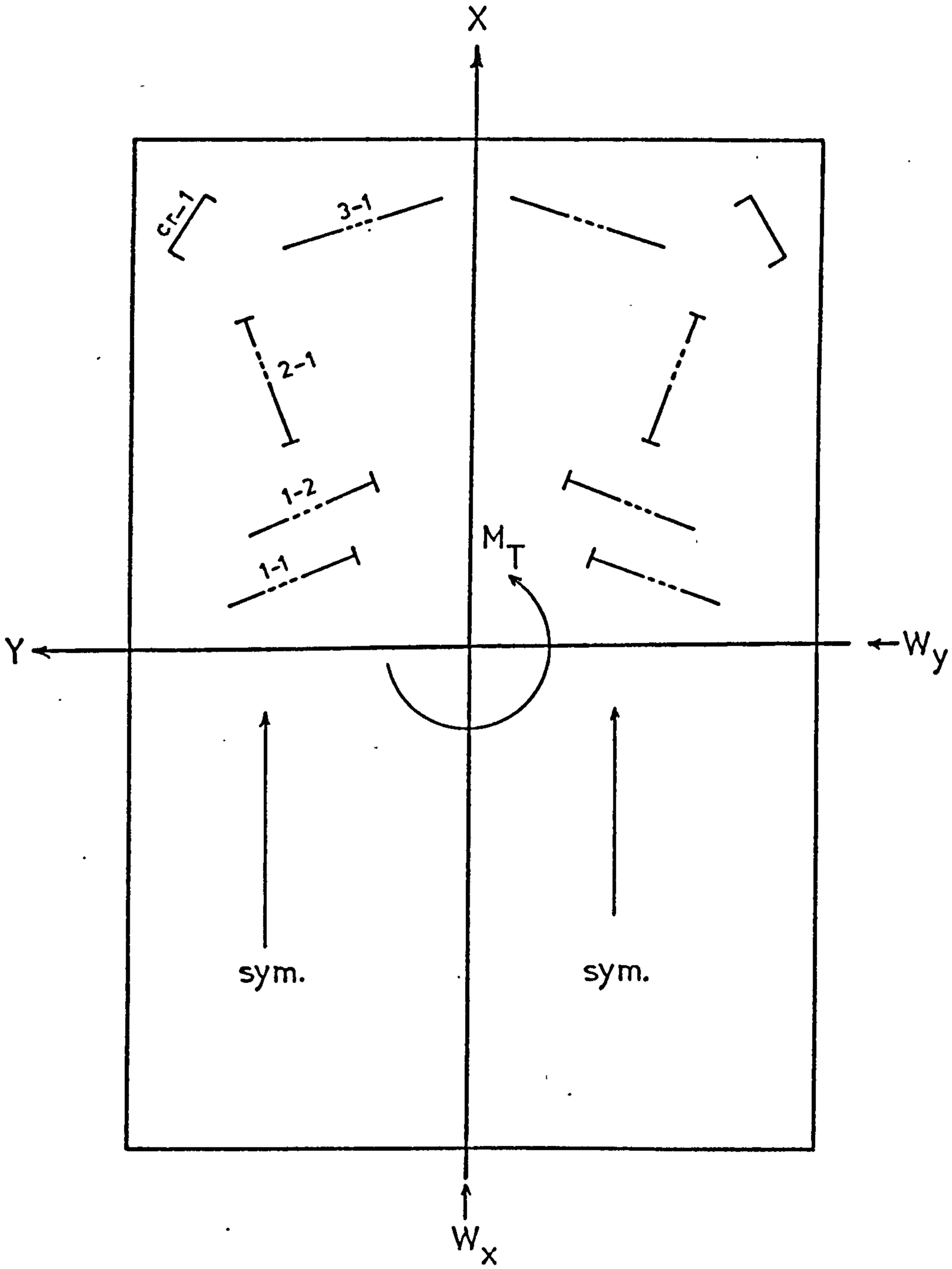

Symmetrical structure with in-plane symmetrical coupled wall assemblies

Fig. 4.3

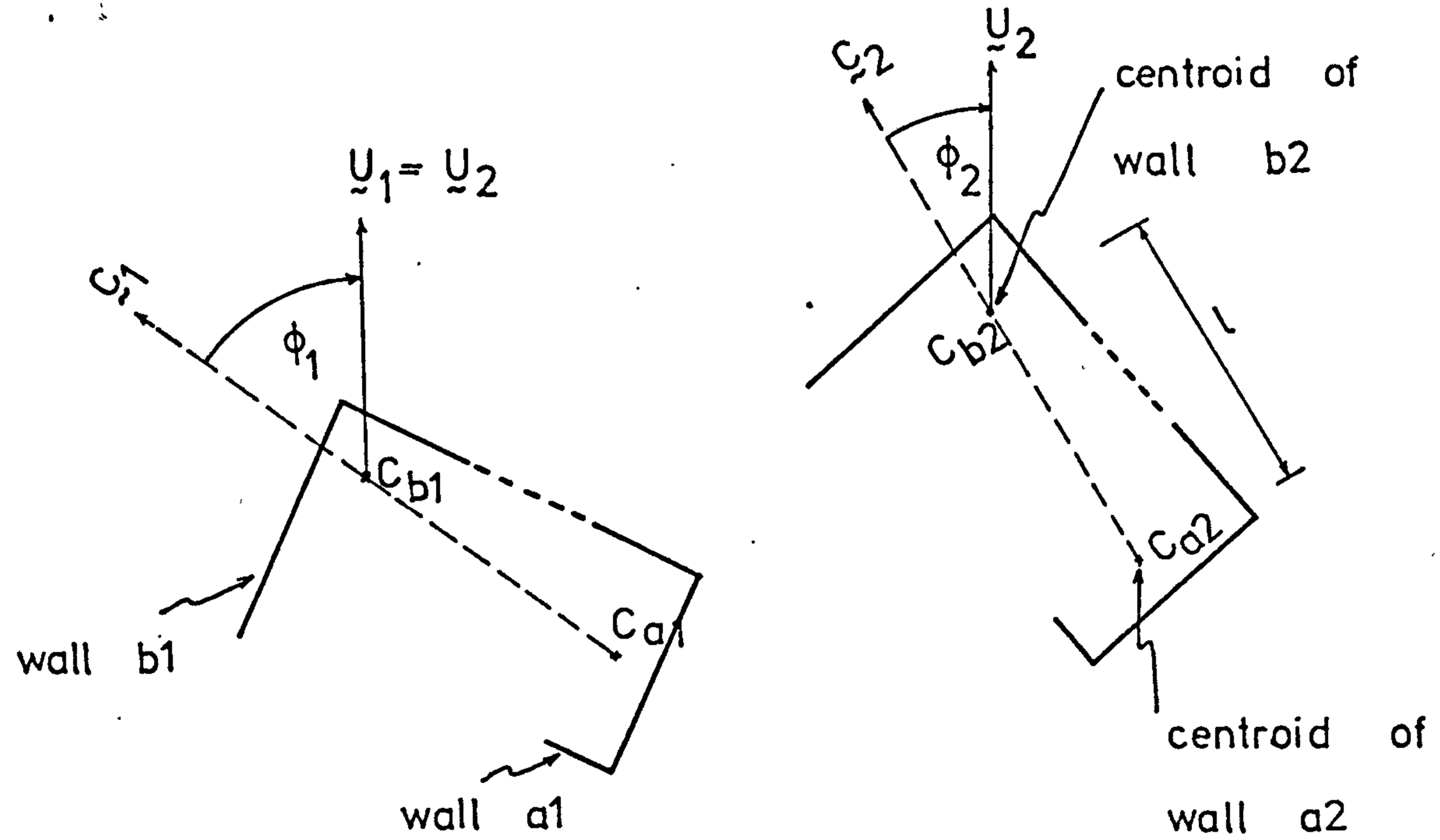

Constrained translation of identical coupled wall assemblies

Fig. 4.4

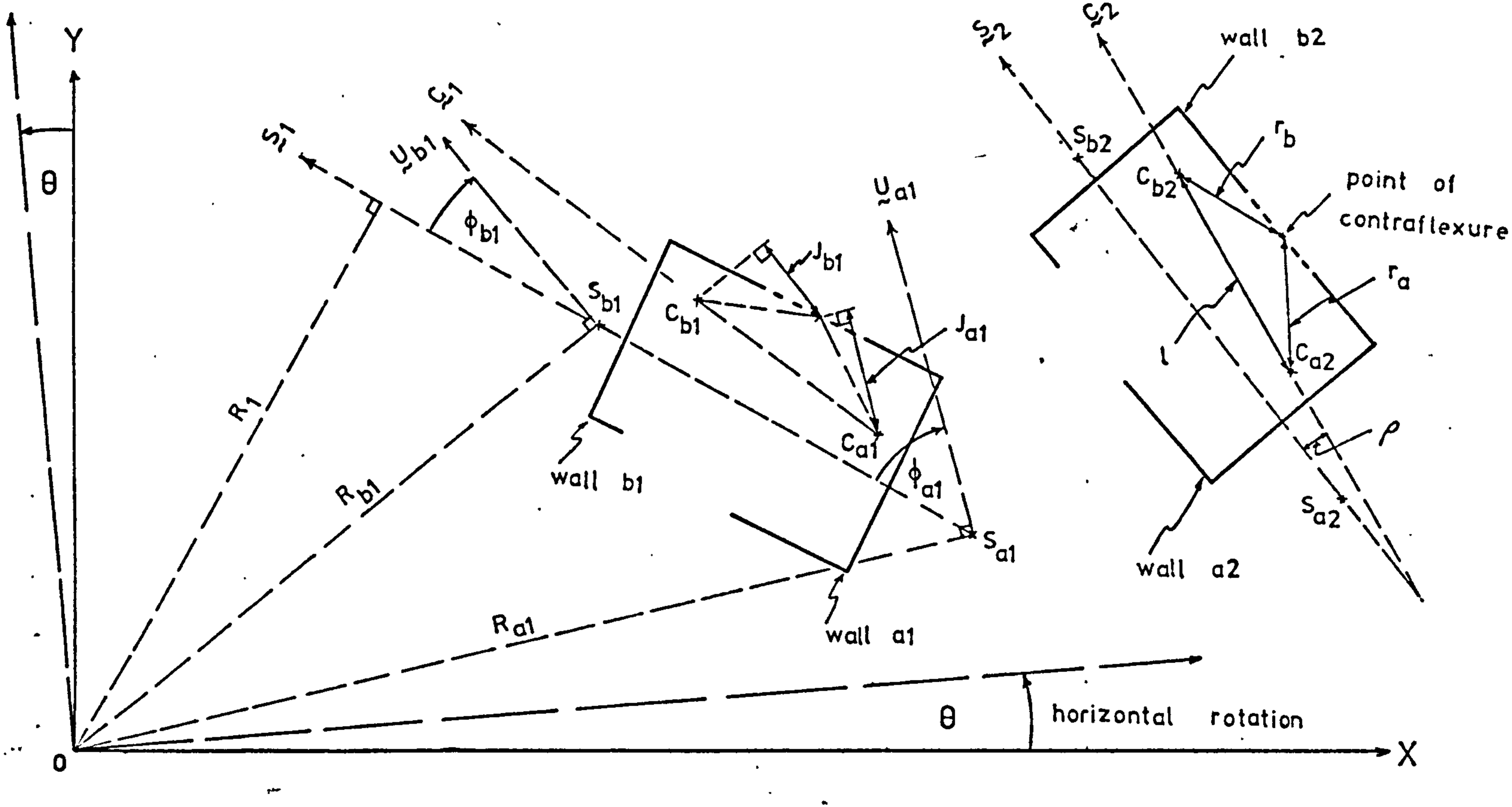

Constrained rotation of identical coupled wall assemblies

Fig. 4.5

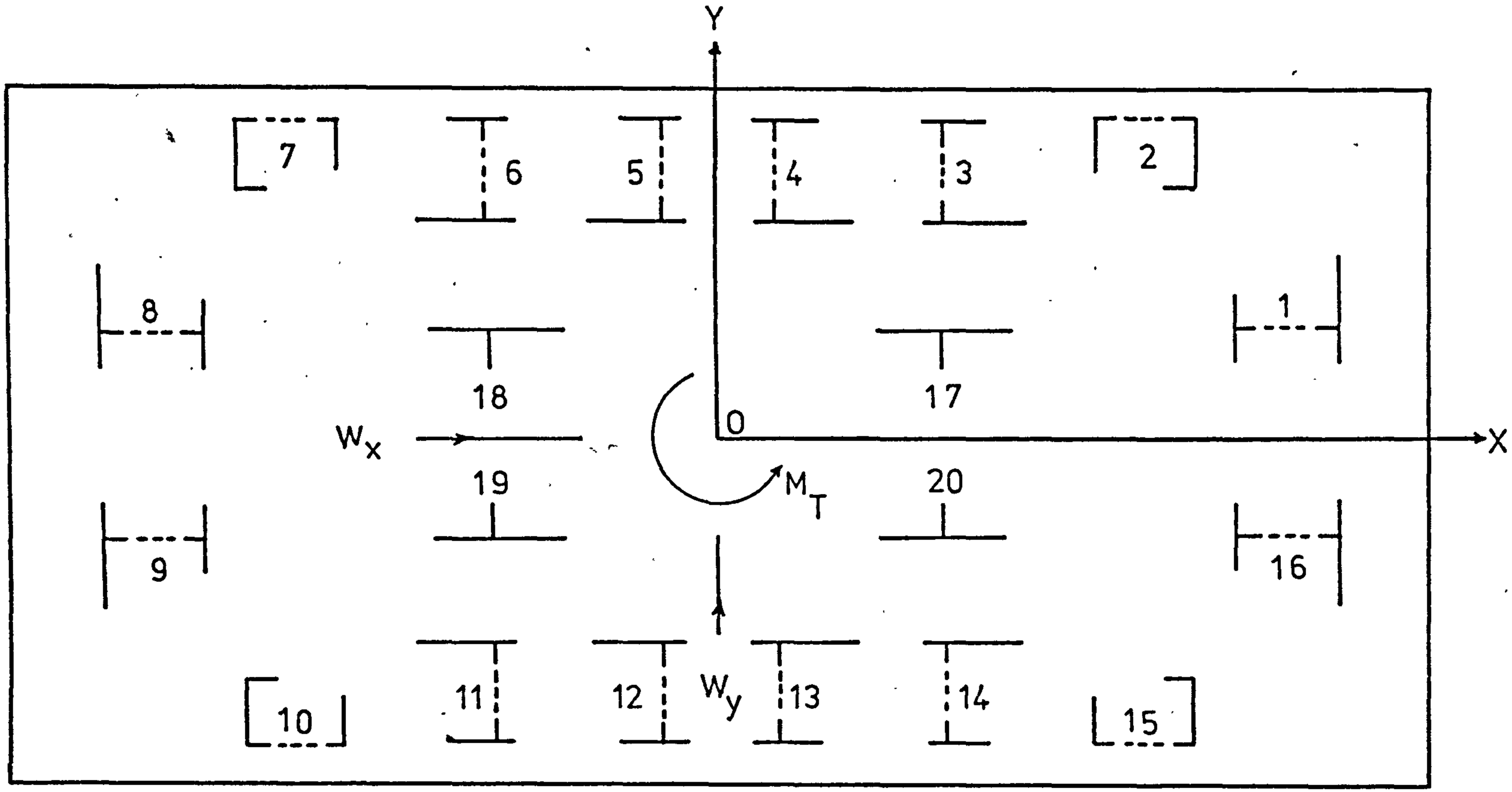

Symmetrical structure with general non-planar coupled wall assemblies

Fig. 4.6

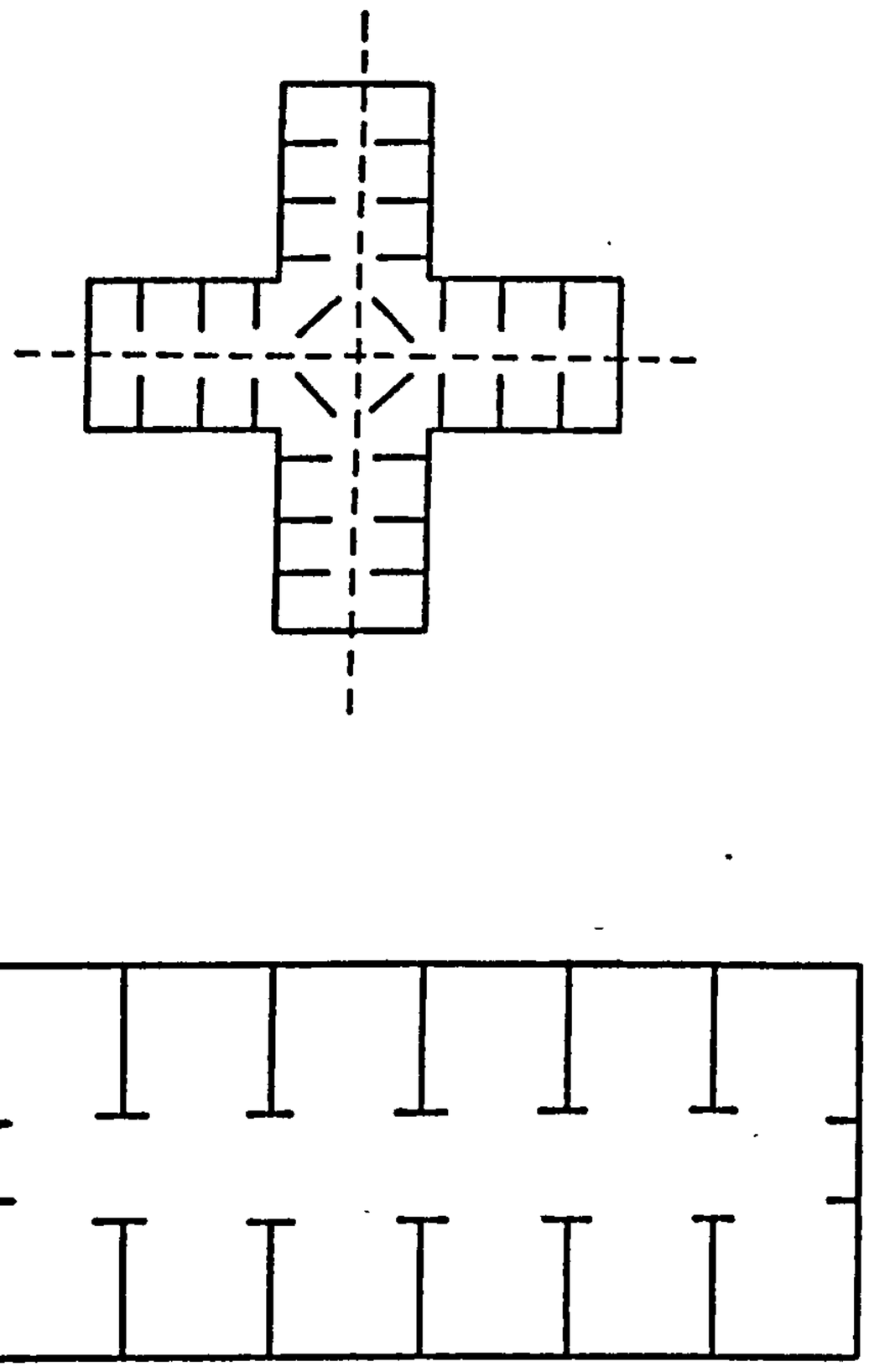

Structures reducible to equivalent plane systems with one analogous coupled wall assembly

Fig. 4.7

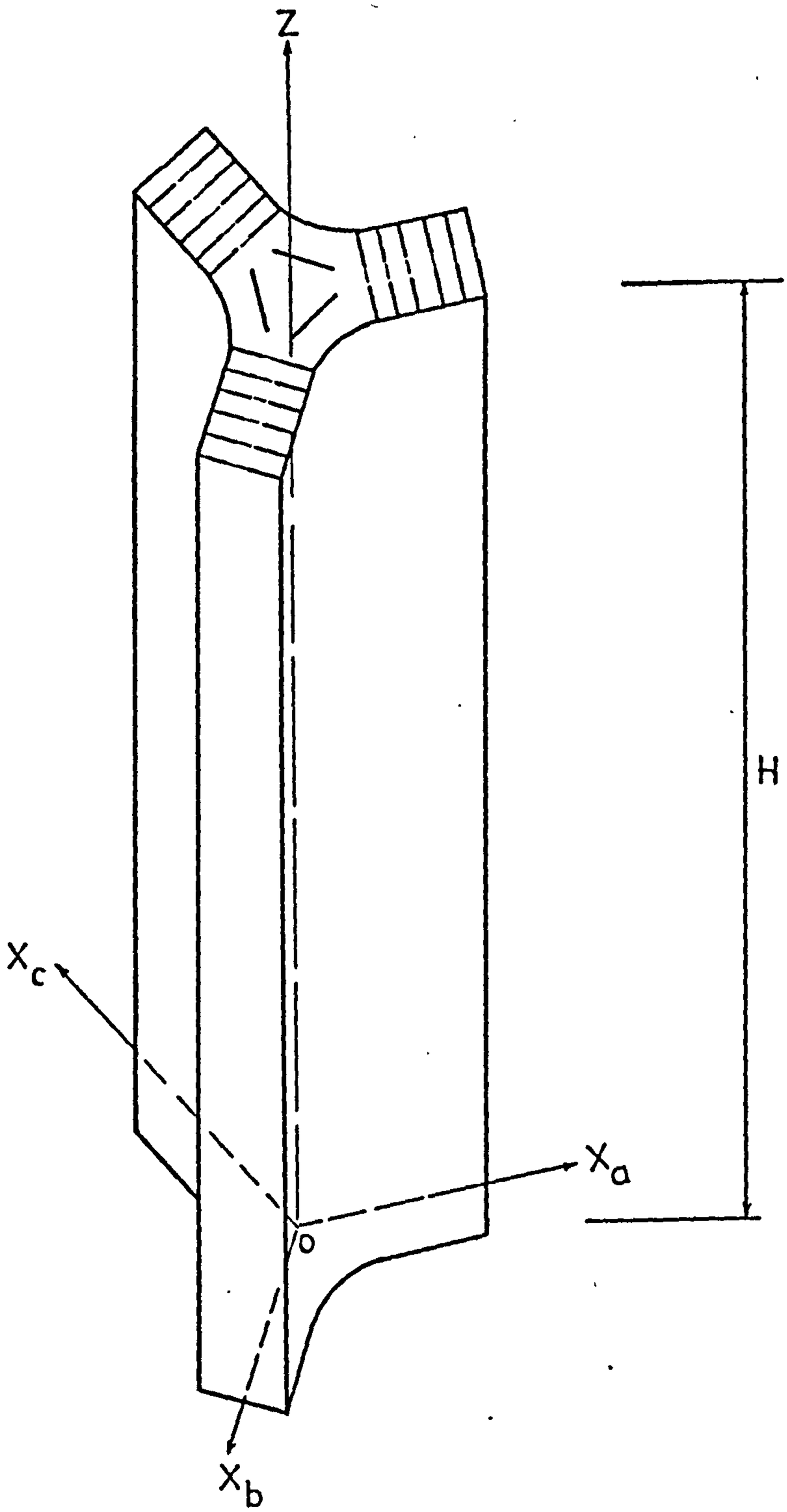

Example problem

(front view)

Fig. 4.8

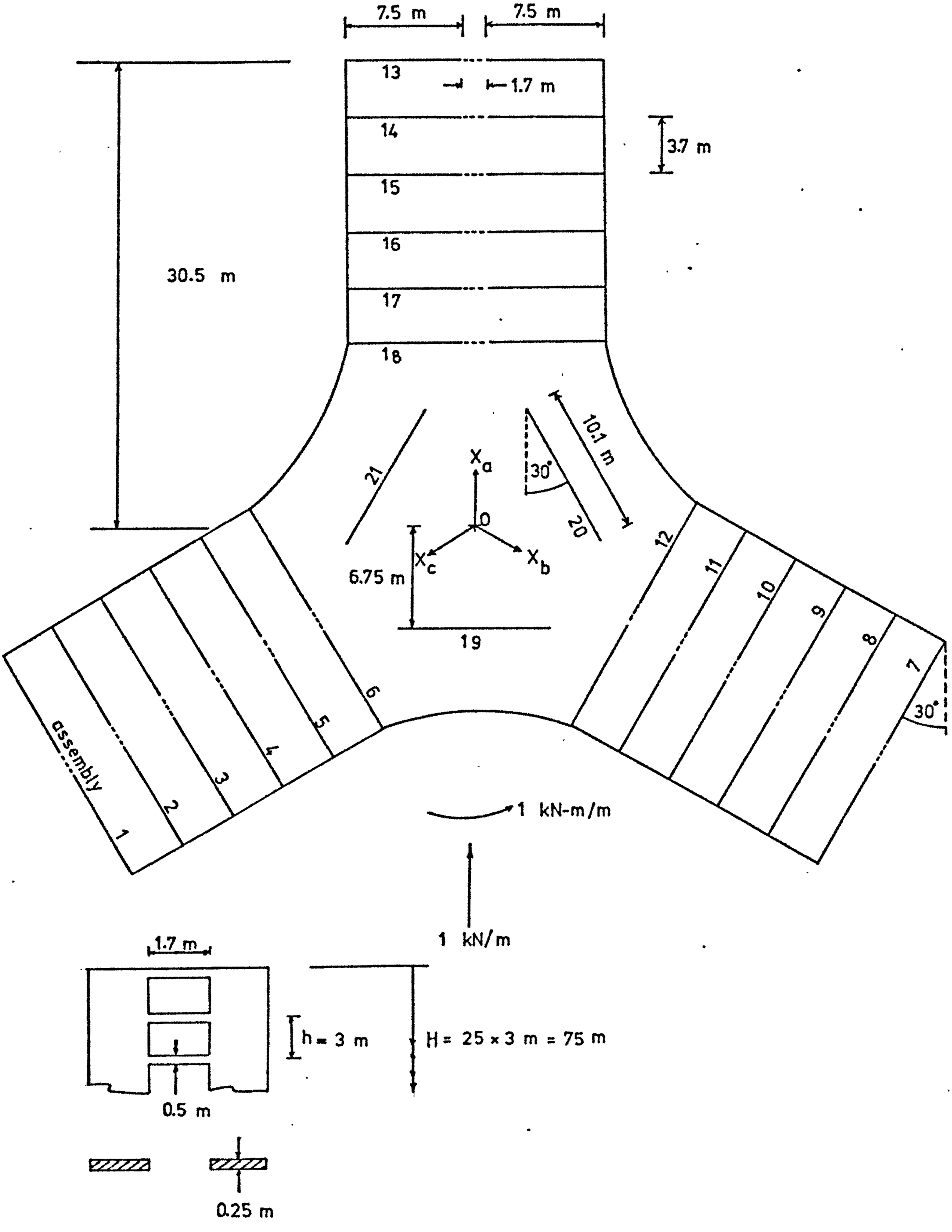

Example problem

Fig. 4.9

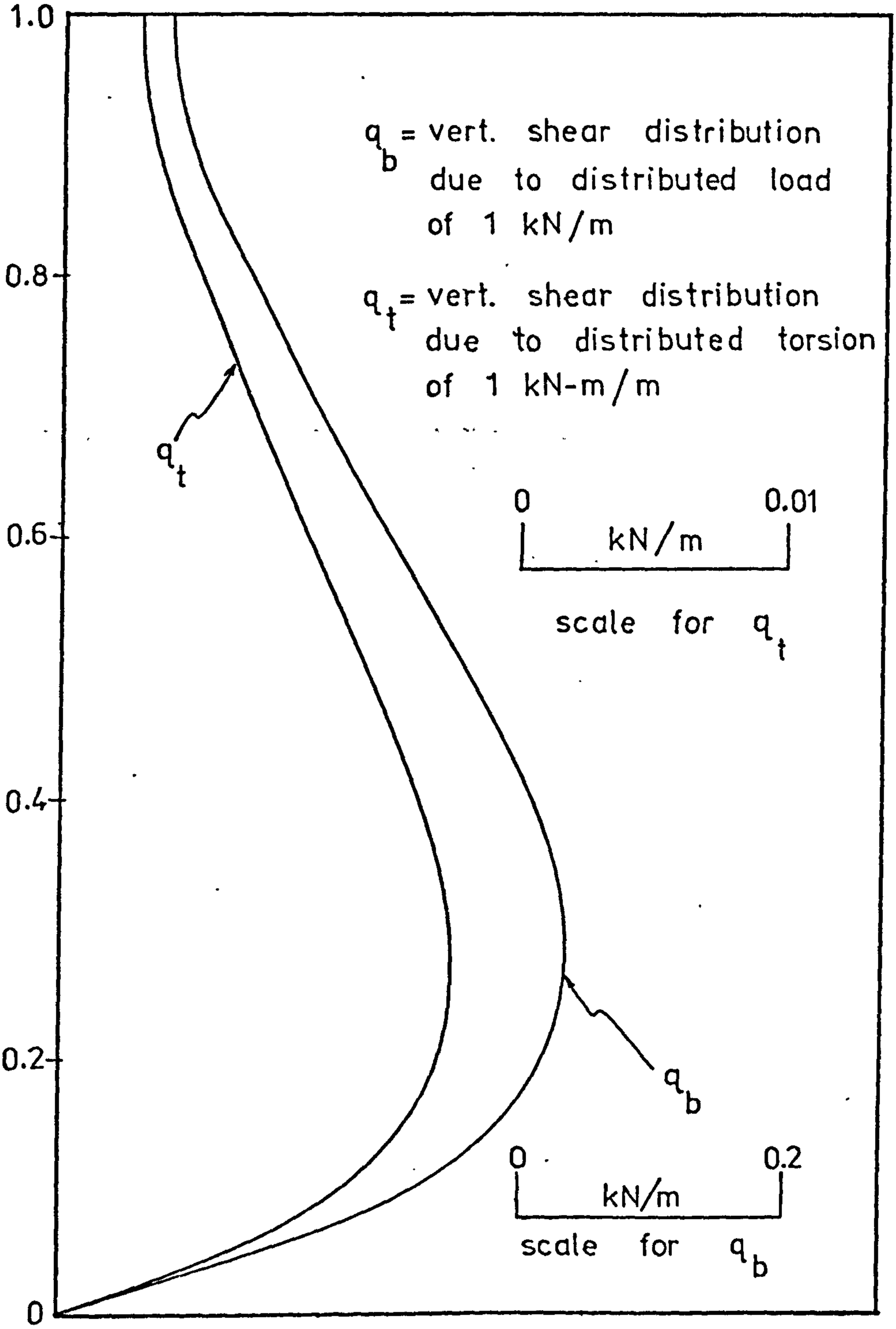

vertical shear distribution

Vertical shear distribution in assembly 1 (example)

Fig. 4.10

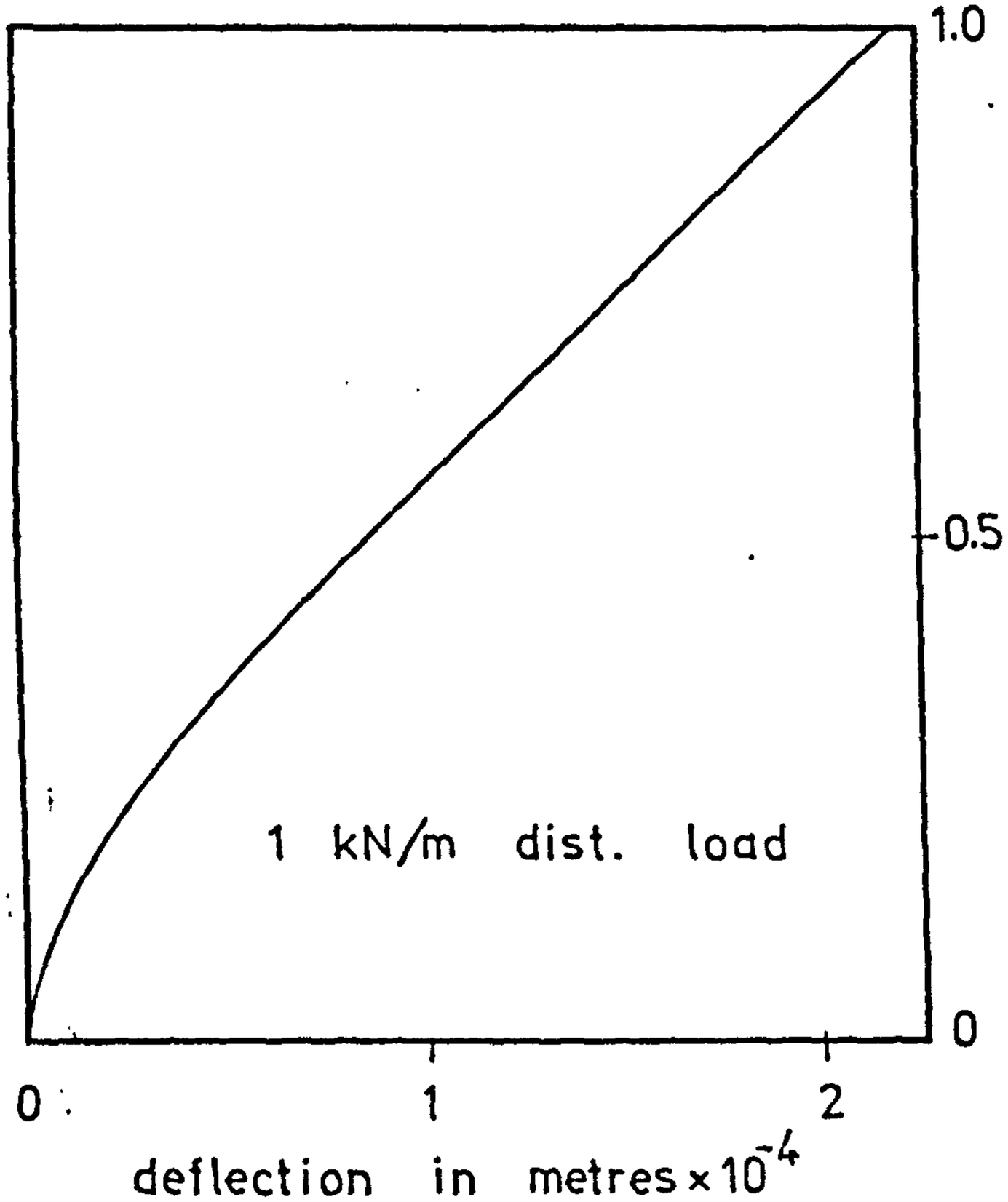

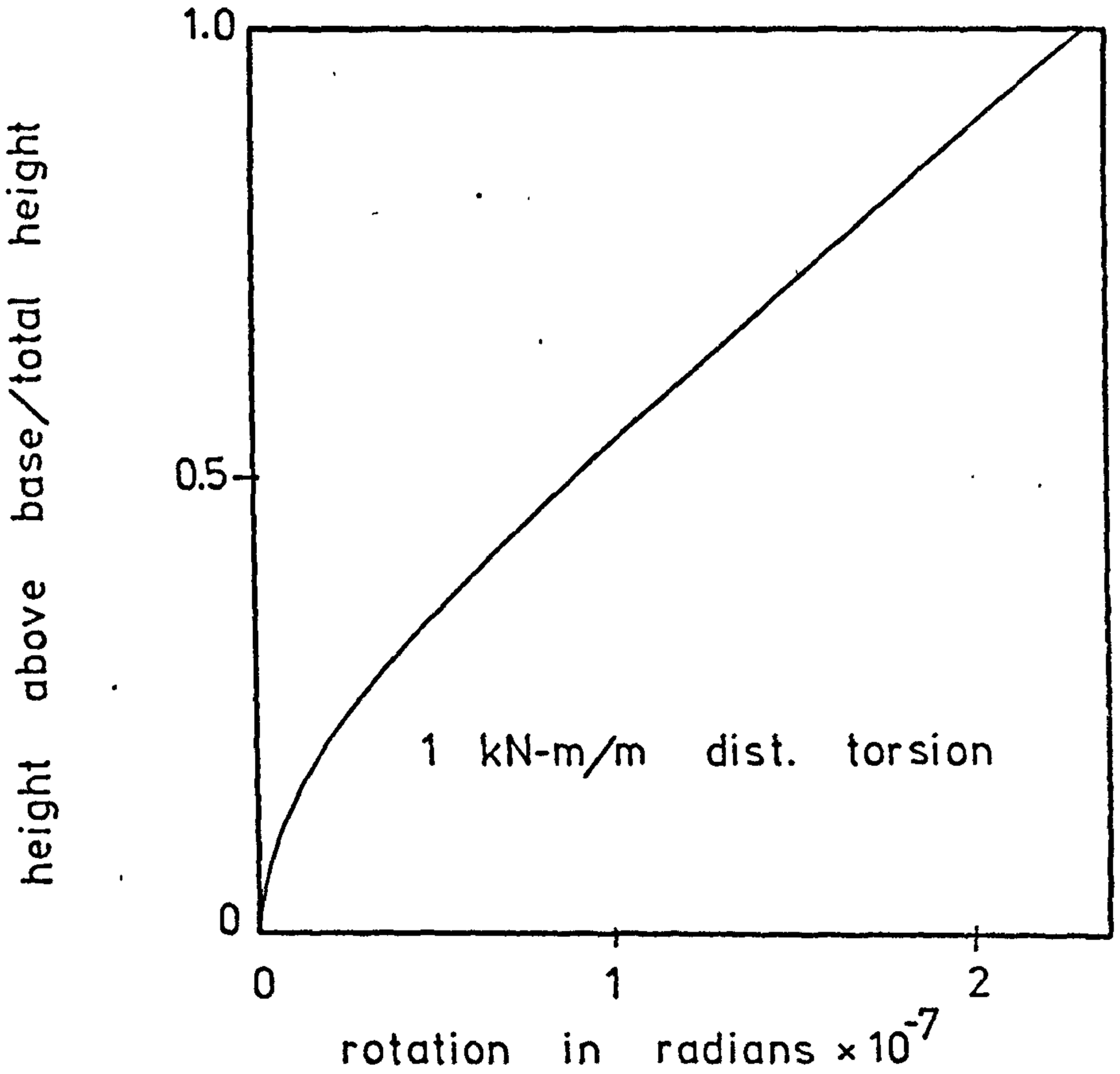

Example problem : (deflection and rotation of structure)

Fig. 4.11

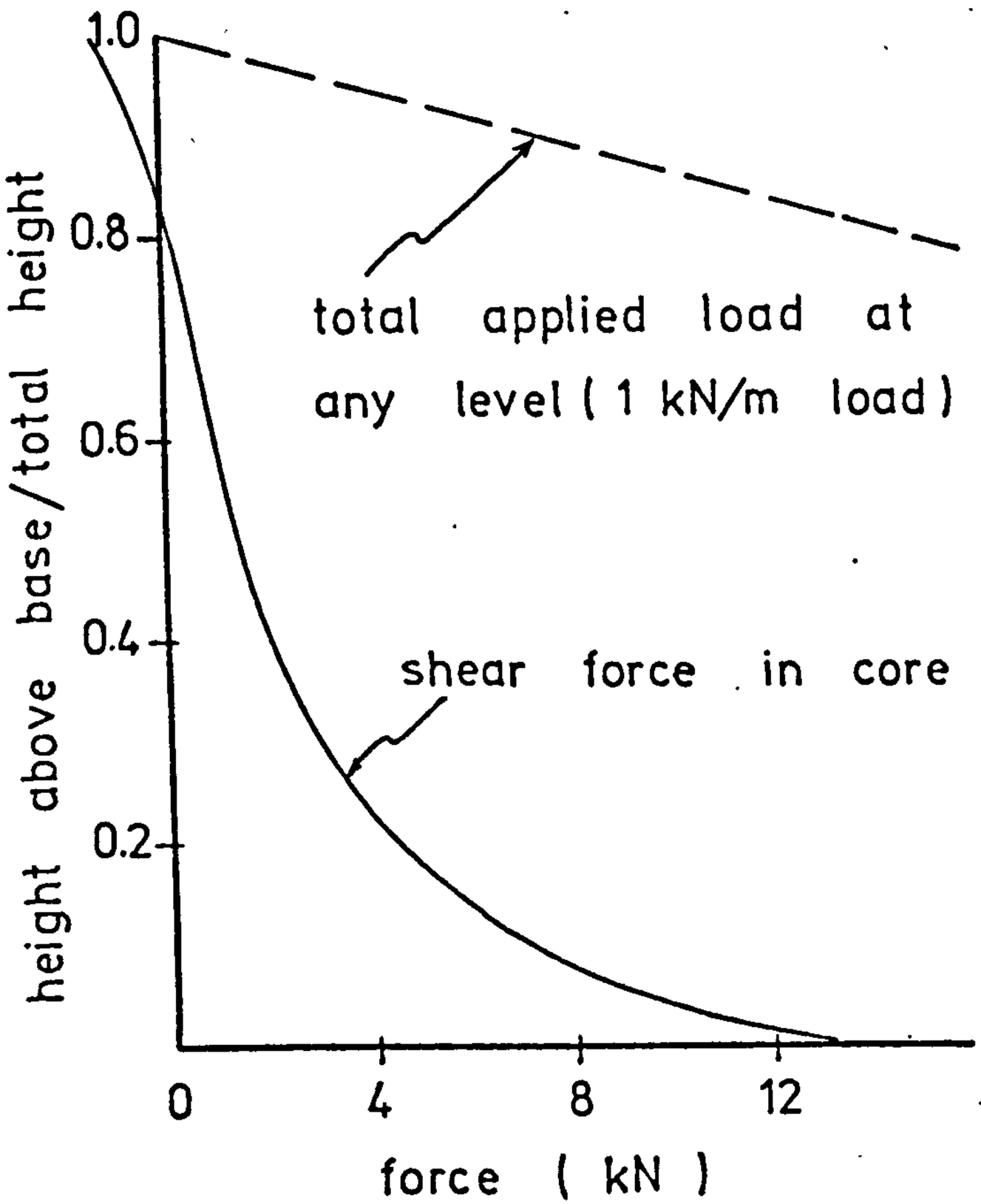

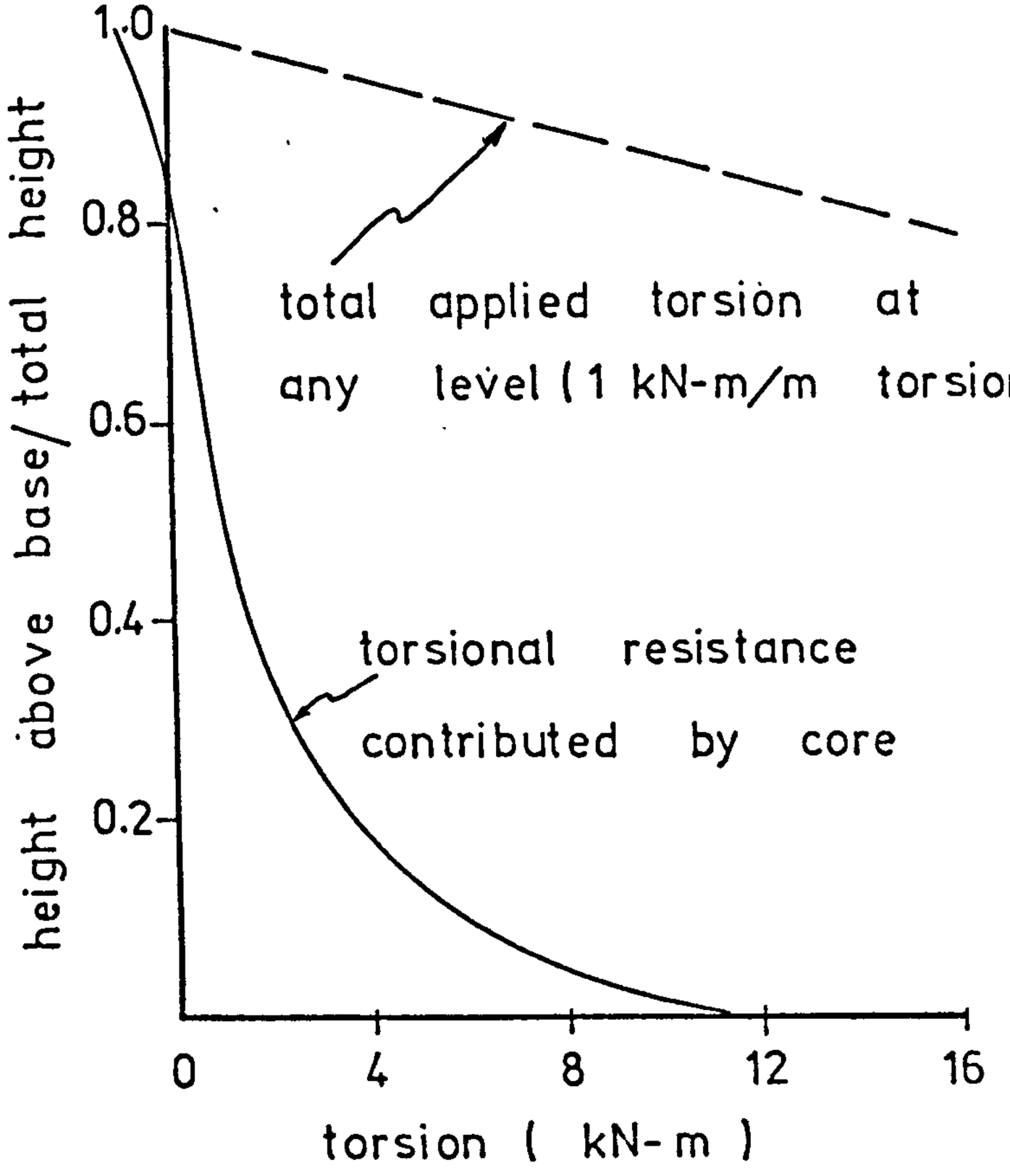

Example problem : (shear forces and torsional resistances)

Fig. 4.12

CHAPTER 5

SYMMETRICAL SHEAR WALL-FRAME STRUCTURES

5.1 Introduction

Structures consist entirely of cantilevered walls and coupled walls have been analysed in Chapter 4. The method of analysis may also be used to analyse directly symmetrical shear wall and frame (wall-frame) structures provided that the lateral stiffnesses of the frames are negligible in comparison with those of the walls and, in addition, the connections between walls and frames do not provide significant bending restraint. However, if the frames are relatively stiff it is necessary to consider the effects of interaction between the walls and frames.

If a cantilevered wall and a frame are allowed to deform independently under similar horizontal load conditions, the former will deform in bending configuration and the latter in shear configuration[15,18,19], as shown in Fig. 5.1. For a coupled wall, the mode of deformation will be based on a bending configuration since it is assumed that the ordinary beam theory is valid for individual wall. Therefore, any wall-frame structure may be considered as consisting of a combination of two types of structural units, which are basically different in the deformed configurations, constrained to act together by the rigid floor slabs. An analysis of symmetrical wall-frame structures in which frames are treated as shear beams acting with flexural

beams (walls) will be presented in this Chapter.

5.2 Cantilevered Wall-Coupled Wall-Frame Structure

Consider initially the behaviour of the basic flexural and shear beams shown in Fig. 5.2. The moment in the flexural beam is proportional to the rate of change of the rotation, whereas the shear force in the shear beam is assumed proportional to the rate of change of the lateral deflection. The force-deformation relationship for each type of beam may be expressed mathematically as,

$$M_B = K_B \frac{d^2 u_B}{dz^2} \qquad (5.1)$$

$$S_S = K_S \frac{du_S}{dz}$$

in which the subscripts B and S refer to the flexural and shear beams respectively.

M = bending moment

S = shear force

K_B = flexural rigidity of the flexural beam

K_S = shear rigidity of the shear beam

z = height ordinate

u = lateral displacement in the X direction

The flexural and shear rigidities are given by,

$$K_B = EI \qquad (5.2)$$

$$K_S = GA$$

where E, I = modulus of elasticity and second moment of area, respectively, of the flexural beam

G, A = shear modulus and effective cross-sectional area in shear, respectively, of the shear beam.

From consideration of the equilibrium of elemental elements of both types of beams, Fig. 5.3, the following relationships may be obtained,

$$S_B = -\frac{dM_B}{dz} = -K_B \frac{d^3u_B}{dz^3}$$

$$w_B = \frac{d^2M_B}{dz^2} = K_B \frac{d^4u_B}{dz^4}$$

(5.3)

$$S_S = -\frac{dM_S}{dz} = K_S \frac{du_S}{dz}$$

$$w_S = \frac{d^2M_S}{dz^2} = -K_S \frac{d^2u_S}{dz^2}$$

where w_B and w_S are the distributed horizontal forces acting on the flexural and shear beams respectively.

If the flexural beam is also subjected to a distributed vertical load q per unit height, such as in the case of a coupled wall, the horizontal shear and the distributed horizontal load may be shown to be respectively, Fig. 5.4,

$$S_{BH} = -\frac{dM_B}{dz} + \frac{dM_{BV}}{dz} \qquad (5.4)$$

$$w_{BH} = \frac{d^2M_B}{dz^2} - \frac{d^2M_{BV}}{dz^2} \qquad (5.4)\ \text{contd.}$$

where

$$M_{BV} = \int_z^H q\ L\ dz$$

= bending moment resulting from the distributed vertical load q acting at a distance L from the centroid of the cross-section.

Equations (5.1)-(5.4) are the basic equations from which the governing differential equations for a symmetrical wall-frame structure may be derived. A symmetrical wall-frame structure shown in Fig. 5.5 will be considered. The structure consists of four identical planar coupled wall assemblies, two cantilevered walls and four frames. The structure is assumed acted upon by a horizontal loading system which produces a horizontal moment M and a torsional moment M_T about the vertical axis of symmetry. The pure bending action and the pure torsional action are analysed separately. All the assumptions made in Chapter 4 are assumed to be valid.

In the analysis, the cantilevered walls and the individual coupled walls are treated as flexural beams. The plane frames are treated as shear beams. The shear rigidity of any plane frame depends on the member stiffnesses, the frame configuration and the rigidity of the joints. The contribution of a single column to the shear rigidity of an equivalent shear beam is determined

by assuming that points of contraflexure occur at mid-length positions of beams and columns. The total shear rigidity of a plane frame is the combined shear rigidity of all the columns in a typical storey of the frame. The expression for the shear rigidity contributed by a single column may be obtained by considering the horizontal force-deflection relationship for a single interior column shown in Fig. 5.6. The shear rigidity may be shown to be

$$K_S = E \times \left(\frac{12\ I_{col}}{h^2}\right) \times \frac{1}{\left[1 + \frac{2\ I_{col}}{h\left(\frac{I_{d1}}{d_1} + \frac{I_{d2}}{d_2}\right)}\right]} \qquad (5.5)$$

where,

I_{col} = second moment of area of the column

h = storey height

d_1, d_2 = total length of adjacent beams

I_{d_1}, I_{d_2} = second moment of areas of corresponding adjacent beams

Equation (5.5) is also valid for an exterior column provided that the second moment of area of one of the adjacent beams is assumed to be zero.

5.2.1 Analysis of Pure Bending Action

Consider the structure shown in Fig. 5.5, subjected to a lateral load which acts along the X axis. The loading system will produce only pure bending of the

structure. As the displacements of all the components are identical, the continuity equation for the substitute lamina of any coupled wall assembly is given by, for a structure on a rigid foundation,

$$1\ \frac{du}{dz} - \frac{1}{E}\left(\frac{b^3h}{12I_c}\right)q - \frac{1}{E}\left(\frac{1}{A_a} + \frac{1}{A_b}\right) \int_0^z \int_\xi^H q\ d\lambda\ d\xi = 0 \qquad (5.6)$$

The horizontal shear forces in coupled wall assembly i, cantilevered wall cr-k and frame f-j are given by, respectively (cf. equations (5.1)-(5.4)),

$$S_i = - K_i \frac{d^3u}{dz^3} + 1q$$

$$S_{cr-k} = - K_{cr-k} \frac{d^3u}{dz^3} \qquad (5.7)$$

$$S_{f-j} = K_{f-j} \frac{du}{dz}$$

where

$K_i = E\ I_i = E(I_a + I_b)$

I_a, I_b = second moment of areas of walls a and b of coupled wall assembly

$K_{cr-k} = E\ I_{cr-k}$

I_{cr-k} = second moment of area of cantilevered wall cr-k

K_{f-j} = shear rigidity of frame f-j

The total applied horizontal shear at any level may be expressed in terms of the applied moment M as,

$$\text{applied shear} = -\frac{dM}{dz} \tag{5.8}$$

The total internal horizontal shear becomes, from equation (5.7),

$$\text{internal shear} = EK_{BB}\frac{d^3u}{dz^3} + EK_{SB} + n_1 lq \tag{5.9}$$

where

K_{BB} = bending-flexural rigidity

$$= \frac{1}{E}\left(\sum_{i=1}^{n_1} K_i + \sum_{k=1}^{n_{cr}} K_{cr-k}\right)$$

K_{SB} = bending-shear rigidity

$$= \frac{1}{E}\sum_{j=1}^{n_f} K_{f-j}$$

n_1, n_{cr}, n_f = 2, 4, 4 respectively for the structure considered.

For the horizontal equilibrium of the structure, the applied shear must be balanced by the internal shear, hence,

$$EK_{SB}\frac{du}{dz} = EK_{BB}\frac{d^3u}{dz^3} - n_1 lq - \frac{dM}{dz} \tag{5.10}$$

Substitution of $\frac{du}{dz}$ from equation (5.10) into (5.6), and then differentiating twice with respect to z yields,

$$(1EK_{BB})\frac{d^5u}{dz^5} = K_{SB}\left(\left(\frac{b^3h}{12I_c}\right)\frac{d^2q}{dz^2} - \left(\frac{1}{A_a} + \frac{1}{A_b}\right)q\right) + 1\frac{d^3M}{dz3}$$

$$+ n_1 l^2 \frac{d^2q}{dz^2} \tag{5.11}$$

Differentiating equation (5.6) four times with respect to z leads to,

$$(EI)\frac{d^5u}{dz^5} - (\frac{b^3h}{12I_c})\frac{d^4q}{dz^4} + (\frac{1}{A_a} + \frac{1}{A_b})\frac{d^2q}{dz^2} = 0 \qquad (5.12)$$

From equations (5.11) and (5.12), $\frac{d^5u}{dz^5}$ may be eliminated and the fourth-order governing differential equation for q is obtained as,

$$\frac{d^4q}{dz^4} - \alpha_B^2\frac{d^2q}{dz^2} + \kappa_B^4 q = \beta_B^2\frac{d^3M}{dz^3} \qquad (5.13)$$

$$\beta_B^2 = (\frac{12I_c}{b^3h})\frac{1}{K_{BB}}$$

$$\alpha_B^2 = \beta_B^2 1\left[n_1 + \frac{K_{BB}}{1^2}(\frac{1}{A_a} + \frac{1}{A_b}) + \frac{K_{SB}}{1^2}(\frac{b^3h}{12I_c})\right]$$

$$\kappa_B^4 = \beta_B^2\frac{K_{SB}}{1}(\frac{1}{A_a} + \frac{1}{A_b})$$

(5.14)

The four constants of integration for the solution of q may be determined from the following boundary conditions:-

$$\text{At } z = 0, \quad \frac{du}{dz} = 0 \qquad (5.15)$$

evaluating equation (5.6) at z = 0, using equation (5.15), gives

$$(q)_0 = 0 \qquad (5.16)$$

At z = H, the bending moments in the coupled walls vanish,

hence,

$$\left(\frac{d^2u}{dz^2}\right)_H = 0 \qquad (5.17)$$

Differentiating equation (5.6) with respect to z, then evaluating at z = H yields

$$\left(\frac{dq}{dz}\right)_H = 0 \qquad (5.18)$$

From equations (5.10), (5.15) and (5.16), the third derivative of the displacement u at z = 0 becomes,

$$\left(\frac{d^3u}{dz^3}\right)_0 = \frac{1}{EK_{BB}}\left(\frac{dM}{dz}\right)_0 \qquad (5.19)$$

Differentiating equation (5.6) twice with respect to z, then evaluating at z = 0, using equations (5.16) and (5.19), gives

$$\left(\frac{d^2q}{dz^2}\right)_0 = \beta_B^2\left(\frac{dM}{dz}\right)_0 \qquad (5.20)$$

Differentiating equation (5.10) with respect to z, then evaluating at z = H, using equations (5.17), (5.18), leads to

$$\left(\frac{d^4u}{dz^4}\right)_H = \frac{1}{EK_{BB}}\left(\frac{d^2M}{dz^2}\right)_H \qquad (5.21)$$

Differentiating equation (5.6) three times with respect to z, then evaluating at z = H, using equations (5.18) and (5.21), yields

$$\left(\frac{d^3q}{dz^3}\right)_H = \beta_B^2\left(\frac{d^2M}{dz^2}\right)_H \qquad (5.22)$$

Hence, the boundary conditions for q are,

$$\text{at } z = 0, \qquad q = 0$$

$$\frac{d^2q}{dz^2} = \beta_B^2 \frac{dM}{dz} \tag{5.23}$$

$$\text{at } z = H, \qquad \frac{dq}{dz} = 0$$

$$\frac{d^3q}{dz^3} = \beta_B^2 \frac{d^2M}{dz^2}$$

After the vertical shear distribution q has been solved, the displacement u may be obtained by integrating equation (5.6), i.e.

$$u = \frac{1}{EI}\left[\left(\frac{b^3h}{12I_c}\right)\int_0^z q\, d\lambda + \left(\frac{1}{A_a} + \frac{1}{A_b}\right)\int_0^z\int_0^{\psi}\int_{\xi}^{H} q\, d\lambda\, d\xi\, d\psi\right] + (u)_0 \tag{5.24}$$

in which $(u)_0$ is the displacement at the base, which is zero for a structure on a rigid foundation.

If there are J groups of identical in-plane symmetrical coupled wall assemblies in the structure, the J fourth-order differential equations will be of the form,

$$\frac{d^4q_e}{dz^4} - (\alpha_B^2)_e \frac{d^2q_e}{dz^2} + (\kappa_B^4)_e q_e - \left[(\beta_B^2)_e l_e\right]\cdot$$

$$\left[\sum_{r=1}^{J}\left(\frac{l_r n_r}{l_e}\right)\frac{d^2q_r}{dz^2} - n_e\frac{d^2q_e}{dz^2}\right] - (\beta_B^2)_e \frac{d^3M}{dz^3} = 0 \tag{5.25}$$

$$e = 1, 2 \ldots J$$

where

$$(\beta_B^2)_e = \frac{12(I_c)_e \, l_e}{K_{BB} \, h \, b_e^3}$$

e = subscript denoting properties associated with a typical assembly of coupled wall group e

$$K_{BB} = \left(\sum_{k=1}^{n_{cr}} K_{cr-k} + \sum_{e=1}^{J} \bar{K}_e\right) \frac{1}{E}$$

$\bar{K}_e$ = sum of flexural rigidity of all assemblies of coupled wall group e

$$(\alpha_B^2)_e = (\beta_B^2)_e \, l_e \left[n_e + \frac{K_{BB}}{l^2} \left(\frac{1}{A_{ae}} + \frac{1}{A_{be}}\right) + \frac{K_{SB}}{l^2} \, h \, \frac{b_e^3}{12(I_c)_e} \right]$$

n_e = number of identical assemblies in coupled wall group e

$$(\kappa_B^4)_e = (\beta_B^2)_e \frac{K_{SB}}{l_e} \left(\frac{1}{A_{ae}} + \frac{1}{A_{be}}\right)$$

(5.26)

The boundary conditions given by equation (5.23) are valid for each q_e. The number of differential equations is equal to the number of distinct groups of coupled shear wall assemblies, and does not depend on the number of the frames. All the frames are not necessarily identical since only the symmetry of overall structure is required. Once the vertical shear distributions and the displacement

u have been obtained, all other forces in each component may be easily determined from equations (5.1)-(5.4).

Although all the derivations are based on the structural configuration with parallel walls and frame, there will be little difficulty in dealing with walls and frames of different orientation. Indeed, non-planar wall components can also be treated employing the same general procedure given in detail in Chapter 4.

5.2.2 Analysis of Pure Torsional Action

Consider the symmetrical structure shown in Fig. 5.5 under the torsional moment M_T. From symmetry, the structure will rotate about the vertical axis of symmetry. The horizontal displacement u of any point will be proportional to its distance (Y ordinate) from the axis of symmetry, i.e. $u = y\theta$, where θ is the angle of twist of the structure.

The continuity equation for the substitute lamina of any coupled wall assembly i may be written as,

$$1\ y_i \frac{d\theta}{dz} - \frac{1}{E}\frac{b^3 h}{12 I_c} q_i - \frac{1}{E}\left(\frac{1}{A_a} + \frac{1}{A_b}\right) \int_0^z \int_\xi^H q_i \, d\lambda \, d\xi = 0 \qquad (5.27)$$

where

y_i = Y ordinate of coupled wall assembly i

q_i = vertical shear distribution in coupled wall assembly i

As the coupled wall assemblies in Fig. 5.5 are in-plane symmetrical, the vertical shear distributions are

linearly related (this has been shown in the previous Chapter). The linear relationship is given by,

$$\frac{q_i}{y_i} = \frac{q_1}{y_1} = \text{constant} \qquad (5.28)$$

Consequently, there exists only one independent continuity equation for the structure. Adopting the coupled wall assembly 1 as the datum assembly, the continuity equation for the structure becomes,

$$1\ y_1 \frac{d\theta}{dz} - \frac{1}{E} \frac{b^3 h}{12 I_c} q_1 - \frac{1}{E} \left(\frac{1}{A_a} + \frac{1}{A_b}\right) \int_0^z \int_\xi^H q_1\ d\lambda\ d\xi = 0 \qquad (5.29)$$

From equations (5.1)-(5.4), the horizontal shear forces in the coupled wall assembly i, cantilevered wall cr-k and frame f-j may be written as, respectively,

$$S_i = - K_i\ y_i \frac{d^3\theta}{dz^3} + 1\ q_i$$

$$S_{cr-k} = - K_{cr-k}\ y_{cr-k} \frac{d^3\theta}{dz^3} \qquad (5.30)$$

$$S_{f-j} = K_{f-j}\ y_{f-j} \frac{d\theta}{dz}$$

in which y_i, y_{cr-k}, y_{f-j} are the Y ordinates of the coupled wall assembly, cantilevered wall and frame respectively. The parameters K_i, K_{cr-k}, K_{f-j} are as defined previously.

By assuming that the St. Venant's torsion may be neglected due to small value of the torsional stiffness of an individual component relative to the bending

stiffness, the torsional resistance of the structure is solely developed by the shearing actions of the components. The contribution of torsional resistance due to coupled wall assembly i, cantilevered wall cr-k and frame f-j are then, respectively,

$$(M_R)_i = S_i y_i = - K_i y_i^2 \frac{d^3\theta}{dz^3} + y_i l q_i$$

$$(M_R)_{cr-k} = S_{cr-k} y_{cr-k} = - K_{cr-k} y_{cr-k}^2 \frac{d^3\theta}{dz^3} \qquad (5.31)$$

$$(M_R)_{f-j} = S_{f-j} y_{f-j} = K_{f-j} y_{f-j}^2 \frac{d\theta}{dz}$$

For the structure considered, the total torsional resistance, M_R, may be written as,

$$M_R = \sum_{i=1}^{n_1} S_i y_i + \sum_{k=1}^{n_{cr}} S_{cr-k} y_{cr-k} + \sum_{j=1}^{n_f} S_{f-j} y_{f-j} \qquad (5.32)$$

and upon substitution, using equations (5.31) and (5.28),

$$M_R = - \frac{d^3\theta}{dz^3} \left(\sum_{i=1}^{n_1} K_i y_i^2 + \sum_{k=1}^{n_{cr}} K_{cr-k} y_{cr-k}^2 \right) + \frac{d\theta}{dz} \sum_{j=1}^{n_f} K_{f-j} y_{f-j}^2 + q_1 \frac{1}{y_1} \sum_{i=1}^{n_1} y_i^2 \qquad (5.33)$$

For the torsional equilibrium of the structure, the total torsional resistance and the applied torsional moment must be equal. Hence,

$$M_R = M_T \qquad (5.34)$$

Substituting M_R from equation (5.33) into (5.34), and

then dividing by y_1^2 yields

$$E\left(\frac{d^3\theta}{dz^3} K_{BT} - \frac{d\theta}{dz} K_{ST}\right) - q_1 \frac{1}{y_1} R_T = - \frac{M_T}{y_1^2} \qquad (5.35)$$

where

K_{BT} = torsional-flexural rigidity, with respect to assembly 1, of the flexural components

$$= \frac{1}{Ey_1^2} \left(\sum_{i=1}^{n_1} K_i y_i^2 + \sum_{k=1}^{n_{cr}} K_{cr-k} y_{cr-k}^2\right)$$

K_{ST} = torsional-shear rigidity, with respect to assembly 1, of the shear components

$$= \frac{1}{Ey_1^2} \sum_{j=1}^{n_f} K_{f-j} y_{f-j}^2$$

$$R_T = \frac{1}{y_1^2} \sum_{i=1}^{n_1} y_i^2$$

(5.36)

Following exactly the same steps of derivation which have led to equations (5.11)-(5.13), a fourth-order differential equation for the structure under the pure torsional action may be shown to be,

$$\frac{d^4 q_1}{dz^4} - \alpha_T^2 \frac{d^2 q_1}{dz^2} + \kappa_T^4 q_1 = - \beta_T^2 \frac{d^2 (M_T/y_1)}{dz^2} \qquad (5.37)$$

where

$$\beta_T^2 = \left(\frac{12 I_c}{b^3 h}\right) \frac{1}{K_{BT}} \qquad (5.38)$$

$$\kappa_T^4 = \beta_T^2 \frac{K_{ST}}{l}\left(\frac{1}{A_a} + \frac{1}{A_b}\right)$$

$$\alpha_T^2 = \beta_T^2\, l \left[R_T + \frac{K_{BT}}{l^2}\left(\frac{1}{A_a} + \frac{1}{A_b}\right) + \frac{K_{ST}}{l^2}\,\frac{b^3 h}{12 I_c} \right]$$

(5.38) contd.

Proceeding in a similar manner as in the case of pure bending action, the boundary conditions for the pure torsional action are found to be as follows:-

$$(q_1)_0 = 0$$

$$\left(\frac{dq_1}{dz}\right)_H = 0$$

$$\left(\frac{d^2 q_1}{dz^2}\right)_0 = -\beta_T^2\,(M_T/y_1) \qquad (5.39)$$

$$\left(\frac{d^3 q_1}{dz^3}\right)_H = -\beta_T^2\,\frac{d}{dz}\,(M_T/y_1)$$

Once the vertical shear distribution q_1 has been solved, the values of all other q_i may be obtained using the linear relationship given by equation (5.28). The angle of rotation, θ , may be obtained by integrating equation (5.29), i.e.

$$= \frac{1}{E l y_1}\left[\frac{b^3 h}{12 l I_c}\int_0^z q_1\, d\lambda + \left(\frac{1}{A_a} + \frac{1}{A_b}\right)\cdot \int_0^z \int_0^{\psi} \int_{\xi}^{H} q_1\, d\lambda\, d\xi\, d\psi \right] + (\theta)_0 \qquad (5.40)$$

in which $(\theta)_0$ is the horizontal rotation at the base, which is equal to zero for a structure on a rigid foundation.

It has been shown previously in Chapter 4 that under a pure torsion the vertical shear distributions of identical in-plane symmetrical coupled wall assemblies are linearly related. Therefore, if there are J groups of identical coupled wall assemblies in the structure there will be only J independent fourth-order differential equations. Consider a symmetrical wall-frame structure similar to that shown in Fig. 5.5, but with J groups of identical coupled wall assembly, subjected to a torsional moment M_T. Select one assembly from each group of identical wall assemblies, groups 1 to J, and designate the vertical shear distribution in the respresentative assemblies as q_{i-1}, $i = 1, 2, \ldots J$ respectively.

Following the foregoing method of analysis and taking assembly 1-1 as the datum assembly, it may be shown that the J fourth-order differential equations for pure torsion will be of the form,

$$\frac{d^4 q_{i-1}}{dz^4} - \alpha_i^2 \frac{d^2 q_{i-1}}{dz^2} - \beta_i^2 \left[\sum_{j=1}^{J} (R_j t_j / t_i) l_i \, q_{j-1} - R_i l_i q_{i-1} \right]$$

$$+ \kappa_i^4 \, q_{i-1} = - \beta_i^2 \left(\frac{1}{t_i y_{1-1}} \right) \frac{d^2 M_T}{dz^2} \qquad (5.41)$$

$$i = 1, 2, \ldots J$$

where

$$\beta_i^2 = \frac{1}{K_{BT}} \left(\frac{12\ I_{ci}\ l_i}{b_i^3\ h}\right)$$

K_{BT} = torsional-flexural rigidity, with respect to assembly 1-1, of all the flexural components in the structure, cf. equation (5.36).

i = subscript referring to coupled wall group i

$$\kappa_i^4 = \beta_i^2 \frac{K_{ST}}{l_i} \left(\frac{1}{A_{ai}} + \frac{1}{A_{bi}}\right)$$

K_{ST} = torsional-shear rigidity, with respect to assembly 1-1, of all the shear components in the structure, c.f. equation (5.36).

$$\alpha_i^2 = \beta_i^2\ l_i \left[R_i + \frac{K_{BT}}{l_i^2} \left(\frac{1}{A_{ai}} + \frac{1}{A_{bi}}\right) + \frac{K_{ST}}{l_i^2} \left(\frac{b_i^3 h}{12 I_{ci}}\right)\right]$$

$$t_i = \frac{y_{1-1}}{y_{i-1}}$$

y_{i-1} = Y ordinate of assembly i-1

$$R_i = \frac{1}{y_{1-1}^2} \sum_{j=1}^{n_i} y_{i-j}^2$$

n_i = number of identical assemblies in coupled wall group i

y_{i-j} = Y ordinate of assembly i-j, i.e. assembly j of coupled wall group i

(5.42)

The four boundary conditions for each q_{i-1} may be

shown to be as follows,

$$(q_{i-1})_0 = 0$$

$$(\frac{dq_{i-1}}{dz})_H = 0$$

$$(\frac{d^2q_{i-1}}{dz^2})_0 = -\beta_i^2 (\frac{1}{t_i y_{1-1}}) (M_T)_0 \qquad (5.43)$$

$$(\frac{d^3q_{i-1}}{dz^3})_H = -\beta_i^2 (\frac{1}{t_i y_{1-1}})(\frac{dM_T}{dz})_H$$

After the shear distributions q_{i-1} have been determined, the vertical shear distribution q_{i-j} in any assembly i-j with the y ordinate y_{i-j} may be obtained using the linear relationship,

$$q_{i-j} = (\frac{y_{i-j}}{y_{i-1}}) q_{i-1} \qquad (5.44)$$

The analysis is still valid even though the frames are not all identical. Also, as in the case of pure bending, the analysis of pure torsional action presented can be readily extended to deal with general wall-frame structures with non-planar flexural components. However, when dealing with truly non-planar coupled wall assemblies it should be recognised, as have been shown in Chapter 4, that the relationships between the vertical shear distributions of identical coupled wall assemblies are not necessarily linear.

5.2.3 Closed Form Solutions for Standard Load Cases

If there is only one governing differential equation for the structure, i.e. when the coupled wall assemblies are identical and in-plane symmetrical, a closed form solution may be easily obtained. A solution for the differential equation (5.13) is given by,

$$q = c_1 e^{\lambda_1 z} + c_2 e^{-\lambda_1 z} + c_3 e^{\lambda_2 z} + c_4 e^{-\lambda_2 z} + q_p \qquad (5.45)$$

in which,

$$\lambda_1^2 = \left(\frac{\alpha_B^2}{2}\right) + \sqrt{\left(\frac{\alpha_B^2}{2}\right)^2 - \kappa_B^4} \qquad (5.46)$$

$$\lambda_2^2 = \left(\frac{\alpha_B^2}{2}\right) - \sqrt{\left(\frac{\alpha_B^2}{2}\right)^2 - \kappa_B^4}$$

q_p = particular integral solution

c_i = constants of integration which may be determined from the boundary conditions, equation (5.23).

When the characteristic roots, λ_1, λ_2, are real number and different, which is usually the case unless the parameter κ_B^4 is relatively large, the solution may be written as,

$$q = k_1 \cosh \lambda_1 z + k_2 \sinh \lambda_1 z + k_3 \cosh \lambda_2 z + k_4 \sinh \lambda_2 z + q_p \qquad (5.47)$$

in which k_1, k_2, k_3, k_4 are constants of integration.

Assume that the characteristic roots of the

differential equation are real and different. The solution for pure bending actions due to the three standard load cases, namely, a uniformly distributed load w per unit height, a concentrated load P at the top and a triangularly distributed load $\vartheta(\frac{z}{H})$ per unit height, are respectively,

$$q_w = \frac{w\,\beta_B^2 H^3}{(\gamma_1^2 - \gamma_2^2)}\,\phi_w(\gamma_1, \gamma_2, \eta)$$

$$q_P = \frac{P\,\beta_B^2 H^2}{(\gamma_1^2 - \gamma_2^2)}\,\phi_P(\gamma_1, \gamma_2, \eta) \qquad (5.48)$$

$$q_\vartheta = \frac{\vartheta\,\beta_B^2 H^3}{(\gamma_1^2 - \gamma_2^2)}\,\phi_\vartheta(\gamma_1, \gamma_2, \eta)$$

where

$$\phi_w(\gamma_1, \gamma_2, \eta) = \frac{1}{\cosh\gamma_2}\left(\cosh\gamma_2(1-\eta) - \frac{\sinh\gamma_2\eta}{\gamma_2}\right)$$

$$- \frac{1}{\cosh\gamma_1}\left(\cosh\gamma_1(1-\eta) - \frac{\sinh\gamma_1\eta}{\gamma_1}\right)$$

$$\eta = z/H$$

$$\gamma_1 = \lambda_1 H$$

$$\gamma_2 = \lambda_2 H$$

$$\phi_P(\gamma_1, \gamma_2, \eta) = \frac{\cosh\gamma_2(1-\eta)}{\cosh\gamma_2} - \frac{\cosh\gamma_1(1-\eta)}{\cosh\gamma_1}$$

$$\phi_\vartheta(\gamma_1, \gamma_2, \eta) = \left\{\frac{1}{\gamma_2^2} - \frac{\sinh\gamma_2\eta}{\gamma_2} - \left(\frac{1}{\gamma_2^2} - \tfrac{1}{2}\right)\cdot\right.$$

(5.49)

$$\left. \frac{\cosh \gamma_2(1-\eta)}{\cosh \gamma_2} \right\}$$

$$-\left\{ \frac{1}{\gamma_1^2} - \frac{\sinh \gamma_1 \eta}{\gamma_1} - \left(\frac{1}{\gamma_1^2} - \tfrac{1}{2}\right) \frac{\cosh \gamma_1(1-\eta)}{\cosh \gamma_1} \right\} \qquad (5.49)$$

contd.

The corresponding displacement functions for the three standard load cases are, respectively,

$$u_w = \frac{w \beta_B^2 H^4}{EI(\gamma_1^2 - \gamma_2^2)} F_w(\gamma_1, \gamma_2, \eta)$$

$$u_P = \frac{P \beta_B^2 H^3}{EI(\gamma_1^2 - \gamma_2^2)} F_P(\gamma_1, \gamma_2, \eta) \qquad (5.50)$$

$$u_\vartheta = \frac{\vartheta \beta_B^2 H^4}{EI(\gamma_1^2 - \gamma_2^2)} F_\vartheta(\gamma_1, \gamma_2, \eta)$$

where

$$F_w(\gamma_1, \gamma_2, \eta) = \left(\frac{b^3 h}{12 I_c}\right)\left(\psi_w(\gamma_2, \eta) - \psi_w(\gamma_1, \eta)\right)$$

$$- \left(\frac{H^2}{\gamma_1^2 \gamma_2^2}\right)\left(\frac{1}{A_a} + \frac{1}{A_b}\right) \cdot$$

$$\left[\gamma_1^2 \psi_w(\gamma_2,\eta) - \gamma_2^2 \psi_w(\gamma_1,\eta) - (\gamma_1^2-\gamma_2^2)(\eta - \tfrac{1}{2}\eta^2)\right]$$

$$\psi_w(\gamma,\eta) = \frac{1}{\gamma}\left[\sinh\gamma\eta + (1-\cosh\gamma\eta)\left(\frac{1}{\gamma\cosh\gamma} + \tanh\gamma\right)\right]$$

$$F_P(\gamma_1,\gamma_2,\eta) = \left(\frac{b^3h}{12I_c}\right)\left\{\psi_P(\gamma_2,\eta) - \psi_P(\gamma_1,\eta)\right\}$$

$$- \left(\frac{H^2}{\gamma_1^2\ \gamma_2^2}\right)\left(\frac{1}{A_a} + \frac{1}{A_b}\right)\cdot$$

$$\left[\gamma_1^2\ \psi_P(\gamma_2,\eta) - \gamma_2^2\ \psi_P(\gamma_1,\eta) - (\gamma_1^2 - \gamma_2^2)\eta\right]$$

$$\psi_P(\gamma,\eta) = \frac{1}{\gamma}\left(\ \sinh\gamma\eta\ + \tanh\gamma\cdot(1 - \cosh\gamma\eta)\right)$$

$$F_\vartheta\ (\gamma_1,\gamma_2,\eta) = \left(\frac{b^3h}{12I_c}\right)\left\{\psi_\vartheta(\gamma_2,\eta) - \psi_\vartheta(\gamma_1,\eta) + \left(\frac{1}{\gamma_2^2} - \frac{1}{\gamma_1^2}\right)\eta\right\}$$

$$-\left(\frac{H^2}{\gamma_1^2\ \gamma_2^2}\right)\ \left(\frac{1}{A_a} + \frac{1}{A_b}\right)\cdot$$

$$\left[\gamma_1^2\ \psi_\vartheta(\gamma_2,\eta) - \gamma_2^2\ \psi_\vartheta(\gamma_1,\eta) + \tfrac{1}{6}(\gamma_1^2 - \gamma_2^2)\ \eta^3\right.$$

$$+\ \left(\gamma_1^2\ \sinh\gamma_2 - \gamma_2^2\ \sinh\gamma_1 - (\gamma_1^2 - \gamma_2^2)\ \right)\eta^2$$

$$\left. - \left(\tfrac{1}{2}(\gamma_1^2 - \gamma_2^2) + \left(\frac{\gamma_2}{\gamma_1}\right)^2 - \left(\frac{\gamma_1}{\gamma_2}\right)^2\right)\eta\ \right]$$

$$\psi_\vartheta(\gamma,\eta) = \frac{1}{\gamma}\ \left[\frac{\cosh\gamma}{\gamma} + \frac{1}{\gamma} + \left(\frac{1}{\gamma^2} - \tfrac{1}{2}\right)\cdot\right.$$

$$\left.\left(\frac{\sinh\ \gamma(1-\eta) - \sinh\gamma}{\cosh\gamma}\right)\right]$$

(5.51)

It may be shown that there are correspondences

between the expressions for the solutions for pure bending and pure torsional actions, between the following pairs of standard loadings,

1. Uniformly distributed load w per unit height and uniformly distributed torsional moment M_w per unit height.
2. Concentrated load P at the top and concentrated torsional moment M_P at the top.
3. Triangularly distributed load $\vartheta \frac{z}{H}$ per unit height and triangularly distributed moment $M_\vartheta \left(\frac{z}{H}\right)$ per unit height.

The solutions for pure torsional actions for the three standard torsional moments, namely, a uniformly distributed torsional moment per unit height, a concentrated torsional moment at the top and a triangularly distributed torsional moment per unit height, are given by, respectively,

$$q_{wm} = \frac{(M_w/y_1)\ \beta_T^2\ H^3}{(\ \gamma_1^2 - \gamma_2^2)} \quad \phi_w\ (\ \gamma_1,\ \gamma_2, \eta\ )$$

$$q_{Pm} = \frac{(M_P/y_1)\ \beta_T^2\ H^2}{(\ \gamma_1^2 - \gamma_2^2)} \quad \phi_P\ (\ \gamma_1,\ \gamma_2, \eta\ )$$

$$q_{\vartheta m} = \frac{(M_\vartheta/y_1)\ \beta_T^2\ H^3}{(\ \gamma_1^2 - \gamma_2^2)} \quad \phi_\vartheta\ (\ \gamma_1,\ \gamma_2, \eta\ )$$

$$\theta_{wm} = \frac{(M_w/y_1^2)\ \beta_T^2\ H^3}{EI(\ \gamma_1^2 - \gamma_2^2)} \quad F_w\ (\ \gamma_1,\ \gamma_2, \eta\ )$$

$$\theta_{Pm} = \frac{(M_P/y_1^2)\ \beta_T^2\ H^2}{El(\ \gamma_1^2 - \gamma_2^2)}\ F_P\ (\ \gamma_1,\ \gamma_2, \eta\ )$$

$$\theta_{\upsilon m} = \frac{(M_\upsilon/y_1^2)\ \beta_T^2\ H^3}{El(\ \gamma_1^2 - \gamma_2^2)}\ F_\upsilon\ (\ \gamma_1,\ \gamma_2, \eta\ )$$

(5.52)

where

θ = horizontal rotation of the structure

$$\gamma_1 = H \sqrt{(\frac{\alpha_T^2}{2}) + \sqrt{(\frac{\alpha_T^2}{2})^2 - \kappa_T^4}}$$

$$\gamma_2 = H \sqrt{(\frac{\alpha_T^2}{2}) - \sqrt{(\frac{\alpha_T^2}{2})^2 - \kappa_T^4}}$$

(5.53)

y_1 = y ordinate of the datum assembly

q_{wm}, q_{Pm}, $q_{\upsilon m}$ = vertical shear distributions in the datum assembly due to the standard torsional moments M_w, M_P, M_υ $(\frac{z}{H})$, respectively.

Other functions, namely, ϕ_w, ϕ_P, ϕ , F_w, F_P, F_υ are as given previously.

5.3 Cantilevered Wall-Frame Structures

When the symmetrical structure consists of frames and cantilevered walls only, the continuity equations (5.6) and (5.27) become trivial. The equilibrium equations (5.10) and (5.35) then become the governing

differential equations for pure bending and pure torsion, respectively. As there is no coupled walls in the system, the distributed vertical shear force q is zero, and the equilibrium equations (5.10) and (5.35) reduce to, respectively,

$$\frac{d^3u}{dz^3} - \rho_B^2 \frac{du}{dz} = \frac{1}{K_C} \left(\frac{dM}{dz}\right) \qquad (5.54)$$

$$\frac{d^3\theta}{dz^3} - \rho_T^2 \frac{d\theta}{dz} = - \frac{M_T}{K_{CA}} \qquad (5.55)$$

where

$$\rho_B^2 = \frac{K_F}{K_C} \quad , \quad \rho_T^2 = \frac{K_{FA}}{K_{CA}}$$

$$K_F = \sum_{j=1}^{n_f} K_{f-j} \quad , \quad K_C = \sum_{k=1}^{n_{cr}} K_{cr-k} \qquad (5.56)$$

$$K_{FA} = \sum_{j=1}^{n_f} K_{f-j}\, y_{f-j}^2 \quad , \quad K_{CA} = \sum_{k=1}^{n_{cr}} K_{cr-k}\, y_{cr-k}^2$$

Equation (5.54) is the governing differential equation for pure bending, and (5.55) for pure torsion. The boundary conditions for zero moment at the top and complete fixity at the base yield,

$$\begin{aligned} &\text{at } z = 0, && u = = 0 \\ & && \frac{du}{dz} = \frac{d\theta}{dz} = 0 \qquad (5.57) \\ &\text{at } z = H, && \frac{d^2u}{dz^2} = \frac{d^2\theta}{dz^2} = 0 \end{aligned}$$

The complete solutions for equations (5.54) and (5.55) may be written as,

$$u = C_1 \cosh \eta\gamma_B + C_2 \sinh \eta\gamma_B + C_3 + u_p \qquad (5.58)$$

$$\theta = k_1 \cosh \eta\gamma_T + k_2 \sinh \eta\gamma_T + k_3 + \theta_p \qquad (5.59)$$

where

$\gamma_B = \rho_B H$, $\gamma_T = \rho_T H$

$\eta = \frac{z}{H}$

u_p, θ_p = particular integral solutions for pure bending and pure torsion respectively.

c_i, k_i = constants of integration for pure bending and pure torsion respectively; these constants may be determined from the boundary conditions given in equation (5.57).

If the structure is subjected to a uniformly distributed lateral load w per unit height acting with a constant eccentricity e, the horizontal and rotational displacements of the structure may be shown to be, respectively,

$$u = \frac{1}{K_C}\left(\frac{wH^4}{\gamma_B^4}\right)\left[\frac{(\gamma_B \sinh \gamma_B + 1)}{\cosh \gamma_B}(\cosh \eta\gamma_B - 1) - \gamma_B \sinh \eta\gamma_B + \gamma_B^2(\eta - \tfrac{1}{2}\eta^2)\right]$$

$$= \frac{1}{K_C}\left(\frac{wH^4}{\gamma_B^4}\right) f_\gamma(\gamma_B, \eta) \qquad (5.60)$$

$$\theta = \frac{1}{K_{CA}} \left(\frac{ewH^4}{\gamma_T^4}\right) \quad f_\gamma \quad (\gamma_T, \eta) \tag{5.61}$$

It may be noted that both the horizontal and the rotational displacements possess the same form of solutions, i.e. involving the function f_γ . It may be shown that the similarity between the expressions for the horizontal and the rotational displacements occurs also in the other standard load cases of a concentrated load at the top and a triangularly distributed load.

If the lateral stiffnesses of the frames are small in comparison with those of the cantilevered walls and may thus be neglected, the governing differential equations for pure bending and pure torsion may be shown to be, respectively,

$$\frac{d^2u}{dz^2} = \frac{M}{K_C}$$

$$\frac{d^3}{dz^3} = -\frac{M_T}{K_{CA}} \tag{5.62}$$

The solutions for the horizontal and the rotational displacements, i.e. u and θ , may be easily obtained by directly integrating equation (5.62). For the particular cases of a uniformly distributed lateral load w per unit height and a uniformly distributed torsional moment we per unit height the solutions, subjected to the boundary conditions given in equation (5.57), are given by, respectively,

$$u = \frac{1}{K_C}\left(\frac{wH^4}{24}\right)\left(6\eta^2 - 4\eta^3 + \eta^4\right)$$

$$= \frac{1}{K_C}\left(\frac{wH^4}{24}\right) f(\eta) \qquad (5.63)$$

$$\theta = \frac{1}{K_{CA}}\left(\frac{weH^4}{24}\right) f(\eta)$$

It may again be noted that the solutions for the horizontal and the rotational displacements possess the same form, i.e. involving the function $f(\eta)$. The solutions for other standard load cases may be similarly obtained by direct integrations.

5.4 Example Problem

To give an example of the effects of incorporating the lateral stiffness of frames in the analysis, a structure shown in Fig. 5.7 is considered. Both bending and torsional actions, due to a uniformly distributed load 1 KN/m and a uniformly distributed torsion 1 KN-m/m respectively, are analysed. The results obtained by considering wall-frame interaction are compared with those obtained by assuming that the lateral stiffness of the frames may be neglected.

From Fig. 5.7,

H	=	45.0 m	I_c	=	3.125×10^{-3} m^4
h	=	3.0 m	$A_a = A_b$	=	1.8 m^2
l	=	8.0 m	E	=	2.4×10^7 KN/m^2

and based on datum assembly 1, the following parameters are obtained,

(i) Lateral Stiffness of Frames Considered

K_{BB} = 45.278 m^4

K_{SB} = 4.3566×10^{-2} m^2

κ_B^4 = 1.6705×10^{-6} m^{-4} bending action

α_B^2 = 1.1533×10^{-2} m^{-2}

γ_1 = 4.8017

γ_2 = 0.54504

K_{BT} = 22.464 m^4

K_{ST} = 1.6846×10^{-2} m^2

κ_T^4 = 1.3019×10^{-6} m^{-4}

torsional action

α_T^2 = 1.1745×10^{-2} m^{-2}

γ_1 = 4.8548

γ_2 = 0.46404

(ii) Lateral Stiffness of Frames Neglected

I = 45.278 m^4

μ = 1.1965

B = 4 bending action

γ = 4.6266

I = 22.464 m^4

μ = 1.1875

D = 2.08 torsional action

γ = 4.7186

Three functions, namely, the vertical shear distribution, wall moment in the coupled wall assembly 1, and the displacement of the structure, are shown graphically in Figs. 5.8 - 5.13. When the lateral stiffness of the frames is considered, vertical shear distribution and displacement are obtained using equations (5.48) to (5.52). Equations (4.76) and (4.77) are used when the lateral stiffness of the frames is neglected. The wall moment is determined using the moment-curvature relationship.

It may be seen from Figs. 5.8-5.13 that in neglecting the lateral stiffness of the frames, the displacement, vertical shear distribution and the maximum wall moment are all overestimated. In the lower region of the structure, a considerable proportion of bending moment is carried by the frame system.

5.5 Conclusion

From the analysis the following conclusions can be drawn. For a symmetrical coupled wall-frame structure, the governing differential equations for pure bending and pure torsion are fourth-order equations. In each case, provided that the coupled wall assemblies are planar or in-plane symmetrical, the number of the differential equations will be equal to the number of distinct groups of coupled wall assemblies. For a symmetrical cantilevered wall-frame structure the differential equations for the displacement functions are third-order equations.

The analysis is also applicable to structure with non-planar components.

From consideration of equation (5.1) it may be deduced that the rotation at the base of the shear beam and that of the support will generally be incompatible. For any loading system, the rotation at the base of the beam is proportional to the shear force at the base, whereas the rotation of the support is proportional to the imposed moment. Therefore, it should be noted that the behaviour of the shear beam as represented by equation (5.1) is valid only when the beam acts in conjunction with flexural beam. The interactive forces between the flexural and shear beams provide additional force system to satisfy the rotational compatibility at the base of the shear beam.

Regarding the load distributions between walls and frames, the following points may be noted. From the top boundary condition of zero moment at the top it is evident that the distributed load acting on the frame must vanish at the top (c.f. equation (5.3)). The base boundary condition of zero rotation implies that the shear forces at the bases of all the frames vanish. Therefore, at the base, all the shear forces are taken by the walls.

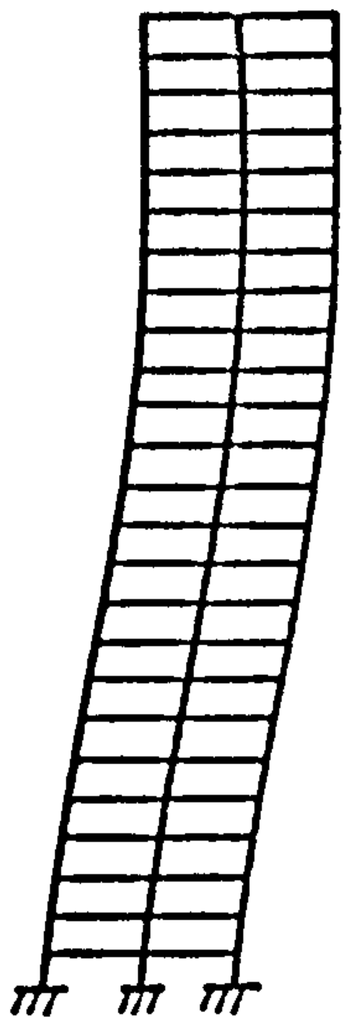

frame

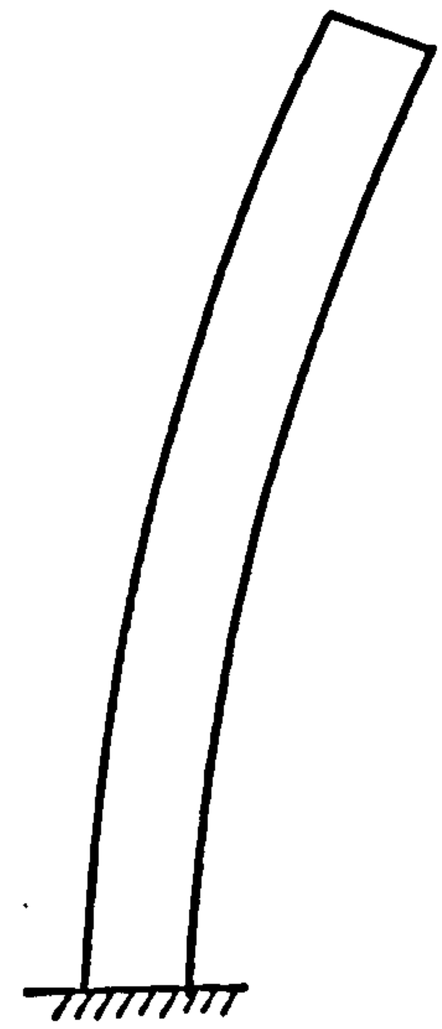

cantilevered wall

Deformed configurations of frame and cantilevered wall

Fig. 5.1

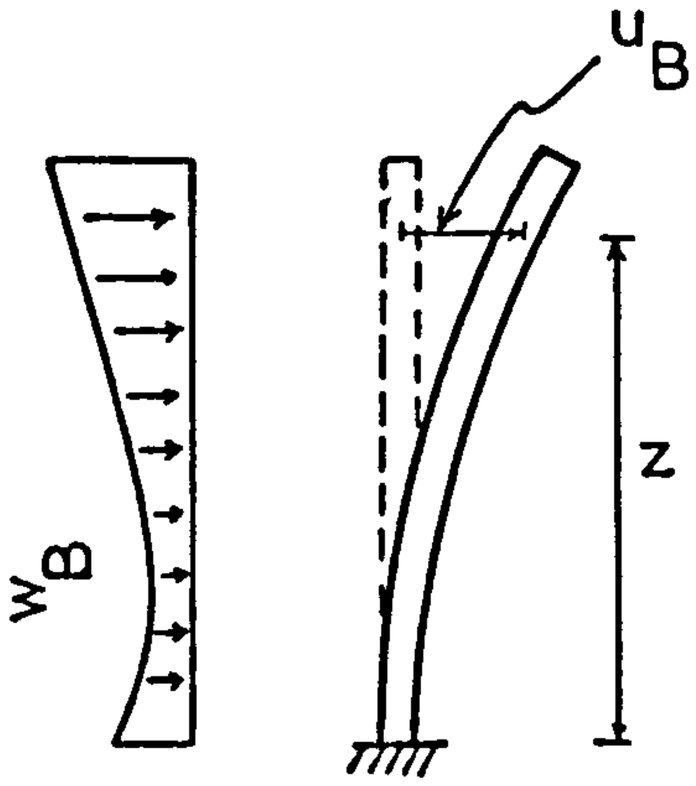

flexural beam

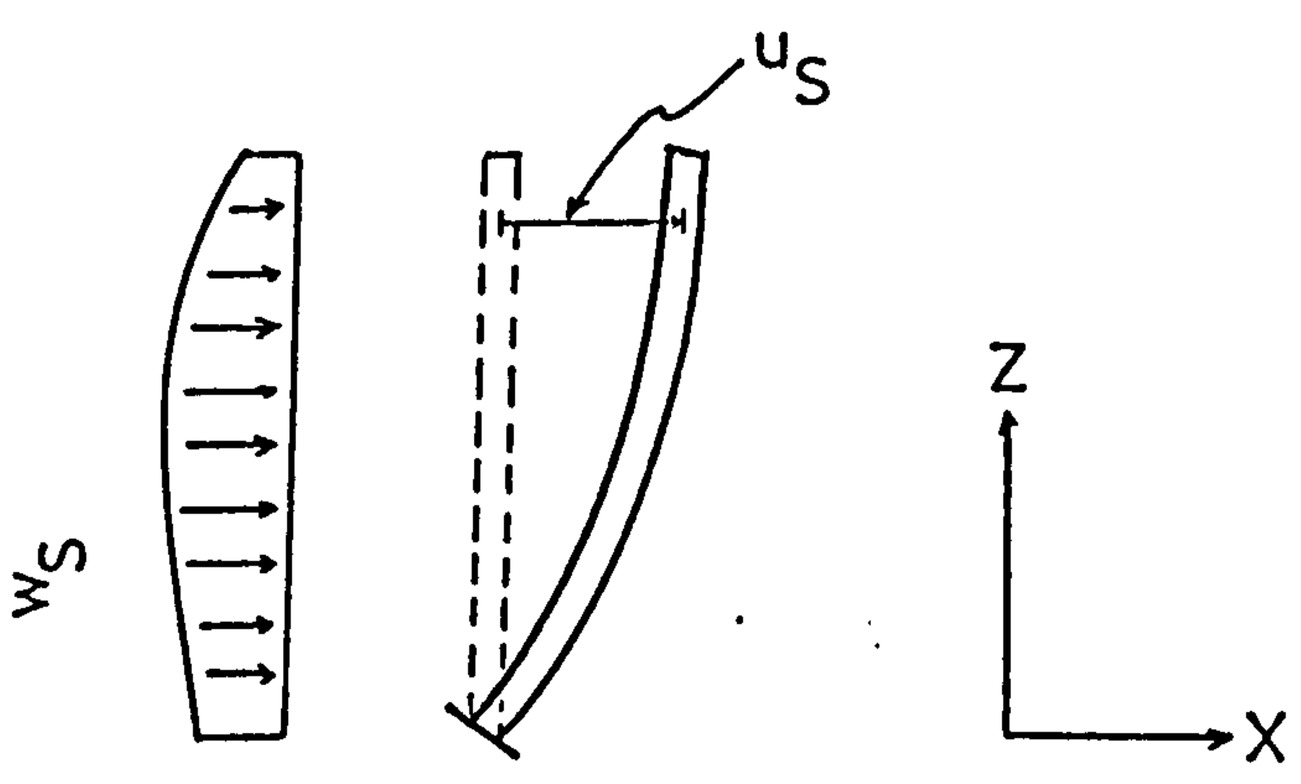

cantilevered shear beam

Horizontally loaded flexural beam and shear beam

Fig. 5.2

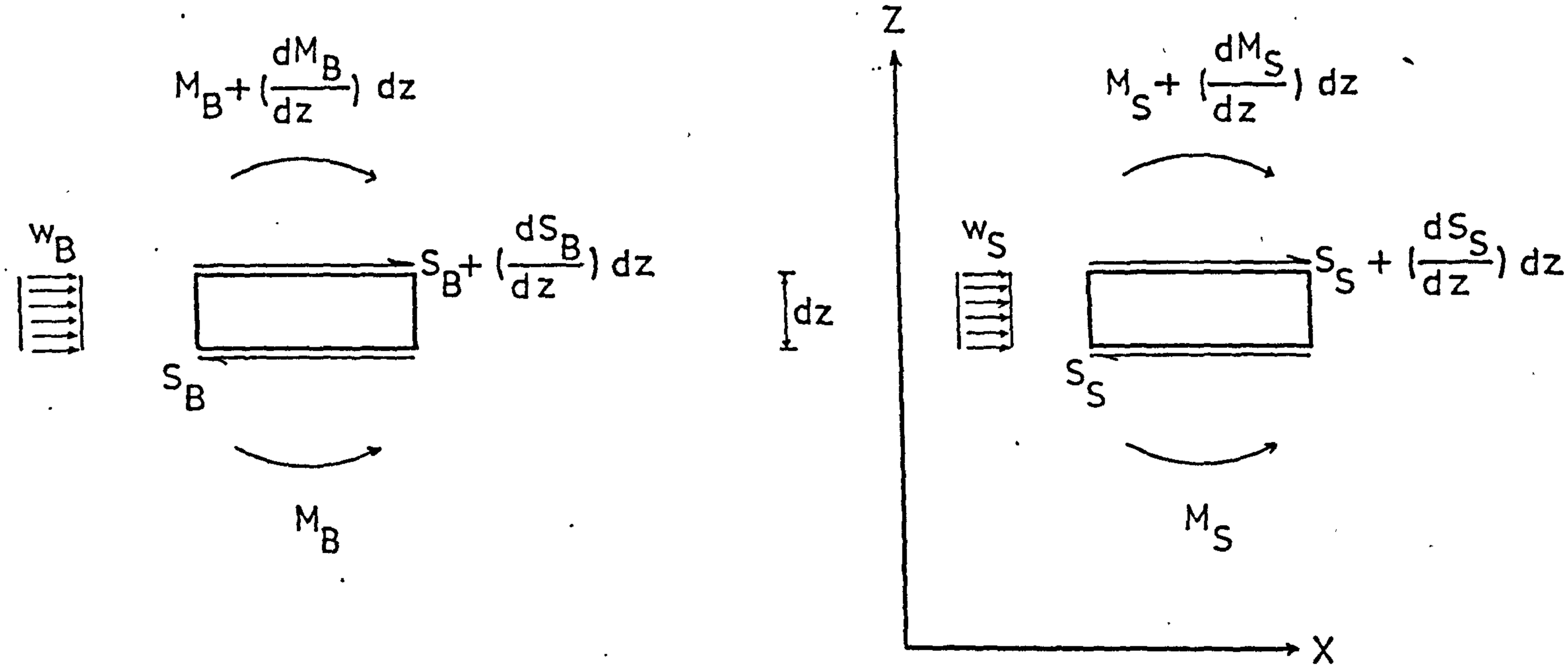

Forces acting on elements of cantilevered wall and shear beam

Fig. 5.3

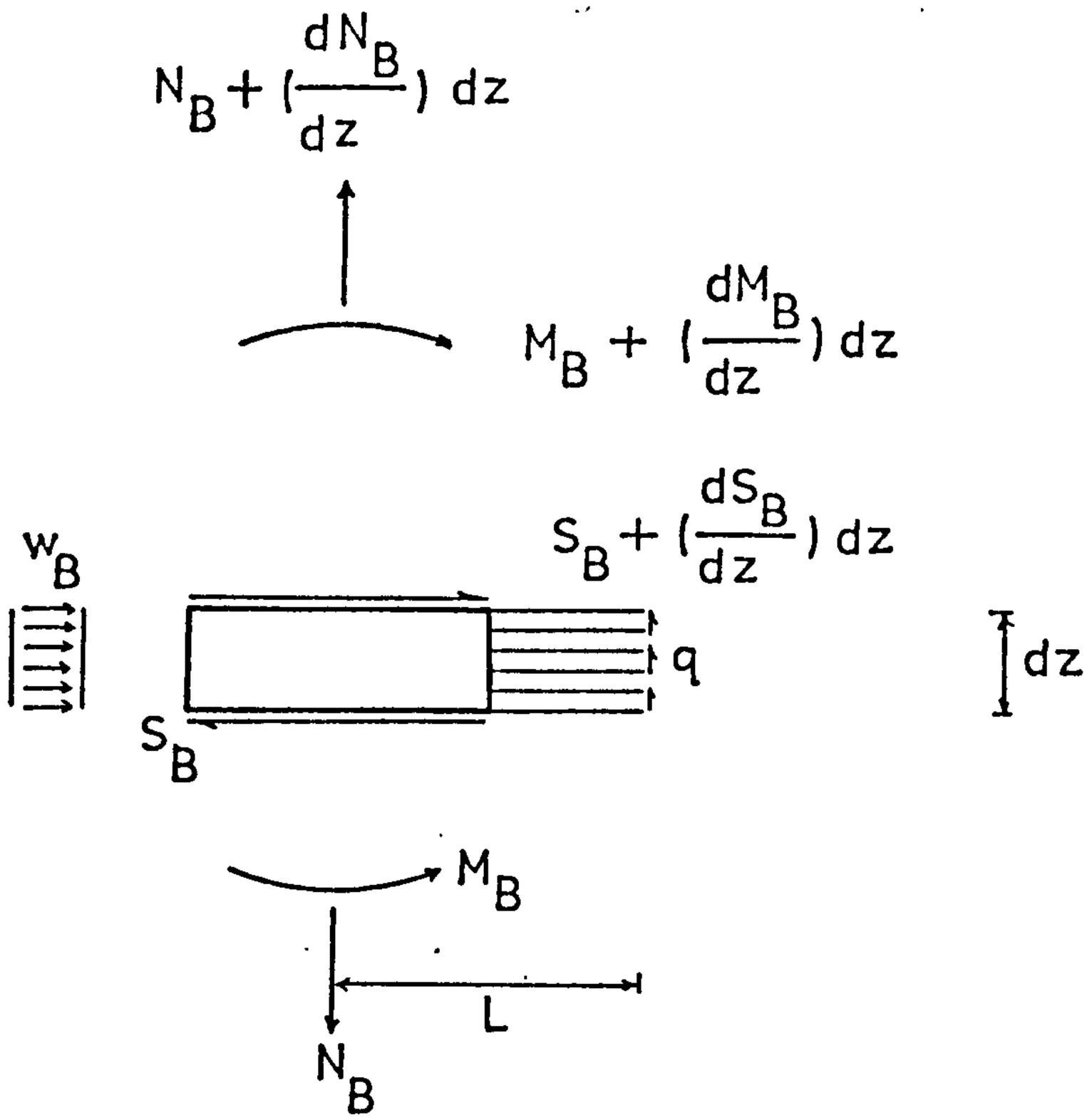

Forces acting on an element of coupled wall

Fig. 5.4

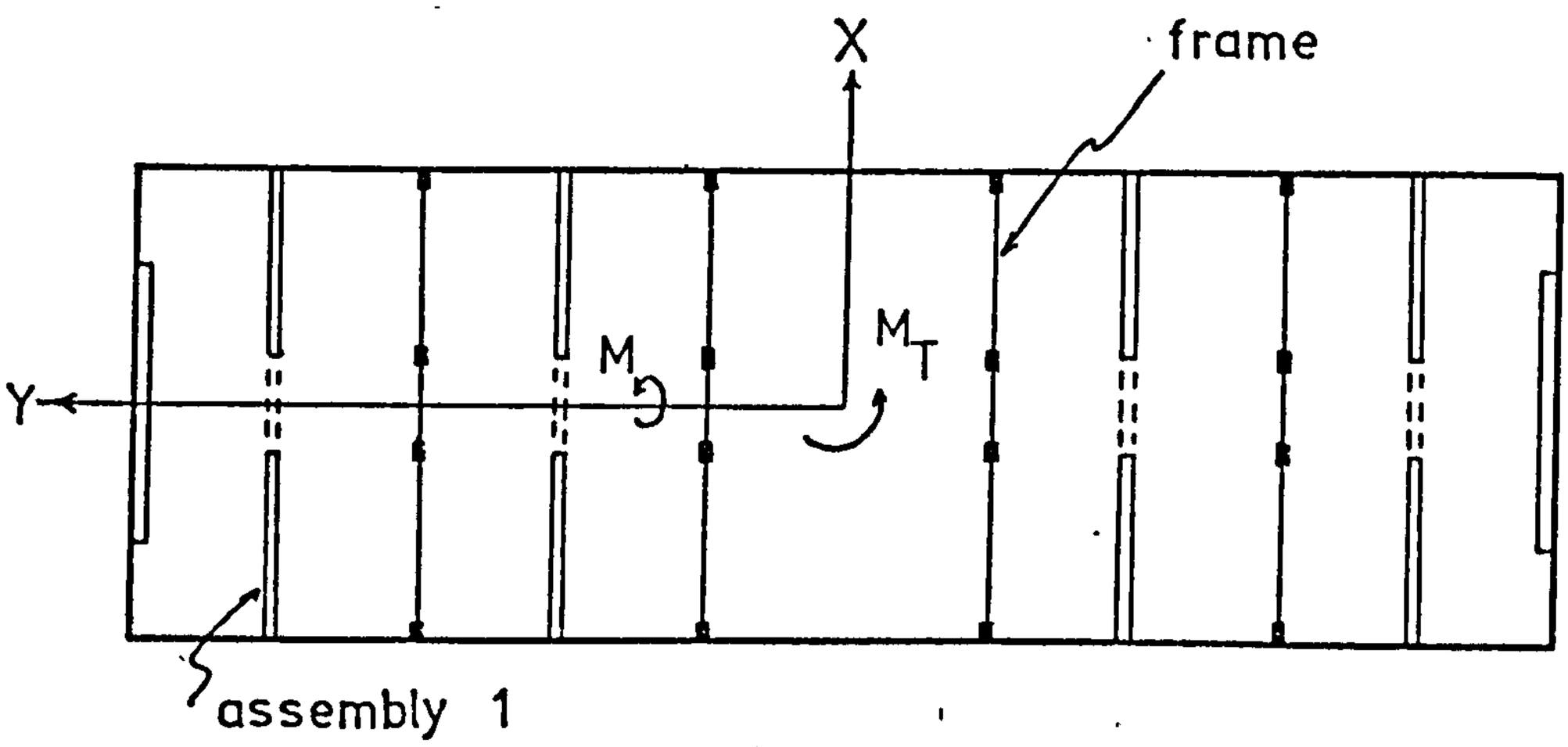

Symmetrical shear wall-frame structure

Fig. 5.5

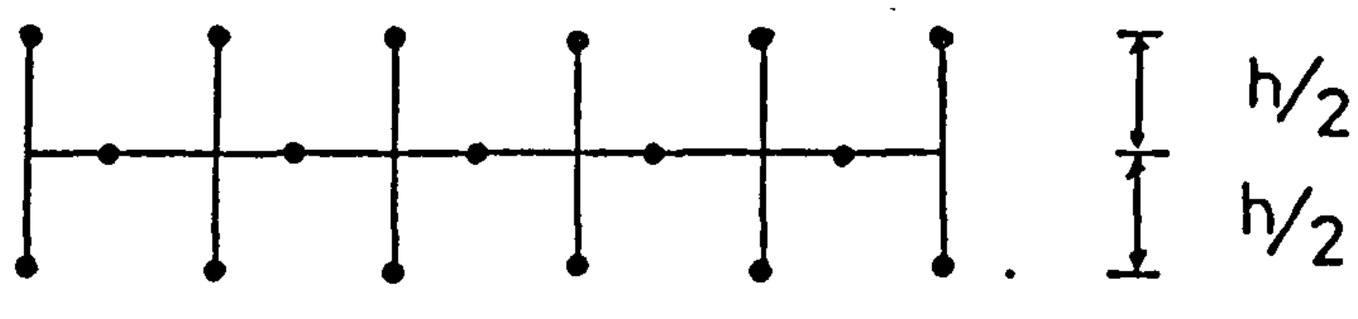

(a) one-storey frame segment

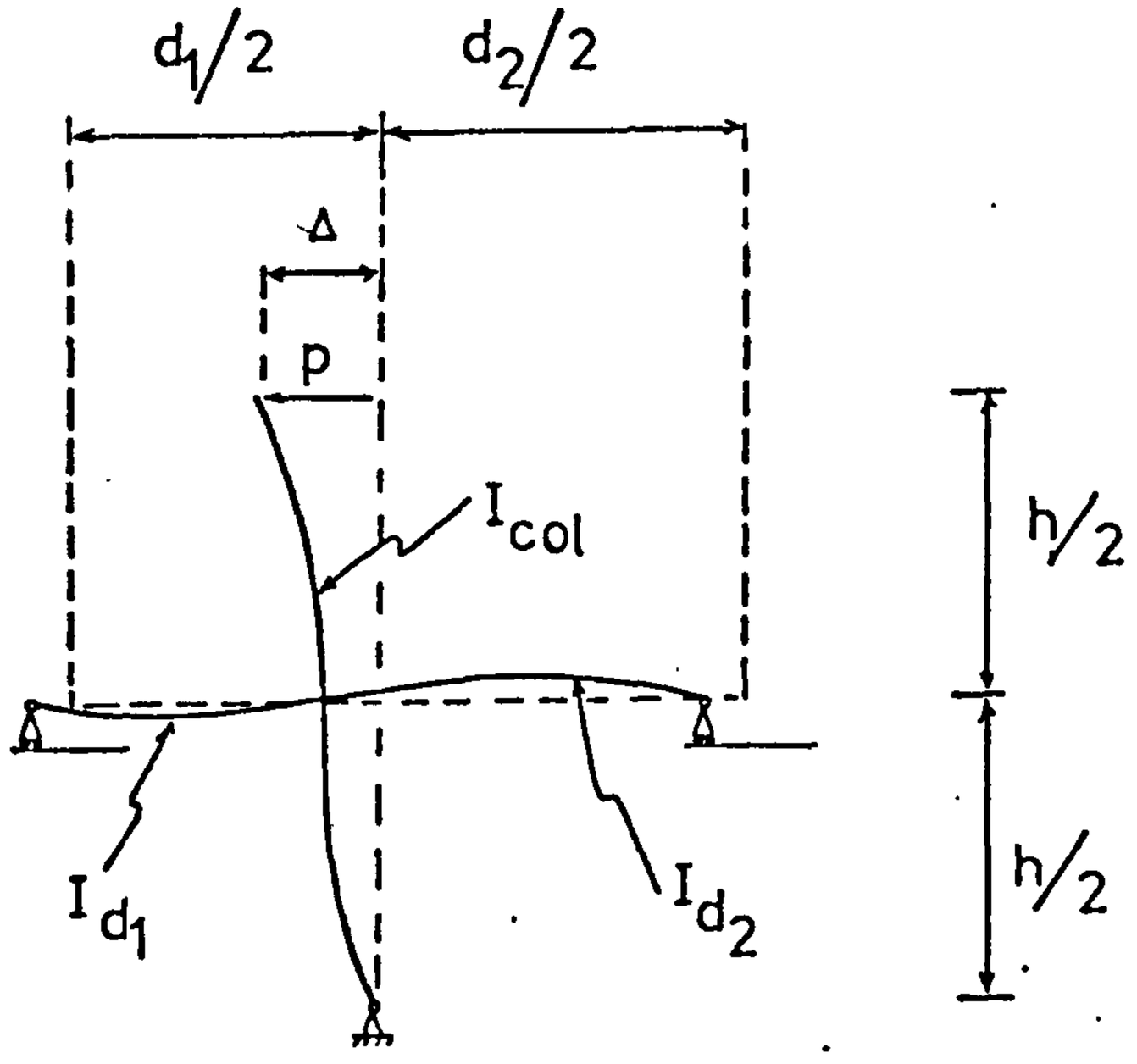

(b) horizontal deformation of one column

Deformation of frame

Fig. 5.6

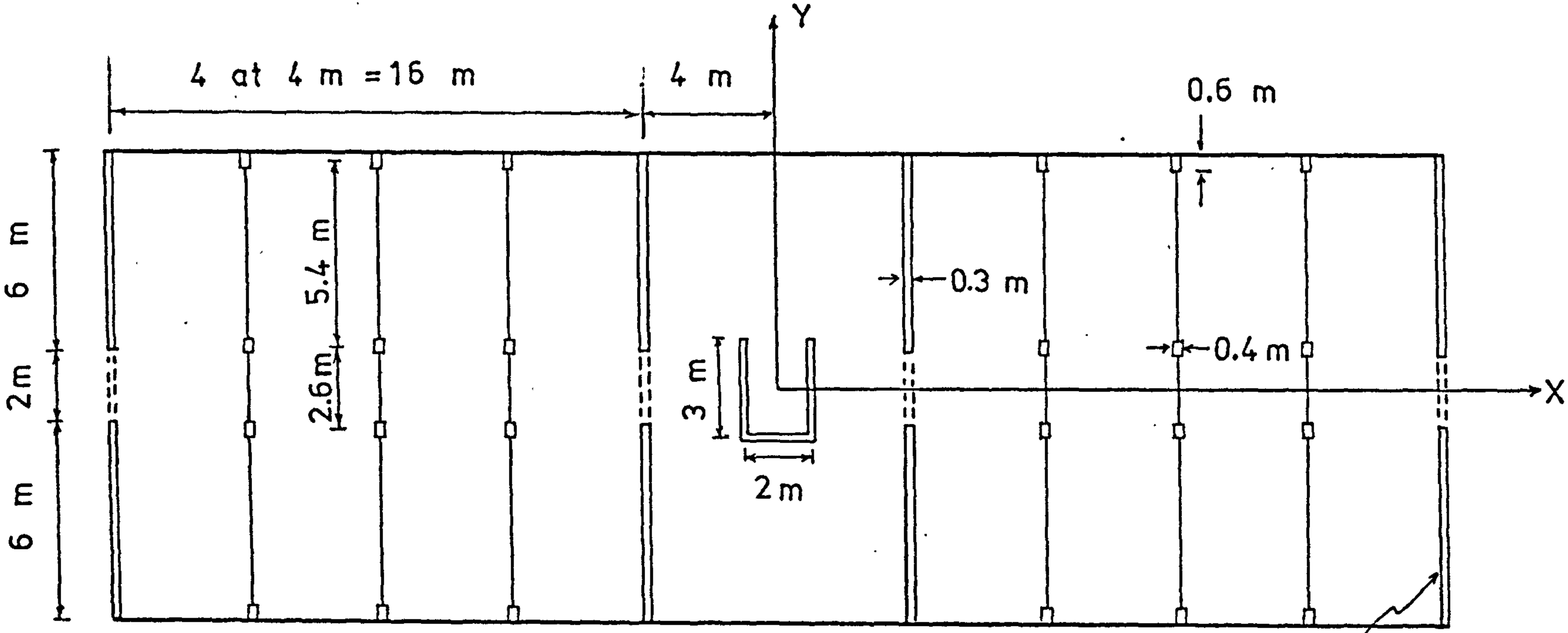

all beams are 0.5 m deep

total height = 45 m ; storey height = 3 m

Example problem

Fig. 5.7

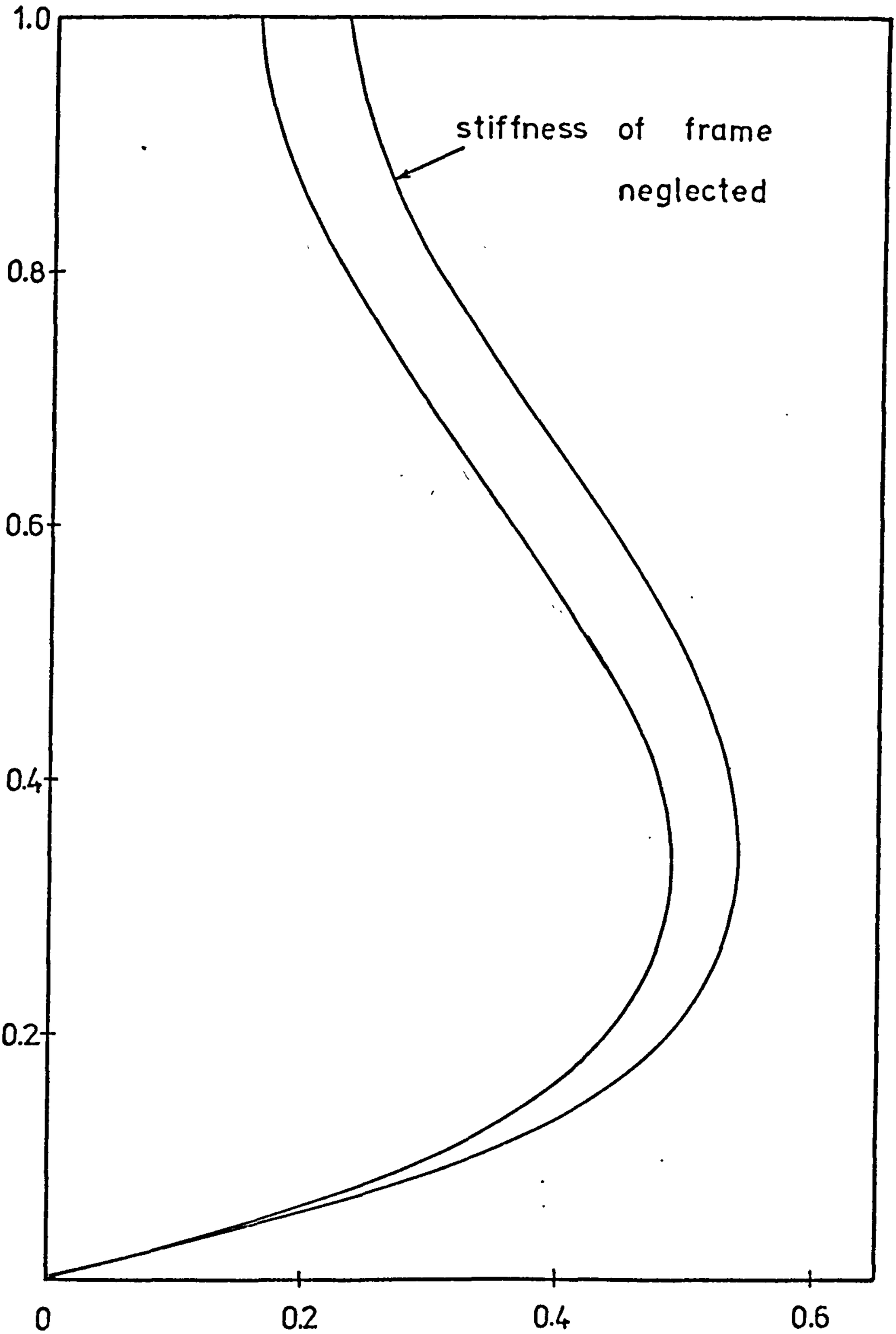

Example problem :- (bending load of 1 kN/m)

Fig. 5.8

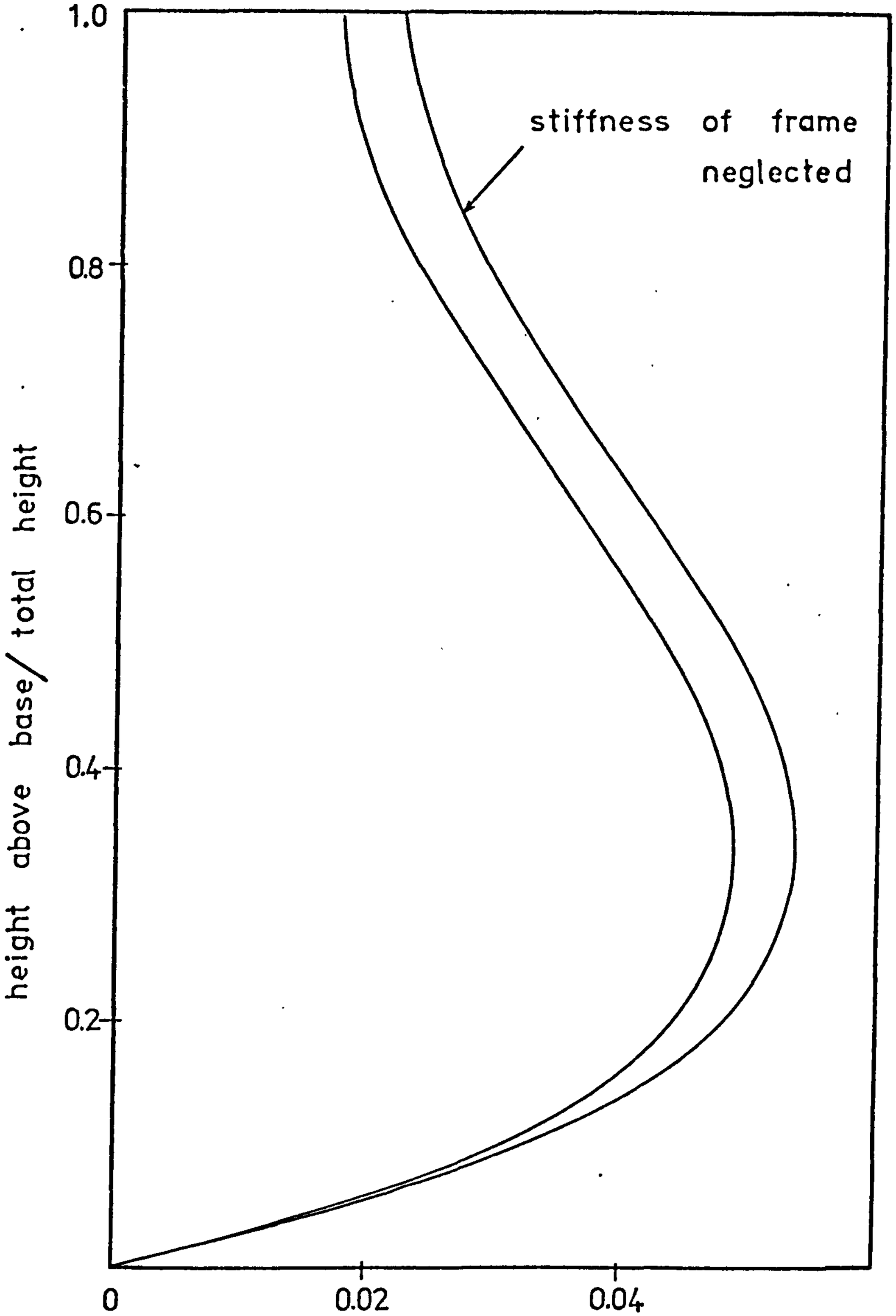

Example problem:- (torsional loading of 1 kN-m/m)

Fig. 5.9

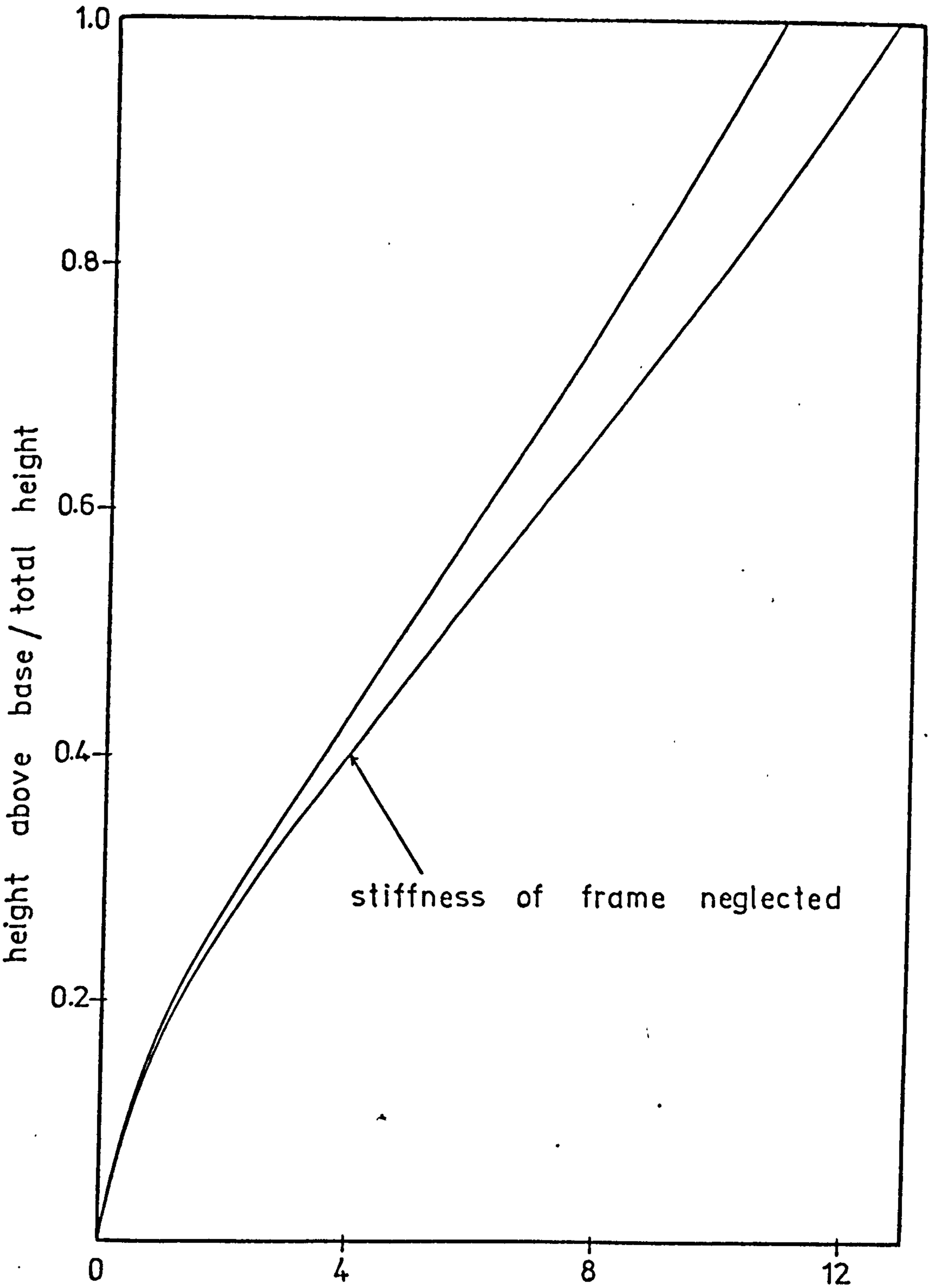

Example problem:-(bending load of 1 kN/m)

Fig. 5.10

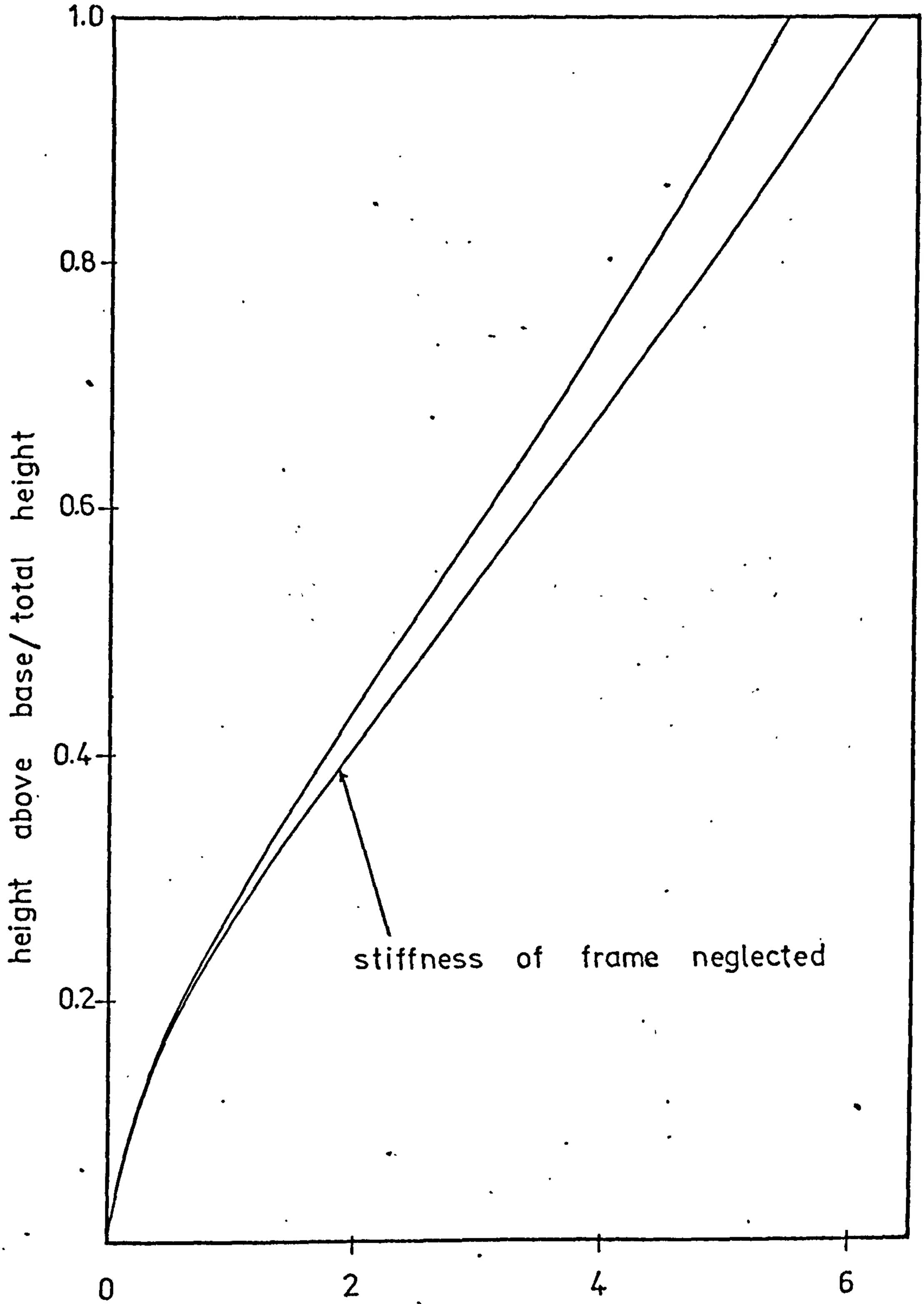

Example problem :- (torsional loading of 1 kN-m/m)

Fig. 5.11

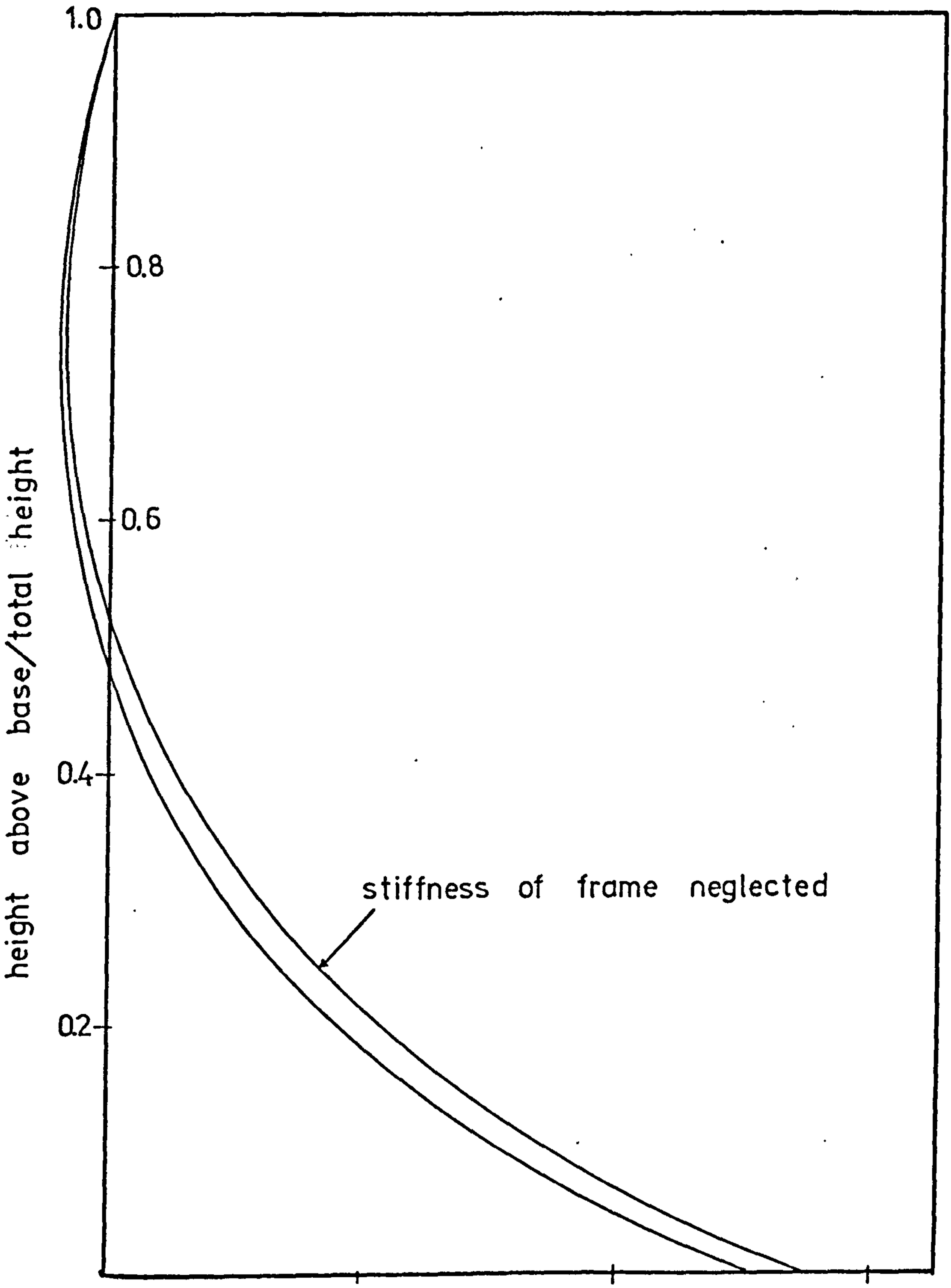

Example problem:- (bending load of 1 kN/m)

Fig. 5.12

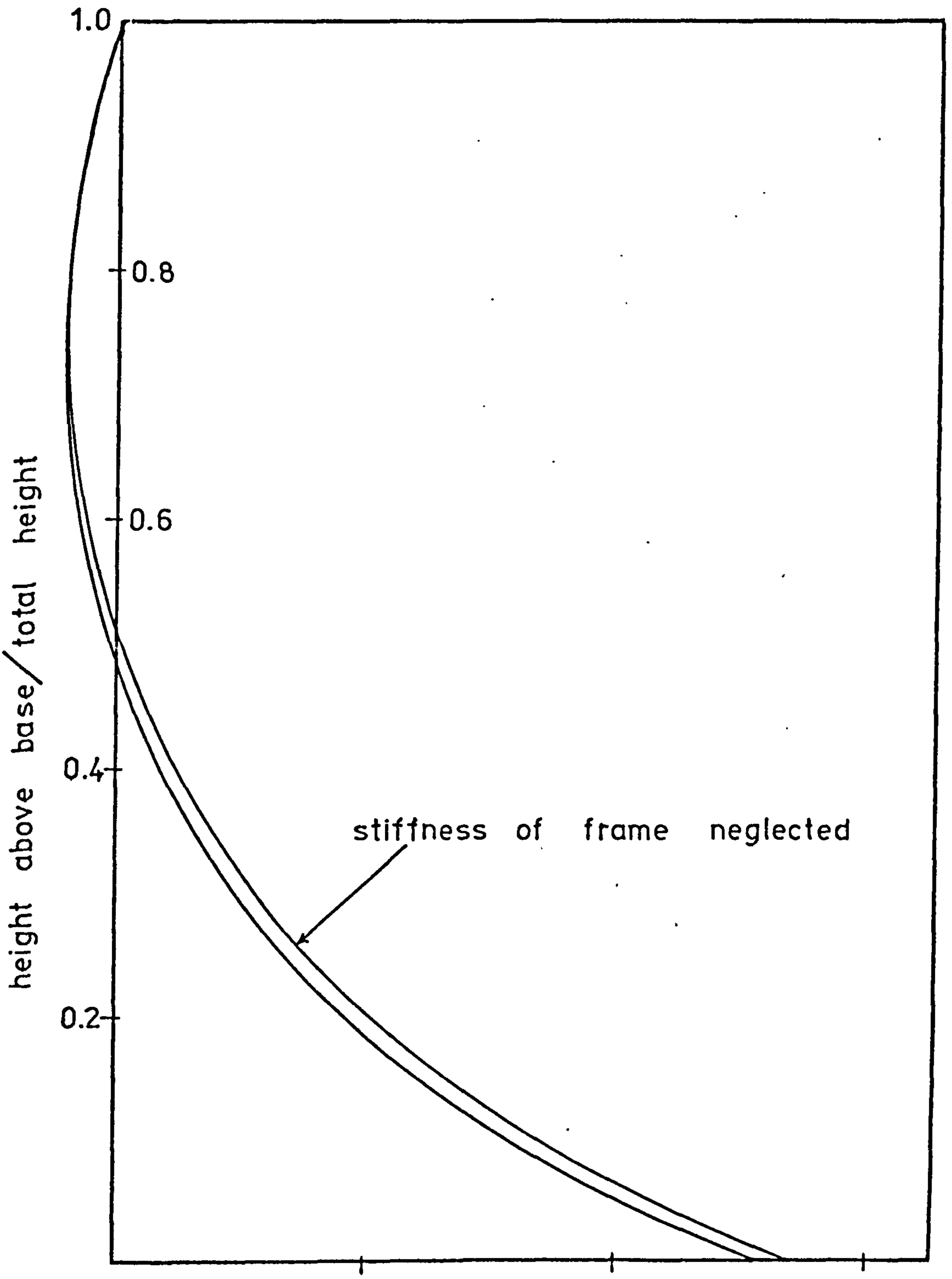

Example problem:- (torsional loading of 1 kN-m/m)

Fig. 5.13

CHAPTER 6

ASYMMETRICAL STRUCTURES

6.1 Introduction

The relatively simple methods of analysis presented in Chapters 4 and 5 are able to be achieved because of the symmetry of the structures. Due to symmetry, any lateral loading in a plane of symmetry will produce only pure bending of the structure, and under a pure torsional moment the structure will rotate about its axis of symmetry. With these known characteristics of a symmetrical structure, any lateral loading system may be replaced by an equivalent system which consists of a torsional moment and the loads which produce only pure bendings of the structure. The analyses for pure bending action and pure torsional action can be carried out separately, and the solutions are then superimposed to give the actual solutions. Under the pure bending action the vertical shear distributions in identical in-plane symmetrical coupled wall assemblies are linearly related (cf. section 4.7.1). Under the pure torsional action the vertical shear distributions in identical coupled wall assemblies with the same relative orientation with respect to the axis of symmetry are equal (cf. section 4.7.2), and are linearly related irrespective of their relative orientations whenever the identical assemblies are in-plane symmetrical. Therefore, for a structure consisting of groups of identical coupled wall assemblies, the number

of the indeterminate functions to be determined is usually small.

If the structure is asymmetrical the methods of analysis employed in Chapters 4 and 5 are not directly applicable. The structure must be analysed by considering the total loading system which is capable of producing both bending and torsion of the structure simultaneously. As a result, the number of governing differential equations for the vertical shear distributions will generally be equal to the number of coupled wall assemblies present in the structure, even though some of the assemblies may be identical. However, for an asymmetrical structure consisting of a few coupled wall assemblies or consisting of cantilevered walls and frames, the methods are still relatively economical in comparison with the conventional stiffness or flexibility analyses.

6.2 Cross-wall Structures Composed of Cantilevered Walls and Coupled Wall Assemblies

Consider a simple cross-wall structure shown in Fig. 6.1. The axes OX, OY, OZ are structural co-ordinate system with OZ as vertical axis. A loading function W is assumed acting perpendicular to the long face of the structure, and with eccentricity e with respect to the plane OYZ. The same set of assumptions stated in section 4.4 is assumed to be valid.

The geometrical relationships between the displacements of the reference axis OZ and the displace-

ments of the axis of individual wall J are given by

$$v_J = v + x_J \theta$$

$$\theta_J = \theta \qquad (6.1)$$

in which

v, θ = translational displacement in the Y direction, and rotational displacement about the vertical axis, respectively, of a point on the reference axis OZ

v_J, θ_J = the corresponding displacements of the axis of wall J

x_J = X ordinate of the axis of wall J

Using the continuous medium approach, the continuity equation for the substitute lamina of any coupled wall assembly i is given by, for a structure on a rigid foundation,

$$l_i \frac{dv_i}{dz} - \frac{1}{E}\left(\frac{b_i^3 h}{12 I_{ci}}\right) q_i - \frac{1}{E}\left(\frac{1}{A_{ai}} + \frac{1}{A_{bi}}\right) \int_0^z \int_\xi^H q_i \, d\lambda \, d\xi = 0 \qquad (6.2)$$

where the parameters E, h, H, b_i, l_i, q_i, A_{ai}, A_{bi}, I_{ci} are as previously defined in Chapter 4.

From ordinary beam theory, the internal moments in the coupled wall assembly i and cantilevered wall cr-k are given by, respectively,

$$EI_i \frac{d^2 v_i}{dz^2} = M_i - l_i \int_z^H q_i \, d\lambda$$

$$EI_{cr-k} \frac{d^2 v_{cr-k}}{dz^2} = M_{cr-k} \qquad (6.3)$$

where

M_i = component of moment due to the transmitted horizontal force acting on coupled wall assembly i

M_{cr-k} = moment due to the transmitted horizontal force acting on cantilevered wall cr-k

I_{cr-k} = second moment of area of cantilevered wall cr-k

$I_i = I_{ai} + I_{bi}$

I_{ai}, I_{bi} = second moment of areas of walls a and b respectively, of coupled wall assembly i

v_{cr-k} = displacement in the Y direction of the axis of cantilevered wall cr-k.

The corresponding cross-sectional shear forces are,

$$S_i = - \frac{dM_i}{dz} = - EI_i \frac{d^3 v_i}{dz^3} + l_i q_i \qquad (6.4)$$

$$S_{cr-k} = - \frac{dM_{cr-k}}{dz} = - EI_{cr-k} \frac{d^3 v_{cr-k}}{dz^3}$$

in which S_i, S_{cr-k} are the cross-sectional shear forces in the coupled wall assembly i and the cantilevered wall cr-k respectively.

For the force equilibrium of the structure, it may be shown that,

$$E\left[\sum_{i=1}^{n} I_i \frac{d^3 v_i}{dz^3} + \sum_{k=1}^{n_{cr}} I_{cr-k} \frac{d^3 v_{cr-k}}{dz^3}\right] = \frac{dM}{dz} + \sum_{i=1}^{n} l_i q_i \qquad (6.5)$$

in which

M = applied static moment

n = number of coupled wall assemblies in the structure

n_{cr} = number of cantilevered walls in the structure.

By assuming that the St. Venant's torsion is comparatively insignificant since the thickness of each wall is relatively small in comparison with its width, the torsional resistance of the structure may be considered as arising solely from the differential shearing action of all the walls. Therefore, the torsional equilibrium equation for the structure becomes,

$$M_T = \sum_{i=1}^{n} S_i x_i + \sum_{k=1}^{n_{cr}} S_{cr-k}\, x_{cr-k} \qquad (6.6)$$

where

M_T = static applied torsion due to the eccentricity e of the applied load

x_i = X ordinate of the plane of coupled wall assembly i

x_{cr-k} = X ordinate of the axis of cantilevered wall cr-k

Substitution of equation (6.4) into (6.6) leads to,

$$E\left(\sum_{i=1}^{n} I_i x_i \frac{d^3 v_i}{dz^3} + \sum_{k=1}^{n_{cr}} I_{cr-k} x_{cr-k} \frac{d^3 v_{cr-k}}{dz^3}\right) = -M_T + \sum_{i=1}^{n} l_i q_i \qquad (6.7)$$

Using the geometrical relationships given by equation (6.1), the force and torsional equilibrium equations become, respectively,

$$K \frac{d^3v}{dz^3} + K_x \frac{d^3\theta}{dz^3} = \frac{dM}{dz} + \sum_{i=1}^{n} l_i q_i \qquad (6.8)$$

$$K_x \frac{d^3v}{dz^3} + K_A \frac{d^3\theta}{dz^3} = - M_T + \sum_{i=1}^{n} l_i x_i q_i \qquad (6.9)$$

$$K = E\left(\sum_{i=1}^{n} I_i + \sum_{k=1}^{n_{cr}} I_{cr-k}\right)$$

$$K_x = E\left(\sum_{i=1}^{n} I_i x_i + \sum_{k=1}^{n_{cr}} I_{cr-k}\ x_{cr-k}\right) \qquad (6.10)$$

$$K_A = E\left(\sum_{i=1}^{n} I_i\ x_i^2 + \sum_{k=1}^{n_{cr}} I_{cr-k}\ x_{cr-k}^2\right)$$

As the choice of the location of the origin of the co-ordinate system is arbitrary, the differential equations (6.8) and (6.9) may be uncoupled by locating the origin at the equivalent centroid of combined wall stiffness. With the equivalent centroid of combined wall stiffness as the origin,

$$K_x = 0 \qquad (6.11)$$

and equations (6.8) and (6.9) become, respectively,

$$K \frac{d^3v}{dz^3} = \frac{dM}{dz} + \sum_{i=1}^{n} l_i q_i \qquad (6.12)$$

$$K_A \frac{d^3\theta}{dz^3} = - M_T + \sum_{i=1}^{n} l_i x_i q_i \qquad (6.13)$$

In equation (6.13) the torsional moment M_T is the moment with respect to the vertical axis of the new co-ordinate system. Differentiating equation (6.2) twice with respect to z yields,

$$l_i \frac{d^3v}{dz^3} + l_i x_i \frac{d^3\theta}{dz^3} + \frac{1}{E}\left(\frac{1}{A_{ai}} + \frac{1}{A_{bi}}\right) q_i - \frac{d^2 q_i}{dz^2} = 0 \qquad (6.14)$$

For the structure with n coupled wall assemblies, there will be n equations of the form given by equation (6.14). From equations (6.12)-(6.14) it may be shown that the n simultaneous second-order governing differential equations for the structure are of the form,

$$\frac{d^2 q_i}{dz^2} - \alpha_i^2 q_i - F_i = \beta_i^2 \left(\frac{dM}{dz} - M_T\right) \qquad (6.15)$$

$$i = 1, 2, 3 \ldots n$$

where

$$\beta_i^2 = \left(\frac{12 I_{ci}}{b_i^3 h}\right) \frac{l_i}{K}$$

$$\alpha_i^2 = \beta_i^2 l_i \mu_i$$

$$\mu_i = 1 + \frac{K}{K_A} x_i^2 + \frac{K}{E l_i^2} \left(\frac{1}{A_{ai}} + \frac{1}{A_{bi}}\right)$$

$$F_i = \left(\sum_{r=1}^{n} q_r D_{i,r}\right) - q_i D_{i,i}$$

$$D_{i,r} = \beta_r^2 l_i \left(1 + \frac{K}{K_A} x_i x_r\right) \qquad (6.16)$$

With the usual boundary conditions of zero moment at the top and zero rotation at the base, the boundary conditions for q_i become,

$$\begin{aligned} &\text{at } z = 0, \quad q_i = 0 \text{ , for all } i \\ &\text{at } z = H, \quad \frac{dq_i}{dz} = 0 \text{ , for all } i \end{aligned} \qquad (6.17)$$

The displacement functions v and θ may be obtained by integrating equations (6.12) and (6.13) respectively. The boundary conditions for the displacement functions are as follows,

$$\begin{aligned} &\text{at } z = 0, \quad v = \frac{dv}{dz} = \frac{d\theta}{dz} = 0 \\ &\text{at } z = H, \quad \frac{d^2v}{dz^2} = \frac{d^2\theta}{dz^2} = 0 \end{aligned} \qquad (6.18)$$

6.3 Cross-wall Structures Composed of Cantilever Walls and Frames

An analysis of asymmetrical cross-wall structure composed entirely of cantilevered walls and frame will be presented in this section. Consider an asymmetrical structure consisting of n_{cr} cantilevered walls and n_f frames, a typical plan of which is as shown in Fig. 6.2. Each frame component is treated as a vertical cantilevered shear beam. The load-deformation relationships for a

shear beam are those given in Chapter 5 (equation (5.3)).

Following the same procedure in establishing the equilibrium equations carried out in section 6.2, the force and torsional equilibrium equations for the structure considered may be shown to be, respectively,

$$K_C \frac{d^3v}{dz^3} + K_{CX} \frac{d^3\theta}{dz^3} - K_F \frac{dv}{dz} - K_{FX} \frac{d\theta}{dz} = \frac{dM}{dz} \qquad (6.19)$$

$$K_{CX} \frac{d^3v}{dz^3} + K_{CA} \frac{d^3\theta}{dz^3} - K_{FX} \frac{dv}{dz} - K_{FA} \frac{d\theta}{dz} = - M_T \qquad (6.20)$$

where

$$K_C = E \sum_{k=1}^{n_{cr}} I_{cr-k} \;,\; K_{CX} = E \sum_{k=1}^{n_{cr}} I_{cr-k}\, x_{cr-k}$$

$$K_F = \sum_{j=1}^{n_f} K_{f-j} \;,\; K_{FX} = \sum_{j=1}^{n_f} K_{f-j}\, x_{f-j} \qquad (6.21)$$

K_{f-j} = shear rigidity of frame f-j

x_{f-j} = X ordinate of the plane of frame f-j

$$K_{CA} = E \sum_{k=1}^{n_{cr}} I_{cr-k}\, x_{cr-k}^2 \;,\; K_{FA} = \sum_{j=1}^{n_f} K_{f-j}\, x_{f-j}^2$$

The shear rigidity K_{f-j} is evaluated as described in section 5.2.

By choosing the equivalent centroid of combined wall stiffness as the origin for the co-ordinate system,

$$K_{CX} = 0 \qquad (6.22)$$

and equations (6.19) and (6.20) reduce to, respectively,

$$K_C \frac{d^3v}{dz^3} - K_F \frac{dv}{dz} - K_{FX} \frac{d\theta}{dz} = \frac{dM}{dz} \tag{6.23}$$

$$K_{CA} \frac{d^3v}{dz^3} - K_{FX} \frac{dv}{dz} - K_{FA} \frac{d\theta}{dz} = - M_T \tag{6.24}$$

From equations (6.23) and (6.24), a differential equation for the displacement v may be obtained as,

$$\frac{d^5v}{dz^5} - \alpha^2 \frac{d^3v}{dz^3} - \kappa^4 \frac{dv}{dz} = \frac{1}{K_{CA}} \left(\frac{d^3M}{dz^3} - \rho^2 \frac{dM}{dz} - \psi^3 M_T\right) \tag{6.25}$$

$$\alpha^2 = \frac{K_F}{K_C} + \frac{K_{FA}}{K_{CA}}$$

$$\kappa^4 = \frac{K_{FX}^2 - K_F K_{FA}}{K_C K_{CA}} \tag{6.26}$$

$$\rho^2 = \frac{K_{FA}}{K_{CA}}$$

$$\psi^3 = \frac{K_{FX}}{K_{CA}}$$

For the structure on a rigid foundation and free at the top, the boundary conditions may be shown to be,

$$\text{at } z = 0 , \quad v = \frac{dv}{dz} = 0$$

$$\frac{d^3v}{dz^3} = \frac{1}{K_{CA}} \frac{dM}{dz}$$

at $z = H$, $\quad \frac{d^2v}{dz^2} = 0$

$$\frac{d^4v}{dz^4} = \frac{1}{K_{CA}} \frac{d^2M}{dz^2} \qquad (6.27)$$

The solution for the displacement v may be written as,

$$v = c_1 \cosh r_1 z + c_2 \sinh r_1 z + c_3 \cosh r_2 z$$

$$+ c_4 \sinh r_2 z + c_5 + v_p \qquad (6.28)$$

$$r_1^2 = \tfrac{1}{2}\left(\alpha^2 + \sqrt{\alpha^4 - 4\kappa^4} \right)$$

$$r_2^2 = \tfrac{1}{2}\left(\alpha^2 - \sqrt{\alpha^4 - 4\kappa^4} \right) \qquad (6.29)$$

c_i = constants of integration which may be evaluated from equation (6.27)

v_p = particular integral solution of equation (6.25)

By integrating equation (6.23), the rotational displacement is obtained as,

$$\theta = \frac{1}{K_{FX}} \left[K_C \left(\frac{d^2v}{dz^2} - \left(\frac{d^2v}{dz^2} \right)_0 \right) - K_F v + (M)_0 - M \right] \qquad (6.30)$$

in which

$\left(\frac{d^2v}{dz^2}\right)_0$ = curvature at $z = 0$

$(M)_0$ = applied static moment at the base, $z = 0$

If the lateral stiffnesses of the frames are small

in comparison with those of the walls and may be neglected, the governing differential equations become, from equations (6.23) and (6.24),

$$K_C \frac{d^3 v}{dz^3} = \frac{dM}{dz} \qquad (6.31)$$

$$K_{CA} \frac{d^3 \theta}{dz^3} = - M_T$$

The boundary conditions are given by,

$$\text{at } z = 0, \quad v = \quad = \frac{dv}{dz} = \frac{d}{dz} = 0 \qquad (6.32)$$

$$\text{at } z = H, \quad \frac{d^2 v}{dz^2} = \frac{d^2 \theta}{dz^2} = 0$$

The solution for the displacement functions are simply, by directly integrating equation (6.31),

$$v = \frac{1}{K_C} \int_0^z \int_0^\xi M \, d\lambda \, d\xi \qquad (6.33)$$

$$= \frac{1}{K_{CA}} \int_0^z \int_0^\xi \int_\zeta^H M_T \, d\lambda \, d\zeta \, d\xi \qquad (6.34)$$

It may be seen that equations (6.33) and (6.34) represent the pure bending action and the pure torsional action respectively. Under the pure torsion the structure rotates about the vertical axis OZ. To produce pure bending the applied load must act along the plane OYZ.

6.4 Structures with Non-planar Walls

Although sections 6.2 and 6.3 dealt only with

asymmetrical cross-wall structure, with slight modifications the analyses can be readily extended to deal with fully three dimensional structures. For a fully three dimensional structure there will be three equilibrium equations, namely, a torsional equilibrium equation and two force equilibrium equations in two orthogonal directions. The number of independent displacement functions will likewise be three, i.e. corresponding to the number of equilibrium equations. The shear centre axis of each wall must be used as the wall axis instead of the centroidal axis. From geometry, the relationships between the displacements of the shear centre axis of any wall i and the displacements of the reference axis OZ may be shown to be, Fig. 6.3,

$$\begin{Bmatrix} u_i \\ v_i \\ \theta_i \end{Bmatrix} = \begin{bmatrix} \cos \phi_i & \sin \phi_i & 0 \\ -\sin \phi_i & \cos \phi_i & 0 \\ 0 & 0 & 1 \end{bmatrix} \begin{bmatrix} 1 & 0 & -y_i \\ 0 & 1 & x_i \\ 0 & 0 & 1 \end{bmatrix} \begin{Bmatrix} u \\ v \\ \theta \end{Bmatrix} \tag{6.35}$$

where

u, v, θ = displacements along X and Y axes and rotation about vertical axis, respectively, of the reference axis OZ

u_i, v_i, θ_i = displacements along $\bar{x}_i$ and $\bar{y}_i$ axes and rotation about vertical axis, respectively, of the shear centre axis of wall i

$\bar{x}_i, \bar{y}_i$ = principal axes of wall i

x_i, y_i = X and Y ordinates respectively of the shear centre axis of wall i

ϕ_i = the angle the $\bar{x}_i$ axis makes with the X axis

Following similar procedure carried out earlier, expressions for the three equilibrium equations for an asymmetrical structure composed of cantilevered walls and coupled wall assemblies may be established. These equations are expressible in terms of applied loads, vertical shear distribution functions, and the third derivative of displacement functions (i.e. $\frac{d^3u}{dz^3}$, $\frac{d^3v}{dz^3}$, $\frac{d^3\theta}{dz^3}$). Consequently, using the continuity equations for the substitute laminae, a system of simultaneous second-order differential equations for the structure may be obtained. Generally there will be as many differential equations as there are series of connecting beams. Only a brief outline of the analysis has been given here to avoid repetition since detailed analysis may be obtained from the next Chapter, Chapter 7, which treats all walls as thin-walled beams of open sections (thin-walled beam theory is a more general theory which includes ordinary beam theory as a special case).

For an asymmetrical structure consisting of non-planar cantilevered walls and plane frame with different orientations, further assumptions regarding the stiffness of the frame may be made. It may be assumed that out of plane stiffness of each frame can be neglected, and the axis of each equivalent shear beam is located at the equivalent centroid of stiffness of columns within the

frame. With these additional assumptions similar analysis may be carried out as before, and three simultaneous third-order differential equations for the three displacement functions, i.e. u, v, θ , may be obtained from the three equilibrium equations.

Special Case of Asymmetrical Cantilevered Wall Structures

Provided that the stiffnesses of the frames may be neglected, it can be shown that an asymmetrical structure composed of non-planar cantilevered walls and frames may be analysed as a combination of pure bending and pure torsional actions.

Consider again Fig. 6.2, but now assume that all the walls are non-planar and the stiffnesses of the frames may be neglected. Following the method of analysis outlined earlier, treating each wall as a three dimensional component with three degrees of freedom of displacements, the equilibrium equations for the structure may be expressed as (c.f. equation (7.7)-(7.10) of the next Chapter).

$$\begin{bmatrix} c_{11} & c_{12} & c_{13} \\ c_{21} & c_{22} & c_{23} \\ c_{31} & c_{32} & c_{33} \end{bmatrix} \begin{Bmatrix} \frac{d^3u}{dz^3} \\ \frac{d^3v}{dz^3} \\ \frac{d^3\theta}{dz^3} \end{Bmatrix} = \begin{Bmatrix} -P_X \\ -P_Y \\ -M_T \end{Bmatrix} \qquad (6.36)$$

where,

P_X, P_Y = total (from the top to level z) applied loads along the X and Y directions respectively

M_T = total (from the top to level z) twisting moment about OZ axis, due to eccentricity of the applied loads

X, Y, Z = axes of an arbitrarily chosen auxiliary co-ordinate system

c_{ij} = c_{ji} if $i \neq j$, i.e. the coefficient matrix is symmetric

u, v, θ = as defined previously

The expressions for c_{ij} are those given in equation (7.12). As the choice of the auxiliary co-ordinate system is arbitrary, any point at the base level may be chosen as the origin and an arbitrary orientation of the vertical axis selected. Assume that a new co-ordinate system with axes O_cX_c, O_cY_c, O_cZ_c is selected (Fig. 6.4). Let ϕ be the angle of relative orientation of the two systems, and x_0, y_0 the ordinates of the new origin with respect to the original system. It can be shown, using expression for c_{ij} given in equation (7.12), that x_0, y_0, ϕ, may be uniquely determined such that the equilibrium equations in this new frame of reference reduce to,

$$\begin{bmatrix} k_{11} & 0 & 0 \\ 0 & k_{22} & 0 \\ 0 & 0 & k_{33} \end{bmatrix} \begin{Bmatrix} \frac{d^3u_c}{dz^3} \\ \frac{d^3v_c}{dz^3} \\ \frac{d^3\theta}{dz^3} \end{Bmatrix} = \begin{Bmatrix} -P_{x_a} \\ -P_{y_a} \\ -M_{T_a} \end{Bmatrix} \qquad (6.37)$$

where

P_{x_a}, P_{y_a} = total applied loads along the X_c and Y_c directions respectively

M_{T_a} = total twisting moment about $0_c Z_c$ axis due to eccentricity of the applied loads with respect to this axis

u_c, v_c, θ = displacements in the X_c and Y_c directions and rotation about vertical axis, respectively, of the new reference axis $0_c Z_c$

From equation (6.37) it is evident that Z_c axis is the axis of rotation of the structure under pure torsion. Loading along the $0_c X_c Z_c$ and $0_c Y_c Z_c$ planes will produce deflections in the X_c and Y_c directions respectively. Thus, it can be concluded that an asymmetrical structure of the type considered may be analysed as a combination of pure bending and pure torsional actions.

6.5 Conclusions

The analysis of asymmetrical structures consisting of cantilevered and coupled walls shows that the behaviour of the structure may be described by a system of simultaneous second-order differential equations for the vertical shear distributions. The number of differential equations will generally be equal to the number of series of connecting beams although some of the coupled wall assemblies are identical. However, since the differential equations are of second-order only, the method may still be economical if the number of the coupled wall assemblies present in the structure is not large.

In the case of asymmetrical structures consisting of cantilevered walls and frames, a closed form solution may be achieved by solving a fifth-order differential equation, equation (6.25). If the lateral stiffnesses of the frames are small in comparison with those of the walls and may be neglected, the two equilibrium equations lead to two independent third-order differential equations, equation (6.31), which may be solved separately. Effectively, the structure may be analysed as subjected to pure bending and pure torsion. This is possible since it has been shown that (cf. equations (6.33)-(6.34)) the axis of rotation and the plane in which the load must act in order to produce pure bending can be determined from geometry alone.

The analyses can be readily extended to cover cases where the walls are non-planar and the frames are differently orientated. It has also been shown, for the special case of non-planar cantilevered walls structure, that the axis of rotation and the orthogonal vertical planes which the loads must act in order to produce pure bending actions may be determined from geometry of the structure. Hence, this type of structure may be analysed as a combination of pure bending and pure torsional actions. The pure bending and pure torsional actions can be analysed independently, and solution for each action may be easily obtained by solving a single third-order differential equation.

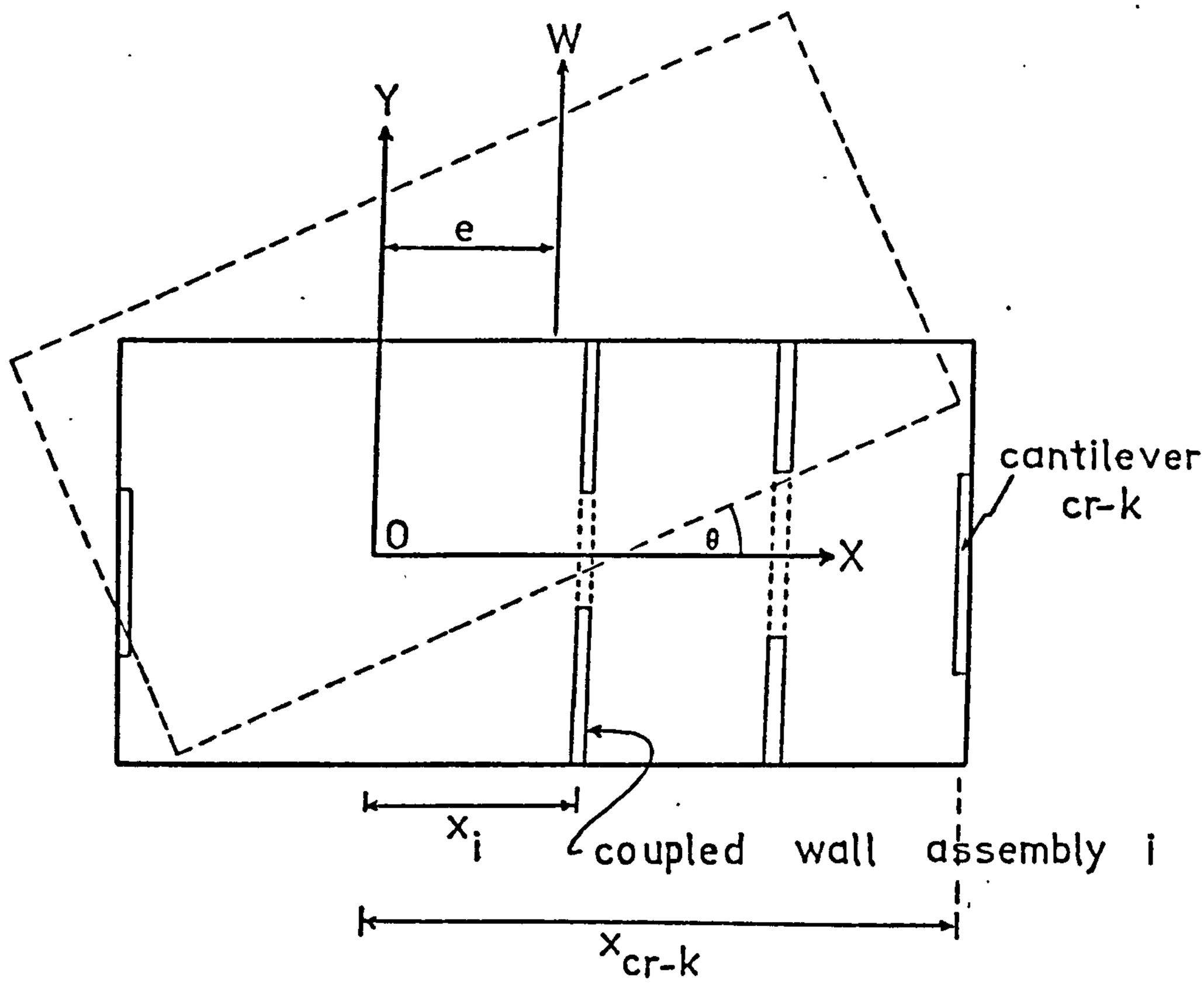

Cantilevered wall-coupled wall structure

Fig. 6.1

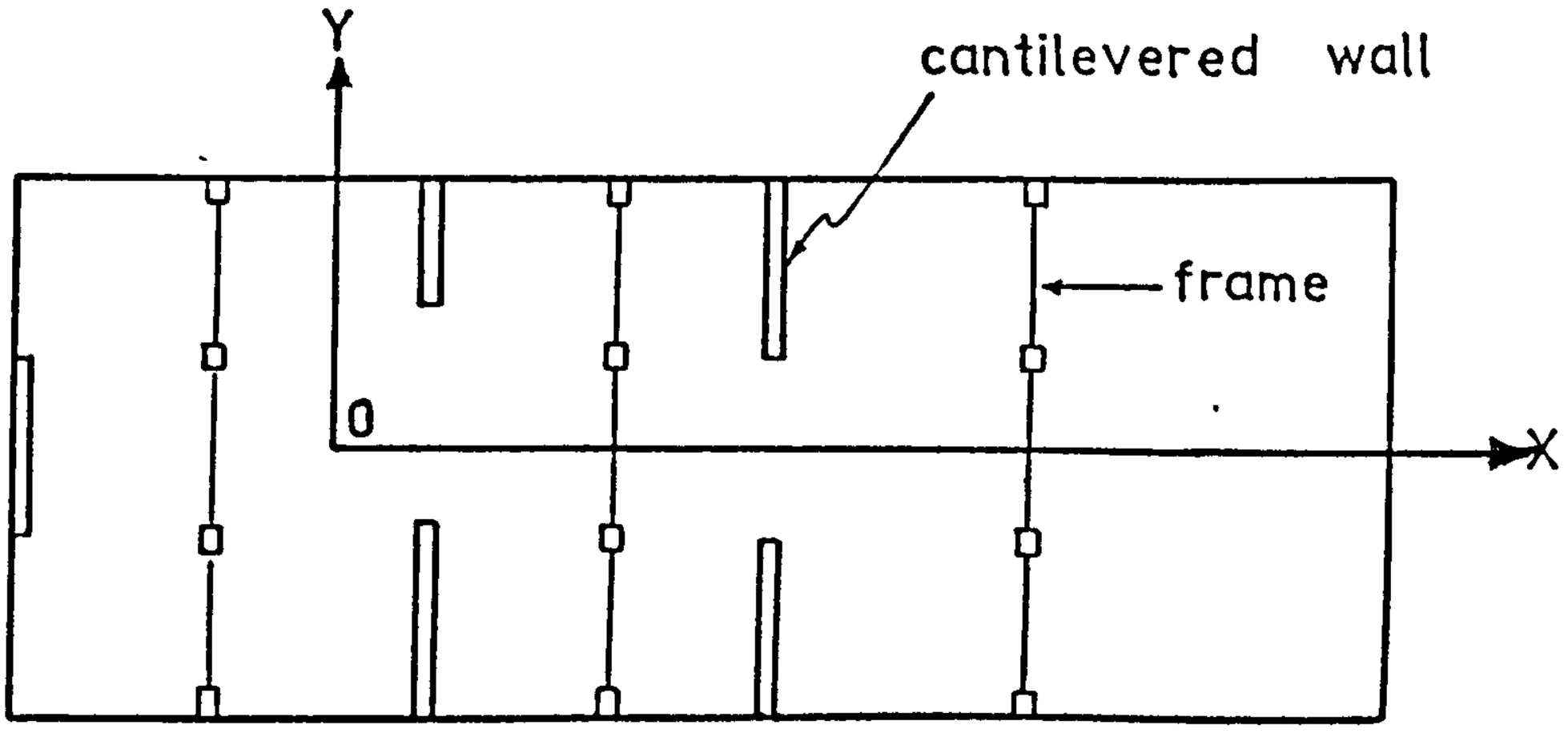

Cantilevered wall-frame structure

Fig. 6.2

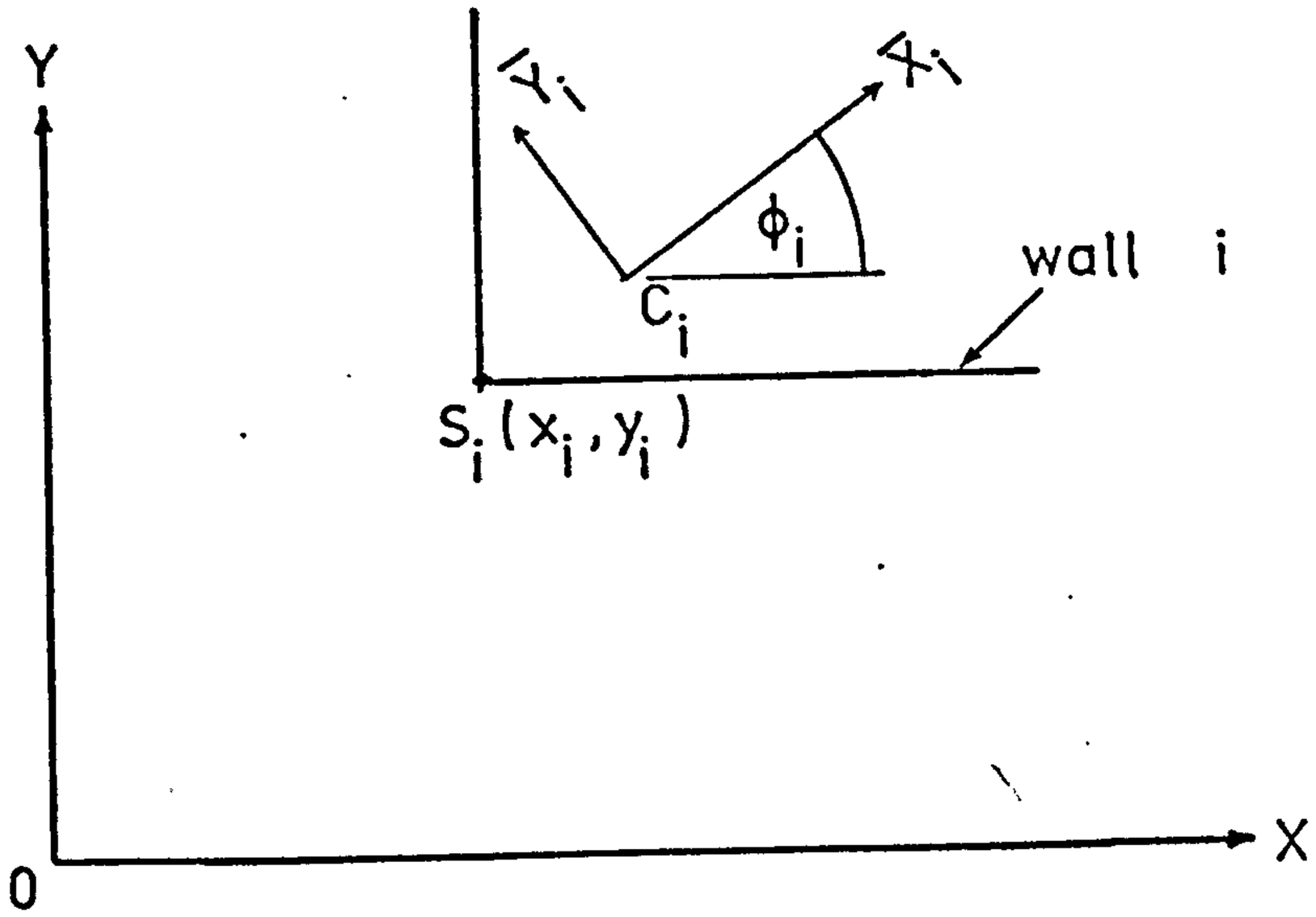

Fig. 6.3

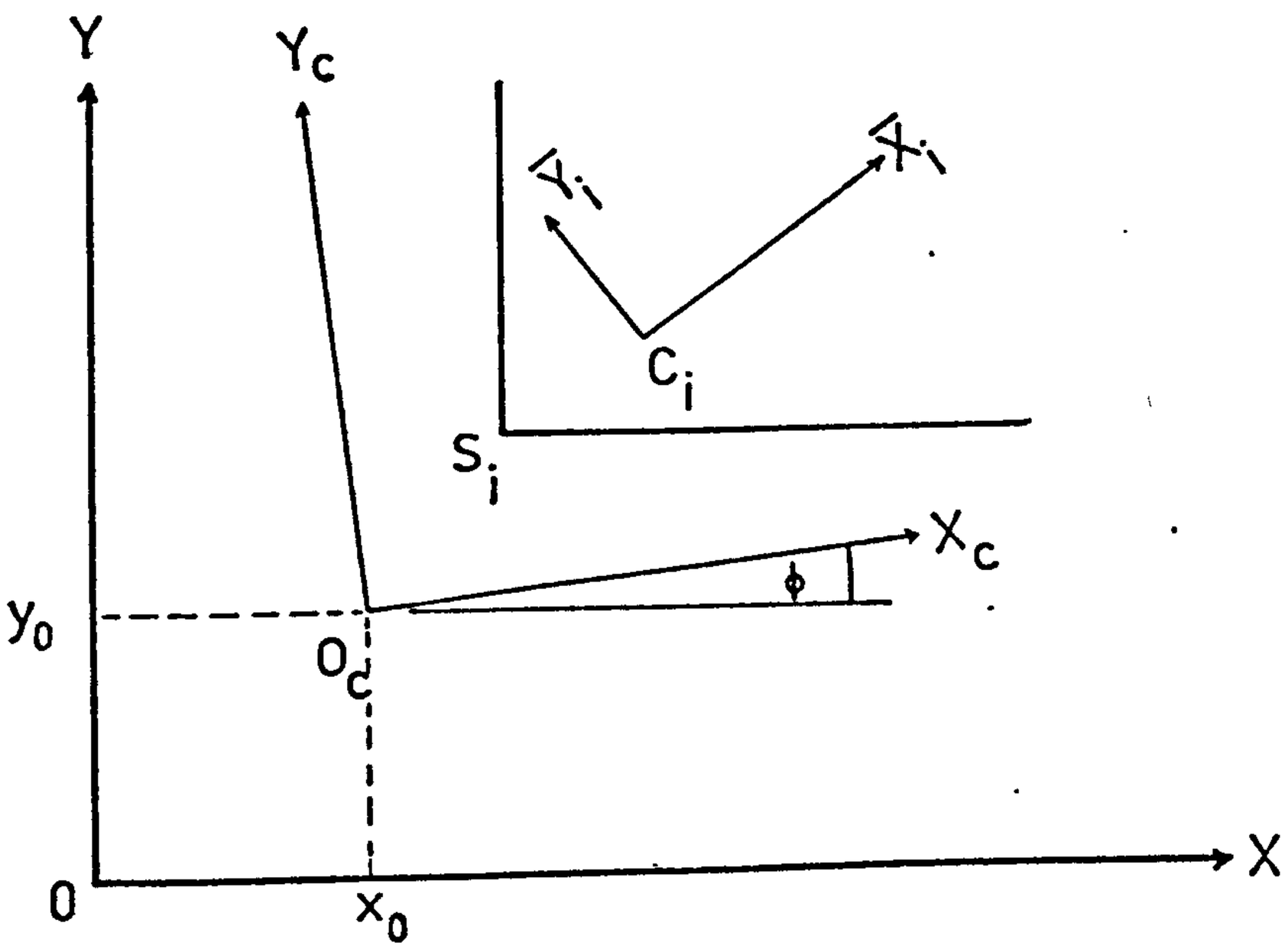

Fig. 6.4

CHAPTER 7

SPATIAL STRUCTURES COMPOSED OF THIN-WALLED ASSEMBLIES

7.1 Introduction

Throughout Chapters 4 to 6 it has been tacitly assumed that the plane cross-sections of wall assemblies before loading remain plane during loading. The St. Venant's torsion of each wall is also neglected since it is assumed that it does not contribute significantly to the overall torsional resistance of the structure. For most tall buildings the St. Venant's torsion may safely be neglected since the thicknesses of the wall assemblies are generally small in comparison with other dimensions. On the other hand, the assumption that plane cross-sections remain plane during loading may lead to a significant error in the solutions.

Generally most walls have a fairly large degree of restraint against rotation at the base level. In consequence, the wall cross-sections will warp under torsional loading, and warping or constraint torsion will be developed. Although the thicknesses of the walls may be small, the effects of warping of the cross-sections may be significant. This is particularly true regarding the stress conditions at the corners or edges of thin-walled assembly subjected to severe torsion. It is then desirable that an analysis which takes into account the effects of warping of the cross-sections of the wall assemblies should be developed.

In this Chapter an analysis of a general spatial structure composed of thin-walled assemblies is presented. Each wall is treated as a thin-walled beam of open section, and Vlasov's theory for thin-walled beams of open section[31] is taken to be valid for individual walls. In addition, in order to simplify the analysis, it will be assumed that the St. Venant's torsion may also be neglected. The method developed is particularly suitable for analysing structures with a few series of connecting beams since with only a few series of connecting beams the analysis may be carried out using only a small desk calculator.

7.2 Formulation of Problem

The plan of a general thin-walled structure containing typical elements is shown in Fig. 7.1. It will be assumed that the storey height, h, is constant and the wall cross-sections are uniform throughout the height of the structure.

7.2.1 Assumptions

The analyses are based on the following assumptions:

1. The floor slabs are rigid in their own planes so that the contour of the cross-section retains its shape.
2. Deformation of the connecting beams occurs only in the vertical plane, with points of contraflexure at the mid-span positions.
3. Out-of-plane deformations of the floor slabs can occur with negligible accompanying bending moments and vertical forces, i.e. the slabs effectively transmit

only direct in-plane forces.

4. Vlasov's theory for thin-walled beams of open section is valid for individual walls.

5. The St. Venant's torsion may be neglected. Therefore, the total torsional resistance of the structure consists of,

   (i) torsional moments developed by cross-sectional shear forces of all the walls (i.e. differential shearing action)

   (ii) warping torsional moments of all the walls.

7.2.2 Compatibility Condition

Each series of connecting beams is replaced by a corresponding series of independently acting laminae or a continuous medium of equivalent flexural rigidity. The medium is assumed 'cut' along the line of the points of contraflexure, and a self-equilibrating vertical shear distribution force system is assumed acting along the cut edges.

Consider two walls, i and j, connected by a series of connecting beams i-j as shown in Fig. 7.2(a). The walls i and j are also connected to walls k and l respectively.

The following symbols are used:-

S_i = the shear centre of wall i

C_i = the centroid of wall i

$\bar{X}_i$, $\bar{Y}_i$ = the principal axes of wall i

O_{i-j} = point of contraflexure of connecting beams i-j

X, Y, Z = structural co-ordinate axes, positive Z direction

is upwards.

The vertical displacement at the edge of the cut lamina i-j, belonging to wall i, is made up of five components of deformation, namely,

1. Axial deformation of wall i, (Δ_{ai}), due to vertical forces,
2. bending about the principal axis $\bar{X}_i$, (Δ_{xi}),
3. bending about the principal axis $\bar{Y}_i$, (Δ_{yi}),
4. warping of the cross-section, ($\Delta_{\theta i}$),
5. cantilevered bending action of the lamina due to the shear distribution of the cut edge, (Δ_{bi}).

Similar components of deformation exist at the cut edge belonging to wall j. Assuming that the vertical shear distribution along the contraflexure points 0_{i-j} is acting upwards on wall i, the relative vertical displacements of the cut edges at 0_{i-j} resulting from the corresponding five components of deformation may be shown to be, respectively (cf. Fig. 7.3),

$$(\Delta_a)_{i-j} = (\Delta_{ai}) - (\Delta_{aj})$$

$$= \frac{1}{E} \int_0^z \int_\xi^H \left[\frac{1}{A_i} (\bar{q}_{i-j} + \bar{q}_{i-k}) \right.$$

$$\left. - \frac{1}{A_j} (\bar{q}_{j-i} + \bar{q}_{j-l}) \right] d\lambda \, d\xi$$

$$(\Delta_x)_{i-j} = (\Delta_{xi}) - (\Delta_{xj})$$

$$- \bar{v}_i' \bar{y}_{i,i-j} + \bar{v}_j' \bar{y}_{j,i-j}$$

$$(\Delta_y)_{i-j} = (\Delta_{yi}) - (\Delta_{yj})$$

$$= \bar{u}_i' \bar{x}_{i,i-j} + \bar{u}_j' \bar{x}_{j,i-j}$$

$$(\Delta_\theta)_{i-j} = -(\Delta_{\theta i}) + (\Delta_{\theta j})$$

$$= +\bar{\theta}_i' w_{i,i-j} - \bar{\theta}_j' w_{j,i-j}$$

$$(\Delta_b)_{i-j} = (\Delta_{bi}) - (\Delta_{bj})$$

$$= \left(\frac{b_{i-j}^3 h}{24EI_{ci-j}}\right)(\bar{q}_{i-j} - \bar{q}_{j-i}) \qquad (7.1)$$

where

A_i = cross-sectional area of wall i

b_{i-j} = length of connecting beams i-j

H = total height of structure

λ , ξ = auxiliary height ordinates

I_{ci-j} = second moment of area of connecting beams i-j

$\bar{q}_{i-j}$ = signed vertical shear distribution acting on wall i at the cut edge of the lamina i-j, positive if acting along positive Z direction

$\bar{x}_{i,i-j}$, $\bar{y}_{i,i-j}$ = $\bar{X}_i$ and $\bar{Y}_i$ ordinates of the point 0_{i-j}

$\bar{x}_{j,i-j}$, $\bar{y}_{j,i-j}$ = $\bar{X}_j$ and $\bar{Y}_j$ ordinates of the point 0_{i-j}

$\bar{u}_i$, $\bar{v}_i$ = displacements along the $\bar{x}_i$ and $\bar{y}_i$ axes respectively, of the shear centre S_i

$\bar{\theta}_i$ = rotation about the vertical axis of the shear centre S_i

' (prime) = symbol denotes differentiation with respect

to z

$w_{i,i-j}$ = principal sectorial ordinate of the point 0_{i-j}, with respect to wall i (cf. Appendix III).

The expressions for ($\Delta_{\theta i}$), ($\Delta_{\theta j}$) are obtained from Vlasov's theory for thin walled beams of open section[31]. Equation (7.1) and subsequent derivations will be based on the right-hand system of co-ordinate axes.

For displacement compatibility at the cut edges of the lamina i-j, the relative vertical displacement at the cut edges must vanish, hence,

$$(\Delta_a)_{i-j} + (\Delta_b)_{i-j} + (\Delta_x)_{i-j} + (\Delta_y)_{i-j} + (\Delta_\theta)_{i-j} = 0 \tag{7.2}$$

From geometry, the local wall displacements $\bar{u}_i$, $\bar{v}_i$, θ_i can be expressed in terms of the structural (global) displacements by the following transformation relationships,

$$\begin{Bmatrix} \bar{u}_i \\ \bar{v}_i \\ \bar{\theta}_i \end{Bmatrix} = \begin{bmatrix} \cos \phi_i & \sin \phi_i & 0 \\ -\sin \phi_i & \cos \phi_i & 0 \\ 0 & 0 & 1 \end{bmatrix} \begin{bmatrix} 1 & 0 & -y_i \\ 0 & 1 & x_i \\ 0 & 0 & 1 \end{bmatrix} \begin{Bmatrix} u \\ v \\ \theta \end{Bmatrix} \tag{7.3}$$

where

u, v and θ = displacements along the X, Y axes, and the rotation about the vertical axis, respectively, of a point along the reference Z axis

ϕ_i = the angle the axis $\bar{x}_i$ makes with the X axis,

counter-clockwise angle is positive,

x_i, y_i = X- and Y-ordinates of the shear centre S_i.

Substituting equations (7.1) into (7.2), differentiating twice with respect to z, and then transforming the local displacements into the global displacements by means of equation (7.3) leads to,

$$R_{u_{i-j}} u''' + R_{v_{i-j}} v''' + R_{\theta_{i-j}} \theta''' + \left(\frac{hb^3_{i-j}}{24EI_{ci-j}}\right)(\bar{q}''_{i-j} - \bar{q}''_{j-i}) + \frac{1}{A_j}(\bar{q}_{j-i} + \bar{q}_{j-l}) - \frac{1}{A_i}(\bar{q}_{i-j} + \bar{q}_{i-k}) = 0 \qquad (7.4)$$

where

$$R_{u_{i-j}} = E(x_{ci} - x_{cj})$$

E = modulus of elasticity

$$R_{v_{i-j}} = E(y_{ci} - y_{cj})$$

$$R_{\theta_{i-j}} = E\left[w_{i,i-j} - w_{j,i-j} + y_i(x_{i-j} - x_{ci}) - x_i(y_{i-j} - y_{ci}) - y_j(x_{i-j} - x_{cj}) + x_j(y_{i-j} - y_{cj})\right] \qquad (7.5)$$

x_{ci}, y_{ci} = X- and Y-ordinates of the centroid C_i

x_{i-j}, y_{i-j} = X- and Y-ordinates of the point O_{i-j}

The compatibility equations for the other series of connecting beams may be similarly established.

7.2.3 Equilibrium Conditions

Let

F_{xi}, F_{yi}, f_{xi}, f_{yi} = cross-sectional shear forces of wall i in directions X, Y, $\bar{X}_i$ and $\bar{Y}_i$ respectively

T_i = torsional moment of resistance about the axis OZ, contributed by the cross-sectional shear forces of wall i

t_i = warping torsion contributed by wall i

M_t = total applied moment above any level z, about the axis OZ

P_x, P_y = components of total applied force above any level z, in the X and Y directions respectively

For the equilibrium of the structure in the X and Y directions, the following equations must be satisfied,

$$\sum_{i}^{m} F_{xi} = P_x$$

$$\sum_{i}^{m} F_{yi} = P_y \qquad (7.6)$$

and for the torsional equilibrium,

$$\sum_{i}^{m} (T_i + t_i) = M_t \qquad (7.7)$$

in which $\sum_{i}^{m}$ is the summation taken over all the walls

in the structure.

Equations (7.6) and (7.7) may be expressed as,

$$\sum_{i}^{m} (f_{xi} \cos \phi_i - f_{yi} \sin \phi_i) = P_x$$

$$\sum_{i}^{m} (f_{yi} \cos \phi_i + f_{xi} \sin \phi_i) = P_y \qquad (7.8)$$

$$\sum_{i}^{m} \left[t_i - (f_{xi} \cos \phi_i - f_{yi} \sin \phi_i) y_i + (f_{yi} \cos \phi_i + f_{xi} \sin \phi_i) x_i \right] = M_t$$

in which ϕ_i, x_i, y_i are as defined previously.

From Vlasov's theory, the cross-sectional shear forces f_{xi}, f_{yi} and the warping torsion t_i are given by (cf. Appendix III),

$$f_{xi} = \sum_{r} \bar{q}_{i-r} \bar{x}_{i,i-r} - EI_{yi} \bar{u}_i'''$$

$$f_{yi} = \sum_{r} \bar{q}_{i-r} \bar{y}_{i,i-r} - EI_{xi} \bar{v}_i'''$$

$$t_i = - \sum_{r} (\bar{q}_{i-r} \; w_{i,i-r}) - EI_{wi} \bar{\theta}_i'''$$

where

I_{xi}, I_{yi} = second moments of area of wall i about axes $\bar{X}_i$ and $\bar{Y}_i$ respectively

I_{wi} = principal sectorial moment of inertia[31] of wall i

$\sum_{r} (\bar{q}_{i-r} \bar{x}_{i,i-r})$ = sum of all $\bar{q}_{i-r} \bar{x}_{i,i-r}$ for wall i

$\sum_r (\bar{q}_{i-r}\ \bar{y}_{i,i-r})$ and $\sum_r (\bar{q}_{i-r}\ w_{i,i-r})$ are similarly defined.

From equations (7.3), (7.8) and (7.9), the equilibrium conditions for the structure may be expressed as,

$$\begin{bmatrix} C_{11} & C_{12} & C_{13} \\ C_{21} & C_{22} & C_{23} \\ C_{31} & C_{32} & C_{33} \end{bmatrix} \begin{Bmatrix} u''' \\ v''' \\ \theta''' \end{Bmatrix} = \begin{Bmatrix} Q_1 \\ Q_2 \\ Q_3 \end{Bmatrix} \qquad (7.10)$$

or simply,

$$\left[\ C\ \right]\left\{d'''\right\} = \left\{Q\right\} \qquad (7.11)$$

in which,

$$C_{11} = E \sum_i^m (I_{yi} \cos^2\phi_i + I_{xi} \sin^2\phi_i)$$

$$C_{22} = E \sum_i^m (I_{yi} \sin^2\phi_i + I_{xi} \cos^2\phi_i)$$

$$C_{33} = E \sum_i^m \left[I_{\omega i} + I_{yi} (y_i \cos\phi_i - x_i \sin\phi_i)^2 + I_{xi} (y_i \sin\phi_i + x_i \cos\phi_i)^2\right]$$

$$C_{12} = - E \sum_i^m \cos\phi_i \sin\phi_i (I_{xi} - I_{yi})$$

$$= C_{21}$$

$$C_{13} = - E \sum_i^m \left[I_{yi} \cos\phi_i (y_i \cos\phi_i - x_i \sin\phi_i) + I_{xi} \sin\phi_i (y_i \sin\phi_i + x_i \cos\phi_i)\right]$$

$$= C_{31}$$

$$C_{23} = - E \sum_{i}^{m} \Big[I_{yi} \sin \phi_i \, (y_i \cos \phi_i - x_i \sin \phi_i)$$

$$- I_{xi} \cos \phi_i \, (y_i \sin \phi_i + x_i \cos \phi_i) \Big]$$

$$= C_{32}$$

$$Q_3 = \sum_{i}^{m} \sum_{r} \bar{q}_{i-r} \, (x_i L_{i,i-r} - y_i K_{i,i-r} - \omega_{i,i-r})$$

$$- M_t$$

$$L_{i,i-r} = \bar{x}_{i,i-r} \sin \phi_i + \bar{y}_{i,i-r} \cos \phi_i$$

$$K_{i,i-r} = \bar{x}_{i,i-r} \cos \phi_i - \bar{y}_{i,i-r} \sin \phi_i$$

$$Q_2 = \sum_{i}^{m} (\sum_{r} \bar{q}_{i-r} \, L_{i,i-r}) - P_y$$

$$Q_1 = \sum_{i}^{m} (\sum_{r} \bar{q}_{i-r} \, K_{i,i-r}) - P_x$$

(7.12)

7.2.4 Governing Differential Equations

From equation (7.11), the third derivatives of the displacements become,

$$\{d'''\} = [F] \{Q\} \qquad (7.13)$$

in which $[F]$ is the inverse matrix of $[C]$.

Consequently, equation (7.4) may be written as,

$$\{Q\}^T [F]^T \{R_{i-j}\} + \left(\frac{hb_{i-j}^3}{12I_{ci-j}}\right) \bar{q}''_{i-j} - \left(\frac{1}{A_i} + \frac{1}{A_j}\right) \bar{q}_{i-j}$$

$$+ \frac{1}{A_j} \bar{q}_{j-1} - \frac{1}{A_i} \bar{q}_{i-k} = 0 \qquad (7.14)$$

in which $\{Q\}^T$ and $[F]^T$ are the transposed matrices of $\{Q\}$ and $[F]$, and,

$$\left\{ \begin{bmatrix} R \\ \end{bmatrix}_{i-j} \right\} = \left\{ \begin{bmatrix} R_{u_{i-j}} \\ R_{v_{i-j}} \\ R_{\theta_{i-j}} \end{bmatrix} \right\} \qquad (7.15)$$

For a structure with n series of connecting beams, there will be n differential equations of the form given by equation (7.14). These equations form a system of governing differential equations for the structure. The system of differential equations may be expressed in matrix form as,

$$[\beta]\{\bar{q}''\} + [\alpha]\{\bar{q}\} = \{R\} \qquad (7.16)$$

where

$\{q\}$ = column matrix of vertical shear distributions (n elements)

$\{\bar{q}''\} = \frac{d^2}{dz^2} \bar{q}$

$\{R\}$ = column matrix (n elements)

$[\beta], [\alpha]$ = square matrices (n x n elements)

The elements of matrices $[\beta]$, $[\alpha]$ and $\{R\}$ may be determined using the differential equation (7.14).

7.2.5 Boundary Conditions

For a structure on a rigid foundation and free at the top, the following boundary conditions apply:-

At the base, $z = 0$,

$$\bar{u}_i,\ \bar{u}_i',\ u,\ u' \quad = 0$$

$$\bar{v}_i,\ \bar{v}_i',\ v,\ v' \quad = 0 \qquad (7.17)$$

$$\bar{\theta}_i,\ \bar{\theta}_i',\ \theta,\ \theta' \quad = 0$$

at the top, $z = H$,

$$\bar{u}_i'',\ u'' \quad = \quad 0$$

$$\bar{v}_i'',\ v'' \quad = \quad 0 \qquad (7.18)$$

$$\bar{\theta}_i'',\ \theta'' \quad = \quad 0$$

From equations (7.1), (7.2), (7.17) and (7.18), the boundary conditions for the system of governing differential equations are given by, in terms of the shear distributions,

$$\text{at } z = 0, \qquad \bar{q}_{i-j} = 0 \ , \quad \text{all } i\text{-}j$$

$$\text{at } z = H, \qquad \bar{q}_{i-j}' = 0 \ , \quad \text{all } i\text{-}j \qquad (7.19)$$

7.2.6 Solutions

From equations (7.16) and (7.19) the solutions for the vertical shear distributions may be obtained by using any standard method of solving a system of simultaneous differential equations with constant coefficients. The displacements u, v, θ are then determined by directly

integrating equation (7.13), using the boundary conditions given by equations (7.17) and (7.18). The local wall displacements $\bar{u}_i$, $\bar{v}_i$, $\bar{\theta}_i$ follow from the transformation relationships, equation (7.3).

The longitudinal stress, σ_p, at any point in the cross-section of wall i is given by (cf. Appendix III),

$$\sigma_p = \frac{1}{A_i} \int_z^H (\sum_r \bar{q}_{i-r})d\lambda - E(\bar{u}_i''\bar{x}_p + \bar{v}_i''\bar{y}_p - \bar{\theta}_i''\omega_p) \quad (7.20)$$

where

$\bar{x}_p$, $\bar{y}_p$ = $\bar{X}_i$- and $\bar{Y}_i$- ordinates, respectively, of the point considered

ω_p = principal sectorial ordinate of that point

7.3 Experimental Investigation

In order to substantiate the validity of the assumptions made in the analysis and to enable the accuracy of the method of analysis to be assessed, the experimental investigation described in the present section was undertaken.

7.3.1 Model Shear Wall Structure

From the various model material available such as araldite, perspex, aluminium etc., perspex acrylic was chosen as an appropriate material for model construction owing to its ease of machining, fabricating, and availability in a wide range of sizes and thicknesses, and relative cost. As relatively complex model was

needed, considerable wastage of construction material was difficult to avoid in fabricating the model. In consequence, the cost of the construction material became one of the important factors in dictating the choice of the material adopted. Perspex has the mechanical property advantages of having a reasonably linear stress-strain relationship and a low value of the modulus of elasticity which allows for reasonably large deflections and strains under loads. Its less desirable properties are sensitivity to humidity and temperature changes and tendency to creep under load, whilst the thickness variation is greater than one would normally desire.

Construction of Model

It was decided to build and test a 14-storey high model consisting of 3 non-planar walls interconnected by two series of connecting beams. The storey height adopted was 50 mm. Fig. 7.4 shows the plan view of the wall assembly.

Perspex sheets of two standard thicknesses were chosen for the construction of the model. The nominal thicknesses of the coupled wall assembly and the floor slabs were $\frac{1}{8}$ inch and $^1/16$ inch respectively. The coupled wall assembly was assembled from 9 components of plane perspex sheet. All components were made with an extra length of material at the base for fixing into slots in the base plate which was a 20" x 18" plate of 1 inch thick perspex. The connecting beams and wall openings were made by cutting away the perspex to form

rectangular openings. These openings were made with small radius fillets at all corners to reduce stress concentration at the connecting beam-wall junctions. Fig. 7.5 shows the configuration for openings and connecting beams.

The slots in the floor slabs required to accommodate the wall assembly were cut slightly oversize for ease in sliding the floor slabs along the height of the walls during assembly. The out-of-plane rigidity of the floor slabs were minimised by using thin perspex, $^1/16$ inch thick perspex sheets, and by cutting out material from the slabs in several areas to form openings and prevent coupling of the walls. The continuity and general in-plane rigidity of the floor slabs, needed for transmitting direct in-plane forces and for retaining the overall contour of the assembly, were ensured by providing at least 20 mm minimum width of material around the assembly. Small holes of 3 mm diameter were drilled in the floor slabs for the purpose of hanging weights. The slab configuration is shown in Fig. 7.6.

The wall components were first assembled, then fitted into the slots in the base plate and cemented. The floor slabs were slid down along the wall assembly, kept in positions and then cemented to the assembly. Tensol No. 7 cement was used throughout for the assembly of the model. The complete model fixed to the test frame is shown in Fig. 7.9.

Strain Gauges

Electrical resistance strain gauges, Japanese type PL 10, were used for measuring the strains induced in the model when tested. The gauges were attached to the wall assembly at a height of 125 mm above the base, midway between the second and the third floor slabs. This position which was in the region of relatively high stresses was selected in order that the strain readings would be reasonable. It was also far enough above the base not to be affected by any local effects caused by the base-to-wall connection. At the mid-floor position the localized effects of slab-wall and connecting beam-wall interactions would also be minimum.

The positions of the strain gauges along the contour of the wall assembly is shown in Fig. 7.7. All gauges were placed parallel to the longitudinal direction of the assembly, to give the measured strain along the longitudinal direction. The gauges and terminal strips for the wire leads were glued to the perspex by Eastman 710 adhesive, and varnished over for insulation and protection.

7.3.2 Test Frame

The frame on which the model was mounted during the tests is shown in Fig. 7.10. It consisted of a pair of vertical mounting units 1 metre apart, connected by horizontal and inclined bracing members to form a stiff self-supporting box frame. The end of the frame which it was intended to use to support the base plate of the

model was further stiffened by bracing an additional mounting unit to it at a short distance apart.

Each mounting unit consisted of two vertical legs of 3" x 1.5" steel channels welded to 6" x 6" base plates, and set at 0.75 metre apart by welding to two 0.5 inch thick by 6 inch wide steel plates. The steel plates were provided with a regular array of holes for use in fixing models to the frame, and were set near the upper ends of the supporting legs to provide adequate clearance below the model to hang weights. The bracing consisted of cut lengths of 2" x 1" rectangular hollow sections with welded end plates which were tapped for bolting to the mounting units.

To strengthen the mounting units used to support the base plate of the model, 0.5" diameter screwed rods and several short lengths of hollow sections were used to bolt and brace the horizontal steel plates of the two adjacent mounting units to make them act together more effectively as a unit (cf. Fig. 7.10). Three 0.5" steel plates were placed vertically across the horizontal steel plates of the mounting unit; the base of the model was then placed in direct contact with these vertical steel plates. To minimise movements of the perspex base during the tests, two strips of 0.5" steel plates and two hollow sections were placed vertically and horizontally, respectively, across the base. (Fig. 7.11). The hollow sections, the steel plates and the base of the model were firmly attached to the mounting units by 0.5"

diameter screwed rods to form a stiff foundation for the wall assembly.

7.3.3 Test Procedure

The model was set up in the test frame such that wall 2 was nearest to the ground and the plane of symmetry of the model lay in a vertical plane. Fig. 7.12 illustrated the model orientation as used in the tests. The lateral loading was simulated by applying loads at each floor level in the form of 0.5 kg. weights on light alloy hangers suspended by "Terylene" cord connected to the floor slabs through the 3 mm dimeter holes. In each test the plane of the loads was a vertical plane parallel to the plane of symmetry of the model. Loads were applied with great care to avoid any impact effect on the structure. The loads were applied in increments of 0.5 kgf per load point to a maximum of 2 kgf per load point. A standard time of 10 minutes was allowed to elapse after each load increment before gauge readings were taken, to permit the gauges to settle to reasonably stable values. The sequences of the gauge readings for every load increment were kept the same. In order to minimise errors due to creep in the perspex, the model was unloaded by increments and gauge readings were again taken. The mean of the results obtained from the loading and unloading of the model was used in the comparison of the experimental and analytical results.

Three tests were carried out using the same model orientation. The three tests undertaken were as follows

(cf. Fig. 7.6).

Test number 1 : Applied loads lay in the plane of symmetry of the model.

Test number 2 : The plane of the applied loads bisected the web of wall 3 (80 mm eccentricity).

Test number 3 : The plane of the applied loads passed through the outer corners of wall 3 (120 mm eccentricity).

7.3.4 Measurements of Strains and Deflections

Strains

A Baldwin-Lima-Hamilton strain indicator was used in measuring the strains induced in the model by the applied loads. The equipment gave strain readings directly in units of microstrains. To minimise any effect on the readings due to temperature and humidity changes in the laboratory during tests, and local heating caused by the current passing through the gauge during the actual measurement of strain, compensating "dummy" gauges were incorporated in the circuit.

Deflections

Arrangements were made to measure the deflections at various points on the model using "John Bull" dial gauges, type 2U, with a maximum travel of 12.7 mm and a sensitivity of 0.002 mm. The deflections, in the direction of the applied loads, of the model were measured by gauges supported on a light "Dexion" frame-

work attached to the test frame. Two parallel sets of dial gauges were positioned above the assembly, near the outer corners of walls 1 and 3. Each set consisted of 7 dial gauges for measuring the deflections at alternate mid-storey levels. The positions of the 14 points (D1 to D14) along the walls at which their deflections in the direction of the applied load were measured are shown in Fig. 7.8. It was attempted to detect any rotation of the base plate about a horizontal axis parallel to the plane of the base by using two dial gauges to measure the displacements normal to the base. The two gauges were set 100 mm apart along a vertical line, and held in positions by magnetic stands attached to the steel backing plates. One additional gauge was used to try to detect any vertical movement of the base plate.

7.3.5 Determinations of the Modulus of Elasticity and Poisson's Ratio of Perspex

In order to compare analytical results with experimental results it was necessary to evaluate the elastic properties of the model material. The modulus of elasticity and Poisson's ratio were determined from specimens cut out from the same sheet of perspex used to make the wall assembly. Two beam specimens, nominally 2 inches wide by 12 inches long were used. Standard beam testing procedures using equal loading at the third points of the span, were followed. Each specimen was tested twice and the mean values of the modulus of

elasticity and Poisson's ratio were adopted. The modulus of elasticity and Poisson's ratio were found to be 310 kgf/mm^2 and 0.36 respectively.

7.3.6 Experimental Results

The measured longitudinal strains in the walls for the three tests are given in Table 7.1. The deflections in the direction of the applied load are given in table 7.2. The values of the deflections tabulated in Table 2 have already been adjusted to allow for the base movements detected in the tests. The rotations of the model as calculated from the relevant experimental deflections are tabulated in Table 7.3.

In order to be able to compare the experimental and analytical deflections in the direction normal to the plane of symmetry of the model, an additional set of dial gauges was used in test No. 3 to measure horizontal. deflections of the model. The positions of the dial gauges, D15 to D21, are shown in Fig. 7.8. The experimental results for the deflections normal to the plane of symmetry are given in Table 7.4.

7.4 Analytical Results

Theoretical analyses of the model were carried out, using the equations derived in Sections 7.2.1 to 7.2.6 and the elastic properties of the perspex given in Section 7.3.5. In the analyses each loading system was taken to be equivalent to a combination of a uniformly distributed load and a concentrated load at the top. The

top concentrated load was taken to be one half of the load actually applied at the top of the model, and the uniformly distributed load equivalent to the total applied load distributed uniformly across the whole length (height) of the model. To simply assume that the loading system could be treated as equivalent to the total applied load distributed uniformly across the length of the model would be less logical. The applied load at the top of the model could not realistically be considered as arising from a load distributed over one half of the 14th storey and one half of an imaginary 15th storey. The combination of loads mentioned earlier was then adopted since it was thought to be a more realistic representation of the actual loading of the model.

The positions of the shear centres and the centroids of the walls and the structural co-ordinate system are shown in Fig. 7.13. The shear centre axis of wall 2 is taken to be the reference vertical axis OZ. In all the tests the components of the applied loads along the X axis were zero because the loads were applied normal to the X axis.

7.4.1 Solutions of Differential Equations

From equation (7.14), the governing differential equations for the model may be written as,

$$\left(\frac{b^3 h}{12 I_c}\right) q''_{2-1} - \left(\frac{1}{A_1} + \frac{1}{A_2}\right) q_{2-1} - \frac{1}{A_2} q_{2-3}$$

$$= - \left(R_{u_{2-1}} u''' + R_{v_{2-1}} v''' + R_{\theta_{2-1}} \theta'''\right)$$

$$\left(\frac{b^3 h}{12 I_c}\right) q''_{2-3} - \left(\frac{1}{A_2} + \frac{1}{A_3}\right) q_{2-3} - \frac{1}{A_2} q_{2-1}$$

$$= - \left(R_{u_{2-3}} u''' + R_{v_{2-3}} v''' + R_{\theta_{2-3}} \theta'''\right) \qquad (7.21)$$

in which q_{2-1} and q_{2-3} are assumed acting upwards on wall 2.

From geometry and structural properties of the model, and relevant expressions derived previously, equation (7.21) becomes,

$$q''_{2-1} - B_1 q_{2-1} - B_2 q_{2-3} = J_1 P_y + J_2 M_t$$

$$q''_{2-3} - B_1 q_{2-3} - B_2 q_{2-1} = J_3 P_y + J_4 M_t \qquad (7.22)$$

where

$$B_1 = 1.17287 \times 10^{-5} \quad mm^{-2}$$

$$B_2 = 5.52039 \times 10^{-6} \quad mm^{-2}$$

$$J_1 = J_3 = -6.47724 \times 10^{-8} \quad mm^{-3}$$

$$J_2 = -J_4 = 1.31875 \times 10^{-10} \quad mm^{-3}$$

Closed form solutions for the vertical shear distributions q_{2-1} and q_{2-3} may be obtained. It may be shown that the solutions are given by,

$$q_{2-1} = w \left[K_1 \phi_w(\gamma_1) + K_2 \phi_w(\gamma_2) + K_3 \left(1 - \frac{z}{H}\right)\right]$$

$$+ \frac{P}{H} \left[K_1 \phi_p(\gamma_1) + K_2 \phi_p(\gamma_2) + K_3\right]$$

$$q_{2-3} = w \left[K_1 \phi_w (\gamma_1) - K_2 \phi_w (\gamma_2) + K_4 (1 - \frac{z}{H}) \right]$$

$$+ \frac{P}{H} \left[K_1 \phi_p (\gamma_1) - K_2 \phi_p (\gamma_2) + K_4 \right] \qquad (7.23)$$

where

w = uniformly distributed applied load per unit height

P = top concentrated load

H = total height of the model (700 mm)

$$\gamma_1 = H \sqrt{B_1 + B_2}$$

$$\gamma_2 = H \sqrt{B_1 - B_2}$$

$$\phi_w(\gamma) = \frac{\cosh \gamma(1 - \eta)}{\cosh \gamma} - \frac{\sinh \gamma \eta}{\gamma \cosh \gamma}$$

$$\phi_p(\gamma) = \frac{\cosh \gamma(1 - \eta)}{\cosh \gamma}$$

$$\eta = z/H$$

$$K_1 = \frac{H(R_1 + R_2)}{2(B_1 + B_2)}$$

$$R_1 = - J_1 + J_2 e$$

$$R_2 = - J_3 + J_4 e$$

e = eccentricity of the applied loads; equal to 0.0 mm, - 80.0 mm and -120 mm for the test Nos. 1, 2 and 3 respectively.

$$K_2 = \frac{H(R_1 - R_2)}{2(B_1 - B_2)}$$

$$K_3 = \frac{H(R_2B_2 - R_1B_1)}{(B_1^2 - B_2^2)}$$

$$K_4 = \frac{H(R_1B_2 - R_2B_1)}{(B_1^2 - B_2^2)}$$

The displacement functions u, v, θ are then determined by integrating equation (7.13). From the geometrical relationships, equation (7.3), the displacements of any point in the model may be evaluated. The analytical displacements are compared with those obtained experimentally and are shown graphically in Figs. 7.14-7.19.

The longitudinal stresses in the walls are determined from equation (7.20) and the results are compared with those obtained from the tests, Figs. 7.20-7.22.

To investigate the effects of neglecting warping deformation of the cross-sections of the walls, the model is again analysed by assuming that plane cross-sections of the walls remain plane during loading, i.e. using ordinary beam theory. The results are shown by superimposing the analytical curves onto Figs. 7.14-7.22, so that direct comparisons can be made between the experimental results and the results obtained by using the ordinary beam theory and the thin-walled beam theory.

7.5 Comparison and Discussion of Results

In the comparison of results, the limitation imposed by the degree of accuracy attainable experimentally and any deviation of the real structure from the idealised

mathematical model must be recognised. For any practical experimental investigation it is inevitable that a number of sources of errors are present. Some errors may be minimised with little extra care whereas others are not determinable. Some of the possible sources of errors will be indicated.

The electrical resistance strain gauges and the strain indicator equipment are items of precision scientific equipment, therefore, the inherent inaccuracy in strain readings would be very small. Effects of changes in humidity, temperature were taken into account by using compensating gauges. One possible source of error which might have influenced the results of the strains obtained could be the local stiffening of the perspex due to the strain gauges and their adhesive. This would result in strain readings which were lower than the actual values. Strain readings of gauges near the corners of the model could also be affected by localized stress concentrations.

In the experimental studies where full fixity at the base of the structure was required, it was usually found that this requirement could rarely be met. The flexibility of the base was a source of errors encountered in most of the experiments. In this study considerable effort had been made to stiffen the test frame, but it was found that base movements were still detectable. Although the model deflections were adjusted to compensate for the movements of the base, it was anticipated that undetected residual frame deformations arising from the

flexibility of the frame existed, and this would contribute to errors in the measured deflections. Deformations local to the foot of the wall assembly and within the depth of the perspex base could also occur. It was difficult, to the point of being impractical, to measure accurately these deformations. The tendency would be, therefore, to produce results for the deflection and rotation of the model rather larger than would be the case if the base of the wall assembly was truly rigid. As noted earlier, one of the undesirable properties of the perspex is its tendency to creep under sustained loading, therefore, creep effects would also contribute to errors in the measured deflections. Furthermore, as several components were made and then assembled to form the complete structure, the inaccuracy in fabrication, misalignment and non-uniform joint rigidity could well be potential sources of errors.

The estimation of the inaccuracy due to any particular source of error was extremely difficult to determine. However, the combined strain inaccuracy due to experimental deficiencies could be estimated using static checks. As test number 1 produced only pure bending of the assembly, any variation of stresses or strains across the thickness of the walls would be small. Therefore, with little loss in accuracy, the strains measured along the outer surface of the walls could be considered as representative of strain distributions in the walls. The static checks results, per load increment, of test number 1 are as follows:-

Forces

tensile force in the model = 10090 gmf

compressive force in the model = 8530 gmf

unbalanced force = 1560 gmf

error as percentage of combined forces = 8.4 %

Moments

moment due to the applied loads = 1,800,000 gmf-mm

moments calculated from the stress distributions:-

(i) moment about an axis along the webs of walls 1 and 3,

moment = 1,726,000 gmf-mm

error = 4.1 %

(ii) moment about an axis along the web of wall 2,

moment = 1,960,000 gmf-mm

error = 8.9 %

Average error for moment = $\frac{1}{2}(4.1 + 8.9) = 6.5\%$

The static checks results show that the errors for forces and moments are less than 10%. Hence, the accuracy of the experimentally determined strains may be estimated to be within 10% of the actual values. However, this estimation does not truly reflect the degree of accuracy attainable regarding the deflections of the model. Since some sources of errors only marginally affect the static checks but can produce large errors in the measured deflections. For instance, a rigid body rotation of the base has insignificant effects on the static check

results but will produce large errors for the measured deflection at the top of the model.

Deflections

Comparisons between the experimental and analytical results for the deflections in the direction of the applied loads are shown graphically in Figs. 7.14-7.16. The measured deflections of almost all the points are greater than the analytical deflections. At the top of the model the maximum deflections obtained analytically was approximately 80 per cent of the experimental values. As noted earlier, flexibility of the base and creep effects were expected to be the sources of discrepancy in the results. Creep tends to increase the deflections and has a cumulative effect on points further away from the base. The effect of rotational flexibility of the base on the deflections also amplifies towards the top. Both sources of errors have a tendency to produce increasingly larger deflection towards the top, which was verified by Figs.7.14-7.16.

The differences between the analytical deflections obtained by using the ordinary beam theory and the thin-walled beam theory are not great; and for the test number 1 the solutions are identical since the structure underwent only pure bending.

Comparison for the deflections normal to the plane of symmetry is shown in Fig. 7.17. The experimental results agree reasonably well with the analytical results.

Rotations

Comparisons of rotations for test numbers 2 and 3, Figs. 7.18 - 7.19, show that analytical results are again smaller than the experimental results. The discrepancies are of similar magnitudes to those of the deflections. The rotation at the top calculated from the thin-walled beam theory was approximately 82 per cent of the experimental results. The ordinary beam theory predicted slightly smaller rotation; approximately 77 per cent of the experimental value.

Strains

Comparisons of strains are shown graphically in Figs. 7.20-7.22. The strains in the walls obtained experimentally show a general pattern of distribution which bears a close relationship to the distribution predicted by the thin-walled beam theory. With the exception of strains in the straight flange of wall 2 and at a few positions near the corner points, the experimental results and analytical results obtained from the thin-walled beam theory agreed reasonably well. The analytical results predicted by the ordinary beam theory, however, were not in good agreement with the experimental results. The discrepancies between the experimental results and the ordinary beam solutions for points near the corners or edges were generally very marked. The agreement was extremely poor at the edges of the return webs of walls 1 and 2, for tests number 2 and 3. It is to be noted that the strain distributions for test

number 1 predicted by both theories were identical since the applied load did not produce torsion of the model.

Relatively large discrepancies between experimental and analytical (thin-walled beam theory) strains in the straight flange of wall 3 for tests number 2 and 3 were not expected because reasonably good agreement was obtained for the rest of the walls. The possibility of the gauges being damaged during assembly was remote since the readings were consistant throughout the tests. Connecting beam-wall interaction was also unlikely to produce errors which were confined to the flange of wall 3 without significantly affecting the connected flange of wall 2. Accepting that the discrepancies could not reasonably be explained in the context of theoretical deficiency, the differences in the results were most likely to be the effects of fabrication or assembly errors. Careful measurements showed that there were slight errors in the model dimensions. The distances between the inner corners of walls 1 and 3 measured at the base and the top of the model were found to be 81 mm and 79 mm respectively instead of a constant distance of 80 mm throughout the height of the assembly. This indicated that there was a slight distortion of the straight flange of wall 2, which might account for the discrepancies localized to the flange of the wall.

7.6 Conclusion

The experimental investigation shows that the continuous medium approach can be successfully used to

analyse non-planar thin-walled coupled wall structure provided that thin-walled beam theory is used instead of ordinary beam theory. The ordinary beam theory, although giving deflections and rotations which are only slightly less than those predicted by the thin-walled beam theory, gives a prediction of strains which is greatly different from those obtained experimentally, particularly in the vicinity of most corners and edges of the walls.

Experimental results obtained were based on a model which had been designed to conform to the assumptions made in the analysis. Therefore, it must be recognized that, strictly, the conclusions drawn are valid for the idealized structure. Idealization of real structures involves a certain degree of approximation, and this will reduce the accuracy of the solutions.

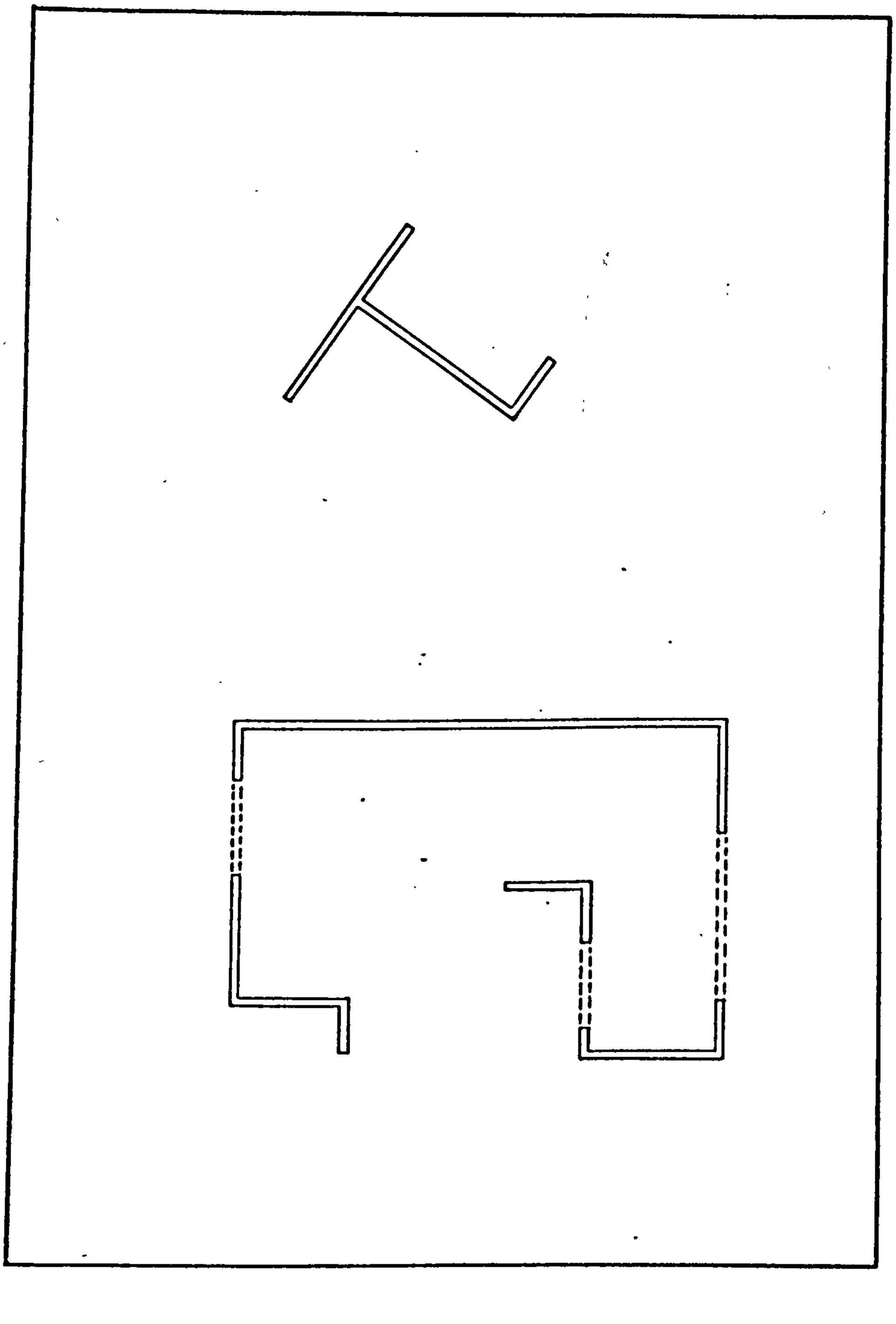

Plan of general coupled wall structure

Fig. 7.1

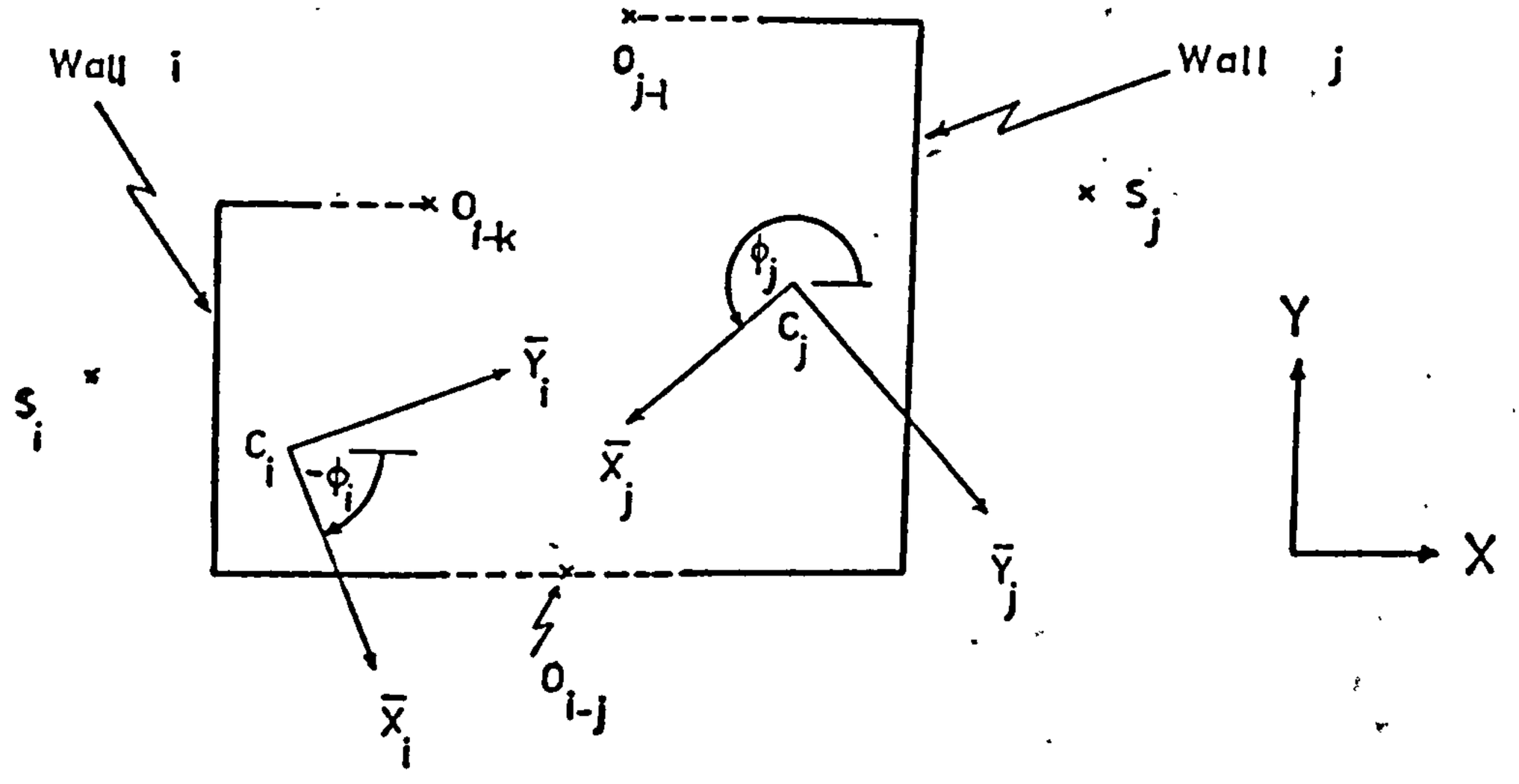

(a) Plan of walls i and j

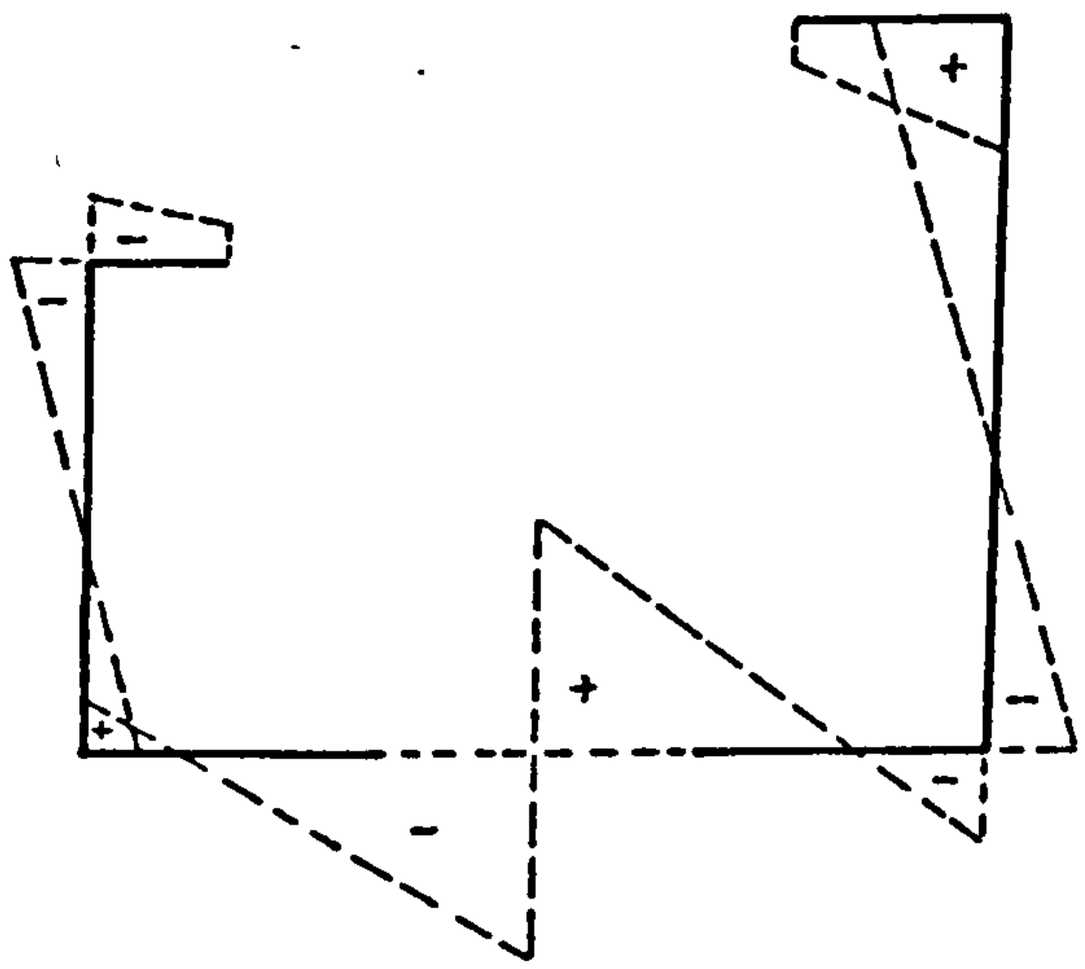

(b) Sectorial co-ordinate diagram

Coupled walls i and j

Fig. 7.2

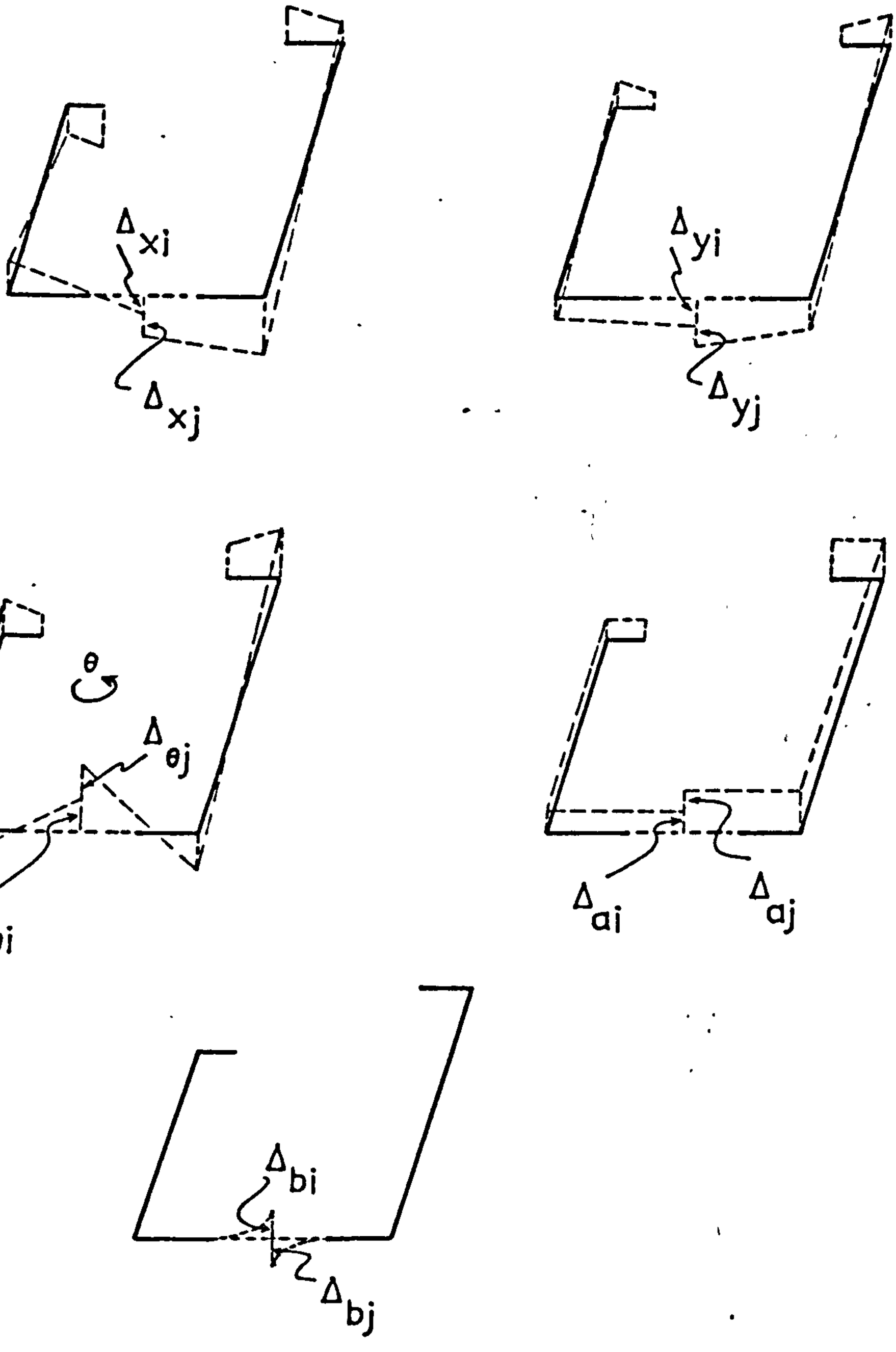

Components of vertical displacement at point of contraflexure

Fig. 7.3

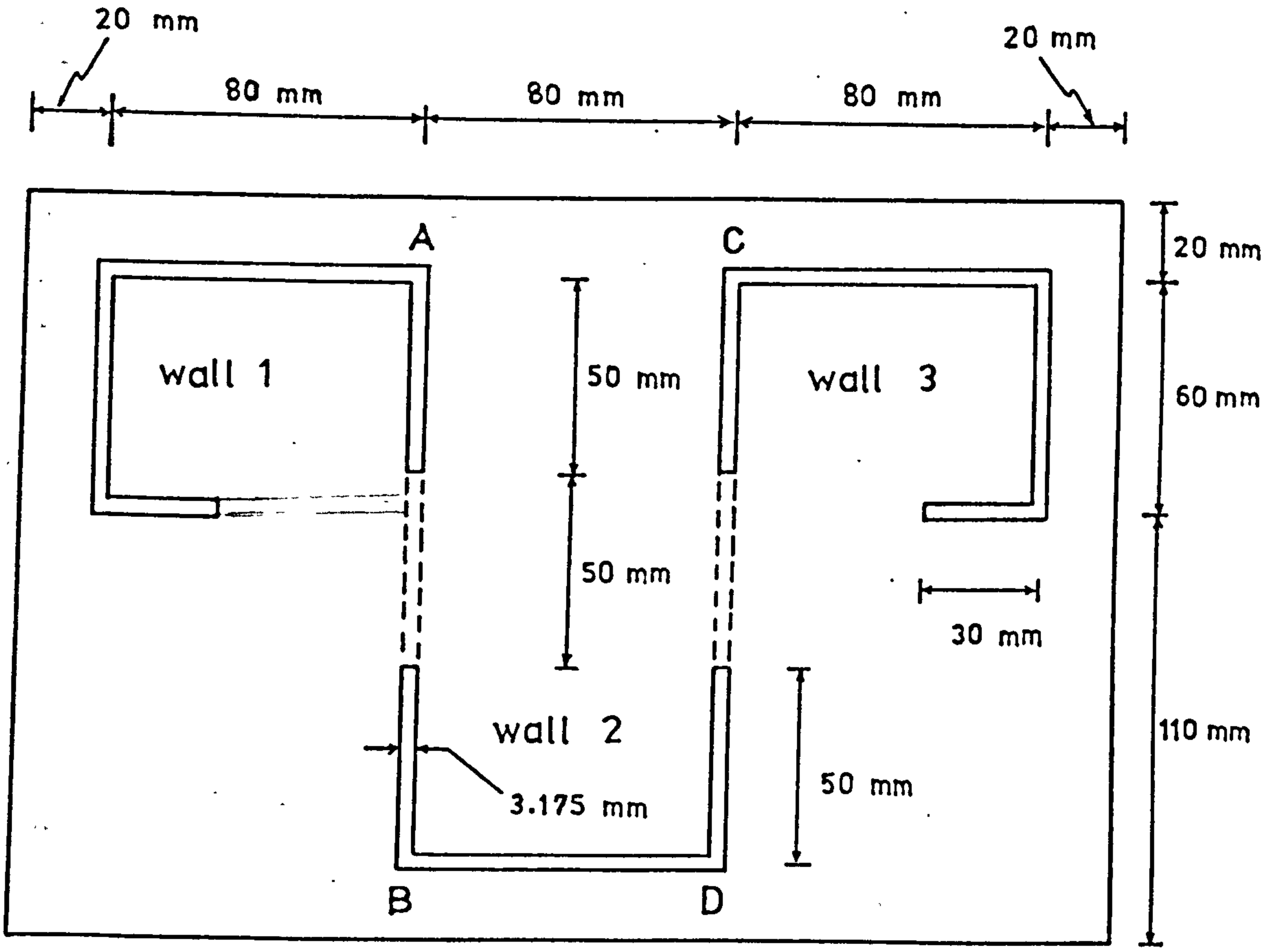

Plan of model structure

Fig. 7.4

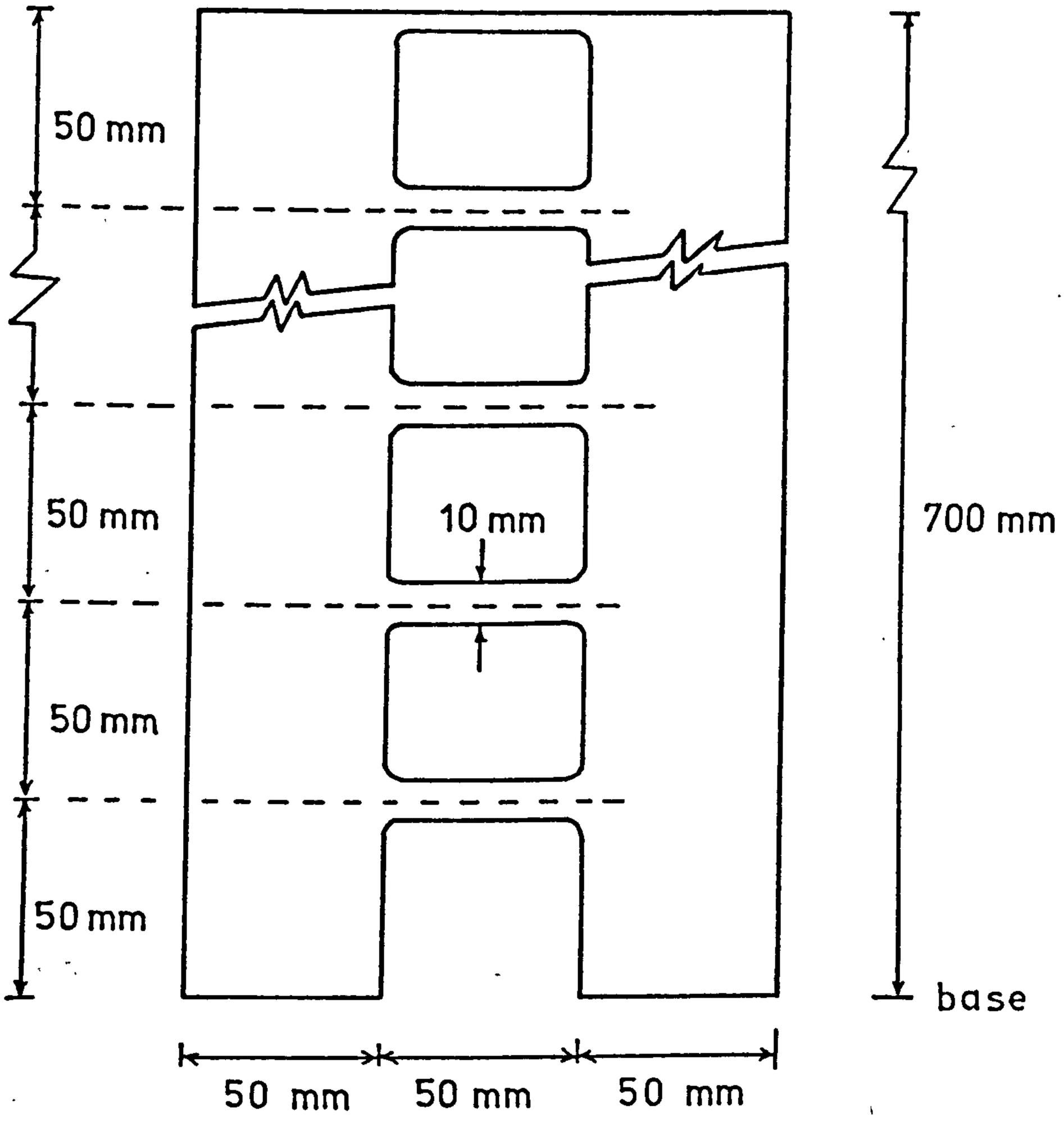

Segments of assembly connected by connecting beams (segments AB and CD of Fig. 7.4)

Fig. 7.5

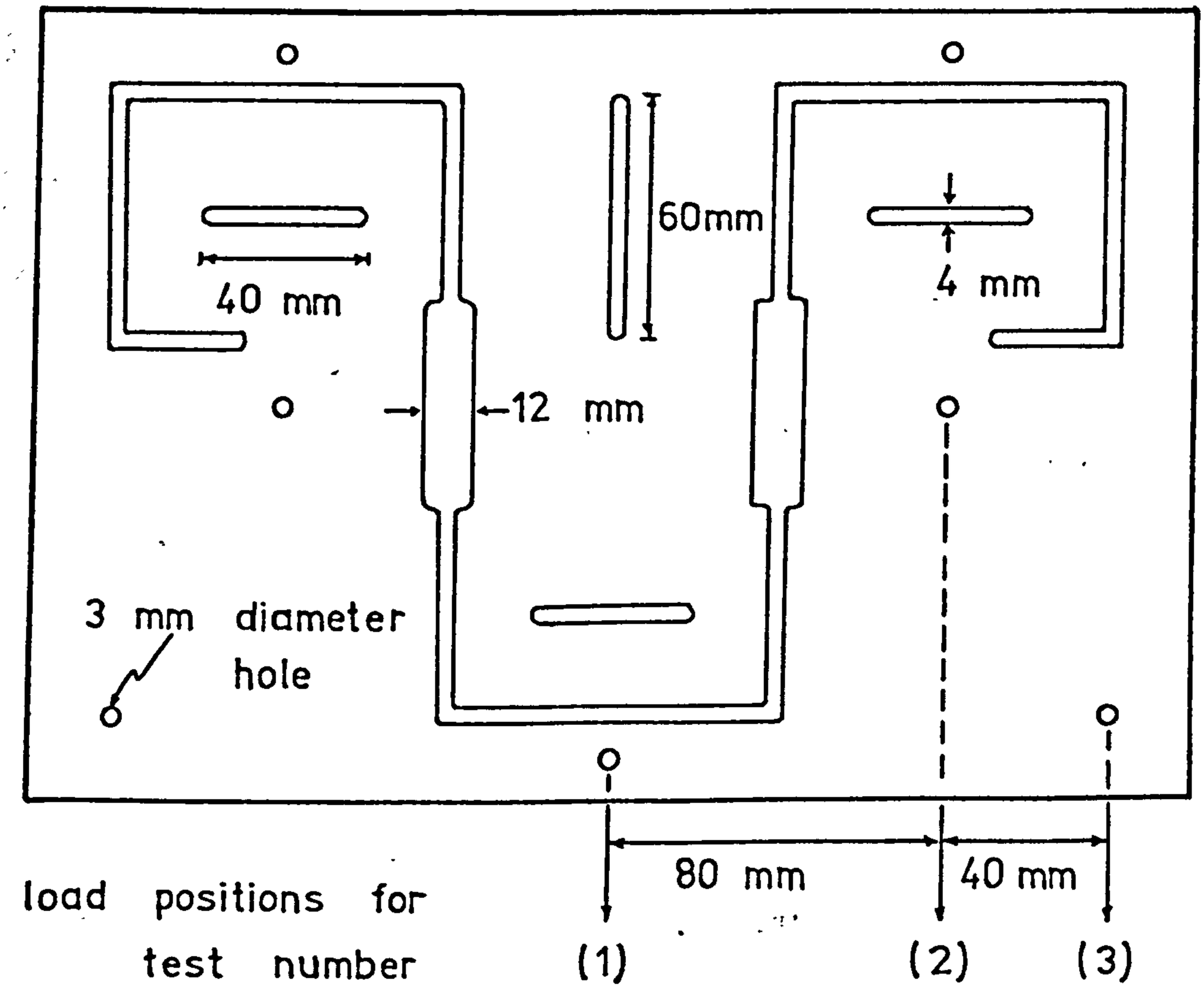

Floor slabs showing slots to avoid coupling and loading points for test numbers 1-3

Fig. 7.6

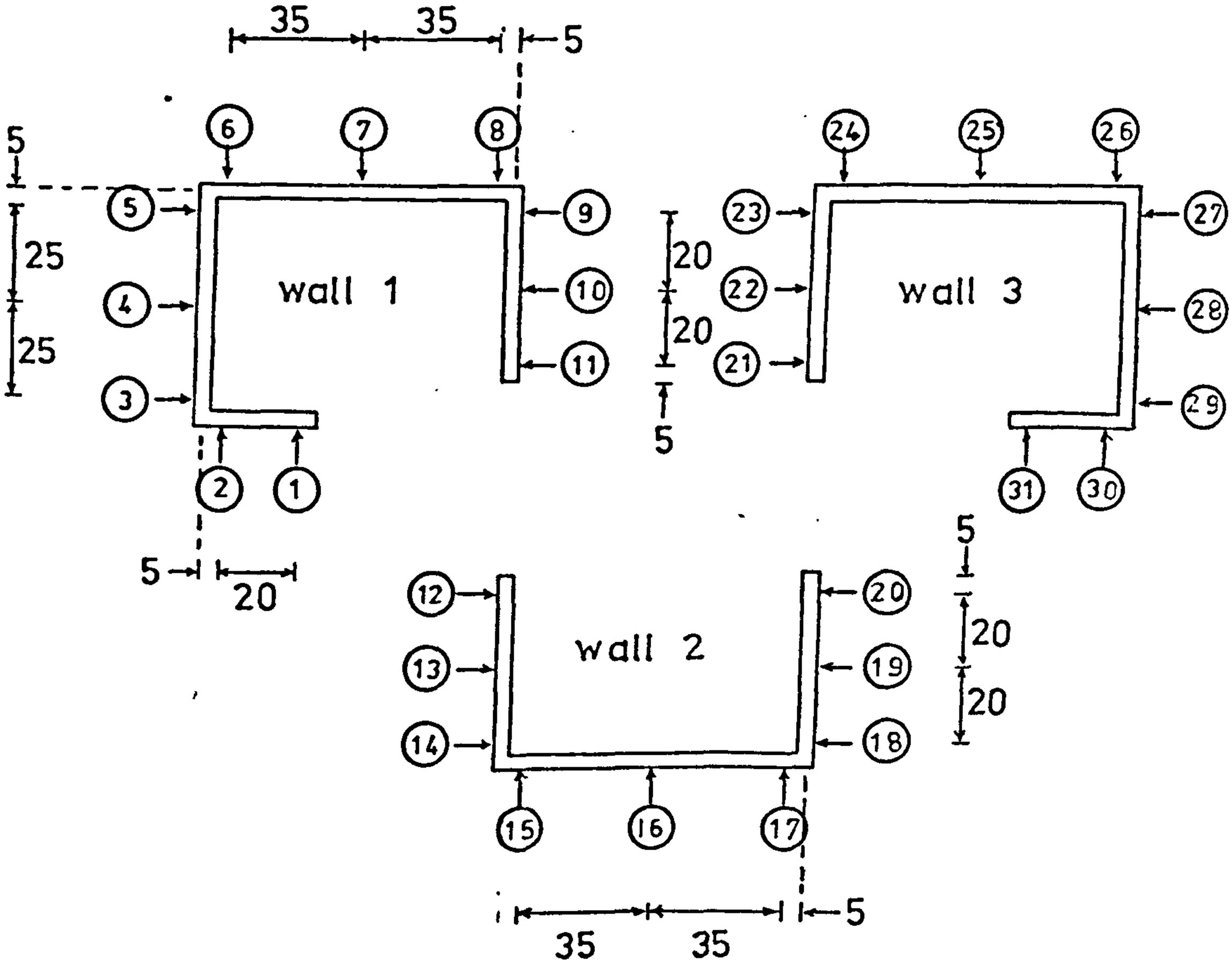

all dimensions in mm

○ strain gauges

Positions of strain gauges

Fig. 7.7

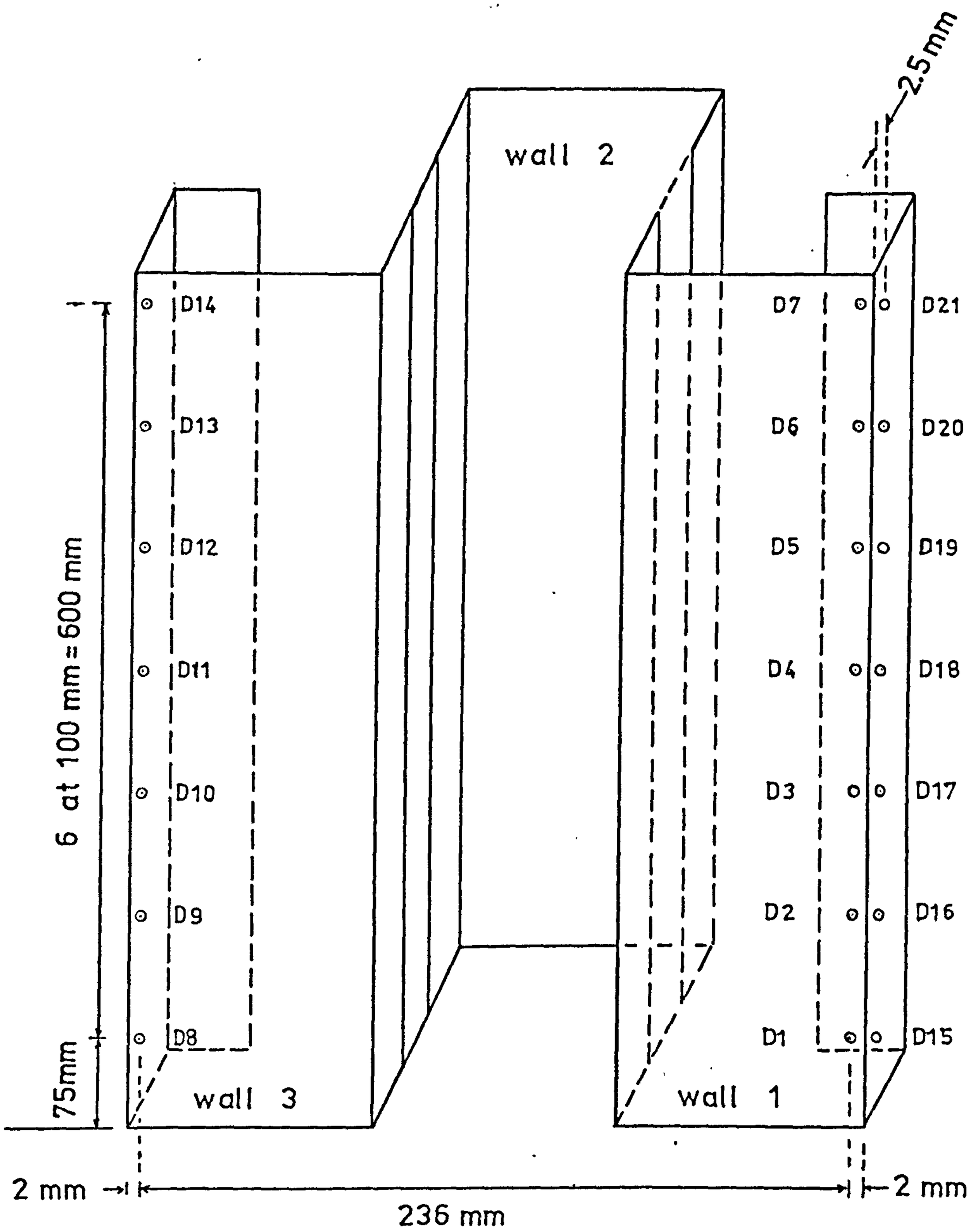

Positions of dial gauges

Fig. 7.8

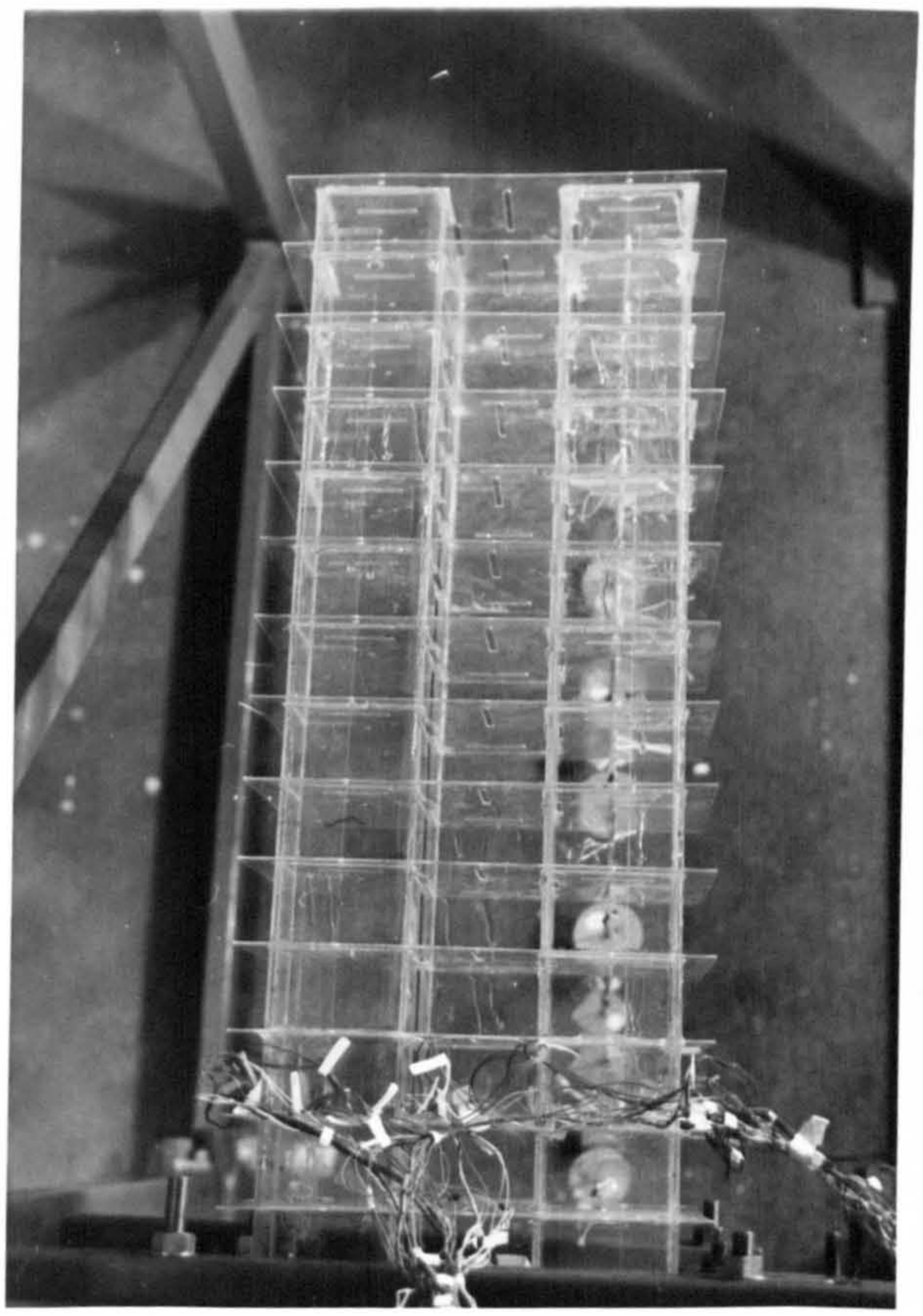

Fig. 7.9

Model structure

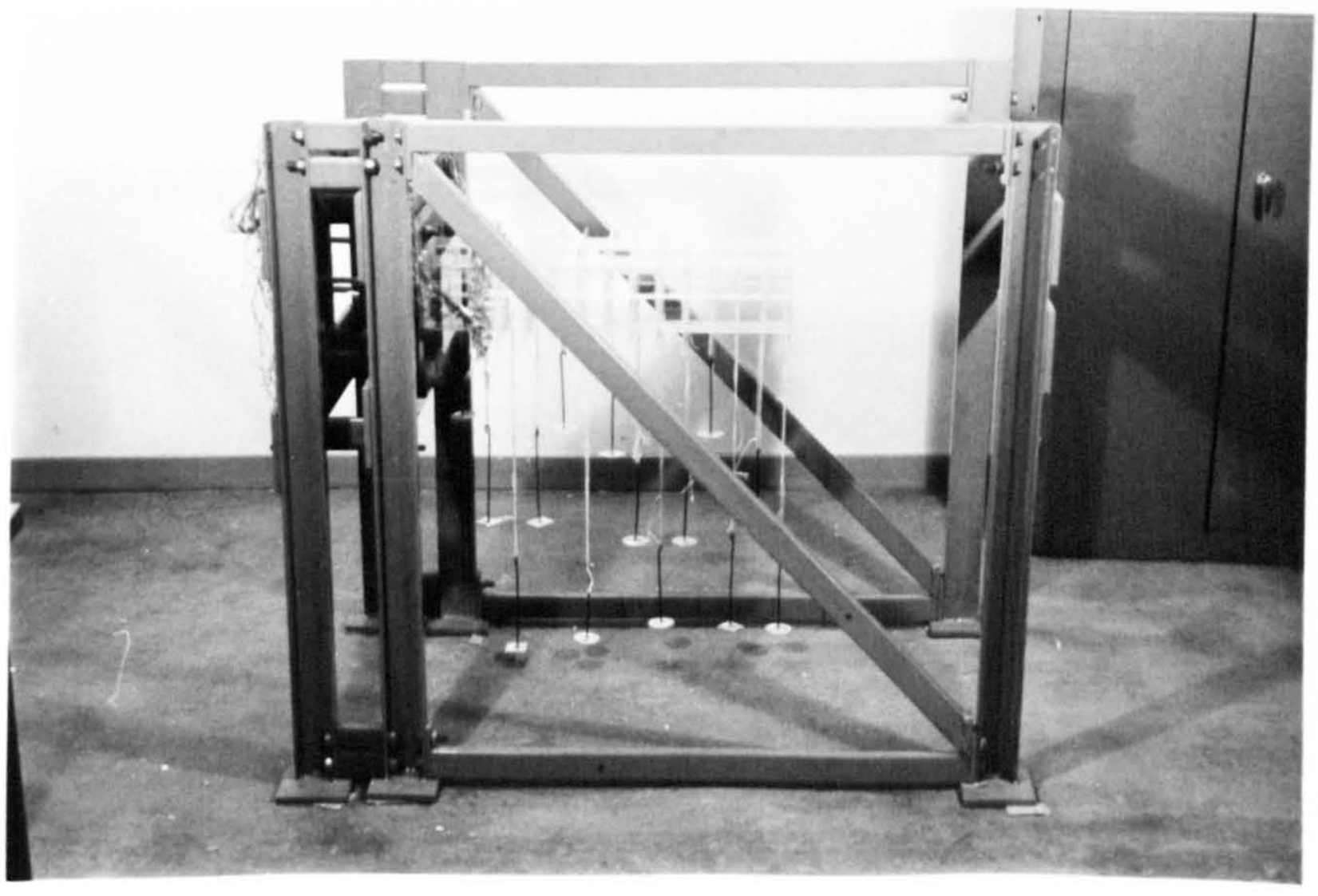

Test frame

Fig. 7.10

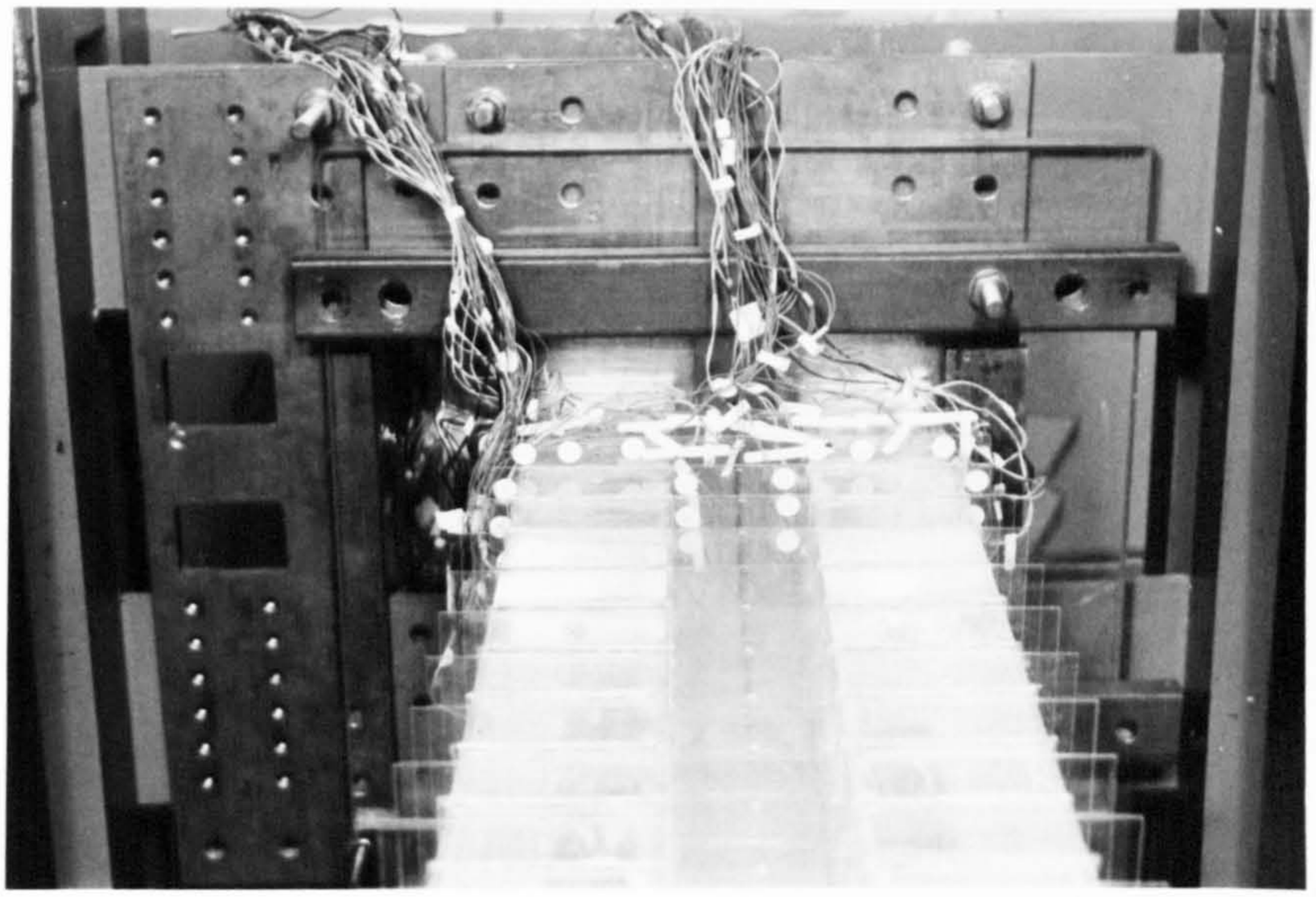

Fixing arrangement at the base

Fig. 7.11

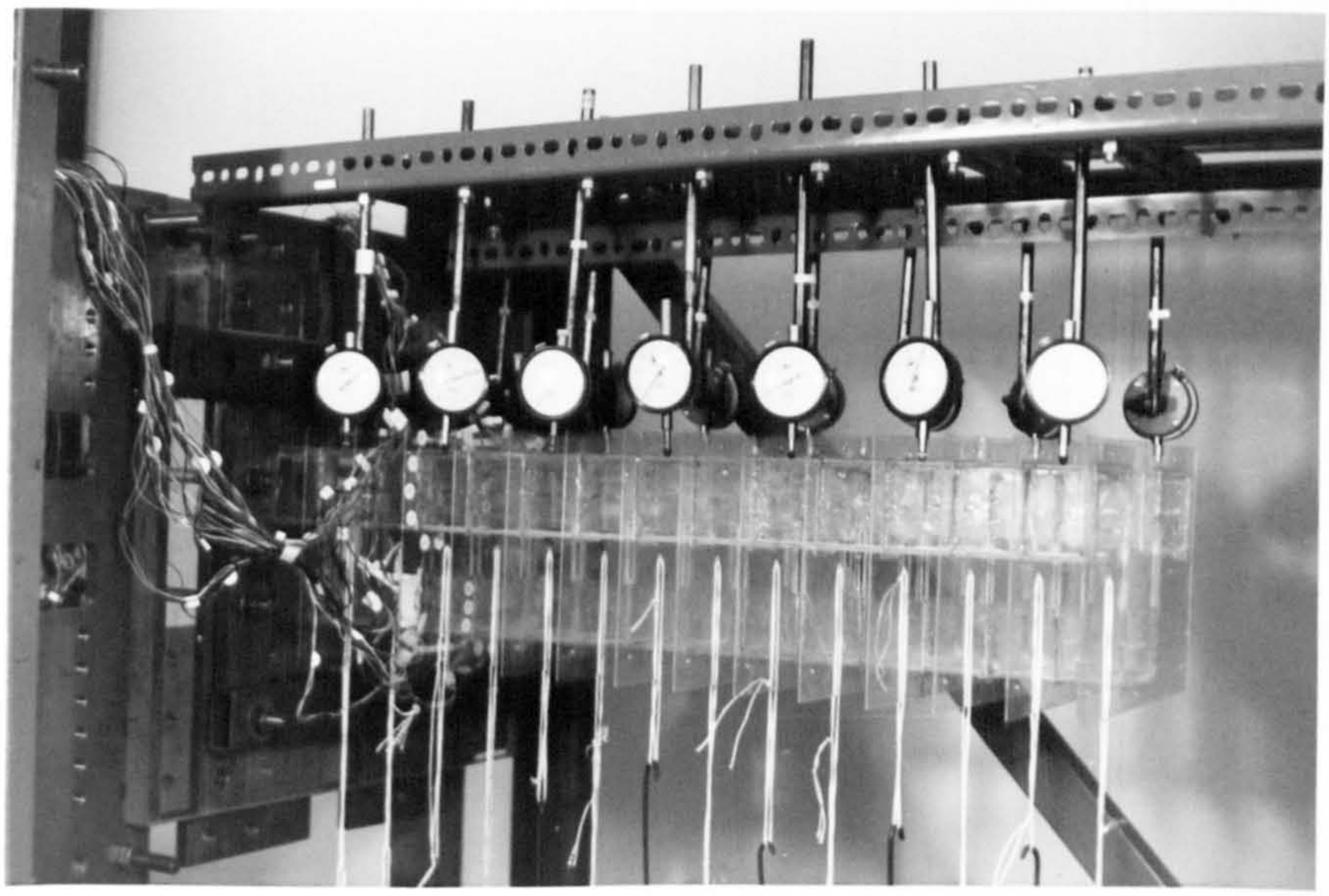

Orientation of model

Fig. 7.12

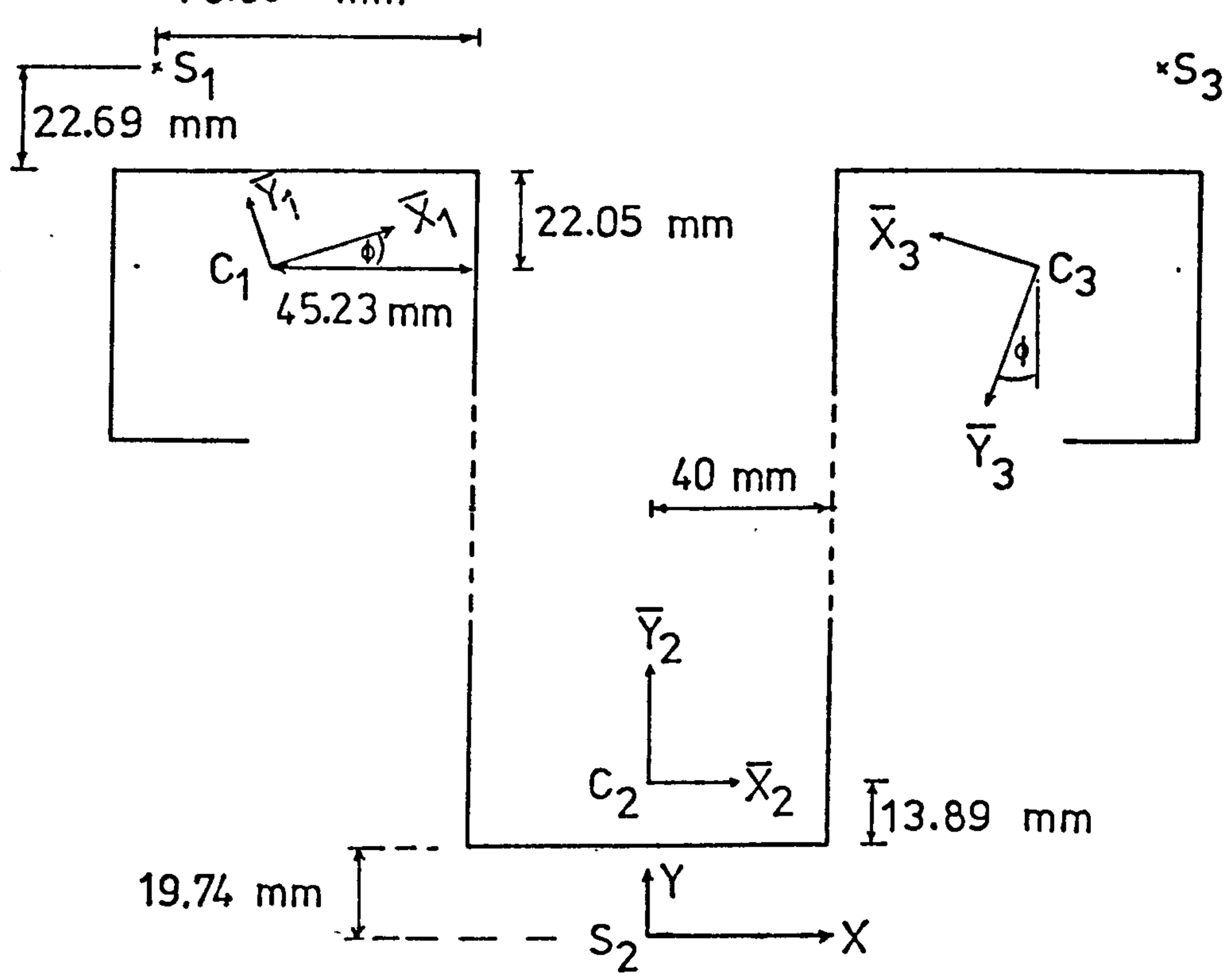

$\phi = \tan^{-1} 0.3154$

Principal co-ordinate systems of coupled walls

Fig. 7.13

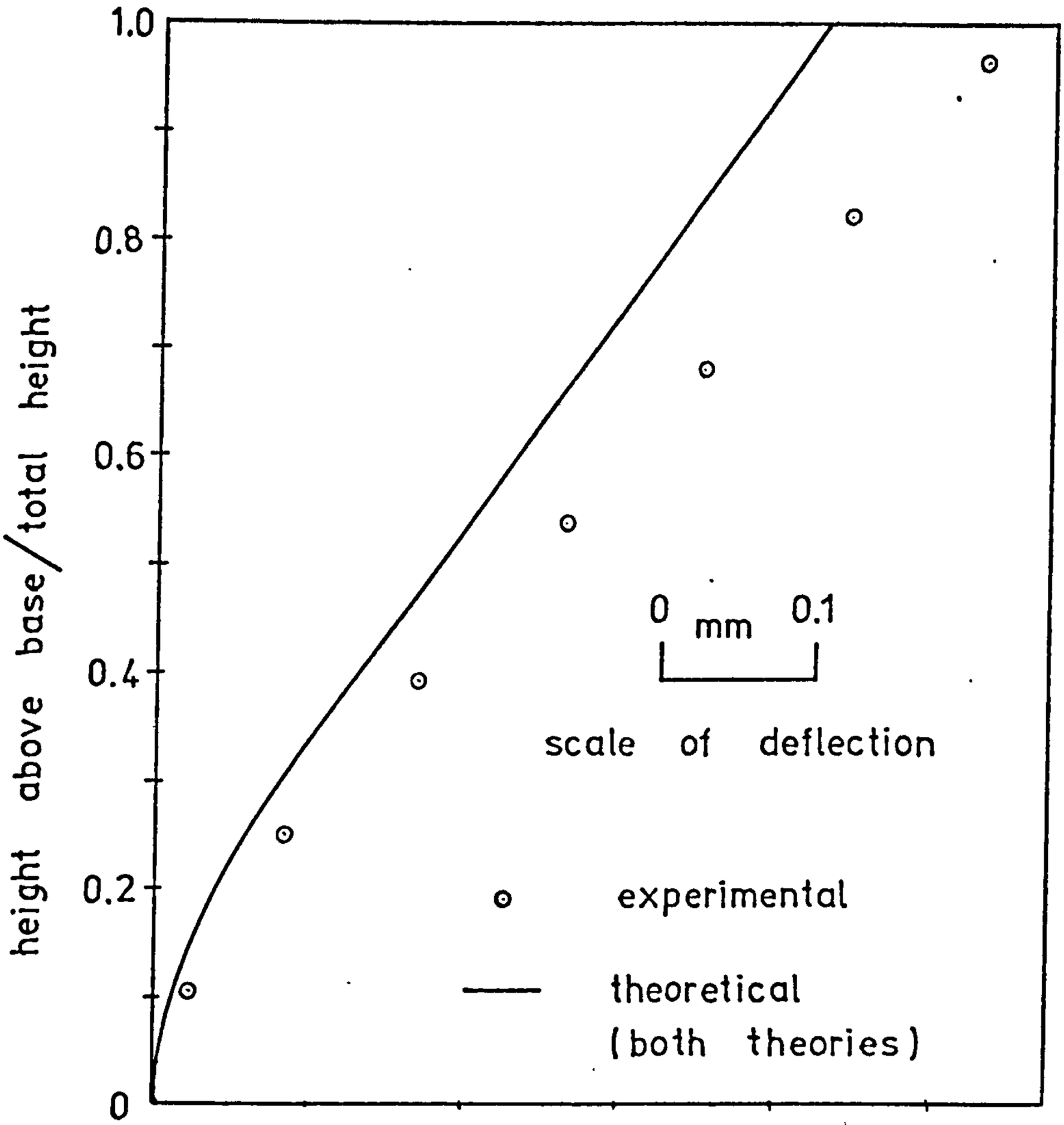

Deflection in the direction of the applied loads for test number 1 (for loading of 0.5 kgf per storey)

Fig. 7.14

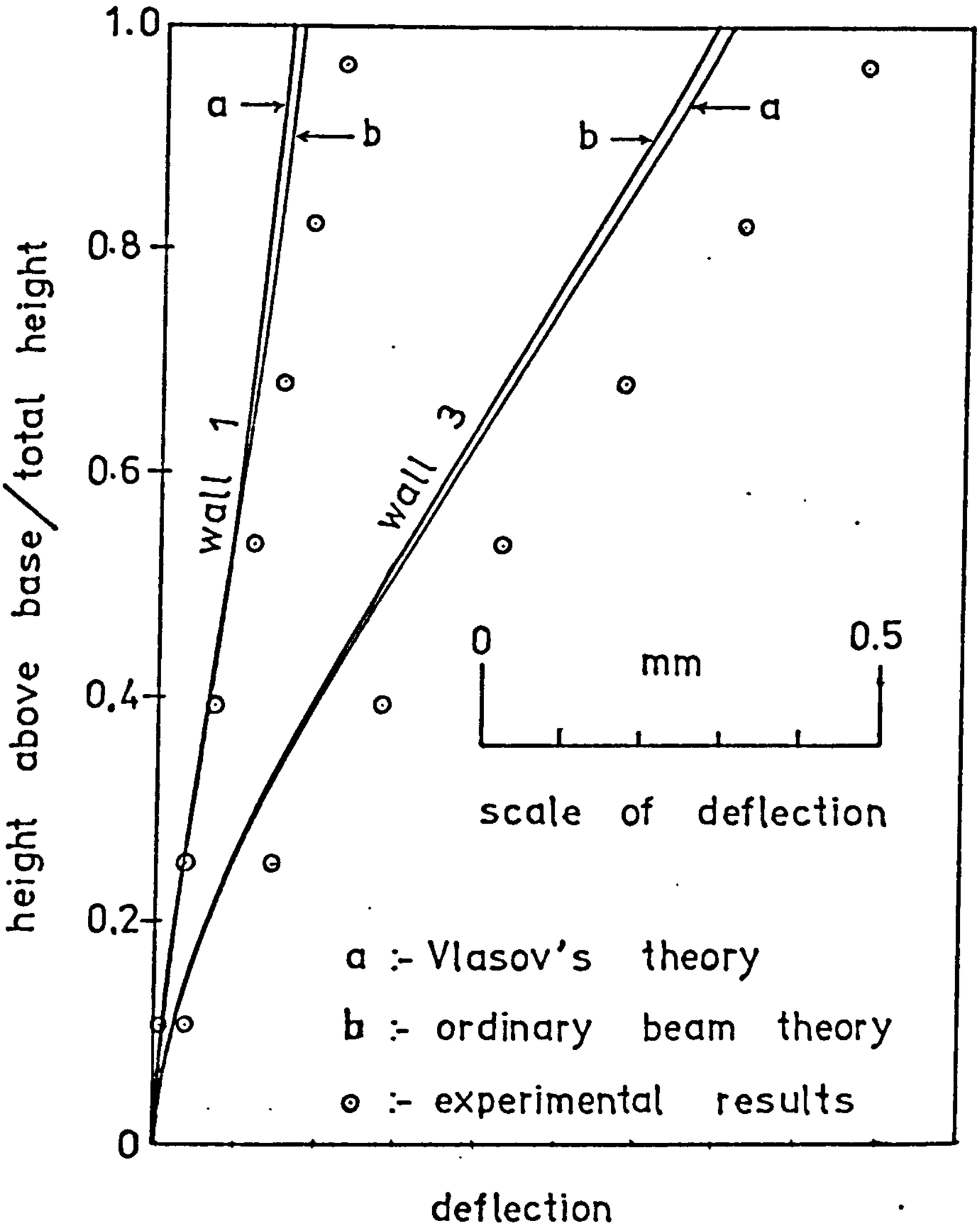

Deflection in the direction of the applied loads for test number 2 (for loading of 0.5 kgf per storey)

Fig. 7.15

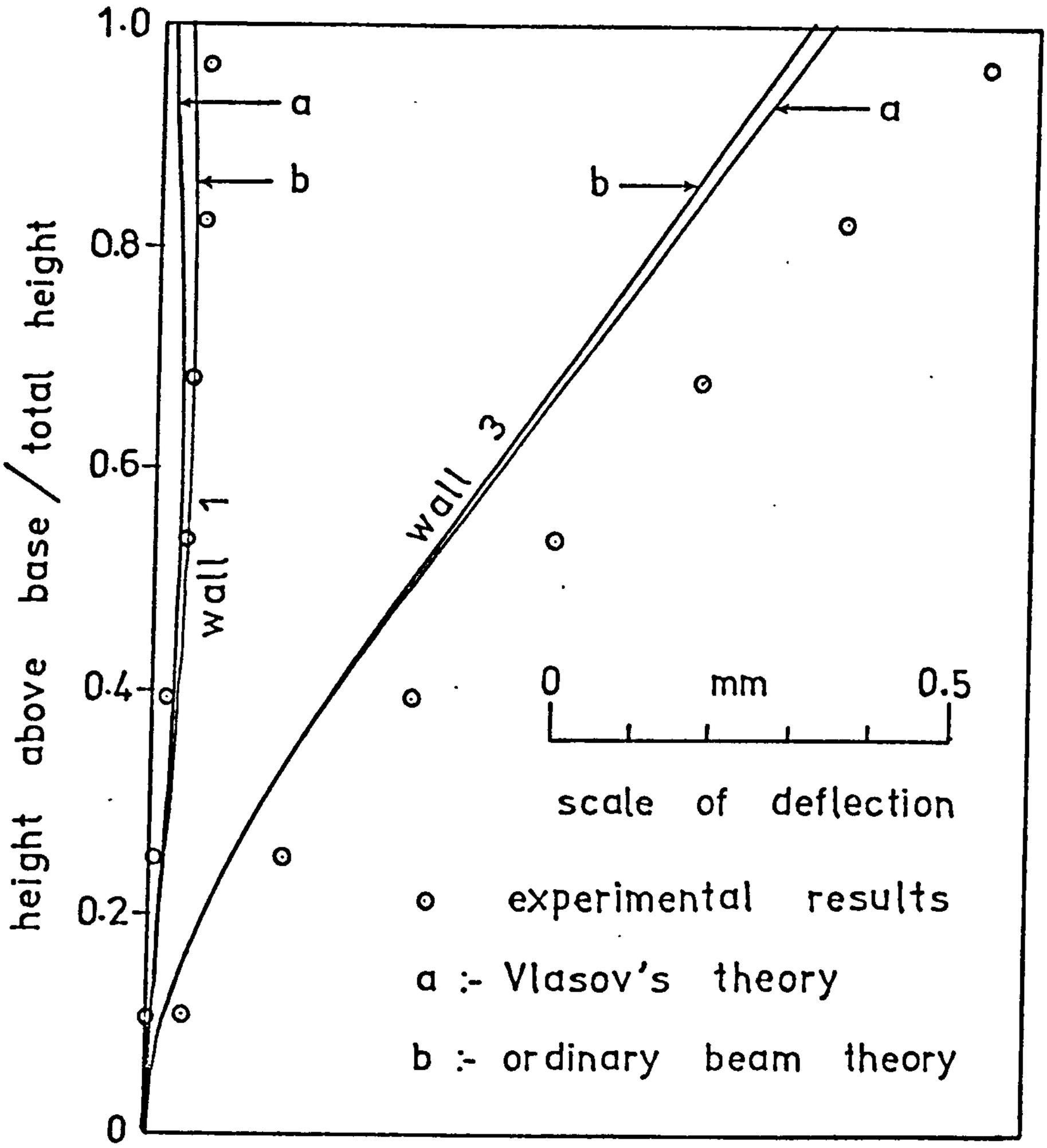

Deflection in the direction of the applied loads for test number 3 (for loading of 0.5 kgf per storey)

Fig. 7.16

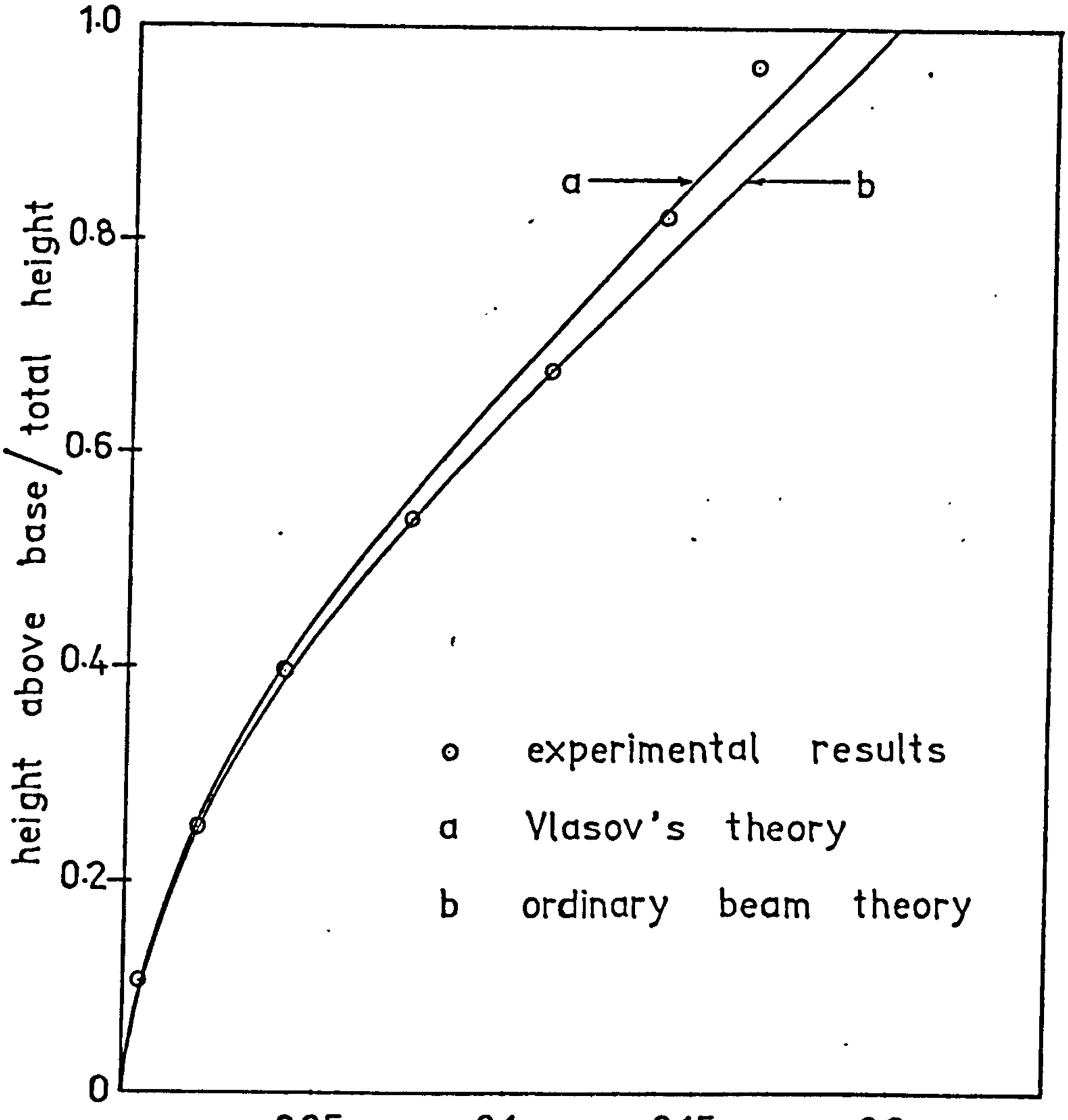

Deflection normal to the plane of symmetry for loading of 0.5 kgf per storey with eccentricity of 120 mm (test number 3)

Fig. 7.17

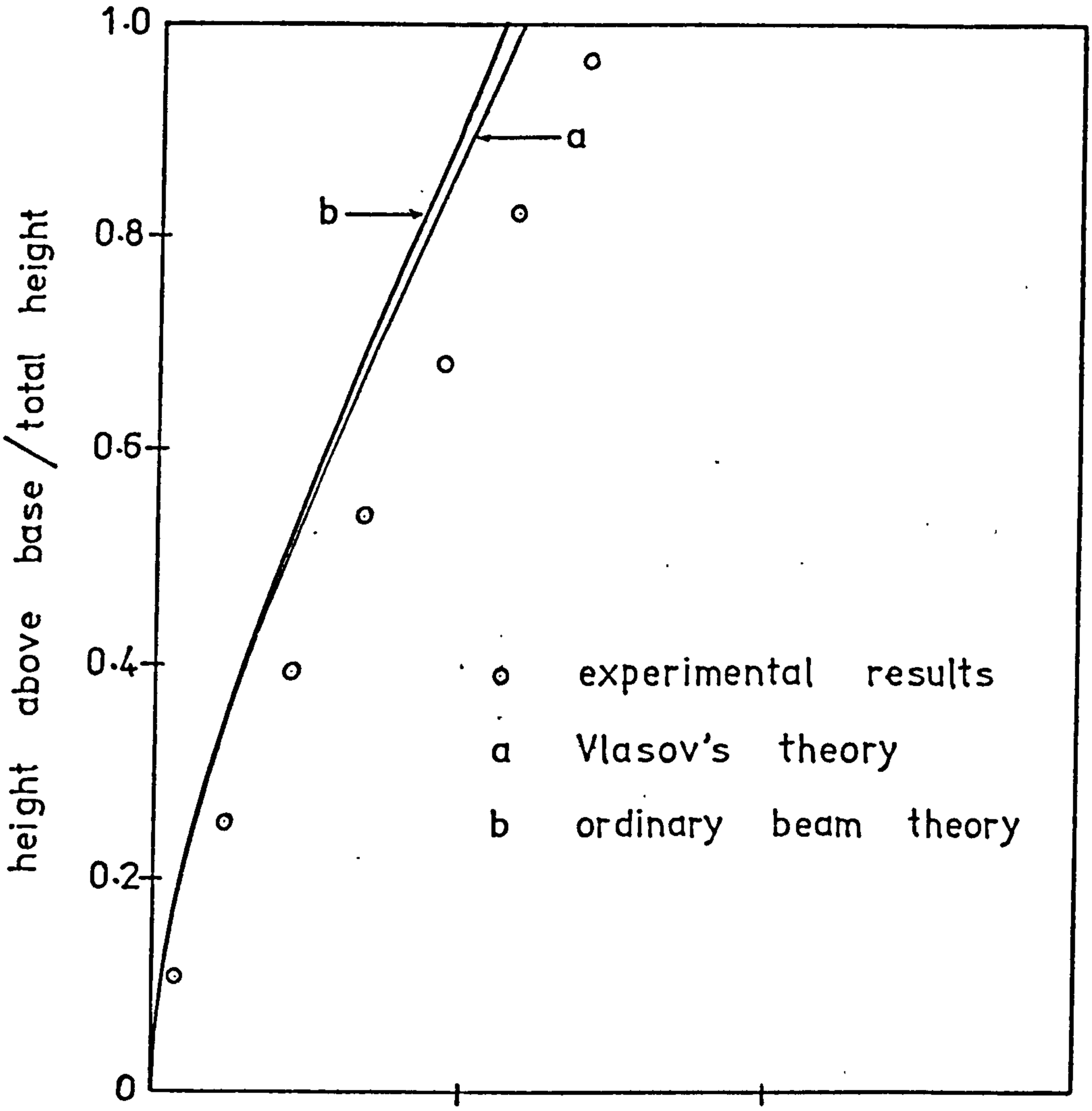

Rotation of model for test number 2 (for loading of 0.5 kgf per storey)

Fig. 7.18

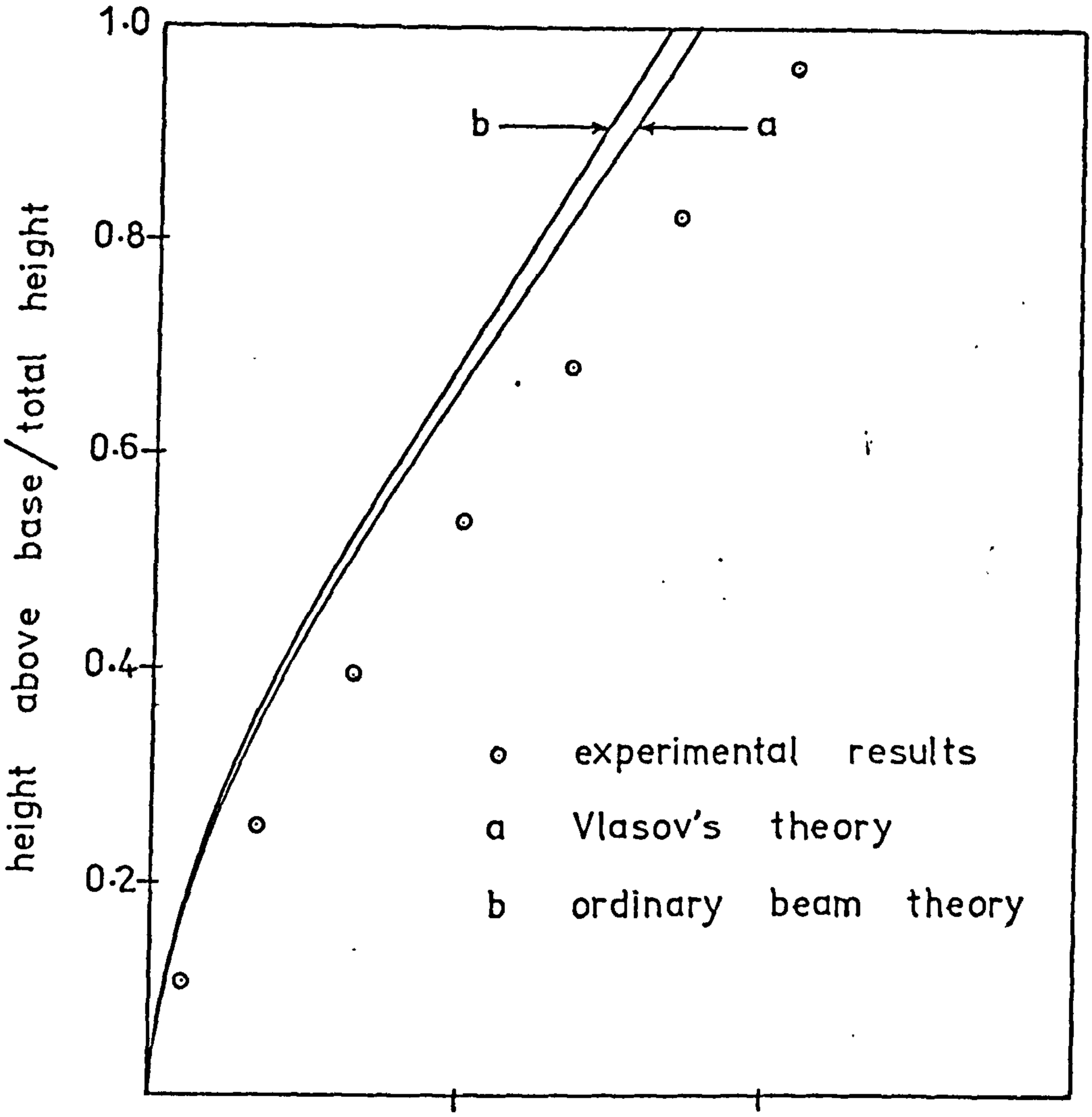

Rotation of model for test number 3
(for loading of 0·5 kgf per storey)

Fig. 7·19

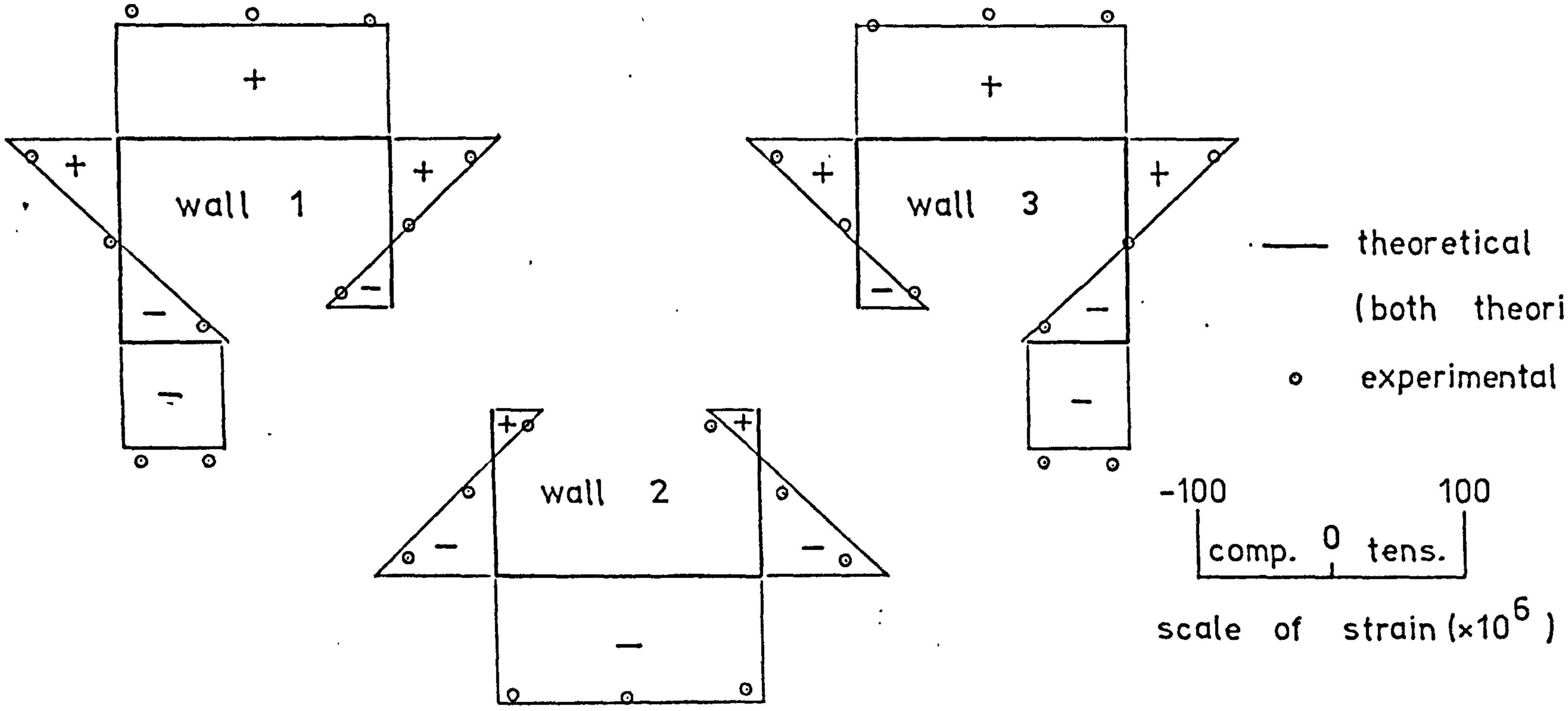

Strains :- test number 1 (for loading of 0.5 kgf per storey)

Fig. 7.20

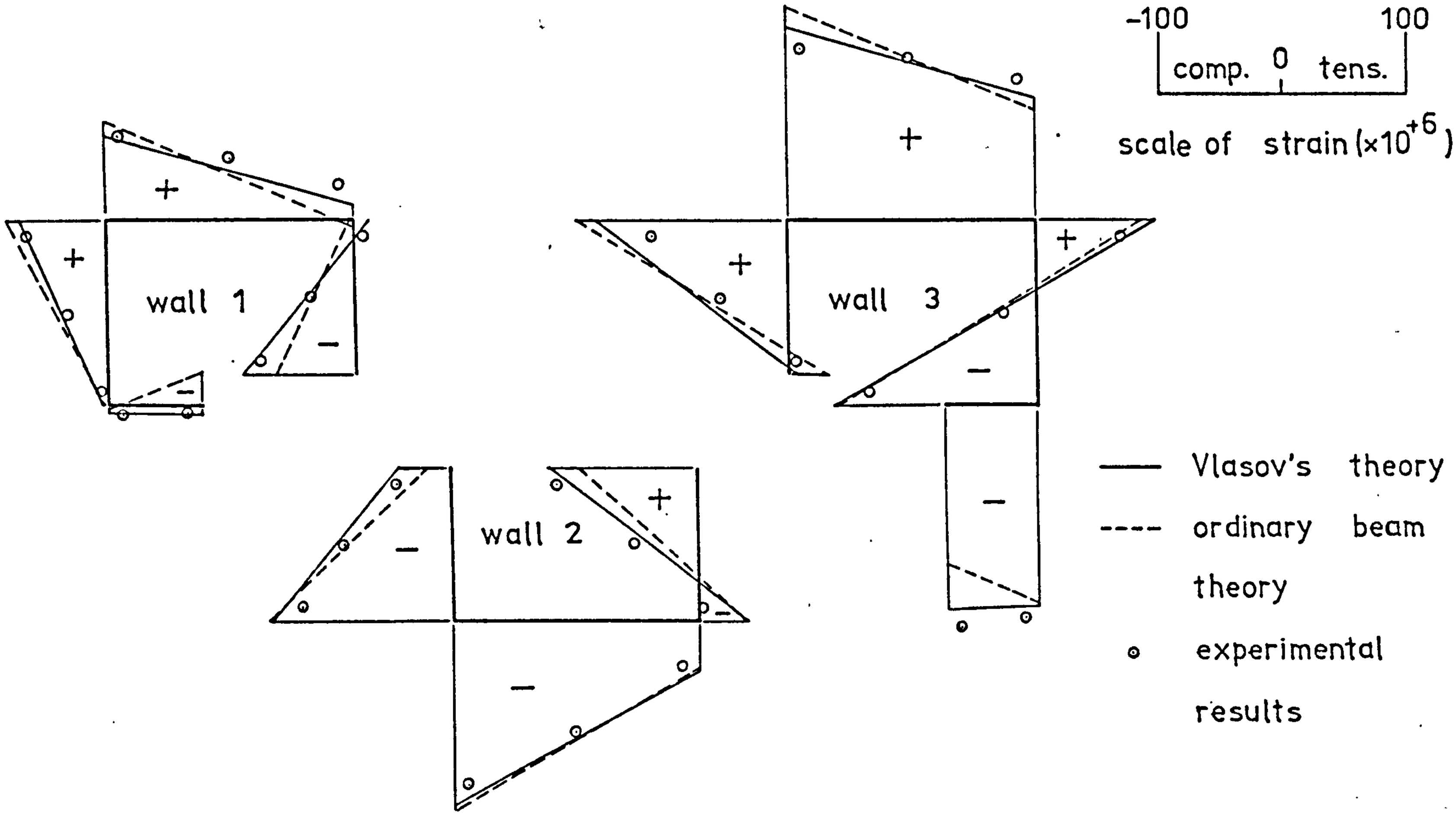

Strains:- test number 2 (for loading of 0.5 kgf per storey)

Fig. 7.21

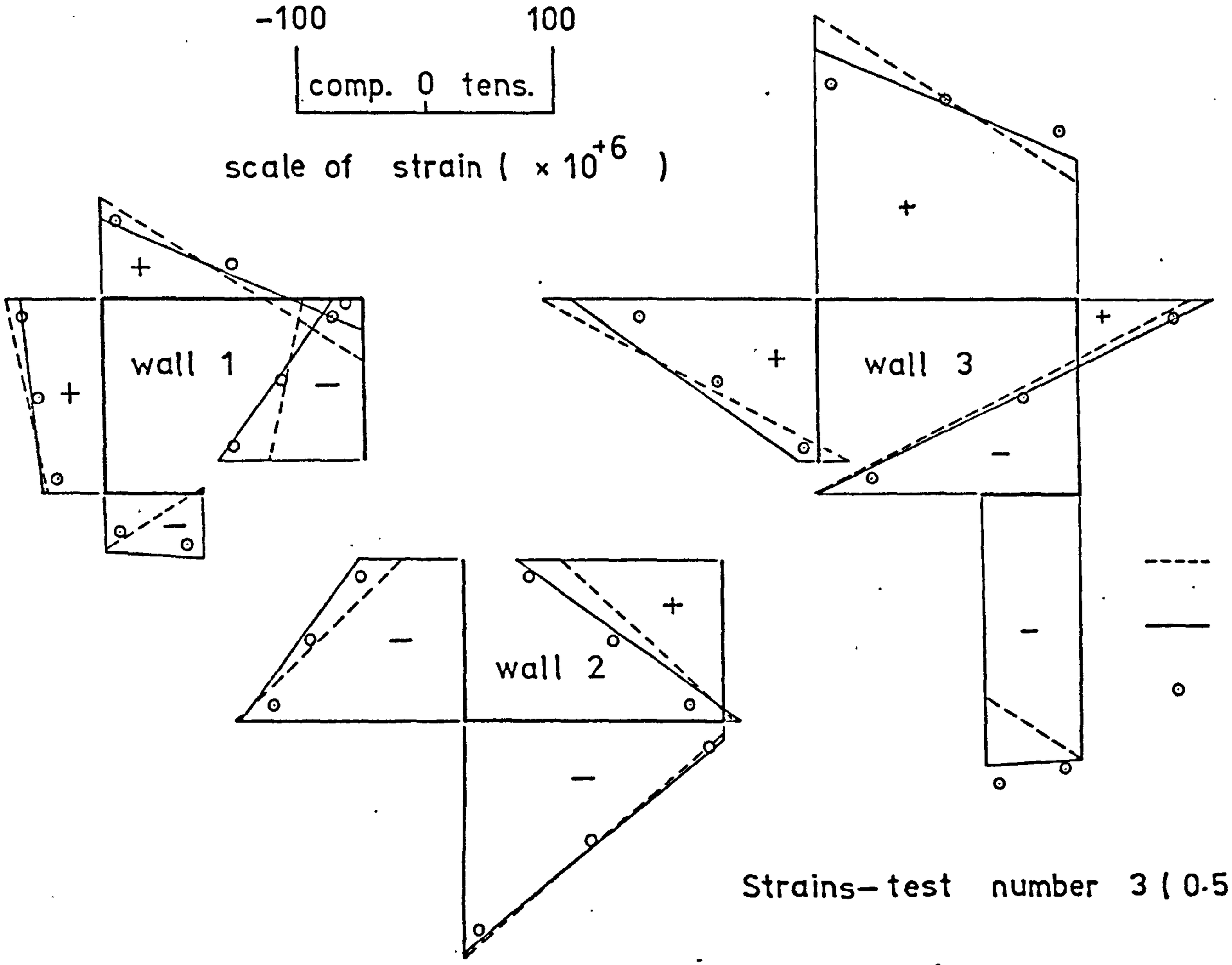

Strains– test number 3 (0·5 kgf per storey)

Fig. 7.22

Table 7.1

Strain in Wall Assembly Due to Loading of 0.5 kgf per Storey

Strain gauge number	Longitudinal strains at 125 mm above base μ in/in		
	Test No. 1	Test No. 2	Test No. 3
1	-90	- 5	37
2	-90	- 8	29
3	-61	4	34
4	7	36	48
5	64	63	61
6	95	69	61
7	93	51	29
8	87	30	- 2
9	63	7	-23
10	14	-36	-64
11	-37	-79	-101
12	27	-42	-78
13	-17	-85	-117
14	-65	-121	-149
15	-87	-131	-157
16	-89	- 88	-89
17	-83	-36	-17
18	-61	- 4	26
19	-16	51	84
20	35	112	148
21	-42	- 9	9
22	9	53	75
23	57	109	135
24	84	136	163
contd.	contd.	contd.	contd.

Table 7.1 (contd.)

Strain gauge number	Longitudinal strains at 125 mm above base μ in/in		
	Test No. 1	Test No. 2	Test No. 3
25	93	131	151
26	93	114	127
27	66	70	75
28	2	-25	-41
29	-61	-129	-158
30	-92	-171	-209
31	-95	-180	-221

Height above base mm	Deflection in the direction of applied loads mm		
	Test No. 1	Test No. 2	Test No. 3
wall 1* (D1 to D7)			
75	0.026	0.006	-0.003
175	0.087	0.038	0.008
275	0.169	0.071	0.020
375	0.266	0.115	0.038
475	0.360	0.150	0.043
575	0.452	0.184	0.053
675	0.541	0.222	0.059
wall 3* (D8 to D14)			
75	0.028	0.039	0.047
175	0.087	0.144	0.168
275	0.167	0.277	0.326
375	0.266	0.425	0.504
475	0.360	0.580	0.685
575	0.450	0.728	0.865
675	0.541	0.876	1.039

* The distances between the points at which the deflections were measured and the plane of symmetry of the model were 118 mm (cf. Fig. 7.8).

Deflection of Model Due to Loading of 0.5 kgf per Storey

Table 7.2

Height above base mm	Rotation of Model (radian)		
	Test No. 1	Test No. 2	Test No. 3
75	0.0	0.00014	0.00021
175	0.0	0.00045	0.00068
275	0.0	0.00087	0.00130
375	0.0	0.00131	0.00197
475	0.0	0.00182	0.00272
575	0.0	0.00231	0.00344
675	0.0	0.00277	0.00415

Rotation of Model Due to Loading of 0.5 kgf per Storey

Table 7.3

Height above base* mm	Deflection normal to the plane of symmetry mm
75	0.004
175	0.019
275	0.042
375	0.074
475	0.110
575	0.140
675	0.162

* Dian gauge positions were shown in Fig. 7.8.

Deflection Normal to the Plane of Symmetry of the Model due to Loading of 0.5 kgf per Storey with eccentricity 120 mm (test number 3)

Table 7.4

CHAPTER 8

GENERAL CONCLUSIONS

The use of the continuous medium method for the analysis of two- and three-dimensional multi-storey shear wall structures has been examined in this thesis. Experimental investigations were undertaken, when they were necessary, to substantiate the analyses.

Plane coupled wall systems with continuously variable stiffness have been analysed, and experimental investigations on coupled walls with tapered width were carried out using perspex models. The strains in the walls predicted by the theory agreed well with the experimental results, but considerable discrepancies occurred regarding the deflections of the walls. In all three models tested, including a model with uniform walls, the deflections obtained experimentally were considerably larger than those predicted by the theory. However, in the case of a uniform coupled wall it has been well established that the continuous medium approach yields accurate results. Therefore, there was considerable indication that experimental deficiencies existed which had the effects of giving larger measured deflections. It is believed that the discrepancies in the deflections were mainly due to undetected support movements caused by deformations of the test frame under loading conditions. Elastic deformations of the perspex base plates and creep of the models could also increase the

measured deflections. Taking these effects into consideration, the analysis can be considered as being reasonably substantiated by the experimental investigations. Between the two methods of solution proposed, the Galerkin method and the finite difference method, the Galerkin method is preferable since it gives analytic solutions and for practical purposes sufficient accuracy is obtained using only three undetermined constants. The effects of an elastic foundation has also been considered in the analysis.

The technique put forward in Chapter 3 is valuable for the investigation or design of coupled shear walls on flexible bases, subjected to lateral or vertical loads or a combination of both loads. The formulae and design curves presented enable important design quantities in coupled walls on flexible bases to be evaluated rapidly. Although only four sets of design curves have been produced, they cover a large number of lateral and vertical load cases (due to the correspondences between the design curves for lateral and vertical load cases). The curves are valid for two coupled walls and any symmetrical system with three walls which are connected by two series of connecting beams, provided that the wall cross-sections are uniform throughout their heights. The design curves presented can be very useful in the design office, since the variation of important design quantities under different sets of proposed base conditions can be investigated rapidly with minimum

computation.

The lateral-load analysis of symmetrical three-dimensional multi-storey shear wall structures has been carried out as two separate analyses, bending and torsion being treated separately. As shown in Chapter 4, each separate analysis is reducible to the analysis of an equivalent analogous plane system. The solution is achieved by solving a system of simultaneous second-order differential equations with vertical shear distributions as dependent variables. The method of analysis is very efficient in dealing with symmetrical shear wall structures comprising a large number of coupled wall assemblies which are identical or of a few distinct groups. The advantages of the method is exemplified by the example problem in Chapter 4, where the shear wall structure consisting of three cantilevered walls and eighteen identical coupled wall assemblies was analysed. The solutions for the eccentrically loaded structure were obtained by solving only two second-order differential equations, one at a time. The amount of computation involved was small and could be achieved easily by hand computation. The method presented is valid whether the coupled wall assemblies are planar or non-planar systems.

By treating frames as vertical cantilever shear beams, i.e. it is assumed that the shear force in each frame is proportional to the rate of change of the lateral deflection of the frame, the method has been extended to deal with symmetrical shear wall-frame structures.

However, for shear wall-frame structures, the governing differential equations become fourth-order equations with vertical shear distributions as dependent variables. Closed form solutions for standard load cases, namely, concentrated lateral load (or torsion) at the top, uniformly distributed lateral load (or torsion) per unit height, triangularly distributed lateral load (or torsion) per unit height, have been presented. These closed form solutions are applicable to symmetrical structures with identical in-plane symmetrical coupled wall assemblies.

Asymmetrical cross-wall structures have been treated in Chapter 6. Under an arbitrary lateral loading system it is not generally possible to separate the analysis into bending and torsional analyses. The centre of rotation of an asymmetrical structure, in general, varies with height and is not predetermined. In consequence, the vertical shear distributions in identical coupled wall assemblies are no longer linearly related. Therefore, the analysis given is suitable only for shear wall or shear wall-frame structures with relatively few coupled wall assemblies.

The analysis of three-dimensional thin-walled structures presented in Chapter 7 has taken into account the warping of the wall cross-sections. Vlasov's theory for thin-walled beams of open section has been assumed valid for individual walls. An associated experimental investigation on a fourteen-storey perspex model structure consisting of three non-planar walls interconnected by two series of connecting beams was undertaken.

The experimental results substantiated the analytical predictions, and indicated that neglecting the warping of the wall cross-sections could result in considerable errors in the prediction of stress distributions in the walls, particularly at the points having relatively large values of sectorial co-ordinates. The method of analysis presented is applicable to thin-walled structures consisting of cantilevered and coupled walls of any configuration. The coupled wall assemblies may be singly- or multiply-connected, or self-connected assemblies. The method can be advantageously used to analyse structures with relatively few series of connecting beams since the solutions can be achieved manually. For structures with a large number of series of connecting beams, the advantages of the method diminish because the amount of computation involved increases with an increasing number of the series of connecting beams.

In the light of the experimental results obtained from the thin-walled model, caution should be exercised when the expressions given in Chapters 4, 5 and 6 are used, since the analyses in these chapters have been based on the assumption that the ordinary beam theory is valid for individual walls. If the thicknesses of the walls are relatively small and the torsional loadings large, slight modification should be made to the torsional analyses in Chapters 4 and 5 and to the analysis presented in Chapter 6 in order to take account of the warping of the wall cross-sections. However, no modification is necessary if each wall is planar or made

up of straight plates intersecting at one common point. For such wall configurations, the sectorial co-ordinates along the cross-sectional profile of each wall are identically equal to zero. In consequence, the expressions obtained using ordinary beam theory or Vlasov's theory for thin-walled beams of open section will be identical.

REFERENCES

1. BECK, H. "Contribution to the Analysis of Coupled Shear Walls" Jnl. ACI, Vol. 59, 1962, pp. 1055-1069.

2. CARDAN, B. "Concrete Shear Walls Combined with Rigid Frames in Multi-storey Buildings Subject to Lateral Loads" Jnl. ACI, Vol. 58, 1961, pp.299-316.

3. CHITTY, L. "On the Cantilever Composed of a Number of Parallel Beams Interconnected by Cross-bars" Philosophical Magazine (London), Vol. 38, Series 7, 1947, pp.685-699.

4. CLOUGH, R.; KING, I.P., and WILSON, E.L. "Structural Analysis of Multi-storey Buildings" Jnl. of the Structural Division, ASCE, Vol. 90, No. ST 3, June 1964, pp. 19-34.

5. COULL, A. "Interactions between Coupled Shear Walls and Cantilevered Cores in Three-dimensional Regular Symmetrical Cross-wall Structures" Proc. Instn. Civ. Engrs., Part 2, Vol. 55, 1973, pp.827-840.

6. COULL, A. "Application of Macaulay's Method to the Analysis of Non-uniform

Beams" Civil Engineering and Public Works Review, London, Vol. 65, 1970, pp.1277-1278.

7. COULL, A., and ADAMS, N.W. "A Simple Method of Analysis of the Load Distribution in Multi-storey Shear Wall Structures" Response of Multi-storey Concrete Structures to Lateral Forces, ACI Publication SP-36, 1973, pp. 187-216.

7. COULL, A., and CHANTAKSINOPAS, B. "Design Curves for Coupled Shear Walls on Flexible Bases" Proc. Instn. Civ. Engrs., Part 2, Vol. 57, 1974, pp. 595-618.

9. COULL, A. and CHOUDHURY, J.R. "Stresses and Deflections in Coupled Shear Walls" Jnl. ACI, Vol. 64, 1967, pp. 65-72.

10. COULL, A., and CHOUDHURY, J.R. "Analysis of Coupled Shear Walls" Jnl. ACI, Vol. 64, 1967, pp. 587-593.

11. COULL, A., and IRWIN, A.W. "Analysis of Load Distribution in Multi-storey Shear Wall Structures" Struct. Engr., Vol. 48, 1970, pp. 301-306.

12. COULL, A., and PURI, R.D. "Analysis of Coupled Shear Walls with Variable Thickness" Build. Sci., Vol. 2, 1967, pp. 181-188.

13. COULL, A., and PURI, R.D. "Analysis of Coupled Shear Walls with Variable Cross-section" Build. Sci., Vol. 2, 1967, pp. 313-320.

14. COULL, A., and STAFFORD SMITH, B. "Analysis of Shear Wall Structures (A Review of Previous Research)" Tall Building, Pergamon Press, 1967, pp. 139-156.

15. COULL, A., and STAFFORD SMITH, B. "Structural Analysis of Tall Concrete Buildings" Proc. Instn. Civ. Engrs., Part 2, Vol. 55, 1973, pp. 151-166.

16. GLUCK, J. "Lateral Load Analysis of Asymmetric Multi-storey Structures" Jnl. of the Structural Division, ASCE, Vol. 96, No. ST2, Feb. 1970, pp. 317-333.

17. HEIDEBRECHT, A.C., and SWIFT, R.D. "Analysis of Asymmetrical Coupled Shear Walls" Jnl. of the Structural Division, ASCE, Vol. 97, No. ST3, May 1971, pp. 1407-1422.

18. HEIDEBRECHT, A.C. and SMITH, B.S. "Approximate Analysis of Tall Wall-Frame Structures" Jnl. of the Structural Division, ASCE, Vol. 99, No. ST2, Feb. 1973, pp. 199-221.

19. KHAN, F.R., and SBAROUNIS, J.A. "Interaction of Shear Walls and Frames" Jnl. of the Structural Division, ASCE, Vol. 90, No. ST3, June 1964, pp. 285-335.

20. MACLEOD, I.A. "Lateral Stiffness of Shear Walls with Openings" Tall Buildings, Pergamon Press, London, 1967, pp. 223-244.

21. MAGNUS, D. "Pierced Shear Walls" Concrete and Constructional Engineering (London), Vol. 60, 1965, pp. 89-98; 127-136; and 177-185.

22. MICHAEL, D. "Coupled Plane Shear Walls of Tapered Thickness" Proc. Instn. Civ. Engrs., Vol. 40, 1968, pp. 511-518.

23. PEARCE, D.J., and MATHEWS, D.D. "An Appraisal of the Design of Shear Walls in Box Frame Structures" HMSO, London, 1973.

24. ROSENBLUETH, E., and HOLTZ, I. "Elastic Analysis of Shear Walls in Tall Buildings" Jnl. ACI, Vol. 56, 1960, pp. 1209-1222.

25. ROSMAN, R. "Approximate Analysis of Shear Walls Subject to Lateral Loads" Jnl. ACI, Vol. 61, 1964, pp. 717-732.

26. ROSMAN, R. "Laterally Loaded Systems Consisting of Walls and Frames" Tall Buildings, Pergamon Press, London, 1967, pp. 273-289.

27. ROSMAN, R. "Statics of Non-Symmetric Shear Wall Structures" Proc. Instn. Civ. Engrs., Supplement XII, paper 7393S, pp. 211-244.

28. SALVADORI, M.G., and BARON, M.L. "Numerical Method in Engineering" Prentice-Hall, 1961.

29. SOKOLNIKOFF, I.S. "Mathematical Theory of Elasticity" McGraw Hill, 1956.

30. STAMATO, M.C. "Three Dimensional Analysis of Tall Buildings" Proceedings, International Conference on Planning and Design of Tall Buildings, Lehigh University, U.S.A., 1972, Vol. 3, Report 24-4, pp. 683-699.

31. VLASOV, V.Z. "Thin-walled Elastic Beams" Israel Program for Scientific Translations, Jerusalem 1967 (Published for the National Science Foundation, Washington, D.C.)

32. ACI COMMITTEE 442 "Response of Buildings to Lateral Forces" Response of Multi-storey Concrete Structures to Lateral Forces, ACI Publication SP-36, 1973, pp. 281-306.

APPENDIX I

FINITE DIFFERENCE OPERATORS

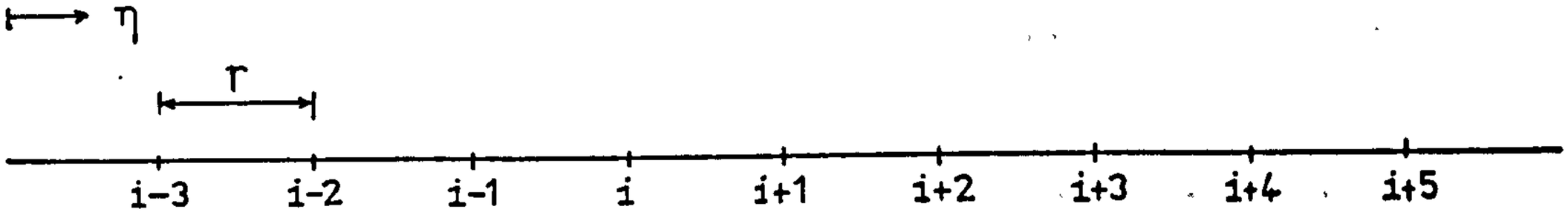

(a) Central Operators (error of order r^2)

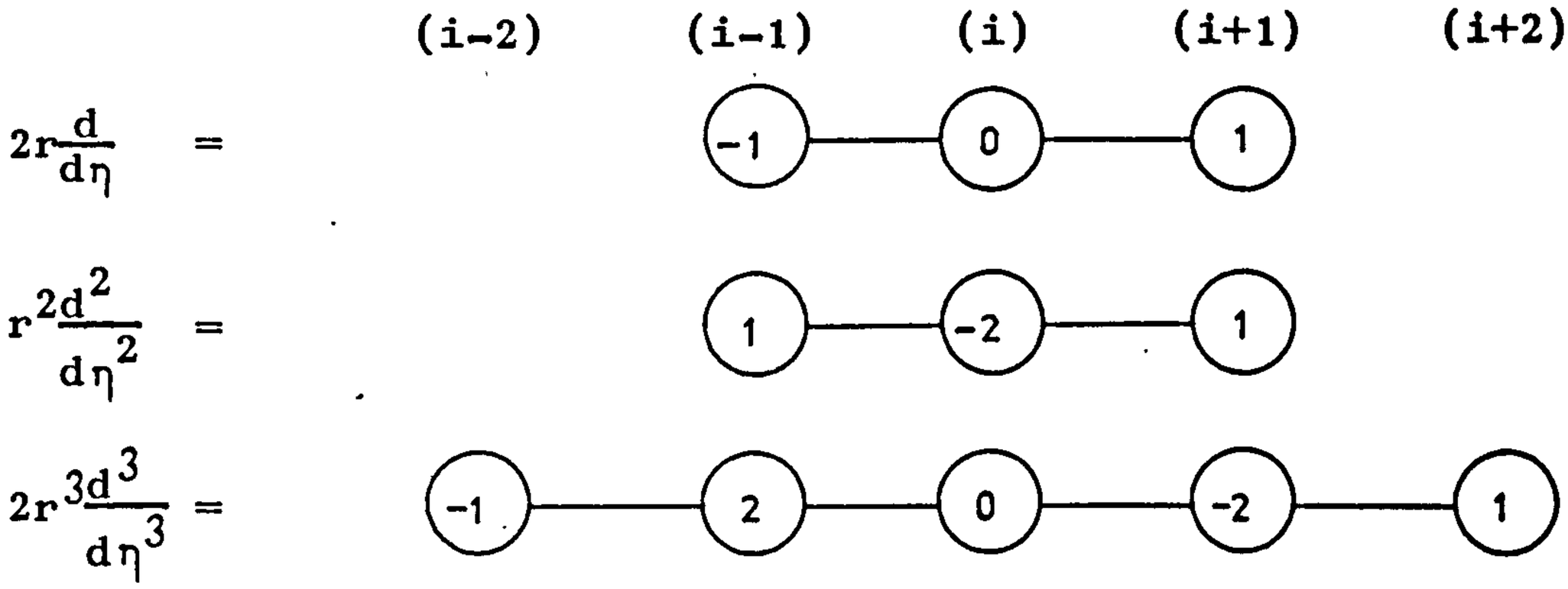

(b) Forward Operators (error of order r^2)

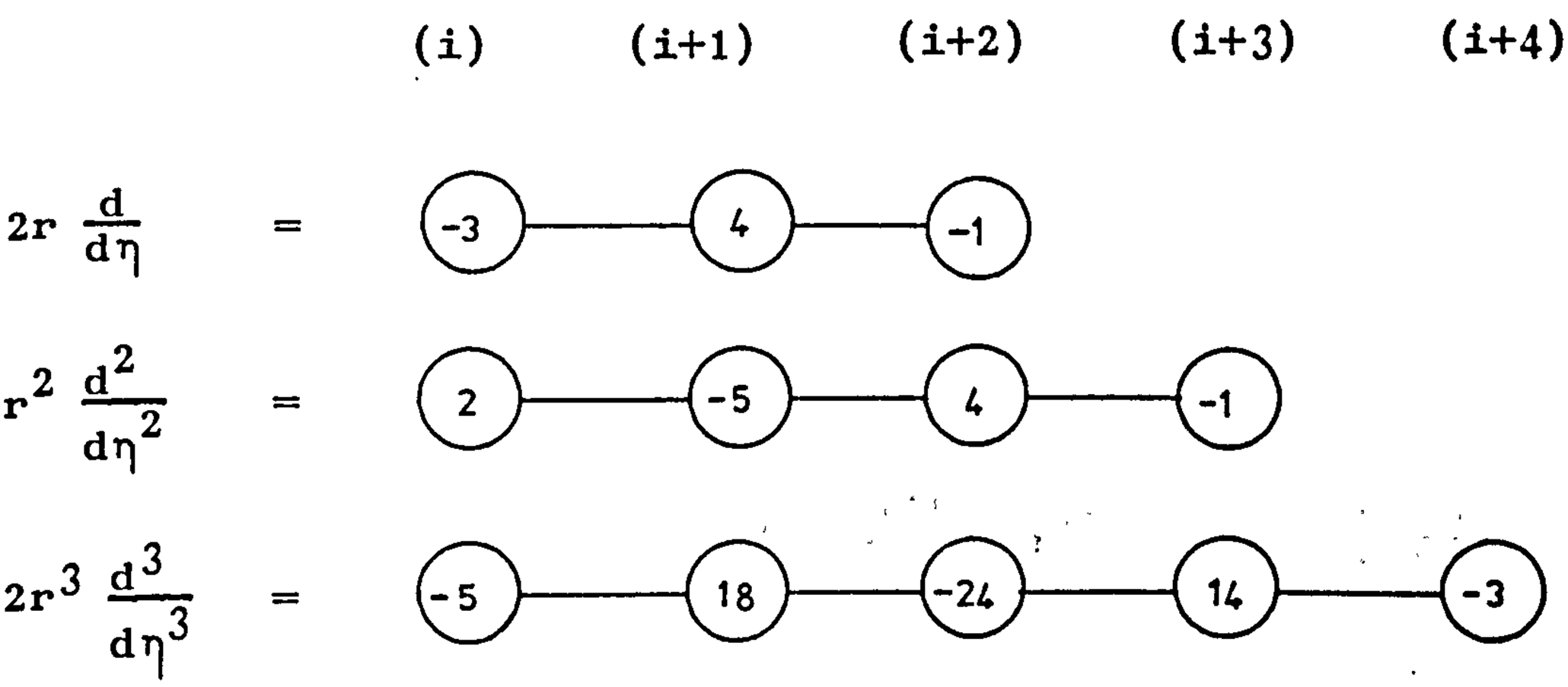

APPENDIX II

DESIGN EXPRESSIONS FOR A POLYNOMIALLY DISTRIBUTED LATERAL LOAD OF INTENSITY $P_n \eta^n$ PER UNIT HEIGHT

Following the same method of analysis established in Chapter 2, the design expressions for a polynomially distributed lateral load of intensity $P_n \eta^n$ per unit height are found to be as follows:-

$$W = P_n H$$

$$f^q = \frac{q l \mu}{W}$$

$$f^T = \frac{T l \mu}{WH}$$

$$f^{u_H} = \frac{EI \mu u_H}{R W H^3}$$

$$F_1^q = \frac{\cosh \gamma(1 - \eta)}{\cosh \gamma}$$

$$F_1^T = \frac{\sinh \gamma(1 - \eta)}{\gamma \cosh \gamma}$$

$$F_1^{u_H} = \frac{\tanh \gamma}{\gamma^3} - \frac{1}{\gamma^2}$$

$$F_2^q = \frac{1}{(n+1)} - \sum_{r=-1}^{n} \frac{n!}{(n-r)!} \frac{\sin^2(\frac{r\pi}{2})}{\gamma^{r+1}} \eta^{(n-r)} + \left(\frac{\sinh \gamma \eta}{\gamma \cosh \gamma}\right) \cdot \left(\sum_{r=-1}^{n} \frac{n!}{(n-r-1)!} \frac{\sin^2(\frac{r\pi}{2})}{\gamma^{r+1}}\right)$$

$$F_2^T = \frac{1 - \eta}{(n+1)} - \sum_{r=-1}^{n} \frac{n!}{(n-r+1)!} \frac{\sin^2(\frac{r\pi}{2})}{\gamma^{r+1}} (1 - \eta^{(n-r+1)})$$

$$+ \sum_{r=-1}^{n} \frac{n!}{(n-r-1)!} \frac{\sin^2(\frac{r\pi}{2})}{\gamma^{r+3}} \left(1 - \frac{\cosh\gamma\eta}{\cosh\gamma}\right)$$

$$F_2^{u_H} = \mu\left[\frac{1}{2(n+2)} - \frac{1}{6(n+1)} + \frac{n!}{(n+4)!}\right]$$

$$+ \tfrac{1}{2} \sum_{r=-1}^{n} \frac{n!}{(n-r+1)!} \frac{\sin^2(\frac{r\pi}{2})}{\gamma^{r+1}}$$

$$- \sum_{r=-1}^{n} \frac{n!}{(n-r+3)!} \frac{\sin^2(\frac{r\pi}{2})}{\gamma^{r+1}} - \frac{1}{3(n+1)}$$

$$- \sum_{r=-1}^{n} \frac{n!}{(n-r-1)!} \frac{\sin^2(\frac{r\pi}{2})}{\gamma^{r+1}} \left(\frac{1}{2\gamma^2} - \frac{1}{\gamma^4} + \frac{1}{\gamma^4\cosh\gamma}\right)$$

$$F_3^{u_H} = \frac{1}{R}\left[r_5\left(r_4 (f^T)_0 + \frac{\mu}{\gamma^2}(f^q)_0\right) + \mu(1 - R)\cdot\right.$$

$$\left.\left(\frac{1}{2(n+1)} - \frac{1}{6(n+1)} + \frac{n!}{(n+4)!}\right)\right]$$

$$B = \frac{r_1\left(\frac{1}{(n+2)} - \frac{h_0}{H(n+1)}\right) - r_2(F_2^T)_0 - r_3(F_2^q)_0}{r_3 + r_2 (F_1^T)_0}$$

In the formulae, $0!$ is equal to unity and a negative factorial is infinite. Other parameters are as defined in Chapter 3.

APPENDIX III

SUMMARY OF VLASOV'S THEORY FOR THIN-WALLED BEAMS OF OPEN SECTION

Vlasov's theory for thin-walled beams of open section is based on two main simplifying assumptions[31], namely,

1. The shape of the out-line of a cross-section remains unchanged under loading, i.e. the contour of the beam profile is invariable (the beam profile is the cross-section of the middle surface of the thin-walled beam).
2. The middle surface of the beam is free of shear deformation, i.e.

$$\frac{\partial \psi}{\partial s} + \frac{\partial \rho}{\partial z} = 0 \qquad \text{(III-1)}$$

where,(Fig. III-1),

ψ = longitudinal displacement of a point along the the profile

ρ = transverse tangential displacement of that point

s = profile ordinate

z = longitudinal axis of the beam

From these two assumptions, the longitudinal displacement $\psi(z,s)$ of a point R in the profile of a cross-section along the Z axis may be shown to be

$$\psi(z,s) = K(z) - u'(z)x - v'(z)y - \theta'(z)\omega \qquad \text{(III-2)}$$

where

$k(z)$ = a function of z only for a given set of the origin 0, sectorial pole p and sectorial origin r (Fig. III-2)

x,y = x- and y- co-ordinates of the point R

ω = sectorial co-ordinate of the point R; it is defined as double the area enclosed by straight lines pr and pR and the curved rR (Fig. III-2),

$u(z)$ = displacement along the X direction, of the sectorial pole p,

$v(z)$ = displacement along the Y direction, of the sectorial pole

$\theta(z)$ = angle of rotation in the plane OXY of the profile; positive if it is a clockwise rotation when viewing by facing the positive Z direction,

' (prime) = symbol denoting differentiation with respect to z

The sectorial co-ordinate ω is positive if the radius pr moves clockwise when viewing by facing the positive Z direction.

Vlasov assumed further that the normal stresses are constant over the thickness of the beam and that the tangential stresses over the beam vary linearly (Fig. III-3). The state of stress in the cross-section can then be expressed by the longitudinal stresses $\sigma(z,s)$, the average tangential stresses $\tau(z,s)$, and the torsional moment $T_a(z)$. The torsional moment $T_a(z)$ which arises from the differences in the tangential

stresses at the outer and inner surface of the beam, (Fig. III-3), is assumed to be distributed uniformly over the cross-section.

From the stress-strain relationship and the assumed inflexibility of the contour of the cross-section it may be shown that,

$$\sigma(z,s) = E \left[k'(z) - u''(z)x - v''(z)y - \theta''(z)\omega \right]$$

$$\tau(z,s) = \frac{1}{\delta} \left[\varkappa(z) - \int_0^s p_z ds - E\left(k''(z)J(s) - u'''(z)J_y(s) - v'''(z)J_x(s) + \theta'''(z)J_\omega(s) \right) \right] \qquad \text{(III-3)}$$

where

E = modulus of elasticity

δ = thickness of the beam

$\varkappa(z)$ = a function of z only

$$J(s) = \int_0^s dA$$

$$dA = d(\delta s)$$

$$J_x(s) = \int_0^s y\,dA$$

$$J_y(s) = \int_0^s x\,dA$$

$$J_\omega(s) = \int_0^s \omega\, dA$$

p_z = projection of the external surface forces on the Z axis

The generalized cross-sectional forces are given by

$$N = \int_A \sigma \, dA \quad = \text{longitudinal force}$$

$$M_x = \int_A \sigma \, y dA \quad = \text{moment about the X axis}$$

$$M_y = \int_A \sigma \, x dA \quad = \text{moment about the Y axis}$$

$$B = \int_A \sigma \, \omega \, dA \quad = \text{bimoment} \qquad \text{(III-4)}$$

$$f_x = \int_L \tau \, \delta \, dx \quad = \text{cross-sectional shear force in the X direction}$$

$$f_y = \int_L \tau \, \delta \, dy \quad = \text{cross-sectional shear force in the Y direction}$$

$$t = \int_L \tau \, \delta \, d\omega \quad = \text{torsional moment about the sectorial pole due to the shear stress } \tau \text{, clockwise torsional moment being positive}$$

where

$\int_A$ = integration taken over the whole cross-section

$\int_L$ = integration taken over the whole curve of the cross-sectional profile.

If the beam is subjected only to transverse surface forces and longitudinal edge forces,(Fig. III-4), the expressions for the generalized forces given by equation

(III-4) become, provided that the co-ordinate system is the generalized principal co-ordinate system[31],

$$N = EA\,\kappa'(z) = \int_{z}^{height} (q_1 + q_2)\,dz$$

$$M_y = EI_y u''(z)$$

$$M_x = - EI_x v''(z)$$

(III-5)

$$B = - EI_\omega\, \theta''(z)$$

$$f_x = (q_1 x_1 + q_2 x_2) - EI_y u'''(z)$$

$$f_y = (q_1 y_1 + q_2 y_2) - EI_x v'''(z)$$

$$t = (q_1 \omega_1 + q_2 \omega_2) - EI_\omega\, \theta'''(z)$$

where

$$I_x = \int_A y^2 dA \quad , \quad I_y = \int_A x^2 dA$$

$$I_\omega = \int_A \omega^2 dA$$

q_1, q_2 = longitudinal shear distributions at edges 1 and 2, (Fig. III-4)

x_1, x_2 = X co-ordinates (principal) at edges 1 and 2

y_1, y_2 = Y co-ordinates (principal) at edges 1 and 2

ω_1, ω_2 = principal sectorial co-ordinates at edges 1 and 2

The principal generalized co-ordinate system for a cross-section is defined as follows:-

(i) The X and Y axes are the principal axes.

(ii) The sectorial pole is located at the shear centre

of the cross-section.

(iii) The sectorial origin is located at the point which results in $\int_A \omega \, dA = 0$

The expression for the longitudinal stress, equation (III-3), then becomes,

$$\sigma(z,s) = \frac{N}{A} - E\left(u''(z)x + v''(z)y + \theta''(z)\omega \right)$$

$$= \frac{N}{A} - x\frac{M_y}{I_y} + y\frac{M_x}{I_x} + \frac{B}{I_\omega}\omega \qquad \text{(III-6)}$$

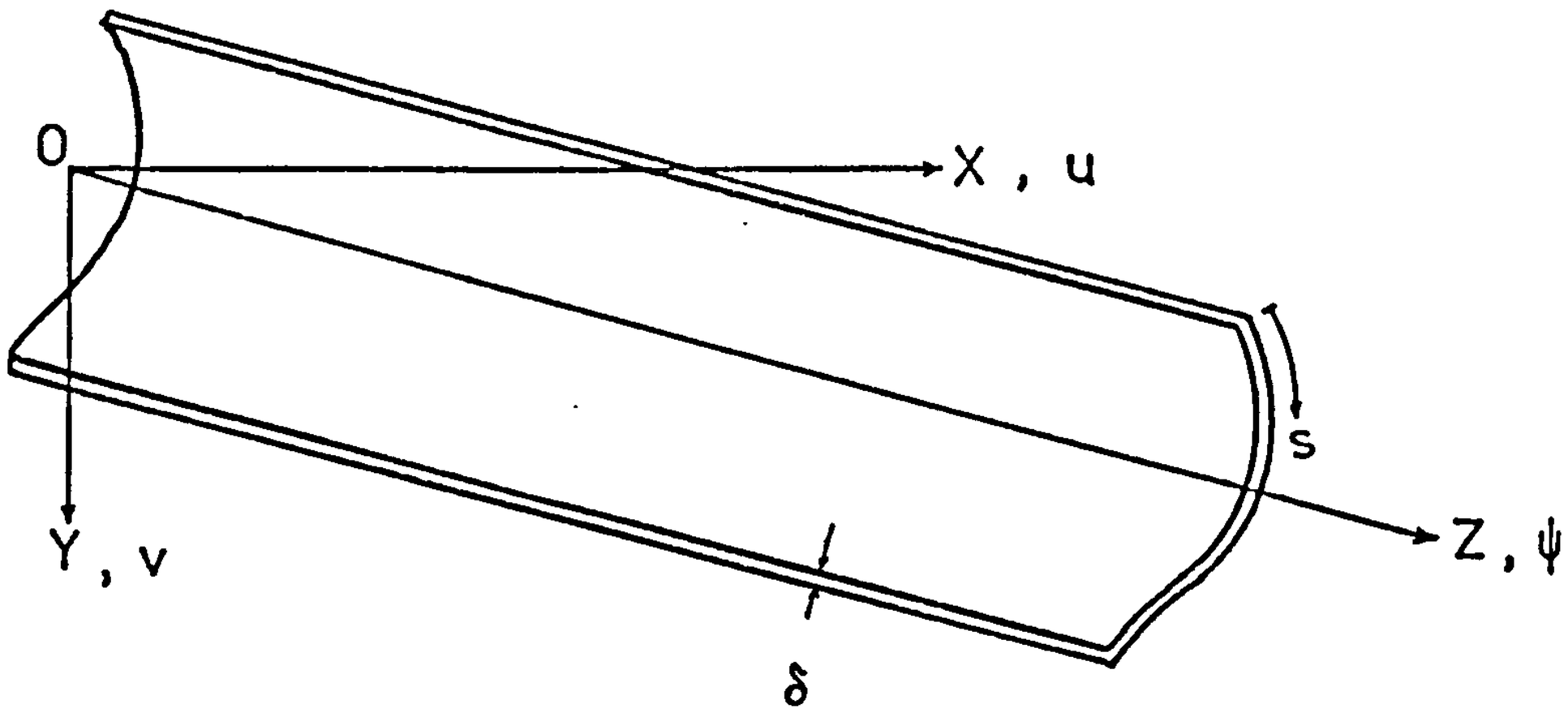

Thin-walled beam

Fig. III-1

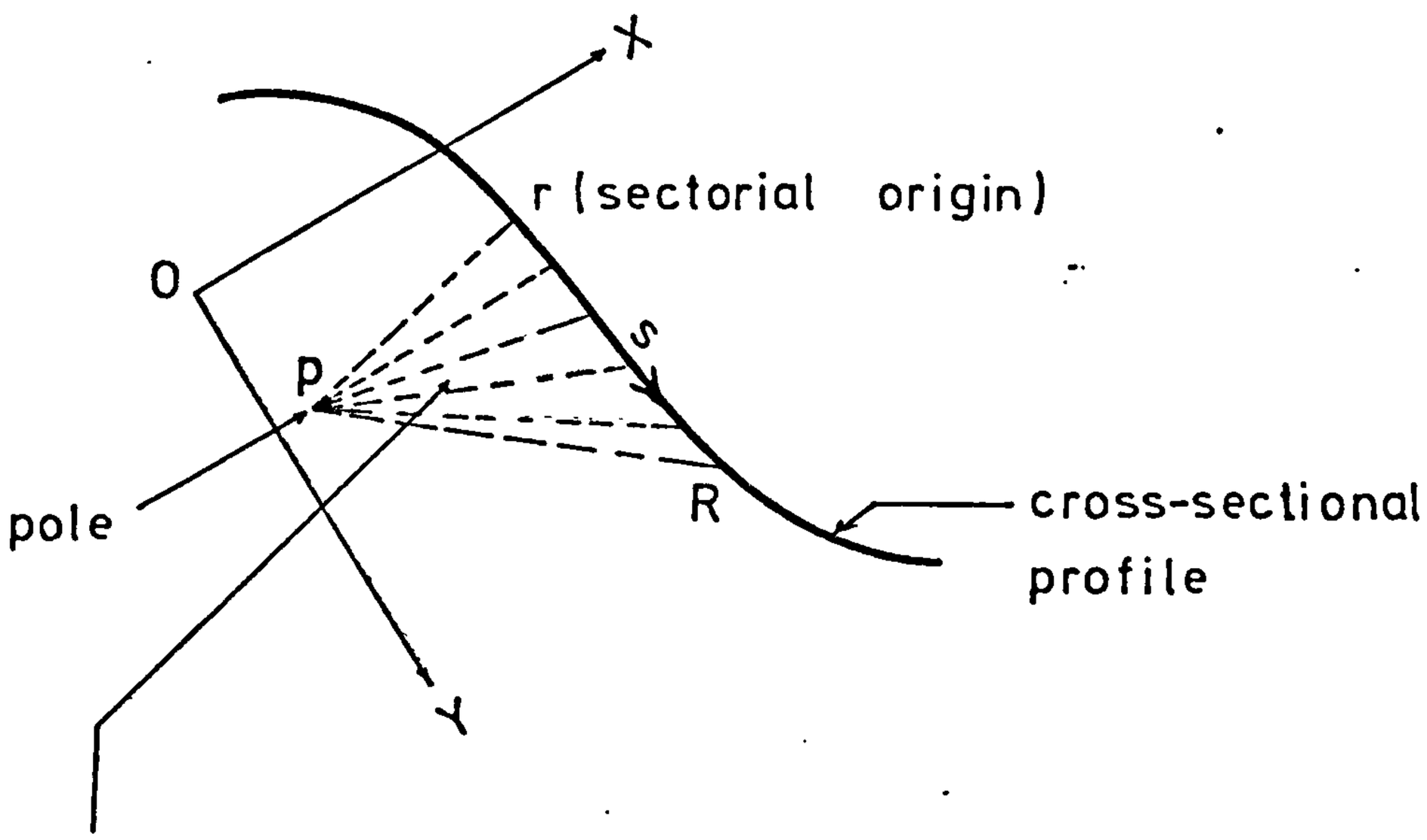

sectorial co-ordinate (ω_R) = 2 × area of prR

Cross-sectional co-ordinates

Fig. III-2

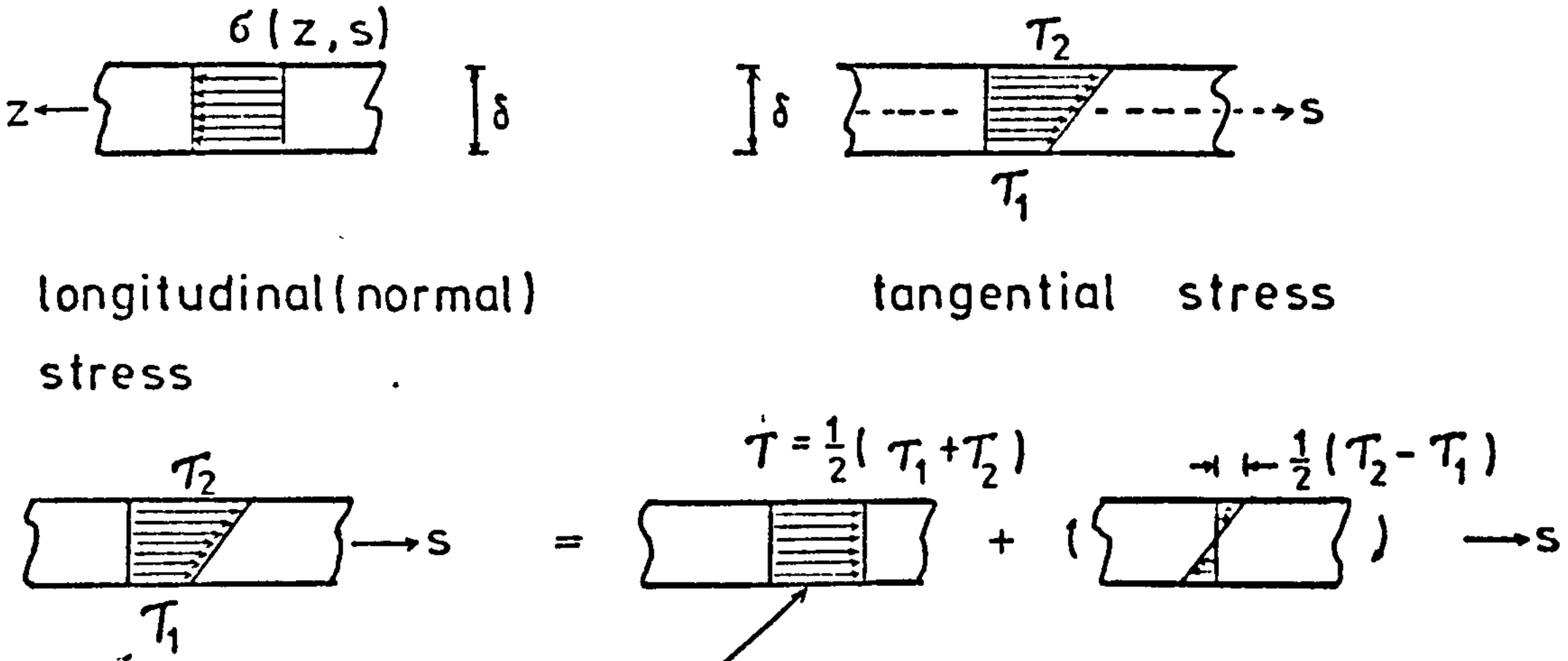

Wall stresses

Fig. III-3

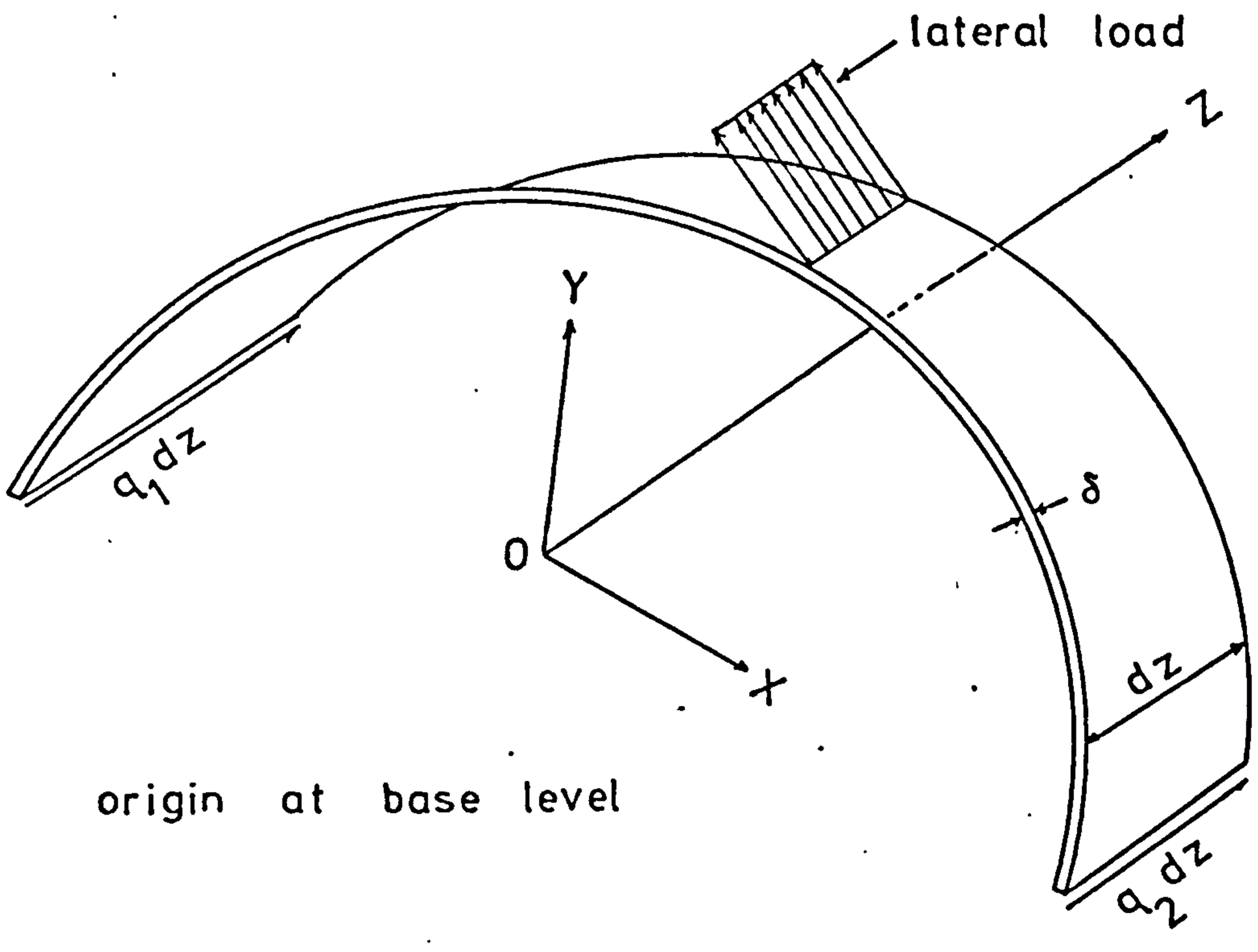

origin at base level

Element of beam subjected to lateral (tranverse) load and longitudinal edged loads

Fig. III-4